UNIVERSITY OF MODENA AND REGGIO EMILIA
PhD program of Clinical and Experimental Medicine (CEM)
Curriculum: Translational Medicine
XXXIV Cycle
Director of the PhD program: Prof. Giuseppe Biagini

FLT3-ITD ACUTE MYELOID LEUKEMIA CELLS: a rationale for the combined use of phosphoinositide 3-kinase and receptor tyrosine kinase inhibitors

Supervisor:
Prof. Sandra Marmiroli

Candidate:
Salihanur Darici

Co-supervisor:
Dr. Xu Huang

Academic Year 2020/2021

Declaration

I declare that this thesis is the result of my own work, unless states otherwise and has not been submitted for any other degree or award. This research was supported by grants from the not-for-profit Association A.Ma.Ri.Ca (Mantova, Italy) as well as from Fondazione Associazione Italiana per la Ricerca sul Cancro (AIRC) MFAG 2018 - ID. 21771.
I was a recipient of an external fellowship, generously granted by the PhD program Clinical and Experimental Medicine (CEM) and, consequently, by the Department of Biomedical, Metabolic and Neural Sciences in loving memory of Professor Paola Loria (1951-2014), previous Director of the PhD School in Clinical and Experimental Medicine.

Salihanur Darici

February 2022

Abstract (in English)

Acute myeloid leukemia (AML) has a very poor 5-year survival of ~20% in Europe. The internal tandem duplication (ITD) mutation of the Fms-like receptor tyrosine kinase 3 (FLT3) (FLT3-ITD) is the most frequent mutation (~25%) in normal karyotype AML. In recent clinical studies, few patients display prolonged remissions with receptor tyrosine kinase (RTK) inhibitors, such as FLT3 inhibitors (FLT3i) therapy, highlighting a substantial unmet need for novel effective treatment. Persistence of leukemia stem cells (LSC) drive AML leukemogenesis, responsible for drug resistance and disease relapse following conventional chemotherapy. Growing evidence recognizes that FLT3-ITD mutation leads to the constitutive activation of FLT3 kinase and its downstream pathways, including PI3K/AKT/mTOR signaling, strongly associated with LSC survival and crosstalk between LSC and stromal cells associated bone marrow (BM) tumor environment (TME). The TME provides protection of FLT3-ITD AML cells against FLT3 inhibitors. Thus, the PI3K/AKT/mTOR pathway may represent as a putative target for FLT3-ITD AML.

This study aims to test the hypothesis that PI3K/AKT/mTOR inhibition could sensitize FLT3-ITD AML cells to RTKi-lead targeted therapy using human AML cell lines and primary patient blasts. First, I uncover the phenotypic profile of FLT3-ITD versus FLT3 wildtype cell lines following treatment with selected FLT3i or PI3K/AKT/mTORi that have failed treatment of AML as monotherapy in clinical studies. More specifically, I determine the drug efficacy by means of cell growth measurement and assessment of cell cycle status and apoptosis. I was able to demonstrate that BAY-806946 (pan PI3Ki) and PF-04691502 (dual PI3K/mTORi) exerted growth inhibitory activity caused by G1 cell cycle arrest and apoptosis, and this effect was irrespective of FLT3 status. Quizartinib (FLT3i) selectively inhibited cell growth in FLT3-ITD AML and this effect was mainly caused by apoptosis. The observed drug-induced apoptotic effect was however not as efficient as chemotherapy.

Next, I provide proof-of-concept for the combination of quizartinib and BAY-806946 using both FLT3-ITD AML cell lines and primary patient blasts. When evaluating on primary patient blasts, I take into consideration the protective role of mesenchymal stromal cells and physiological growth factors to mimic the BM microenvironment. Hereby, I co-cultured FLT3-ITD AML blasts with stromal cell line MS-5 and added growth factors essential for AML survival and differentiation such as IL-3, TPO and G-CSF at physiological concentration. As expected, treatment with BAY-806946

enhanced both cytostatic and cytotoxic effect of quizartinib in FLT3-ITD AML cell line MOLM-13 as well as primary patient blasts in co-culture. More importantly, enhanced apoptosis was measured in the stem cell like CD34+CD38- population.
Lastly, I elucidate the cytokine profile and persistent phosphoproteins as putative targets following combination treatment. Ultimately, this study demonstrates the potential of PI3K/AKT/mTORi to enhance the efficacy of RTKi quizartinib for the treatment of FLT3-ITD AML.

Key words: AML, FLT3-ITD, PI3K/AKT/mTOR, Quizartinib, Target therapy

Abstract (in Italian)

In Europa, la sopravvivenza a 5 anni dei pazienti affetti da leucemia mieloide acuta (LMA) è solo del 20%. La duplicazione interna in tandem del gene FLT3 (FLT3-ITD), che codifica per il recettore della tirosina chinasi FLT3, è la mutazione più frequente (~ 25%) nella LMA con cariotipo normale, dove porta all'attivazione costitutiva della chinasi FLT3. Nonostante risultati iniziali molto promettenti con inibitori di FLT3 (FLT3i) nei pazienti con questa mutazione, pochi pazienti hanno remissioni prolungate, evidenziando la necessità di nuove e più efficaci terapie. La persistenza delle cellule staminali leucemiche guida la leucemogenesi della LMA ed è responsabile della resistenza ai farmaci e della ricaduta dopo chemioterapia convenzionale. L'attivazione costitutiva di FLT3 porta all'attivazione del signaling a valle, e in particolare della via PI3K/AKT/mTOR, una cascata di segnale fortemente associata alla sopravvivenza delle cellule staminali leucemiche e al crosstalk tra le cellule staminali leucemiche e le cellule stromali associate al microambiente tumorale midollare. La nicchia midollare fornisce protezione alle cellule leucemiche FLT3-ITD nei confronti degli inibitori FLT3. Pertanto, la via PI3K/AKT/mTOR può rappresentare un bersaglio terapeutico nella AML FLT3-ITD.

Questo studio mira a verificare l'ipotesi che l'inibizione di PI3K/AKT/mTOR sensibilizzi le cellule AML FLT3-ITD alla terapia mirata con RTKi utilizzando linee cellulari AML umane e blasti di pazienti primari. In particolare, ho definito il profilo fenotipico delle linee cellulari FLT3-ITD rispetto a quelle FLT3 wildtype dopo trattamento con un pannello di FLT3i o PI3K/AKT/mTORi che non hanno dimostrato sufficiente efficacia clinica se utilizzato come monoterapia. Successivamente, ho valutato l'effetto del farmaco sulla crescita cellulare e sul ciclo cellulare e l'apoptosi. I risultati ottenuti dimostrano che BAY-806946 (pan PI3Ki) e PF-04691502 (inibitore duale PI3K/mTORi) sono in grado di inibire la crescita poiché causano arresto del ciclo cellular in fase G1 e apoptosi, un effetto che appare indipendente dallo stato mutazionale di FLT3. Dimostrano inoltre che l'arresto della crescita cellulare indotto dall'inibitore di FLT3 (FLT3i) quizartinib è causato principalmente dall'induzione di apoptosi. Tuttavia l'efficacia rimane inferiore rispetto al trattamento con chemioterpia convenzionale (AraC).

Inoltre, la proof of concept per l'utilizzo della combinazione del quizartinib con BAY-806946 è stata ottenuta in linee cellulari AML FLT3-ITD e blasti primari da paziente. Nel valutare i blasti primari da paziente, è stato considerato il ruolo protettivo delle

cellule stromali mesenchimali in co-coltura, e dei fattori di crescita per riprodurre le condizioni del microambiente midollare. Pertanto, blasti primari da paziente LAM sono stati mantenuti in co-coltura con cellule stromali MS5 in presenza di concentrazioni fisiologiche di fattori di crescita quali IL-3, TPO e GM-CSF. Come atteso, il BAY-806946 potenzia l'effetto citostatico e citotossico del quizartinib nelle cellule MOLM-13 e nei blasti primari da paziente con mutazione FLT3-ITD in condizione di co-coltura. E' importante sottolineare l'incremento di apoptosi osservato anche nella sottopopolazione staminale leucemica CD34+CD38-.

Infine, ho valutato il profilo delle citochine e delle fosfoproteine persistenti come bersagli putativi dopo il trattamento di combinazione. Complessivamente, questo studio dimostra il potenziale di PI3Ki per migliorare l'efficacia di RTKi quizartinib nel trattamento della LMA FLT3-ITD.

Parole chiave: LAM, FLT3-ITD, PI3K/AKT/mTOR, Quizartinib, Target therapy

Acknowledgements

As I look back at this PhD journey, I feel grateful and humble for the support that I have been given by family, friends and colleagues. I would like to express my gratitude and admiration to everyone that has helped me through the good and difficult times and has made it possible for me to accomplish my achievements.

First and foremost, I would like to express my deepest gratitude and appreciation to my supervisors, Prof. Sandra Marmiroli, Dr. Xu Huang, Dr. Heather G. Jørgensen and Dr. Gillian Horne. I feel extremely lucky to have been given advice, guidance, insights and support from such experienced and successful researchers. Thank you for giving me this opportunity to take part of this fruitful collaboration and pushing me to exceed my own expectations. Sandra, thank you for always listening to me and allow me to explore my ideas. I have always highly admired you as a successful female professor that is never afraid to take risks and always works hard to achieve her goals. Although I have been struggling a lot with the language barrier at the very beginning, I felt you always had my back and I felt welcomed in the very social and fun Italian lab family. Thank you for always being there for me, even when I was abroad. Xu, thank you for making me think more critical of my own work and pushing me to perform better. I am immensely grateful for the opportunity you have given me to gain experience in your lab. Heather and Gillian, thank you for the time and efforts you put into reading and correcting my work. I cannot express how grateful I am for your support and for believing in me. I have had many times I doubted my abilities, but thanks to your positivity, patience and guidance I have made it through – thank you!

To my colleagues and everyone else that has helped me during the course of my PhD – thank you! I would like to thank everyone from POG that has helped me over the last two years, in particular Shaun, Laura and Jen. Amy, I am so grateful for meeting such a funny, smart and caring friend like you. From the policlinic in Modena, I would like to thank Manu, Luca, Laura, Tullia, Fra and Marta for their great hospitality, technical advice and of course the banter we had during the coffee breaks with Italian delicacies. In particular, I would like to thank Dr. Luca C. Napoli for always cheering me up and making me laugh. Manu, you are the best lab buddy I could have wished for, thank you for helping me completing my research from 3000 km away. Marta, you are the first person I walk past on the corridor and I am thankful

to you for always making me smile when having our regular chitchats. I could have never had such a great time in Modena if it was not for Nadia's family and the Modena International Friends group. Nadia, I am immensely grateful for what you and your family have done for me – shokran! Even though I do not understand Arabic (but I love the food), I have always had a great time spending time with your family, especially with Presidente Samira! Veronica, you are a wonderful and caring host and I feel honored to be MIF's first member. Thank you for bringing so many internationals together in Modena. I am very much looking forward to seeing all of you again.

Finally, I would like to express my deepest gratitude to my loving family and friends. It has not been easy being away from my family, especially because of the pandemic. Nevertheless, my parents always made sure to call me every other day to make sure I was fine and to remind me that they believe in me. I never felt I was truly away because of your love and support that I could feel anywhere I went. Thank you for being the most caring and loving parents I could have wished for/ İsteyebileceğim en şefkatli ve sevgi dolu anne ve baba olduğunuz için teşekkür ederim. Allah sizden razı olsun! Tashfeen, you are my best friend for almost 15 years and I am once again thankful for having you in my life. Thank you for listening to me for hours on the phone about my PhD drama. I am sure you would have been rich if I had paid you by the hour. ہوں کرتا پیار سے تم میں. Cem, you came into my life towards the very end of my PhD, which was also the most exhausting and stressful time of my studies. With everything that went on in my personal life you have been a wonderful supporter and I cannot thank you enough for the patience, care and love you have shown me. I cannot wait to repay you for all you have done for me.
This thesis is dedicated to my loving parents; I hope I have made you proud.

Table of Contents

List of Tables

Chapter 2:

Chapter 3:

Chapter 4:

Chapter 6:

List of Figures

Chapter 1:

Chapter 2:

Chapter 3:

Chapter 4:

Chapter 5:

Chapter 6:

Abbreviations

4E-BP1	eIF4E -binding protein 1
ALL	acute lymphoblastic leukemia
alt-NHEJ	alternative non-homologous end-joining
AML	acute myeloid leukemia
AMPK	AMP-activated protein kinase
ANG1	angiopoietin 1
ANXA2	annexin 2
ARE	antioxidant response elements
ATM	ataxia telangiectasia mutated
ATR	ataxia telangiectasia and Rad3-related protein
B-NHL	B-cell non-Hodgkin lymphoma
BAD	Bcl-2 associated agonist of cell death
Bcl-2	B-cell lymphoma 2
BER	base excision repair
BET	bromodomain and extra-terminal domain
BH	Bcl-2 homology
BM	bone marrow
CAR	CXCL12-abundant reticular
CCL-1	C-type lectin-like molecule-1
CEBPA	CCAAT/enhancer-binding protein alpha
CI	combination index
CLL	chronic lymphoblastic leukemia
CML	chronic myeloid leukemia
CRc	composite complete remission
CRi	CR with incomplete hematological recovery
CXCL12	CXC-chemokine ligand 12
DCA	dichloroacetate
DDR	DNA damage response
DFS	disease-free survival
DIFP	diisopropyl fluorophosphate
DMEM	Dulbecco's Modified Eagle Medium
DMSO	dimethyl sulphoxide
DNA	deoxyribonucleic acid
DNA-PK	DNA-dependent protein kinase
DNMT3A	DNA methyltransferase 3A
dNTP	deoxynucleotide triphosphate
DSB	double strand breaks
ECM	extracellular matrix

EDTA	ethylenediaminetetraacetic acid
eIF4E	eukaryotic initiation factor-4E
ERK	extracellular signal-regulated kinase
ETC	electron transport chain
FACS	fluorescence activated cell sorting
FBS	foetal bovine serum
FDA	Food and Drug Administration
FGF2	fibroblast growth factor 2
FKBP12	FK506 binding protein 12
FL	follicular lymphoma
FLT3	FMS-like tyrosine kinase 3
FLT3i	FLT3 inhibitor
FMO	fluorescence minus one
FoxO	forkhead box class O
FRB	FKBP rapamycin-binding
G-CSF	granulocyte colony-stimulating factor
GAB2	GRB2-associated binding protein 2
Gal-9	galectin-9
GAP	GTPase-activating protein
gDNA	genomic DNA
GM-CSF	granulocyte-macrophage colony-stimulating factor
GPCR	G protein-coupled receptors
GRB2	growth factor receptor-bound protein 2
GSK	glycogen synthase kinase-3
HBSS	Hank's Balanced Salt Solution
HDAC	histone deacetylase
HIF	hypoxia-inducible factor
HMA	hypomethylating agents
HR	homologous recombination
hrs	hours
HSPC	hematopoietic stem and progenitor cells
IC50	half maximal inhibitory concentration
IDH	isocitrate dehydrogenase
IGF-1	insulin-like growth factor 1
IL-3	interleukin 3
ILK	integrin-linked kinase
IMDM	Iscove Modified Dulbecco Media
IRS	insulin receptor substrate
ITD	internal tandem duplication
JAK	Janus kinase

JMD	juxtamembrane domain
Keap-1	Kelch-like ECH-associated protein 1
LAM	lymphangioleiomyomatosis
LDAC	low dose cytarabine
LEPR	Leptin receptor
LKB1	liver kinase B1
LTC-IC	long-term culture initiating cell
MAF	musculoaponeurotic fibrosarcoma
Mcl-1	myeloid cell leukemia 1
MEC	mitoxantrone/etoposide/cytarabine
MIF	macrophage migration inhibitor factor
Mins	minutes
MM	multiple myeloma
MPAL	mixed phenotype acute leukemia
MPD	myeloproliferative disorders
MR	minimal response
mRNA	Messenger RNA
MSC	mesenchymal stem cells
mSin1	mammalian stress-activated protein kinase interacting protein
MTD	maximum tolerated dose
mTOR	mammalian target of rapamycin
mTORC	mTOR complex
Myr-AKT1	Myristoylated AKT1
NDC	no drug control
NF- κB	nuclear factor kappa-light-chain-enhancer of activated B cells
NK	natural killer
NOD/SCID	nonobese diabetic/severe combined immunodeficiency
noRT	no reverse transcriptase
NPM1	nucleophosmin 1
Nrf-2	nuclear factor erythroid 2-related factor 2
NSG	NOD/SCID/IL2rγ(null)
NTC	no template control
OPN	osteopontin
OS	overall survival
PARP-1	poly(ADP-ribose) polymerase-1
PBS	phosphate-buffered saline
PCR	polymerase chain reaction
PDK1	phosphoinositide-dependent kinase 1
PDX	patient-derived xenograft
PGF	physiological growth factor

PI	propidium iodide
PI3K	phosphoinositide 3-kinase
PI3K/AKT/mTORi	PI3K/AKT/mTOR inhibitor
PIKK	PI3K-related kinase
PIP_2	phosphatidylinositol-4,5-phosphate
PIP_3	phosphatidylinositol-3,4,5-phosphate
PKB	protein kinase B
PR	partial remission
PRAS40	proline-rich AKT substrate 40kDa
PTEN	phosphatase and tensin homolog
Rheb	Ras homolog enriched in brain
RNA	ribonucleic acid
ROS	reactive oxygen species
RPPA	reverse phase protein array
rpS6	ribosomal protein S6
rRNA	ribosomal RNA
RSK	p90 ribosomal S6 kinase
RT	reverse transcriptase
RTK	receptor tyrosine kinase
S	Serine
S6K1	p70 ribosomal S6 kinase
SA-RPE	streptavidin-conjugated R-phycoerythrin
SCF	stem-cell factor
SD	standard deviation
SDF-1	stromal-derived factor-1
SDS	sodium dodecyl sulphate
SFEM	serum-free medium
SFM	serum-free expansion medium
SHIP	Src homology domain-containing inositol phosphatase
SHP-2	SH2 domain-containing protein tyrosine phosphatase-2
SSB	single strand breaks
STAT	signal transducer and activator of transcription
T	Threonine
TAE	tris-acetate-EDTA
TAM	Tyro3-Axl-Mer
TET2	Tet methylcytosine dioxygenase 2
TIM-3	T cell immunoglobulin-3
TKD	tyrosine kinase domain
TKI	tyrosine kinase inhibitor
TNF-α	tumor necrosis factor α

TP53	tumor protein 53
TPO	Thrombopoietin
TSC2	tuberous sclerosis complex 2
VCAM-1	vascular cell adhesion molecule 1
WHO	World Health Organization
Y	Tyrosine

Chapter 1: Introduction part A

1.1 Acute Myeloid Leukemia

Hematological malignancies are cancers that originate in the blood-forming tissue, that is the bone marrow and lymphatic system (Weldetsadik, 2013). Hematological malignancies can be classified in three categories: leukemia, lymphoma and multiple myeloma (Taylor et al., 2017). There are four main types of leukemia, which are acute myeloid leukemia (AML), chronic myeloid leukemia (CML), acute lymphoblastic leukemia (ALL), and chronic lymphocytic leukemia (CLL). AML is the most common leukemia in adults with an incidence rate of 3.7 per 100,000 in Europe and a 5-year relative survival rate of 19% (Visser et al., 2012). AML can be diagnosed in any age group, but occurs more commonly in adults. The median age of diagnosis ranges from 66 to 71 years (Nagel et al., 2017; Oran and Weisdorf, 2012). AML is characterized by aberrant myeloid cell proliferation and differentiation of immature blasts in the bone marrow and peripheral blood, which can result in ineffective erythropoiesis and bone marrow failure (De Kouchkovsky and Abdul-Hay, 2016; Kumar, 2011). The presence of at least 20% leukemic blasts in the BM or blood is characteristic for the diagnosis of AML and common symptoms resulting from the increased production of malignant cells include anemia, recurrent infections, unusual and frequent bruising and bleeding, and fatigue (De Kouchkovsky and Abdul-Hay, 2016; DiNardo et al., 2016).

AML comprises a group of hematological diseases that was traditionally classified based on cell morphology and immunophenotype, but the latest World Health Organization (WHO) classification incorporates genetic abnormalities to define disease entities of clinical significance. According to the WHO classification, AML can be divided into the following categories: AML with recurrent genetic abnormalities; AML with myelodysplasia-related changes; therapy-related myeloid neoplasms; AML not otherwise specified; myeloid sarcoma; and myeloid proliferations associated with Down syndrome (Arber et al., 2016; Hou and Tien, 2020). AML is highly heterogeneous and develops from hematopoietic stem or progenitor cells resulting from genetic and epigenetic changes that deregulate key processes such as self-renewal, proliferation and differentiation (Chopra and Bohlander, 2019; Welch et al., 2012). The presence of mutations in nucleophosmin1

(*NPM1*), FMS-related tyrosine kinase 3 (*FLT3*), and CCAAT/enhancer-binding protein alpha (*CEBPA*) in AML with normal karyotype has prognostic significance (Port et al., 2014). FLT3 alterations including internal tandem duplication (*FLT3*-ITD) and tyrosine kinase domain (TKD) mutations as well as point mutations in the exon 12 of the *NPM1* are reported as the most common mutations in AML (Chauhan et al., 2013; Naseem et al., 2021).

FLT3-ITD mutation, representing the most common type of FLT3 mutation, is detected in approximately 25% of all AML cases (Patnaik, 2018). Given this high frequency of *FLT3* mutations in AML, a number of tyrosine kinase inhibitors (TKI) have been developed for clinical evaluation including first-generation multi-kinase inhibitors (e.g., midostaurin, sunitinib, and sorafenib) and more specific and potent next-generation inhibitors including quizartinib, gilteritinib, and crenolanib (Daver et al., 2019). Although these inhibitors initially demonstrated promising single-agent activity with an overall survival longer than for conventional chemotherapy, the beneficial response was short-lived due to acquired resistance mechanisms (Cortes et al., 2019). An important strategy to overcome therapy resistance is combination therapy. There is ongoing research combining two or more agents that target key leukemic cell survival pathways, which may improve response rates and enable more durable remissions in *FLT3*-ITD AML patients (Daver et al., 2019; Kennedy and Smith, 2020).

1.2 Characterization of LSC

Hematopoietic stem cells (HSC) are defined by their self-renewal and multipotent differentiation capacities (Seita and Weissman, 2010). In normal hematopoiesis, HSC in the bone marrow function by producing uncommitted progenitor cells that proliferate and differentiate into all functional cellular components of the blood as well as immune cells (Rieger and Schroeder, 2012) (Figure 1.1). HSC are mainly quiescent but can enter the cell cycle to differentiate; this process it tightly regulated by HSC-intrinsic and extrinsic mechanisms (Pietras et al., 2011).

A large body of evidence has shown that AML arises from a rare cell population called leukemic stem cells (LSC) – also referred to as leukemia-initiating cells (LIC). LSC possess similar functional and molecular properties with hematopoietic stem and progenitor cells from which they originate, such as quiescence and self-renewal capacity (Hanekamp et al., 2017; Zhou and Chng, 2014) (Figure 1.1). Persistence of LSC following chemotherapy is believed to be at the origin of relapse. More importantly, it is believed that LSC may drive progression of more aggressive forms of AML, leading to worse outcomes (Vetrie et al., 2020). It has therefore become increasingly important to detect and target LSC as a prospective strategy to treat AML.

AML LSC are defined functionally by their ability to initiate, propagate and sustain leukemia after transplantation in the bone marrow compartment of immunodeficient mice (Lapidot et al., 1994; Thomas and Majeti, 2017). AML LSC can subsequently give rise to leukemic blasts that lack the ability to engraft. Initially, it had been reported that LSC capable of reproducing AML after transplantation in nonobese diabetic/severe combined immunodeficient (NOD/SCID) mice were enriched in the immunophenotypically defined CD34+CD38- fraction of leukemic cells (Bonnet and Dick, 1997; Lapidot et al., 1994). CD34 is expressed on the vast majority of HSC and has been reported as a LSC surface marker in AML. Further studies using more permissive mouse models however, cast new light on the origin of LSC. As such, using immunosuppressive mice strain NOD/SCID/IL2rγ(null) (NSG) it has been demonstrated that LSC may co-exist in CD34+CD38+ subpopulation (Sarry et al., 2011; Taussig et al., 2010). AML LSC lacking CD34 expression have additionally been identified, which may originate from healthy CD34- hematopoietic progenitors (Goardon et al., 2011; Quek et al., 2016). Indeed, the LSC hierarchy is complex,

which is responsible for heterogeneity and variation observed in AML cells of different patients as well as the leukemic blasts of individual patients (Bachas et al., 2012; Ho et al., 2016; Li et al., 2016).

There is ongoing research dedicated to further phenotypically characterize LSC according to the expression pattern of numerous surface markers and LSC-specific gene expression signature. Over the years, a number of cell surface markers have been identified that are overexpressed specifically on LSC but not HSC, which are currently under clinical investigation to target LSC. These putative LSC surface markers include CD123, CD44, CD96, C-type lectin-like molecule-1 (CCL-1), and T cell immunoglobulin-3 (TIM-3) (Haubner et al., 2019; Hosen et al., 2007; Jan et al., 2011; Jordan et al., 2000; van Rhenen et al., 2007).

CD123, also known as interleukin 3 (IL-3) receptor α (IL-3Rα), is a ligand activated cytokine receptor (Testa et al., 2019). IL-3 has a prominent role in the regulation of proliferation, growth, and differentiation of hematopoietic cells. The first study reporting CD123 as a LSC marker was by Jordan *et al*. that showed aberrant expression of CD123 on CD34+CD38- AML cells, which was conversely not detected on normal BM-derived CD34+CD38- cells (Jordan et al., 2000). To unravel the functional role of CD123, purified CD34+CD123+ AML cells were transplanted into NOS/SCID mice, which were found to be competent in establishing and propagating leukemic populations *in vivo*, validating CD123 as a LSC marker. Various studies have linked genetic alterations with specific immunophenotypes. As such, screening of CD123 expression in AML patients revealed low expression in erythroid and megakaryocytic leukemia and high CD123 expression in *NPM1* mutated and *FLT3*-ITD AML (Bras et al., 2019; Rollins-Raval et al., 2013). Overexpression of CD123 on leukemic blasts was associated with enhanced proliferation in response to IL-3, failure to achieve complete response to initial induction chemotherapy, and poor survival (Arai et al., 2019; Wittwer et al., 2017).

CD44 is a major hyaluronan receptor and though binding of its ligand, CD44 is best known to control cell-cell adhesion and cell-matrix interaction. CD44 is widely expressed in hematopoietic cells, engaging in the homing and anchorage of HSC in their niche (Ponta et al., 2003; Zöller, 2015). In AML, higher CD44 expression was reported compared to normal HSC, with specific isoforms being differentially expressed among AML patients (Bendall et al., 2000). In particular, strong expression of CD44-6v was correlated with shorter survival of AML patients (Legras

et al., 1998). In a vast majority of LSC, CD44 was found to co-express CD123, identifying CD44 as a potential LSC marker (Florian et al., 2006). Using an activating monoclonal antibody directed to CD44 eradicated AML LSC in PDX assays by inhibition of proliferation, cell cycle progression, differentiation, and impeding LSC trafficking to the BM niche (Gutjahr et al., 2021; Jin et al., 2006; Zada et al., 2003; Zhou and Chng, 2014).

CD96 is a type I membrane protein that belongs to the immunoglobin superfamily. Expressed by both T and NK cells, CD96 plays a role in NK-target cell adhesion, cytotoxicity of NK cells, and may also function in antigen presentation (Fuchs et al., 2004; Georgiev et al., 2018). Hosen *et al*. demonstrated that CD96 was frequently expressed on CD34+CD38- AML LSC, but to lower extend in the normal HSC-enriched population (Chávez-González et al., 2014; Hosen et al., 2007). Furthermore, significant levels of engraftment in murine BM was achieved following implantation of CD96+ fractions, but not CD96- AML cells, demonstrating that AML LSC express CD96.

CLL-1 is a member of type II transmembrane receptor family. CLL-1 was initially identified as a cell surface marker for AML as it is expressed on the majority of primary AML cells (Bakker et al., 2004). Further research by van Rhenen *et al*. however demonstrated that CCL-1 is expressed on 87% of CD34+CD38- AML patients, but not normal HSC (van Rhenen et al., 2007). The same group showed engraftment of CD34+CCL-1+ AML cells, indicating that CCL-1 is expressed on AML LSC.

TIM-3 is a type I membrane-bound glycoprotein that belongs to the Tim domain gene family of immunoregulatory proteins. TIM-3 is mainly expressed in monocytes and in a fraction of NK cells, and is associated with regulation of Th1-dependent immune responses and immune tolerance (Han et al., 2013, p. 3; C. Zhu et al., 2011). Kikushigi *et al*. identified expression of TIM-3 on AML LSC (except promyelocytic leukemia), but was absent on HSC, and myeloerythroid or lymphoid progenitor populations (Jan et al., 2011; Kikushige et al., 2010). TIM-3+ but not TIM-3- AML cells engrafted in AML mice, demonstrating that AML LSC express TIM-3. Further studies revealed that TIM-3 exerts pro-leukemic effects by maintaining LSC function. As such it was shown that TIM-3 and its ligand galectin-9 (Gal-9) form an autocrine loop that co-stimulates activity of nuclear factor kappa-light-chain-enhancer of

activated B cells (NF- κB) and β-catenin, involved in LSC self-renewal (Gonçalves Silva et al., 2016; Kikushige et al., 2015).

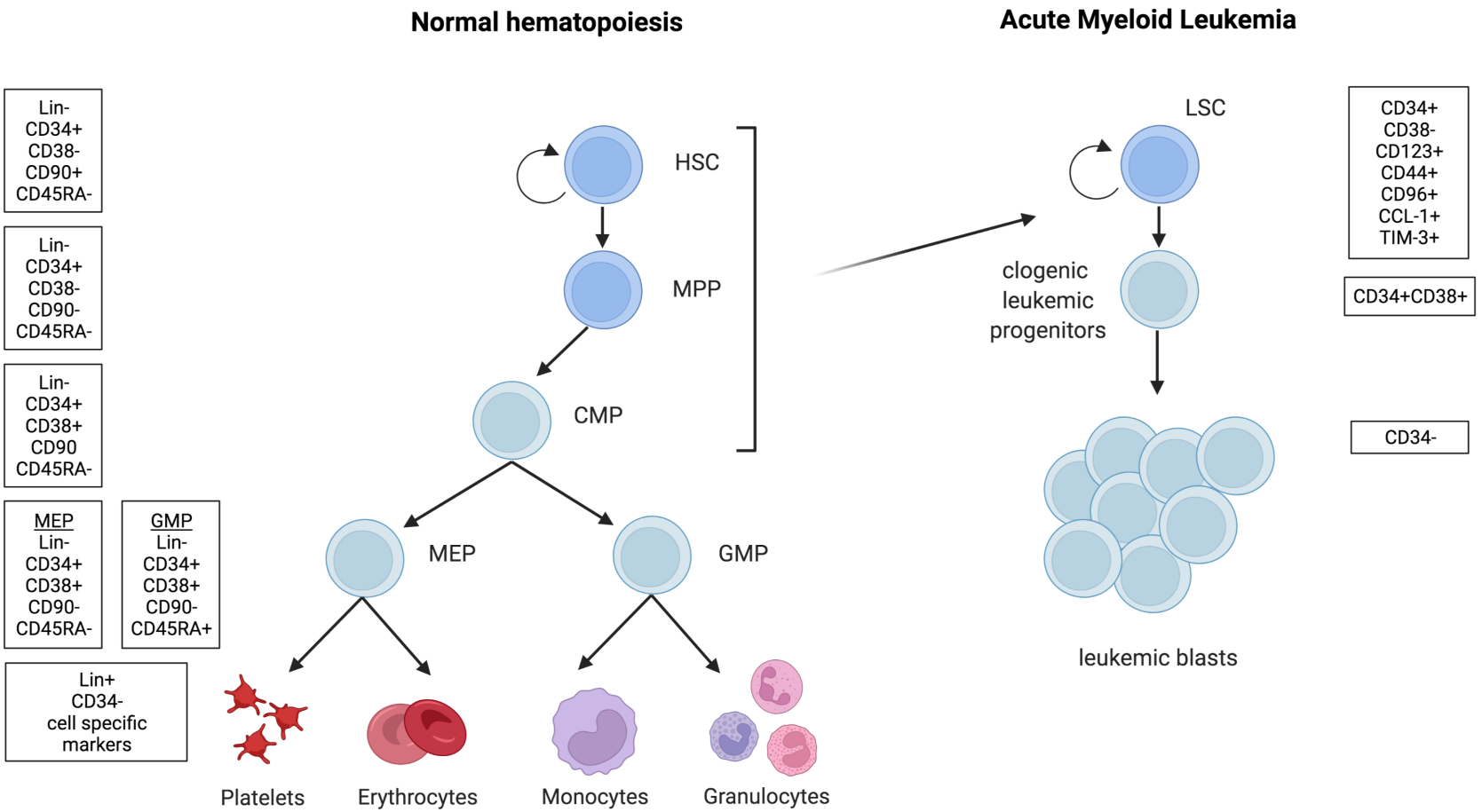

Figure 1.1 Hierarchy of normal hematopoiesis versus AML
A schematic overview depicting the phenotypic characterization of each population in human hematopoiesis and in AML. Lin= lineage markers, HSC= hematopoietic stem cell, LSC= leukemic stem cell, MMP= multipotent progenitor, CMP= common myeloid progenitor, MEP= megakaryocyte/erythrocyte progenitor, GMP= granulocyte/macrophage progenitor. Created with BioRender.com.

1.3 The bone marrow (BM) microenvironment

The BM niche, or also referred to as the BM microenvironment, is a collection of various different cell types and structures that maintain hematopoiesis in the bone marrow (Figure 1.2). The initial BM niche concept depicted by Schofield *et al*. proposed that the BM niche engages in the maintenance of BM self-renewal, and later studies confirmed that HSC-BM niche interactions are determinant of HSC fate (Schofield, 1978). The niche was first functionally ascribed to be located in the endosteal region of the trabecular bone, also referred to as the "endosteal" or "osteoblastic niche", which is comprised of several different cell types, including osteoblasts and osteoclasts, fibroblasts, macrophages, endothelial cells, and adipocytes. Later studies however revealed that HSC are frequently localized near venous sinusoids in the central marrow, which identified the perivascular (also referred to as the endothelial niche). The perivascular niche includes particularly mesenchymal stromal cells and endothelial cells that surround sinusoids. While the exact contributions of the multiple cell types that comprise the niche remains elusive, intensive research has validated the concept that the BM niche is not a single niche, but rather a collection of multiple "micro niches" that collaboratively govern several HSC functions such as homing, quiescence, self-renewal, and lineage commitment (Itkin et al., 2016).

Osteoblasts

In the endosteal niche, there are several cross talk mechanisms between osteoblasts and HSC. Osteoblasts produce numerous soluble growth factors that are essential for the regulation of HSC homing/mobilization and quiescence, such as CXC-chemokine ligand 12 (CXCL12), stem-cell factor (SCF), osteopontin (OPN), granulocyte colony-stimulating factor (G-CSF), annexin 2 (ANXA2), Angiopoietin 1 (ANG1) or thrombopoietin (TPO). CXCL12 or stromal-derived factor-1 (SDF-1) is produced primarily by immature osteoblasts but also by endothelial cells, leptin-receptor expressing perivascular cells (LepR+), CXCL12-abundant reticular (CAR) cells and Nestin+ mesenchymal stem cells (MSC) in the perivascular niche, which regulates HSC homing, retention, and repopulation (Galán-Díez and Kousteni, 2017; Ponomaryov et al., 2000). SCF is important for HSC maintenance and it is also produced by osteoblasts, but primarily by perivascular cells (Ding et al., 2012). Similarly, OPN, a phosphorylated matrix glycoprotein is secreted by osteoblasts among other cell types, and its expression within the BM is restricted to the endosteal bone surface. OPN exerts a critical role in HSC retention, migration, and negative regulation of HSC proliferation and differentiation (Nilsson et al., 2005; Standal et al., 2004; Stier et al., 2005). Osteoblasts support myelopoiesis though the secretion of G-CSF. G-CSF has a central role in

inflammation as it controls the differentiation of progenitors of the myeloid lineage to mature granulocytes (Boettcher and Manz, 2017; Taichman and Emerson, 1994). AXA2 is expressed mainly by osteoblasts and endothelial cells and is involved in the regulation of stem cell adhesion, homing, and engraftment following transplantation (Jung et al., 2007). It has been further demonstrated that AXA2 promotes localization of HSC to the endosteal niche by serving as an anchor for CXCL12 (Jung et al., 2011). ANG1 is expressed by osteoblasts and interaction with the receptor tyrosine kinase (RTK) Tie2 promotes HSC quiescence and adhesion to the bone, thereby protecting the HSC compartment from myelosuppressive stress (Arai et al., 2004). In adult hematopoiesis, TPO and its receptor MPL have a critical role in maintaining quiescence of LT-HSC and interaction with the osteoblastic niche, which is accompanied by increased cycling observed in HSCs in $TPO^{-/-}$ mice (Emerson, 2007; Qian et al., 2007; Yoshihara et al., 2007).

Endothelial cells

Endothelial cells that form the BM vessels deliver nutrients, oxygen and cellular components to the local tissues, and constitute a major component of the BM niche. They promote HSC proliferation and differentiation, homeostasis, and regeneration through expression of angiocrine factors such as growth factors, chemokines, and extracellular matrix (ECM) components (Kobayashi et al., 2010; Poulos et al., 2013; Rafii et al., 1995). Further, endothelial cells exert a critical role regulating trafficking and homing of hematopoietic stem and progenitor cells (HSPC) (Perlin et al., 2017; Rafii et al., 1995). To home to the BM, HPSC recognize and subsequently adhere to endothelial cells in the BM microvessels. Analysis of BM blood vessels revealed that the BM niche contains different types of endothelial cells with different permeability properties (Itkin et al., 2016). It has been demonstrated that less permeable blood vessels in the periarteriolar region maintain HSC in low reactive oxygen species (ROS) state, whereas blood vessels with high permeability in the perisinusoidal region increased ROS levels, thereby promoting their migration capacity. Notably, this metabolically inactive m
icroenvironment is favorable to maintain HSC quiescence.

MSC

Nestin+ MSC, confined in the perivascular region, represent an essential niche component that contain all the bone-marrow colony-forming-unit fibroblastic activity (Méndez-Ferrer et al., 2010). Further, MSC are capable of self-renewal on serial transplantation as well as multilineage differentiation toward osteochondral lineages. It has been demonstrated that MSC co-localize with HSC and express high levels of HSC maintenance factors including CXCL12, SCF, ANG1, IL-7, OPN, and vascular cell adhesion molecule 1 (VCAM-1) in

comparison to other stromal cell types such as osteoblasts (Ehninger and Trumpp, 2011). Conditional depletion of Nestin+ MSC resulted in HSC depletion and altered homing of progenitor cells (Méndez-Ferrer et al., 2010; Szade et al., 2018). Two distinct subpopulations of Nestin+ cells have been identified using a Nestin-GFP transgenic mouse model: Nestin-GFP^{bright} and Nestin-GFP^{dim} cells (Katayama et al., 2006; Kunisaki et al., 2013). Nestin-GFP^{bright} cells localized periarteriolarly and were later identified as neural/glial antigen 2 (NG2) positive with high expression of CXCL12. Nestin-GFP^{dim} cells localized perisinusoidally were marked by Leptin receptor (LEPR) and were shown to express high levels of CXCL12 and SCF.

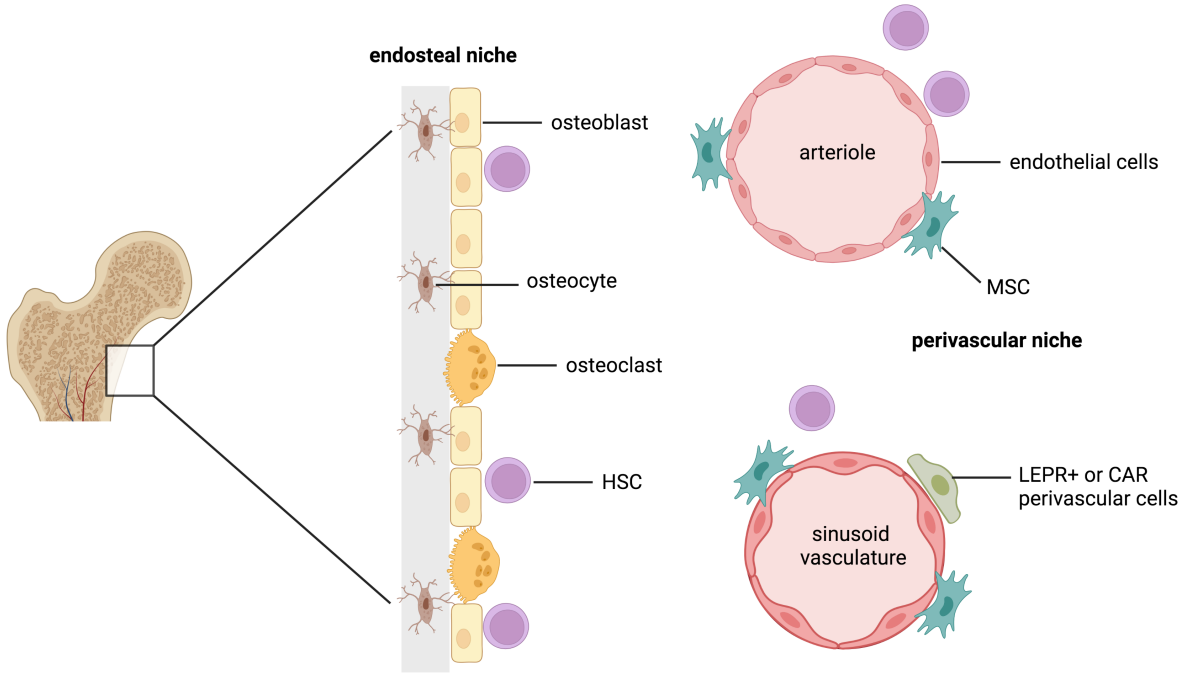

Figure 1.2 A schematic representation of the BM niche

The bone marrow (BM) niche, which can be categorized in the endosteal niche and perivascular niche, is composed of several different cell types, which are involved in the homing, quiescence, self-renewal, and lineage commitment of HSC. HSC= hematopoietic stem cells, MSC= mesenchymal stem cell; leptin-receptor expressing (LEPR+) perivascular cells, CXCL12-abundant reticular (CAR). Created with BioRender.com.

1.4 The role of the BM niche in AML

There is emerging evidence demonstrating that the BM niche is altered in AML and plays a key role in the maintenance and initiation of disease as well as chemoresistance. AML cells remodel their supportive microenvironment via ROS production, adaptability to hypoxia, altered cytokine secretion profile and reshaping the vascular niche into a leukemic niche (Galán-Díez et al., 2018; Ladikou et al., 2020; Yao et al., 2021). In addition, components of the BM niche have been shown to interact with leukemic cells, thereby affecting cellular functions including proliferation, differentiation, adhesion, quiescence, as well as trafficking and clonal expansion (Galán-Díez et al., 2018; O'Reilly et al., 2021; Yao et al., 2021).

In AML, the source of ROS has been shown to derive from the "NOX family" of NADPH oxidases (Brandes et al., 2014). ROS not only drives oncogenic signaling pathways through oxidation of critical cysteine residues, it also facilitates genomic instability by damaging DNA, which in turn promotes chemoresistance (Sillar et al., 2019). Indeed, the BM environment is hypoxic with oxygen tension below 10mmHg and has been addressed to play a critical role in HSC maintenance (Itkin et al., 2016; J. A. Spencer et al., 2014). The BM niche serves as a sanctuary for LSC, which reside in the most hypoxic tissue areas within this niche. In AML, it has been shown that hypoxia induced high constitutive levels of macrophage migration inhibitor factor (MIF) to promote survival and proliferation of AML cells *in vivo* through hypoxia-inducible factor (HIF)-1α signaling (Abdul-Aziz et al., 2018, 2017). It has been demonstrated that hypoxia activates the phosphatidylinositol-3-kinase (PI3K)/AKT and the mammalian target of rapamycin (mTOR) signaling pathway to provide environmental pro-survival support to leukemic cells. Hypoxia stabilizes HIFs which interact with the hypoxia responsive elements (HRE) of several genes, causing upregulated expression of the CXCR4/CXCL12 axis on AML cells and endothelial cells, thereby promoting LSC maintenance, quiescence and chemoresistance (Bruno et al., 2021; Deynoux et al., 2016).

It is further thought that pro-inflammatory cytokines play an important role in leukemogenesis, providing a selective advantage for LSC. In the bone marrow, neighboring stromal cells, normal hematopoietic cells and infiltrating immunocompetent cells secrete numerous cytokines, chemokines and adhesion molecules, which provide an important mechanism of protection (Ladikou et al., 2020). A wide variation of soluble factors have been implicated in this crosstalk, including CXCR2, CXCR4, IL6R, LFA, VLA4, RANK and FAT/CD36 (Shafat et al., 2017). Several of these cytokines can activate a plethora of oncogenic signaling pathways, including Wnt/β-catenin and PI3K/AKT/mTOR, which exert

an important role in regulating self-renewal of LSC (Annageldiyev et al., 2020; Ghosh and Kapur, 2016; Pepe et al., 2022; Wang et al., 2017, 2010). In addition, it has been thought that LSC escape apoptosis by upregulation of NF-κB activity (Bosman et al., 2016; Reikvam, 2020). According to a report by Bruserud *et al*, AML patients can be subclassified based on their constitutive cytokine release profile. Three chemokine clusters could be identified: CCL2-4/CXCL1/8, CCL5/CXCL9-11 and CCL13/17/22/24/CXCL5 (Bruserud et al., 2007). Another means of remodeling the BM niche involves the secretion of leukemia-protective exosomes from bone marrow stromal cells, regulated by fibroblast growth factor 2 (FGF2). It has been shown that exosomes remodel the endosteal niche to promote proliferation, invasion and chemoresistance of leukemia cells, whilst altering normal HSC function (Javidi-Sharifi et al., 2019; Kumar et al., 2018; Lyu et al., 2021).

1.5 Targeting AML LSC

Given the poor prognosis of AML and disappointing clinical outcomes due to a lack of efficacy with standard of care chemotherapy, there remains a pressing need to develop novel targeted therapies. Since AML LSC are often resistant to chemotherapy and are capable to sustain disease, eliminating LSC holds great therapeutic potential to reduce relapse rates and improve survival. Strategies to eradicate AML LSC can be classified in two categories: LSC-specific therapies and therapies that target both the bulk AML cell population as well as the LSC fraction. LSC-specific therapies are based on LSC-specific characteristics such as the immunophenotype, metabolic properties and epigenetic modulators, whereas strategies targeting also the bulk AML population are often directed towards targeting the leukemic-BM niche interactions (Bernasconi and Borsani, 2019; Houshmand et al., 2019; van Gils et al., 2021; Yao et al., 2021).

As previously discussed, LSC were initially enriched in the CD34+CD38− compartment, which is identical to HSC (Bonnet and Dick, 1997; Lapidot et al., 1994). Therefore, to specifically target LSC whilst sparing normal HSC, intensive research has been dedicated to define an LSC-specific immunophenotype (Haubner et al., 2019; Ivanivska et al., 2019; Mitchell and Steidl, 2020). A number of antigenic targets have been identified such as CD123, CD44, CD96, CCL-1, and TIM-3, some of which are currently under clinical investigation (Hosen et al., 2007; Jin et al., 2009, 2006; Kikushige et al., 2010, p. 3; van Rhenen et al., 2007). The main limitation of targeting aberrantly expressed LSC antigens is however the heterogeneity and plasticity in individual patients (Bachas et al., 2012; Ho et al., 2016; Li et al., 2016).

Besides immunophenotype, LSC can also be targeted based on their distinct metabolic features. As such, AML LSC are resistant to standard chemotherapy, take advantage of several molecular and metabolic mechanisms to maintain low ROS state, and preferentially rely on oxidative phosphorylation for the production of high-energy compounds (de Beauchamp et al., 2022). Hypoxia-induced HIF is considered to promote LSC maintenance, and combination of HIF inhibitors with chemotherapy targeting cycling cells is thought to disrupt quiescence and sensitize LSC to cytotoxic chemotherapy (Vukovic et al., 2015; Yao et al., 2021). This approach was however challenging in preclinical setting, which led to the discovery of hypoxia-activated prodrugs (HAP) as an alternative strategy to overcome hypoxia-induced resistance. HAPS, which activated by enzymatic reduction, are considered to be more selective than HIF inhibitors as they are designed to release cytotoxic agents only under hypoxic conditions (Benito et al., 2016). Further, it has been reported by Lagadinou *et al*. that ROS^{low} LSC aberrantly express B-cell lymphoma 2 (Bcl-2), and pharmacological inhibition of Bcl-2 reduced oxidative phosphorylation and selectively eradicated quiescent LSC (Lagadinou et al., 2013).

Other putative strategies to pharmacologically target LSC metabolic activity are directed towards inhibition of glutathione balance, NF-κB, proteasome activity, and HSP function. As mentioned before, oxidative phosphorylation plays an important role in the survival of AML LSC. Recent findings have demonstrated that amino acid metabolism fuels oxidative phosphorylation in LSC in in patients with de novo AML. In particular cysteine, which is metabolized exclusively to glutathione, appeared to be of importance for LSC survival (Forte et al., 2020; Jones et al., 2019; Pei et al., 2013). Impaired glutathione synthesis by cysteine depletion reduced electron transport chain (ETC) II activity, causing inhibition of oxidative phosphorylation and thereby selectively targeted LSC. Cytokine-stimulated NF-κB signaling is required for LSC maintenance, and was found to be constitutively activated in CD34+CD38- subpopulation, but not unstimulated normal CD34+ HSPC (Guzman et al., 2001; Kagoya et al., 2014; Zhou et al., 2018). Currently, NF-κB inhibitor bortezomib is under clinical investigation for the treatment of AML in combination with hypomethylating agent decitabine and/or multi-kinase inhibitor sorafenib (NCT01420926, NCT01861314, NCT01371981). In addition, it has been suggested that in AML both at the blast as well as the LSC level an active signalosome drives addiction of AML cells to a tumor-enriched Hsp90 species (teHsp90). More specifically, it was found that aberrant activation of Janus kinase (JAK)/signal transducer and activator of transcription (STAT) and PI3K/AKT/mTOR signaling pathways were maintained by teHsp90 (Zong et al., 2015).

Recent discoveries identified driver mutations in genes associated with epigenetic regulation. It is therefore not surprising that has been investigated whether LSC can be targeted specifically based on epigenetic modulators. Jung *et al.* demonstrated that the epigenetic signature of AML LSC is largely mutation independent and displays global hypomethylation compared with non-LSC blast cells, which were associated with transcriptional upregulation (Jung et al., 2015). Further, the DNA methylation signature of AML LSC identified 71 genes, which were enriched for members of the *HOX* cluster, and were shown to be prognostic of patient overall survival independent of other known risk factors. Transcriptional analysis of AML LSC additionally revealed a molecular signature underlying "stemness" and leukemia-initiating capacity, which was associated with clinical outcome of AML (Eppert et al., 2011; Ng et al., 2016). A number of approaches have been developed to target AML LSC based on epigenetic modulators including bromodomain and extra terminal protein (BET), DOT1L, enhancer of zeste homolog 2 (EZH2), and lysine-specific demethylase 1 (LSD1) (Bernt et al., 2011; Fong et al., 2015; Harris et al., 2012; Scott et al., 2016).

Finally, given the mounting evidence underscoring the importance of LSC-BM niche interplay in AML pathology, targeting the leukemic stem cell niche is considered a putative therapeutic strategy. Several classes of therapeutic agents have been identified to selectively target the BM-leukemic niche interactions, including strategies targeting angiogenic factor signaling pathways, cytokine secretion, adhesion molecules, and altered oncogenic signaling pathways.

Pro-angiogenic factors like vascular endothelial growth factor (VEGF) is secreted by stromal cells and leukemic cells and contributes to AML progression by promoting the production of nitric oxide, which consequently increases vascular permeability (Passaro et al., 2017). Further, VEGF was shown to protect leukemic cells from chemotherapy-induced apoptotic cell death by upregulation of Bcl-2/Bax ratios (Dias et al., 2002; Katoh et al., 1998). On the other hand, activation of the ANG1/Tie2 axis, which is closely associated with angiogenesis, is suggested to promote LSC quiescence and drug resistance (Arai et al., 2004). Although a number of anti-angiogenic agents have entered clinical trials, the outcomes for the treatment of AML were disappointing due to a lack of anti-leukemic efficacy (Karp et al., 2004; Ossenkoppele et al., 2012).

It has been demonstrated that leukemic cells express high levels of CXCR4 and upon binding of CXCL12 activates a plethora of downstream pro-survival and proliferative pathways such as JAK/STAT, PI3K/AKT/mTOR and MEK/extracellular signal-regulated

kinase (ERK). The CXCR4/CXCL12 axis additionally contributes to AML progression by promoting LSC homing and migration. The therapeutic value of targeting CXCR4 has been investigated and it was demonstrated that CXCR4 inhibition increased sensitivity to kinase inhibitors and chemotherapy in *FLT3*-ITD AML (Zeng et al., 2009). Plerixafor is a well-known potent CXCR4 antagonist that has shown promising results in Phase 1&2 studies in combination with chemotherapeutic agents and hypomethylating agents (Cooper et al., 2017; Roboz et al., 2018; Uy et al., 2012).

Other adhesion molecules highly expressed in AML LSC beside CXCR4 include Very Late Antigen-4 (VLA-4) and CD44 (discussed in section 1.2). VLA-4 interacts with fibronectin, intercellular adhesion molecule 2 (ICAM-2) and VCM-1 in the niche. Interaction of AML LSC with mesenchymal stromal cells, mediated by VCAM-1/VLA-4 axis promoted chemoresistance via stromal upregulation of the NF-κB pathway (Jacamo et al., 2014). Interaction of leukemic VLA-4 with stromal fibronectin additionally drove activation of the PI3K/AKT/Bcl-2 signaling axis to reduce drug-induced cytotoxicity (Nair-Gupta et al., 2020). Antibodies against VLA-4 together with cytarabine improved chemo-sensitivity of leukemic cells and hampered AML development in a patient-derived xenograft (PDX) mouse model (Jin et al., 2006; Layani-Bazar et al., 2014). There is currently one Phase 2 clinical study that investigates VCAM-1 inhibitor AS101 in untreated elderly patients (NCT01010373).

Another promising strategy to target AML LSC is focused on signaling pathways that are of particular importance for the proliferation, differentiation, self-renewal and survival of LSC (Carter et al., 2020; Gurska et al., 2019; Sands et al., 2013; Siveen et al., 2017). These have been briefly addressed and include the PI3K/AKT/mTOR, STAT, Wnt/β-catenin, Hedgehog, Notch, and the TGF-β pathways. Given that there is crosstalk between these pathways that may affect LSC function it is important to decipher these mechanisms of crosstalk in the context of LSC for understanding leukemogenesis and development of new targeted treatment paradigms.

Chapter 2: Introduction part B

In the previous chapter, the clinical importance of targeting AML LSC was highlighted. Targeting altered signaling pathways required to sustain LSC survival has been addressed as a putative therapeutic strategy for AML. An accruing body of scientific knowledge has recognized the PI3K/AKT/mTOR pathway, which is commonly deregulated in AML as a putative target to kill AML LSCs, but despite this, PI3K/AKT/mTORi have not translated into clinical practice.

In this chapter, the laboratory-based evidence of the critical role of PI3K/AKT/mTOR pathway in AML, and outcomes from current clinical studies using PI3K/AKT/mTORi is reviewed. Based on these results, the putative mechanisms of resistance to PI3K/AKT/mTORi are discussed, offering rationale for potential candidate combination therapies incorporating PI3K/AKT/mTORi for precision treatment in AML. This work has been published in the *Journal of Clinical Medicine*:
Darici S, Alkhaldi H, Horne G, Jørgensen HG, Marmiroli S, Huang X. Targeting PI3K/Akt/mTOR in AML: Rationale and Clinical Evidence. J Clin Med. 2020 Sep 11;9(9):2934. doi: 10.3390/jcm9092934. PMID: 32932888; PMCID: PMC7563273.

2.1 PI3K/AKT/mTOR pathway as a druggable target for AML

The PI3K/AKT/mTOR signaling pathway emerges as a promising therapeutic candidate to sensitize LSC to chemotherapy. It plays an important role in both normal and malignant hematopoiesis; components of this pathway govern the expression of genes and proteins essential for cell proliferation, differentiation, and survival. Constitutive activation of PI3K/AKT/mTOR pathway is detected in 50-80% of AML patients, associated with decreased overall survival (OS) (Bertacchini et al., 2014; Martelli et al., 2010; S. Park et al., 2010). One important mechanism leading to deregulation of PI3K/AKT/mTOR signaling is mutation of *FLT3* gene. Among them, FLT3-ITD is one of the most frequent mutations in normal karyotype AML (~25%). In recent clinical studies, few patients display prolonged remissions with RTKi such as FLT3i, highlighting the need for novel and/or partner targeted therapies (Daver et al., 2019; F. Zhou et al., 2019). Targeting the PI3K/AKT/mTOR pathway may be an option for FLT3-ITD AML patients.

Hyperactivation of PI3K/AKT/mTOR has also been associated with attenuated sensitivity to chemotherapy. Several studies have demonstrated that PI3K/AKT/mTOR inhibition may preferentially target LSC. For example, the PI3K/AKT/mTOR pathway may regulate LSC survival through NF- κB. The pro-inflammatory transcription factor NF- κB, has been found to be aberrantly activated in LSC, but is not expressed in normal human CD34+ progenitor cells (Guzman et al., 2002, 2001; Zhou et al., 2015). NF- κB is known to mediate chemoresistance by upregulation of anti-apoptotic genes which enable cells to increase proliferation and evade apoptosis (Jacamo et al., 2014; Li and Sethi, 2010; Zhou et al., 2018). Targeting NF- κB may be selective for LSC and/or sensitize LSC to chemotherapy. Notably, NF-κB is a downstream target of PI3K/AKT/mTOR, and this signaling cascade can trigger NF-κB activation, which suggests a common survival pathway for LSC. Treatment of AML patient samples with PI3Ki LY294002 displayed inhibited AKT phosphorylation and NF-κB DNA-binding activity (Birkenkamp et al., 2004).

Furthermore, PI3K/AKT/mTOR inhibition induced apoptosis in primary AML cells and potentiated response to cytotoxic chemotherapy, while sparing normal HSC function, (Bertacchini et al., 2018; Grandage et al., 2005; Xu et al., 2005, 2003). The LSC population was targeted by PI3K-directed therapies demonstrated by reduced engraftment ability of these cells in NOD/SCID mice (Xu et al., 2005, 2003). PI3K/AKT/mTORi may additionally potentiate LSC kill by synergizing with LSC-directed therapies. An essential feature of quiescent AML-LSC is that they have relative lower production of ROS compared with bulk cells (Lagadinou et al., 2013). These ROS-low LSC were shown to aberrantly overexpress Bcl-2, making them more susceptible to eradication by small-molecule Bcl-2i like venetoclax. The therapeutic potential of venetoclax could be enhanced by PI3K/AKT/mTOR inhibition through myeloid cell leukemia 1 (Mcl-1)-dependent mechanisms, which is a well-known determinant of resistance to venetoclax (Vachhani et al., 2014).

Growing evidence signposts PI3K as a druggable target for AML; indeed, there has been very productive development of small-molecule inhibitors targeting the PI3K/AKT/mTOR pathway. While PI3K/AKT/mTORi have been effective treating other hematological malignancies, such as CLL and follicular lymphoma (FL), in AML, the clinical potential of PI3K/AKT/mTORi has not yet been fully elucidated (Markham, 2017; Miller et al., 2015; Rodrigues et al., 2019). Clinical studies using PI3K/AKT/mTORi as monotherapy have shown limited therapeutic efficacy, likely due to compensatory activation of other survival pathways (Nepstad et al., 2020). Therefore, dissecting these relevant clinical findings and understanding how other signaling pathways impinge on PI3K/AKT/mTOR signaling pathway

activity, may provide us new clues as to how to effectively inhibit this pathway with potential candidate combination strategies to eradicate LSC and so cure AML.

2.2 The PI3K/AKT/mTOR signaling pathway

2.2.1 Regulation of the PI3K/AKT/mTOR pathway in normal hematopoiesis

The PI3K family consists of three distinct classes of PI3Ks (I-III), of which class I is implicated in regulation of hematopoiesis. Class I PI3K can be further divided into class IA and class IB enzymes, both of which are activated by cell surface receptors. Class IA PI3K can be activated by RTKs, G protein-coupled receptors (GPCR), and oncoproteins such as the small G protein Ras, whereas class IB PI3K can be activated by GPCRs only (Fruman and Rommel, 2014; Liu et al., 2009). Class IA PI3Ks form heterodimers between one of three catalytic subunits (p110α, p110β, or p110δ) and a regulatory adaptor molecule (p85α (or its splice variants p55α and p50α), p85β or p55γ) (Vadas et al., 2011; Vanhaesebroeck et al., 2010). Each pair shares some overlap whilst maintaining distinct function. In contrast to the heterogeneity of class IA, a single class IB isoform has been described that associates catalytic subunit p110γ with regulatory adaptor molecule p101 or p84 (Brock et al., 2003; Suire et al., 2005). While catalytic subunits p110α and p110β are consistently expressed in a broad range of tissues, p110γ and p110δ are specifically enriched within the hematopoietic system – preferentially in leukocytes (Kok et al., 2009).

In response to extracellular stimuli (e.g. hormones, growth factors and cytokines) and the subsequent activation of RTKs, class IA PI3K is recruited to the plasma membrane via interaction of p85 with adaptor proteins, such as insulin receptor substrate (IRS) 1/2 or growth factor receptor-bound protein 2 (GRB2)-associated binding protein 2 (GAB2) that bind to the regulatory p85 subunit of PI3K (Hemmings and Restuccia, 2012; Kiyatkin et al., 2006). The class IB p110γ is activated by GPCRs through direct interaction of its regulatory adaptor molecule with Gβγ subunit of trimeric G proteins (Brock et al., 2003). The activated p110 catalytic subunit facilitates the phosphorylation of phosphatidylinositol-4,5-phosphate (PIP_2) to generate phosphatidylinositol-3,4,5-phosphate (PIP_3). PIP_3 recruits phosphoinositide-dependent kinase 1 (PDK1) and AKT/protein kinase B (PKB) to the plasma membrane where PDK1 phosphorylates AKT at Threonine(T)308 residue within the

activation loop of the kinase domain to initiate the activation of AKT (Alessi et al., 1996, p. 1; Toker and Marmiroli, 2014) (Figure 2.1).

AKT is a highly conserved serine/threonine kinase that has multiple diverse functions. Full AKT activation, in addition to PDK1-mediated phosphorylation, requires phosphorylation at Serine(S)473 residue in the regulatory domain, by mTOR complex 2 (mTORC2), integrin-linked kinase (ILK), PDK1 or members of the PI3K-related kinase (PIKK) family, such as DNA-dependent protein kinase (DNA-PK) (Liao and Hung, 2010; Liu et al., 2014). Notably, AKT can activate mTORC2 through a positive feedback loop by direct phosphorylation of mTORC2 component mammalian stress-activated protein kinase interacting protein (mSin1) at T86 (Humphrey et al., 2013; Yang et al., 2015). Activated AKT can phosphorylate a wide spectrum of protein substrates, including forkhead box class O (FoxO), glycogen synthase kinase-3 (GSK3) α/β, and Bcl-2 associated agonist of cell death (BAD), maintaining cell cycling, survival, metabolism, cell growth and other essential cellular functions (Figure 2.2) (Manning and Toker, 2017).

Regulation of PI3K activity is negatively controlled by the tumor suppressor phosphatase and tensin homolog (PTEN) and Src homology domain-containing inositol phosphatase (SHIP) to maintain normal hematopoiesis. PTEN is a lipid phosphatase that hampers PI3K signaling through dephosphorylation of the lipid signaling intermediate PIP3 (Carracedo and Pandolfi, 2008). Loss of function of *PTEN* through mutations, genetic silencing, or epigenetic mechanism is implicated in the pathology of multiple human malignancies and can lead to aberrant PI3K/AKT/mTOR signaling (Milella et al., 2015). SHIP is predominantly expressed in hematopoietic cells and hydrolyzes PIP_3 to generate $PI(3,4)P_2$ (Hazen et al., 2009). Mutation of the *SHIP* gene was detected in a low percentage of AML and ALL patients (Luo et al., 2004).

One of the key downstream targets of the AKT is mTOR, which positively regulates cell growth and proliferation by promoting protein synthesis and inhibition of autophagy (Rabanal-Ruiz et al., 2017; Saxton and Sabatini, 2017). The identification of this serine/threonine kinase stems from the discovery of the natural product rapamycin, originally extracted from the soil bacterium *Streptomyces hygroscopicus* (S. R. Park et al., 2010). mTOR participates in two functionally distinct multiprotein complexes, mTORC1 and mTORC2, of which only mTORC1 is sensitive to inhibition by rapamycin (Gibbons et al., 2009). AKT indirectly activates mTORC1 by phosphorylation of tuberous sclerosis complex 2 (TSC2) at S939 and T1462 (Manning and Cantley, 2003; Potter et al., 2002). TSC2 functions with TSC1 forming a heterodimeric complex, which blocks the activation of Ras homolog

enriched in brain (Rheb). AKT phosphorylation of TSC2 inhibits the GTPase-activating protein (GAP) activity of this complex and in turn permits Rheb to activate mTORC1. AKT can also activate mTORC1 by a TSC2-independent mechanism, which involves phosphorylation of proline-rich AKT substrate 40kDa (PRAS40), a component of mTORC1. Phosphorylation of PRAS40 at T246 results in dissociation of PRAS40 from mTORC1 and attenuates the inhibitory effect of PRAS40 on mTORC1 activity (Kovacina et al., 2003). Upon activation, mTORC1 is phosphorylated on several residues (T2446, S2448, and S2481), but no function has been ascribed to any phosphorylation site (Cheng et al., 2004; Chiang and Abraham, 2005; Holz and Blenis, 2005). S1261 was identified as a site-specific phosphorylation site of mTORC1 that in response to insulin signals via the PI3K/TSC2/Rheb axis regulating mTORC1 function in an amino acid-dependent and rapamycin-insensitive mechanism.

The highly conserved protein kinase mTOR is a central hub of nutrient signaling and cell growth and integrates multiple intracellular signals (Kim and Guan, 2019). With respect to the mTOR signaling pathway, the TSC1/TSC2 complex has emerged as a sensor and integrator of multiple signaling pathways to modulate mTORC1 activity (Huang and Manning, 2008) (Figure 2.1). One important signaling pathway that negatively regulates mTORC1 activity is the liver kinase B1 (LKB1)/ AMP-activated protein kinase (AMPK) pathway (Huang et al., 2008). AMPK is a cellular energy sensor activated in various conditions that deplete cellular energy, such as nutrient deprivation or hypoxia (Dengler, 2020; Hardie, 2005). Phosphorylation of AMPK at T172 in the activation loop is required for its kinase activity and is mediated by LKB1, the upstream serine/threonine kinase of AMPK (Hawley et al., 1996). AMPK inhibits mTORC1 in two different ways i.e. phosphorylation of TSC2 at T1227 and S1345; and phosphorylation of Raptor at S722/792, which is a component of mTORC1 (Gwinn et al., 2008; Inoki et al., 2003). In addition to AMPK, ERK/p90 ribosomal S6 kinase (RSK) pathway also modulates mTORC1 activity. ERK/RSK is one of the other main signaling networks activated in parallel with PI3K by RTKs to control survival, differentiation, proliferation, and metabolism (Mendoza et al., 2011). Both ERK and RSK promote mTORC1 activity by phosphorylation of TSC2 at ERK S664 and S540, and RSK S1798 (Ma et al., 2005; Roux et al., 2004). In addition, ERK1/2 contributes to Ras-dependent activation of mTORC1 through phosphorylation of Raptor at S8, S696, and S863 (Carriere et al., 2011).

Upon activation, mTORC1 phosphorylates its main downstream targets eukaryotic initiation factor-4E (eIF4E) -binding protein 1 (4E-BP1) and rapamycin-sensitive ribosomal protein S6 kinase beta-1/p70 ribosomal S6 kinase (S6K1), involved in the translation of mRNAs. 4E-BP1 inhibits the initiation of cap-dependent translation by binding and inactivating eIF4E.

This binding is reversible, and mTORC1 phosphorylation of 4E-BP1 at T37/46 relieves 4E-BP1 from eIF4E (Gingras et al., 1999). Released eIF4E assembles at the 5' end of mRNA, which facilitates the recruitment of the ribosome and subsequent initiation of translation (Jackson et al., 2010).

S6K1 is the other main target of mTORC1 implicated in the regulation of cell growth. Activation of S6K1 requires phosphorylation at T229 and T389, of which T229 is phosphorylated by PDK1 and T389 by mTORC1 (Alessi et al., 1998; Han et al., 1995; Kim et al., 2002). Activated S6K1 activates 40S ribosomal protein S6 (rpS6) that represents the most extensively studied substrate of S6K1. rpS6 becomes phosphorylated on several serine residues (Ruvinsky and Meyuhas, 2006). While S6K1 phosphorylates rpS6 on all phosphorylation sites (S235/236 and S240/244), RSK phosphorylates rpS6 exclusively on S235/236 in an mTOR-independent mechanism, suggesting that ERK/RSK pathway contributes to rpS6 phosphorylation upon mitogen stimulation (Pende et al., 2004). mTORC1-stimulated S6K1 mediates an important negative feedback regulation of PI3K through phosphorylation of IRS-1. As such, S6K1 phosphorylates IRS-1 proteins at several serine residues (S270, S307, S636, and S1101) of which S270 was found to be required for S6K1/IRS-1 interaction and subsequent phosphorylation of the other S6K1-specific residues (Zhang et al., 2008). Phosphorylation of IRS-1 induces its protein degradation and insulin resistance, thereby inhibiting the insulin-like growth factor 1 (IGF-1) -mediated PI3K activation.

Regulated PI3K/AKT/mTOR signaling is critical for normal hematopoiesis, with deregulation of PI3K/AKT/mTOR activity linked to depletion of HSC pool (Kharas et al., 2010). For example, *Pten* deletion in adult mice HSC activated the PI3K/AKT/mTOR pathway, and promoted HSC proliferation and depletion through induced expression of $p16^{Ink4a}$ and p53, and leukemogenesis (Lee et al., 2010; Magee et al., 2012; Yilmaz et al., 2006). These effects were mostly mediated by mTOR as rapamycin was able to suppress leukemogenesis and restore normal HSC function (Lee et al., 2010). Myristoylated AKT1 (myr-AKT) was introduced into HSC via retroviral transduction of bone marrow cells and subsequent transplantation, to mimic constitutively active AKT, which is frequently observed in AML (Kharas et al., 2010). Results revealed that myr-AKT contributes to myeloproliferative disorders (MPD), and T-cell lymphoma with high frequency, and AML with a lower penetrance. HSC in the myr-AKT1 mice displayed transient expansion of immature myeloid cells in the bone marrow and spleen, and increased cycling, associated with impaired engraftment. The importance of mTOR signaling as a mediator of AKT was demonstrated with rapamycin. Rapamycin rescued cobblestone formation in myr-AKT–transduced bone

marrow cells *in vitro* and increased survival of myr-AKT mice. TSC1 is also potentially involved in leukemogenesis. Deletion of *TSC1* in HSC leads to activation of mTOR signaling, causes rapid HSC cycling and elevated levels of ROS, and impaired HSC self-renewal (Chen et al., 2008). Importantly, treatment with a ROS antagonist *in vivo* demonstrated that the TSC1/mTOR axis is important to maintain HSC quiescence and function by suppressing ROS. These findings indicate that mTOR is an important mediator of PI3K regulation in HSC. Furthermore, FoxO transcription factors are functionally redundant in HSC homeostasis through regulation of HSC response to physiologic oxidative stress, quiescence, and survival (Miyamoto et al., 2007; Tothova et al., 2007; Tothova and Gilliland, 2007). Mice engineered with conditional knockout alleles of *FoxO1*, *FoxO3*, and/or *FoxO4* displayed increased cell cycling and apoptosis of HSC, and a marked increase in ROS levels.

2.2.2 Constitutive PI3K/AKT/mTOR activation in AML

The PI3K/AKT/mTOR signaling pathway is frequently hyperactivated in AML cells, and potentially contributes to uncontrolled growth, proliferation, differentiation, metabolism, and survival (Fransecky et al., 2015; S. Park et al., 2010). The PI3K/AKT/mTOR pathway is also important for the regulation of the AML-LSC population, demonstrated in mouse models with genetic alterations of key PI3K/AKT/mTOR signaling genes. Rheb1 is overexpressed in AML patients which was associated with reduced survival in comparison to patients with lower Rheb1 expression (Gao et al., 2016; Ghosh et al., 2016; Ghosh and Kapur, 2017). Deletion of *Rheb1* induced apoptosis and enhanced cell cycle arrest in LSC, and prolonged survival of MLL-AF9-induced leukemic mice, suggesting that the mTORC1 pathway may be required for LSC maintenance (Gao et al., 2016). PDK1 is overexpressed in over 40% of AML patients and is required for AKT activation (Zabkiewicz et al., 2014). Deletion of *Pdk1* in MLL-AF9-induced mice resulted in a reduction of LSC and upregulated the expression of apoptosis inducers, such as *BAX* and *p53* (Pan et al., 2017; Peña-Blanco and García-Sáez, 2018). Mice transplanted with MLL-AF9-positive LSC were also shown dependent on S6K1 for LSC maintenance (Ghosh et al., 2016). Loss of S6K1 improved survival of MLL-AF9-induced leukemic mice, which was associated with reduced AKT and 4E-BP1 phosphorylation. Furthermore, the PI3K/AKT/mTOR pathway is also implemented in the crosstalk between LSC and the stromal cells associated with its niche that promotes the drug-resistant phenotype of LSC. Several reports have demonstrated that pharmacological inhibition of PI3K/AKT/mTOR signaling may effectively target leukemic cells within the bone marrow niche (Reikvam et al., 2013; Zeng et al., 2012; H.-S. Zhou et al., 2016).

Dysregulation of the PI3K/AKT/mTOR pathway is often the result of loss or inactivation of tumor suppressors, mutation or amplification of PI3K, as well as activation of RTKs or oncoproteins upstream of PI3K (Figure 2.3) (Stemke-Hale et al., 2008; J. Yang et al., 2019). About 50-80% of patients with AML display constitutive PI3K/AKT/mTOR activation and this was associated with significant poorer OS (Gallay et al., 2009). Poor prognosis in AML patients with constitutive PI3K/AKT/mTOR signaling could be related to the fact that this pathway is associated with chemoresistance, which contributes to the short-term survival in AML (Bertacchini et al., 2018; Min et al., 2003; Zhang et al., 2019). However, no correlation was shown to exist between PI3K/AKT/mTOR activity and a particular AML subtype, cytogenetic abnormality or etiology of the disease (Martelli et al., 2006; Nepstad et al., 2018).

Exploring mechanisms of constitutive PI3K/AKT/mTOR activation in AML identified mutations of RTKs (e.g. FLT3-ITD, c-KIT) or GTPases (KRAS, NRAS) as well as autocrine IGF-1/IGF-1R signaling responsible for dysregulation (Brandts et al., 2005; Chapuis et al., 2010a). Aberrant PI3K/AKT/mTOR signaling activation is often associated with enhanced AKT phosphorylation, mediated by phosphorylation at S473 by PDK1 and T308 by mTORC2. The OS of AML patients presenting with AKT phosphorylation at these sites was found to be significantly shorter in several studies (Gallay et al., 2009; Min et al., 2003). Furthermore, mTORC1 is activated in most AML patients, indicated by enhanced phosphorylation of its main downstream substrates 4E-BP1, S6K1, and rpS6 (Tamburini et al., 2009; Xu et al., 2005). However, activation of mTORC1 and its downstream target may also occur independently of PI3K/AKT though parallel signaling pathways (Chow et al., 2006; Qin et al., 2016; Tamburini et al., 2009). It is therefore important to dissect how PI3K/AKT/mTOR signaling converges with other signaling pathways, which may have clinical implications for selection of drugs targeting different signaling molecules.

About 30% of AML patients with normal karyotype present with an activating FLT3 receptor mutation, most often as FLT3-ITD, and is the major intercessory of PI3K/AKT/mTOR pathway dysregulation. FLT3 is a member of the class III RTK family and is important for the maintenance of hematopoietic homeostasis (Chu et al., 2012; Gilliland and Griffin, 2002; Kikushige et al., 2008, p. 3). FLT3-ITD exhibits ligand-independent constitutive tyrosine kinase activity and activates signaling pathways including PI3K/AKT/mTOR (Chen et al., 2010). However, regulatory p85 subunit of PI3K does not bind to the FLT3 receptor, nor is it tyrosine phosphorylated after FLT3 ligand stimulation. Instead, p85 associated with SH2 domain-containing protein tyrosine phosphatase-2 (SHP-2) and SHIP, in murine Ba/F3 cells stably transfected with human FLT3-ITD (Zhang and Broxmeyer, 1999, p. 100). FLT3-ITD

expression in Ba/F3 cells was associated with constitutive activation of AKT and concomitant phosphorylation of FoxO3a (Brandts et al., 2005; Scheijen et al., 2004). FoxO3a has an important role in apoptosis and cell cycle regulation (Zhang et al., 2011). FLT3-ITD was shown to constitutively activate AKT, and concomitantly phosphorylate FoxO3a, suppressing the expression of FoxO3a target genes *p27* and pro-apoptotic Bcl-2 family member, *Bim* (Brandts et al., 2005; Santo et al., 2013). FLT3-ITD negatively regulates FoxO3a, thereby suppressing FoxO3a-mediated apoptosis and bypassing the G1 cell cycle blockade.

2.2.3 Targeting the PI3K/AKT/mTOR signaling pathway in AML

Preclinical evidence underlines the significant role of PI3K/AKT/mTOR signaling in leukemia initiation and maintenance. There is considerable interest targeting PI3K/AKT/mTOR signaling for AML treatment, which has resulted into the rapid development of small molecule compounds that target either a single or multiple kinase (Figure 2.3). PI3K-targeting molecules can be divided into isoform-specific PI3Ki and ATP-competitive pan-PI3Ki.

The PI3K p110δ catalytic subunit is consistently expressed at a high level in AML blasts, making it an attractive therapeutic target for AML (Sujobert et al., 2005). Idelalisib (also referred to as CAL-101), for example, is a p110δ inhibitor that is currently under Phase 3 clinical investigation for the treatment of B-cell malignancies (Gopal and Graf, 2016). Treatment of AML cells with idelalisib inhibited ribosomal RNA (rRNA) synthesis and cell proliferation by suppressing AKT phosphorylation with a greater effect observed in cells expressing higher levels of p110δ (Nguyen et al., 2014).

Pan-PI3Ki target all isoforms of PI3K and may exert broader anti-leukemic effects, but at the expense of higher toxicity. mTORi include both ATP-pocket and allosteric mTOR binding drugs, e.g. rapalogs, such as everolimus and temsirolimus. Both drugs derive from the natural macrolide rapamycin and act by associating with immunophillin FK506 binding protein 12 (FKBP12), which in turn binds and inhibits mTORC1, although after lengthy exposure they inhibit also mTORC2 (Sabers et al., 1995). mTORi represent the first class of PI3K/AKT/mTOR-directed therapies and yielded promising anti-proliferative effects without inhibition of normal CD34+ cells in preclinical settings (Xu et al., 2003). The anti-leukemic effects were associated with reduced phosphorylation of S6K1 and 4E-BP1 and could be enhanced in combination with conventional cytotoxic drugs (Xu et al., 2005). An important drawback of inhibiting mTORC1 is the increased phosphorylation of AKT.

Dual PI3K and mTORi block both the upstream and downstream targets of AKT, thereby circumventing the increased PI3K and AKT signaling subsequent to mTORC1 inhibition (Carneiro et al., 2015). Dual PI3K/mTORi dactolisib efficiently blocked PI3K and mTORC1 signaling and mTORC2 activity (Chapuis et al., 2010b). Furthermore, dactolisib inhibited protein translation in AML cells, reducing cell growth and inducing apoptosis without affecting survival of normal CD34+ cells. A small number of AKTi have been developed, but they are rarely evaluated in preclinical or clinical settings as the development of AKTi has long been hampered by high structural similarity of the AKT catalytic domain to that of other kinases of the AGC kinase family (named after the representative protein kinase A, G, and C families) (Fransecky et al., 2015; Nitulescu et al., 2016).

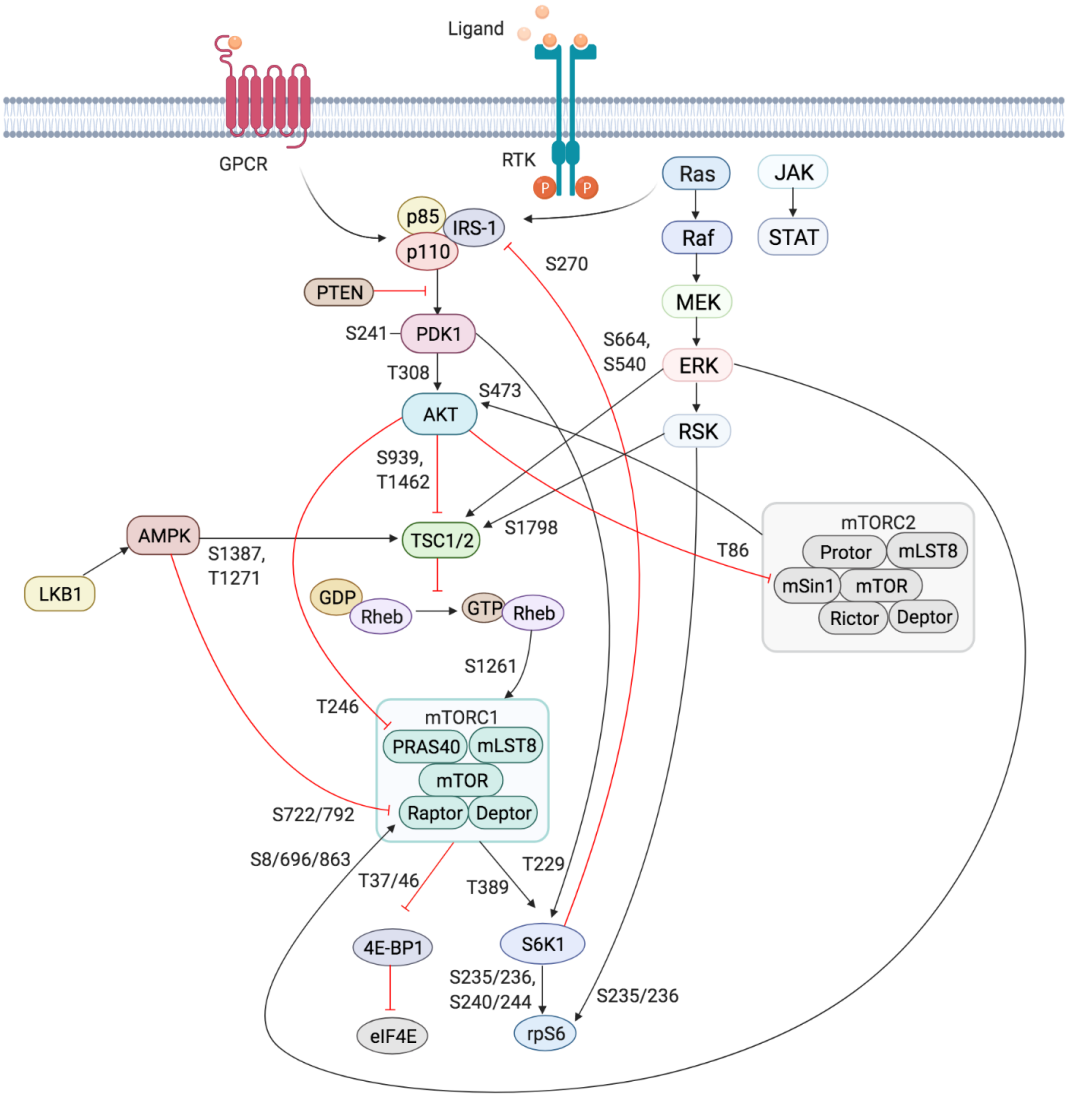

Figure 2.1 Schematic overview of the activation and regulation of the PI3K/AKT/mTOR signaling pathway

Activation of PI3K is stimulated by binding of an extracellular ligand (e.g. hormones, growth factors and cytokines) to a cell surface receptor such as the receptor tyrosine kinase (RTK) in the plasma membrane. Activated RTK recruits adaptor proteins which bind to the regulatory p85 subunit of PI3K

and subsequently activate the catalytic subunits for full PI3K activation. PI3K is also activated by G protein-coupled receptors (GPCR) or small GTPase Ras which bind PI3K directly. Activated PI3K catalyzes the phosphorylation of phosphatidylinositol-4,5-phosphate (PIP_2) to generate phosphatidylinositol-3,4,5-phosphate (PIP_3). PIP_3 recruits phosphoinositide-dependent kinase 1 (PDK1) and AKT to the plasma membrane inducing AKT phosphorylation by PDK1 at T308. AKT activation is completed by phosphorylation at S473 by mTOR complex 2 (mTORC2). The mTOR complex includes two distinct protein complexes, mTORC1 and mTORC2. mTORC1 comprises of mTOR, proline-rich AKT substrate 40 kDa (PRAS40), regulatory-associated protein of mTOR (Raptor), mammalian lethal with Sec13 protein 8 (mLST8, also known as GβL), and DEP-domain-containing mTOR-interacting protein (Deptor) (Laplante and Sabatini, 2009). mTORC2 comprises of mTOR, mLST8, Deptor, protein observed with Rictor-1 (Protor), rapamycin-insensitive companion of mTOR (Rictor), and mammalian stress-activated protein kinase interacting protein (mSin1) (Pearce et al., 2007). AKT indirectly activates mTORC1 by phosphorylation and inhibition of tuberous sclerosis complex 2 (TSC2) at S939 and T1462, releasing the inhibitory effects of this complex on Ras-related GTPase Rheb, an activator of mTORC1. AKT also directly controls activation of mTORC1 in a TSC2-independent manner via phosphorylation of PRAS40 at T246. The extracellular signal-regulated kinase (ERK)/90 kDa ribosomal S6 kinase (RSK) and liver kinase B1/AMP-activated protein kinase (LKB1/AMPK) signaling pathways impinge on several nodes of the PI3K/AKT/mTOR pathway and can modulate mTORC1 activity. Both ERK and RSK modulate mTORC1 activity by phosphorylation of TSC2 at S664 and S540 (ERK), and S1798 (RSK). ERK1/2 can also control mTORC1 activation by phosphorylation of Raptor at S8, S696, and S863. Master metabolic regulator AMPK inhibits mTORC1 activity in two different pathways, the first by phosphorylation of TSC2 at T1271 and S1387; and the second by phosphorylation of Raptor at S722 and S792. Activated mTORC1 promotes cap-dependent mRNA translation via phosphorylation of eukaryotic translation initiation factor 4E (eIF4E)-binding protein 1 (4E-BP1) at T37 and T46, which is a priming event required for subsequent phosphorylation of several carboxy-terminal serum-sensitive sites to release 4E-BP1 from eIF4E. Ribosomal protein S6 kinase beta-1 (S6K1) is a downstream target of mTORC1, activated by phosphorylation at T389 by mTORC1 as well as T229 phosphorylation mediated by PDK1. S6K1 in turn activates ribosomal protein S6 (rpS6), which is dispensable for cell growth and protein synthesis. RSK can also directly activate rpS6 via phosphorylation at S235 and S236. The black arrows represent positive regulation (activation), whereas the red blunt-ended lines indicate negative regulation (inhibition). IRS-1= insulin receptor substrate 1, PTEN= phosphatase and tensin homolog, GDP= guanosine diphosphate, GTP= guanosine triphosphate, JAK= Janus kinase, STAT= signal transducer and activator of transcription. Created with BioRender.com.

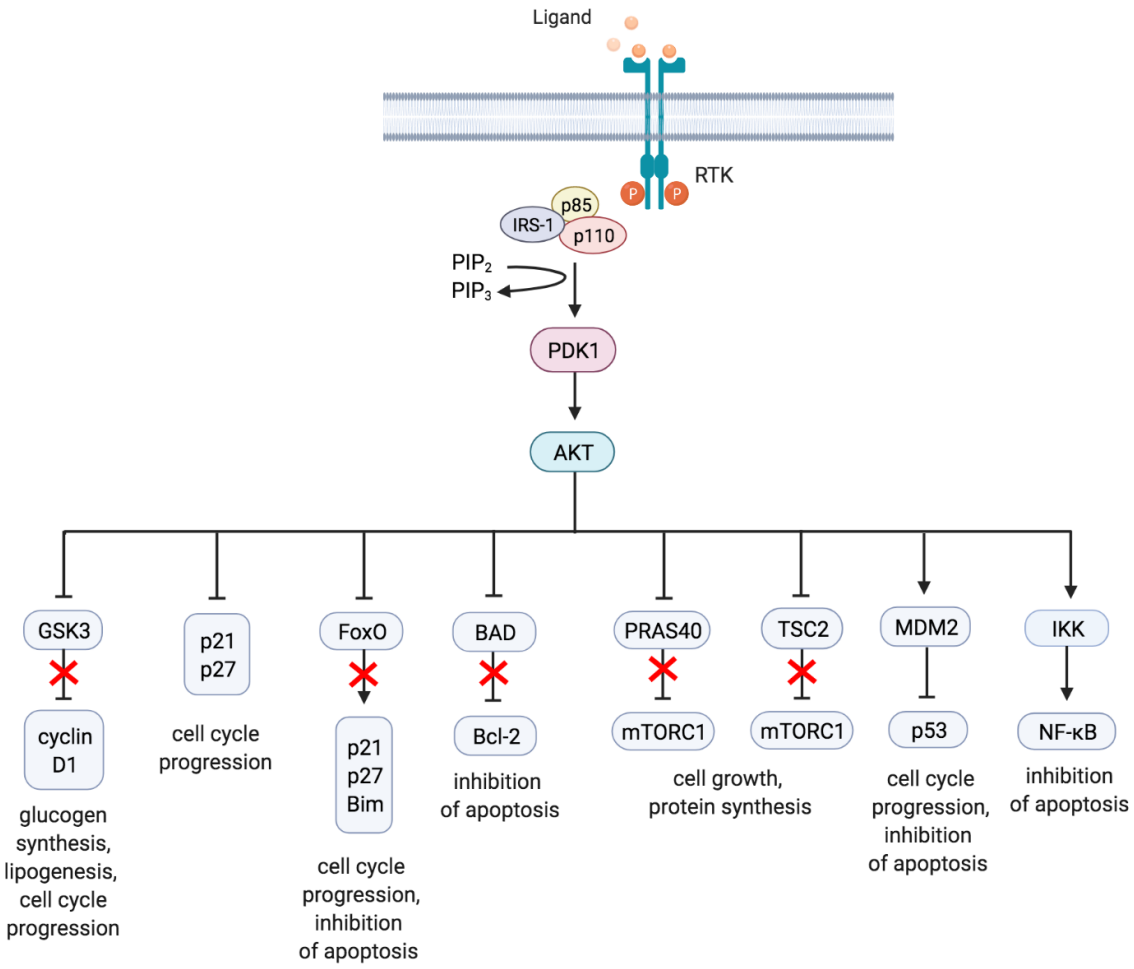

Figure 2.2 A summary diagram of AKT downstream target molecules

Fully activated AKT controls numerous effectors implicated in cell growth, proliferation, differentiation, metabolism, and survival, of which some are highlighted. AKT regulates G1/S cell cycle progression by phosphorylation and inactivation of GSK3/cyclin D1, p21 and p27. AKT controls apoptosis by phosphorylation and inhibition of pro-apoptotic Bcl-2 family members BAD and FoxO. AKT can inhibit apoptosis and promote cell survival by activating NF-κB. AKT was found to regulate cell metabolism by mediating lipogenesis and glucose uptake through phosphorylation and inhibition of GSK3, which inhibits glycogen synthesis. AKT promotes cell growth by activation of mTORC1 though phosphorylation of PRAS40, which prevents its inhibition of mTORC1. AKT can also induce mTORC1 activation through phosphorylation and inhibition of TSC2, relieving the inhibitory effects of the TSC1/TSC2 complex on mTORC1. The arrows represent positive regulation (induction/activation), whereas the blunt-ended lines indicate negative regulation (inhibition/inactivation). RTK= receptor tyrosine kinase, IRS-1= insulin receptor substrate 1, PIP_2= phosphatidylinositol-4,5-phosphate, PIP_3= phosphatidylinositol-3,4,5-phosphate, PDK1= phosphoinositide-dependent kinase-1, MDM2= mouse double minute 2 homolog, GSK3= glycogen synthase kinase 3, TSC2= tuberous sclerosis complex 2, mTORC1= mTOR complex 1, FoxO= forkhead box O, Bim= Bcl-2-like protein 11, BAD= BCL-2 associated agonist of cell death, Bcl-2= B-cell lymphoma 2, IKK= IκB kinase, NF-κB= nuclear factor kappa-light-chain-enhancer of activated B cells. Created with BioRender.com.

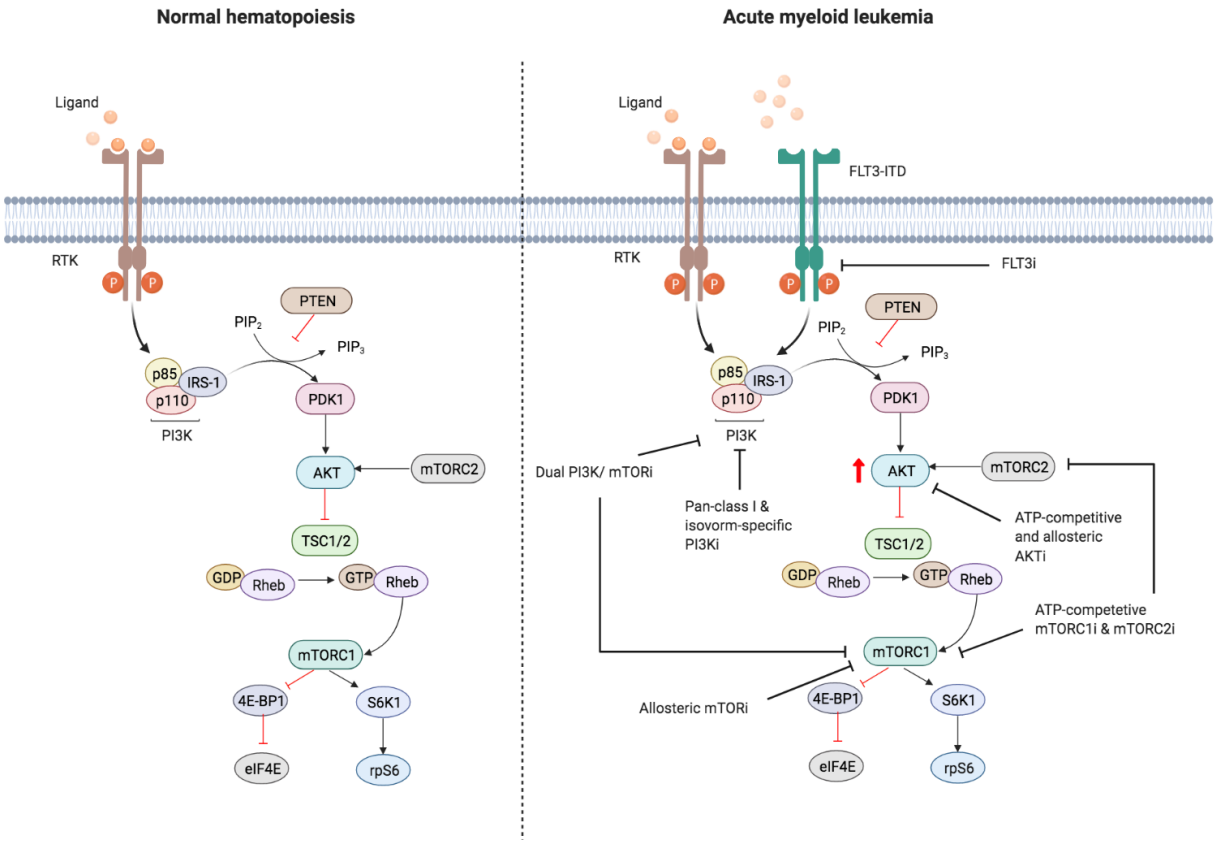

Figure 2.3 Targeting the PI3K/AKT/mTOR pathway in AML

The PI3K/AKT/mTOR pathway is commonly dysregulated in AML caused by mutations in membrane-bound proteins such as receptor tyrosine kinases (RTKs) and small GTPase Ras. Activating mutations in fms-like tyrosine kinase 3 (FLT3), such as the FLT3-internal tandem duplication (FLT3-ITD), are an important mechanism leading to dysregulation of PI3K/AKT/mTOR signaling. The ITD mutation causes ligand-independent activation of the FLT3 receptor, leading to constitutive activation of the PI3K/AKT/mTOR pathway. Numerous small-molecule inhibitors of this pathway include FLT3 inhibitors (FLT3i), dual PI3K/mTORi, allosteric mTORi, pan-class I and isoform-specific PI3Ki, ATP-competitive and allosteric AKTi, and ATP-competitive mTOR complex 1 (mTORC1) and mTOR complex 2 (mTORC2) inhibitors. The red arrow indicates elevated AKT phosphorylation, whereas the red blunt-ended lines represent negative regulation (inhibition). IRS-1= insulin receptor substrate 1, PIP_2= phosphatidylinositol-4,5-phosphate, PIP_3= phosphatidylinositol-3,4,5-phosphate, PTEN= phosphatase and tensin homolog, PDK1= phosphoinositide-dependent kinase-1, TSC 1/2= tuberous sclerosis complex 1/2, ATP= adenosine triphosphate, GDP= guanosine diphosphate, GTP= guanosine triphosphate, Rheb= Ras homolog enriched in brain, 4E-BP1= eukaryotic translation initiation factor 4E (eIF4E)-binding protein 1, S6K1= ribosomal protein S6 kinase beta-1, rpS6= ribosomal protein S6. The black blunt-ended lines indicate the main targets for therapeutic intervention. Created with BioRender.com.

2.3 Crosstalk of the PI3K/AKT/mTOR signaling pathway with other signaling pathways in AML

We have demonstrated the complexity of the PI3K/AKT/mTOR signaling pathway resulting from several feedback loops and crosstalk with other signaling pathways that are able to modulate PI3K/AKT/mTOR signaling. In this section we will particularly focus on FLT3-ITD AML, which is the major driver of dysregulation of PI3K/AKT/mTOR signaling. FLT3-ITD has been shown to induce, in addition to PI3K/AKT/mTOR, other downstream effectors, including MEK/ERK/RSK1 and JAK/STAT pathways, FoxO3a phosphorylation, and ROS production (Hayakawa et al., 2000; Sallmyr et al., 2008a, 2008b). These effectors interact with the PI3K/AKT/mTOR pathway, elucidation of which may reveal possible mechanisms of resistance to PI3K-directed therapies. Recent studies have stressed that FLT3-ITD induces genomic instability through ROS production, which potentially contributes to chemoresistance leading to disease relapse (Ng et al., 2019; Rebechi and Pratz, 2017). The PI3K/AKT/mTOR signaling pathway is linked to both ROS production and the DNA damage response (DDR) pathway, strengthening the premise of further exploiting this pathway as a potential therapeutic target (Juvekar et al., 2016; Liu et al., 2014; Shen et al., 2007).

The Ras/Raf/MEK/ERK and PI3K/AKT/mTOR signaling pathways strongly regulate each other and share overlapping downstream effectors to regulate multiple cellular functions. Several mechanism of integration of these two pathways have been identified, including negative feedback loops, cross-inhibition, cross-activation, and pathway convergence, which have been described in the previous section (Mendoza et al., 2011). Briefly, the Ras/ERK pathway cross-activates PI3K/AKT/mTOR signaling by regulating PI3K, TSC2, and mTORC1. Ras-GTP can directly bind and allosterically activate PI3K (Kodaki et al., 1994). Activated Ras/ERK pathway can positively regulate mTORC1 activity indirectly through phosphorylation of TSC2 or directly through PI3K-independent phosphorylation of proline-directed residues within Raptor (Carriere et al., 2011; Ma et al., 2005; Roux et al., 2004). Furthermore, Ras/ERK and PI3K/AKT/mTOR pathways co-regulate downstream effectors, including FoxO and c-Myc transcription factors, BAD, and GSK3 (Ding et al., 2005; McCubrey et al., 2016; She et al., 2005; Yang et al., 2008; Zhu et al., 2008).

The JAK/STAT pathway is a core oncogenic signaling pathway activated by a plethora of cytokines and hormones, and has a critical role in hematopoietic malignancies (Vainchenker and Constantinescu, 2013). Deregulation of the JAK/STAT pathway, in particular STAT5, is frequently reported in AML and is indispensable for leukemia cell maintenance and survival

(Birkenkamp et al., 2001; Wingelhofer et al., 2018). Persistent STAT5 activity is driven by oncogenic FLT3-ITD independent of JAKs and is associated with resistance to PI3K/AKT/mTORi (Britschgi et al., 2012; Choudhary et al., 2007; Spiekermann et al., 2003). This resistance mechanism involved the increased expression of PIM kinases. PIM kinases are oncogenic serine/threonine kinases overexpressed in several malignancies that promote cellular functions, including cell cycle progression, proliferation, survival, and drug resistance (Green et al., 2015; Keane et al., 2015). PIM-1 is transcriptionally upregulated by constitutively active FLT3 and contributes to FLT3-ITD-mediated survival (Kim et al., 2005). Furthermore, PIM-1 phosphorylates and stabilizes FLT3, promoting FLT3 signaling in a positive feedback loop (Natarajan et al., 2013). It has been reported that PIM kinases are expressed downstream of STAT5 activation in FLT3-ITD AML and are implicated in the regulation of mTORC1 to promote cap-dependent translation in parallel with the PI3K/AKT pathway (Aziz et al., 2018; Zhang et al., 2009, p. 40). PIM and AKT share common substrates of the apoptosis machinery and cellular metabolism which may account for PIM kinases' ability to act as a resistance mechanism (Amaravadi and Thompson, 2005). For instance, it has been reported that PIM-1 elevates RTKs upon inhibition of AKT, leading to drug resistance (Cen et al., 2013; Song et al., 2016). Upregulation of PIM-1 mediated by FLT3-ITD enhanced survival through protection of the mTOR/4E-BP1/Mcl-1 pathway, which was abrogated by inhibition of the STAT5/PIM kinase axis (Nogami et al., 2015, 2019; Okada et al., 2018; Watanabe et al., 2019; Yoshimoto et al., 2009a, p. 1).

Both PI3K/AKT and STAT5 signaling converge to control ROS production, which is induced by FLT3-ITD. ROS are a heterogeneous group of molecules and radicals primarily produced in the ETC of the mitochondria, in particular from Complex I and III (Bleier and Dröse, 2013; Maranzana et al., 2013). ROS have a critical role in the regulation of normal hematopoiesis and is commonly elevated in a wide range of human cancers, including AML (Sillar et al., 2019; Tong et al., 2015). Activating mutations of FLT3 has been shown to increase ROS production, causing DNA damage and affecting the DDR. The DNA damage is repaired by error-prone alternative non-homologous end-joining (alt-NHEJ) pathway, which promotes genomic instability and leukemogenesis (Sallmyr et al., 2008a). Elevated ROS in FLT3-ITD AML is attributable to constitutive activation of nicotinamide adenine dinucleotide phosphate oxidases (NOX). (Hole et al., 2013; Jayavelu et al., 2016; Stanicka et al., 2015). Another proposed mechanism of FLT3-ITD-driven ROS production involves interaction of STAT5 with RAC1, a small GTPase protein which is an essential component of NADPH oxidase (Mi et al., 2018, p. 5; Sallmyr et al., 2008a). Interestingly, ROS can increase phosphorylation of STAT5 via JAK, which acts as a feed-forward loop (Mi et al., 2018, p. 5). It was

demonstrated that inhibition of FLT3-ITD not only decreased tyrosine phosphorylation of STAT5 but also reduced RAC1 activity and its binding to NOX (Bourgeais et al., 2013).

Aberrant PI3K/AKT/mTOR signaling drives ROS production through different molecular mechanisms, including the activation of NOXs (Chatterjee et al., 2012; Koundouros and Poulogiannis, 2018; Moloney et al., 2017). Wortmannin (inhibitor for PI3Ks and PI3K-related enzymes) treatment or *AKT1* knockout, impaired translocation of NOX subunits and reduced production of ROS (Chatterjee et al., 2012; Nakanishi et al., 2014). The PI3K/AKT/mTOR pathway is also involved in the regulation of the gene expression of endogenous antioxidant synthesis. ROS production is tightly regulated by the redox-sensitive signaling system Kelch-like ECH-associated protein 1 (Keap1)/ nuclear factor erythroid 2-related factor 2 (Nrf2)/ antioxidant response elements (ARE). Under physiological conditions, Nrf2 is sequestered in the cytosol via its association with Keap1. When ROS levels increase, the Nrf2 dissociates from Keap1 and enters the nucleus where it forms a heterodimer with a small musculoaponeurotic fibrosarcoma (MAF) protein to activate ARE-dependent gene expression of antioxidative proteins (Bellezza et al., 2018; Zimta et al., 2019). The PI3K/AKT/mTOR signaling pathway contributes to Nrf2-mediated regulation of antioxidative proteins as the nuclear translocation of Nrf2 requires PI3K activation (Nakaso et al., 2003). PI3K inhibition using wortmannin and LY294002 was shown to inhibit Nrf2 activity (Wang et al., 2008). As FLT3-ITD induces phosphorylation of FoxO3a (which requires the presence of AKT phosphorylation sites), it seems apparent that FLT3-ITD promotes ROS production at least in part through dysregulation of the PI3K/AKT/mTOR pathway (Jayavelu et al., 2016; Moloney et al., 2017). Paradoxically, excessive ROS production can promote activation of PI3K/AKT/mTOR signaling through oxidative inhibition of PTEN, causing an increase in cellular PIP_3 levels and activation of AKT (Koundouros and Poulogiannis, 2018; Leslie et al., 2003; Vazquez et al., 2001).

2.4 Clinical implications of PI3K/AKT/mTORi in AML

There is considerable interest in small-molecule drugs targeting the PI3K/AKT/mTOR pathway, of which some have been approved by the United States Food and Drug Administration (FDA) for several human cancers (Table 2.1). However, despite extensive pre-clinical and clinical research of these drugs either as a monotherapy or in conjunction with conventional cytotoxic chemotherapeutics, they have not yet been successfully translated into clinical practice for the treatment of AML. Here we review PI3K/AKT/mTORi

subjected to clinical evaluation for AML therapy, summarized in Tables 2.1 and 2.2. The response criteria for AML are summarized in Table 2.3.

Buparlisib

Buparlisib (BKM120; NVP-BKM120) is a highly selective pan-PI3Ki that has shown promising activity against solid tumors as well as lymphoid malignancies. Buparlisib binds to all class IA p110 catalytic subunits and inhibits PI3K in an ATP-competitive manner (Burger et al., 2011; Maira et al., 2012). Several reports have demonstrated that buparlisib inhibits cell proliferation, diminishes metabolic activity, and exerts cytotoxic effects on solid tumors and hematological malignancies, including AML, by selective inhibition of AKT activity (Allegretti et al., 2015; Jin et al., 2017, p. 120; Yang et al., 2018, p. 120, 2017). The mechanism by which buparlisib impaired viability was associated with the induction of p21-mediated G2/M cell cycle arrest and reduced expression of NF-κB anti-apoptotic proteins (Sadeghi et al., 2020). In AML, buparlisib showed *in vivo* effectiveness in, and prolonged survival of, xenotransplant mouse models (Allegretti et al., 2015). In addition, it has been demonstrated that combination with other small-molecule drugs, such as the glycolitic modulator dichloroacetate (DCA), proteasome inhibitor bortezomib, and c-Myc inhibitor 10058-F4, profoundly enhanced the cytotoxic effect of buparlisib in AML cell lines and/or primary samples (Allegretti et al., 2015; Sadeghi et al., 2020).

Buparlisib was clinically evaluated by Ragon *et al*. in an open label, non-randomized Phase 1 dose escalation study in patients with relapsed/refractory AML (n=12), ALL (n=1) or mixed phenotype acute leukemia (MPAL) (n=1) (Ragon et al., 2017). In the AML population, cytogenetic analysis detected diploid karyotype (n=4), inversion 3 or 3q26 (n=3), and other cytogenic alterations (n=5). Molecular analysis revealed isocitrate dehydrogenase (IDH) and RAS mutation (n=2), FLT3 D835 mutation (n=1), NRAS mutation (n=1), KRAS and NRAS mutation (n=1), tumor protein 53 (TP53) mutation (n=1), and NPM1, NRAS, IDH1, DNA methyltransferase 3A (DNMT3A) mutation (n=1). Three patients experienced clinically significant confusion, supported by earlier studies reporting that buparlisib crosses the blood-brain barrier, and can cause neurotoxicity. Protein profiling by western blot revealed that buparlisib was able to block PI3K/AKT/mTOR signaling, observed by decreased p-S6K1 and p-FoxO3a, and reverse phase protein array (RPPA) analysis showed significant downregulation of PRAS40. However, direct inhibition of PI3K led to AKT induction, pointing towards a compensatory feedback mechanism. These findings confirm that buparlisib can effectively inhibit and target the downstream PI3K/AKT/mTOR pathway, but such biological suppression did not translate into an improved clinical response in this patient population. Overall, only one patient (with inversion 3) had stable disease receiving maximum tolerated dose of BKM120 for a period of 82 days. Notably, three patients (21.4%) with 3q26

abnormalities had the longest OS. As patients carrying 3q26 gene rearrangements present with up-regulation of PI3K/AKT/mTOR signaling and here displayed significantly improved OS, patients with 3q26 aberrations may be more sensitive to pan PI3Ki.

Gedatolisib

Gedatolisib (PF-05212384; PKI-587) is a highly potent, selective and ATP-competitive dual inhibitor of PI3Kα, PIK3γ and mTOR for clinical development (Venkatesan et al., 2010). *In vivo*, gedatolisib has demonstrated antitumor activity in solid tumor xenograft models and has been clinically evaluated in patients with advanced cancers (Del Campo et al., 2016; Iezzi et al., 2016; Langdon et al., 2019; Mallon et al., 2011; Wainberg et al., 2017). Gedatolisib was able to inhibit cell viability in solid tumor models and effectively targeted and inhibited PI3K/AKT/mTOR signaling measured by decreased p-AKT and p-rpS6 expression (Langdon et al., 2019; Mallon et al., 2011). However, many cells were resistant following gedatolisib treatment, which was attributed to over-activation of the MEK/ERK pathway through suppression of mTORC2 (Shah et al., 2018; Soares et al., 2015).

The clinical activity and tolerance of gedatolisib for AML therapy was evaluated in an open, prospective, single arm, multicentric Phase 2 study published by Vargaftig *et al* (Vargaftig et al., 2018). Twelve patients were enrolled of which 10 were retained for analysis. All patients were adults diagnosed with relapsed AML (first relapse [n=5], second relapse [n=5]) and symptomatic uncontrolled AML. One patient had therapy-related AML (prostate adenocarcinoma). Overall, only one patient completed the treatment, and this study was terminated as no objective response was detected in any of the patients. Transcriptomic analysis revealed that gedatolisib treatment weakly affected gene expression pattern, of which four genes found to be upregulated were associated with natural killer (NK) cell immunity. This suggests that gedatolisib might affect immune cells. Current research is focusing on understanding mechanisms of resistance to gedatolisib in solid tumors.

Dactolisib

Dactolisib (BEZ235; NVP-BEZ235) is a dual ATP-competitive pan-class PI3K and mTORi that has been clinically evaluated alone or in combination therapy in Phase 1/2 studies in solid tumors and hematological malignancies (Carlo et al., 2016; Pongas and Fojo, 2016; Salazar et al., 2018). Several reports have demonstrated that dactolisib exerts anti-proliferative and cytotoxic effects *in vitro*. Dactolisib was also shown to induce autophagy and enhance chemosensitivity (Huang et al., 2018; Ma et al., 2019; Mitchell et al., 2018). In AML, dactolisib showed similar biological effects *in vitro* and inhibited the colony-forming capability of LSC (Deng et al., 2017; Gao et al., 2013). Results obtained from clinical

investigation of dactolisib for advanced cancers reported frequent dose-limiting toxicities accounting for adverse effects. Several Phase 2 studies reported poor tolerance of dactolisib with only modest clinical activity, which led to treatment discontinuation (Carlo et al., 2016; Salazar et al., 2018).

A Phase 1 study by Wunderle *et al*. evaluated the safety and efficacy of BEZ235 among 22 patients with relapsed or refractory AML (n=11), B-cell precursor ALL (n=9), T-cell ALL (n=1), and CML in myeloid blast phase (n=9). Clinical responses were observed in four patients (18.2%): complete hematological and molecular remission or hematological improvement in three ALL patients and stable disease of four months in one AML patient. Notably, no activating mutations of PIK3CA, PTEN or AKT were detected in any of the patients [108]. Detection of p-AKT, p-S6 and p-4E-BP1 by western blot and flow cytometry did not correlate with response. Similar to previous clinical findings, dactolisib induced adverse effects such as gastrointestinal implications, pneumonia, and sepsis. Due to disease progression, 19 patients (86.4%) were withdrawn from the study (Wunderle et al., 2013). Together, these data raise the question whether inhibiting both PI3K and mTOR is a viable therapeutic strategy and whether we can do better.

MK-2206

MK-2206 is a highly specific allosteric pan-AKTi for all three isoforms of human AKT that has entered clinical trials for solid tumors as well as hematological malignancies. *In vitro*, MK-2206 induced apoptosis and enhanced the cytotoxicity of chemotherapy (Lu et al., 2015). Although it was reported that MK-2206 effectively suppressed phosphorylation of AKT, MK-2206 monotherapy showed limited clinical activity, due to incomplete target inhibition at tolerable doses, paving the way for combination strategies (Akcakanat and Meric-Bernstam, 2018; Ma et al., 2017, p. 2206; Xing et al., 2019, p. 2206).

A Phase 2 study by Konopleva *et al*. evaluated the clinical efficacy and tolerability of MK-2206 in 19 patients, of which 18 were retained for analysis (Konopleva et al., 2014). All patients were adults with relapsed/refractory AML requiring second salvage therapy. No activating mutations of upstream RTK were detected. In preclinical studies MK-2206 inhibited cell growth and induced apoptosis in AML cell lines and primary samples. In clinical studies, among 18 evaluable patients, only one patient (5.6%) achieved CR with incomplete platelet count recovery. The remaining 17 patients (94.4%) were withdrawn from the study due to disease progression. Proteomic analysis by RPPA following MK-2206 treatment revealed upregulation of a subset of pro-survival proteins, suggesting that other approaches to block AKT signaling should be exploited for AML.

Afuresertib

Afuresertib (GSK21110183) is a reversible, ATP-competitive pan-AKTi that has entered clinical trials, both as monotherapy and combination with other agents, for solid tumors and multiple myeloma (MM) (Blagden et al., 2019; Naymagon and Abdul-Hay, 2016; Tolcher et al., 2015). *In vitro*, afuresertib induced apoptosis and G1 phase arrest, and effectively suppressed phosphorylation of multiple AKT substrates, including FoxO1, GSK3β, mTOR, and p70. Spencer *et al*. evaluated the maximum tolerated dose (MTD), safety, pharmacokinetics and clinical activity of afuresertib in an open-label Phase 1 study for advanced hematological malignancies (A. Spencer et al., 2014). A total of 73 patents were included with MM (n=34), non-Hodgkin lymphoma (NHL) (n=13), AML (n=9), Hodgkin disease (n=8), CLL (n=7), ALL (n=1), and Langerhan's cell histiocytosis (n=1). Among the 73 patients, 26 were evaluated for the dose escalation (part 1) and 47 patients in the expansion cohort (part 2). Disease inclusion criteria for part 2 were CLL, CML, ALL, AML, MM, or NHL. Clinical activity was observed primarily in MM patients and in patients with lymphomas. Overall, three patients (9%) achieved partial remission (PR), three patients (9%) achieved minimal response (MR), and some patients achieved prolonged disease stabilization. Among the nine AML patients, treatment failure was observed in five patients and the other four did not have response assessed. Afuresertib was safe and generally well tolerated but effects related to the gastrointestinal tract or fatigue were noted, suggesting that AKT inhibition with afuresertib may prove beneficial for the treatment of MM.

Sirolimus

Sirolimus, also known as rapamycin, is a naturally occurring macrolide compound that interacts with FKBP12. This complex binds to the FKBP rapamycin-binding (FRB) domain located in the carboxyl terminus of mTOR and inhibits its kinase activity. *In vitro*, sirolimus inhibits cancer cell growth, promotes G1 cell cycle arrest, and enhances cytotoxic effects in combination with other agents (Imrali et al., 2016; Wagner et al., 2012; Yao et al., 2011; Y. Zhou et al., 2016). Sirolimus is clinically often used in renal transplantations and for the treatment of a rare lung disease called lymphangioleiomyomatosis (LAM), but has also been investigated for the treatment of solid tumors and hematological malignancies (Colon-Otero et al., 2017; Grignani et al., 2015; Kolos et al., 2018; Roskoski, 2019; A. X. Zhu et al., 2011).

Kasner *et al*. evaluated the clinical potential of sirolimus for AML therapy in two sequential clinical trials in identical patient populations (NCT00780104 and NCT01184898). In total, 52 patients were enrolled, with 51 undergoing clinical evaluation. Among the 51 patients clinically evaluated, the majority had abnormal cytogenetics (56%) and FLT3-ITD was

detected in seven patients (14%). The pilot study provided evidence that intracellular flow cytometry can be applied to monitor the biochemical efficacy of drugs targeting the PI3K/AKT/mTOR signaling pathway. Results revealed heterogeneity of rpS6 phosphorylation among particular patient populations, suggesting that evaluation of drug sensitivity *ex vivo* or in early therapy may prove useful in predicting response to molecular targeted therapies (Kasner et al., 2011; Perl et al., 2012). In the final clinical and pharmacodynamics study, the clinical response of sirolimus in combination with mitoxantrone/etoposide/cytarabine (MEC) chemotherapy in a larger study cohort was evaluated. Overall, 24 patients responded (47%) with 18 CR (35%), one CRp, and five PRs. Sirolimus combination with MEC was tolerable in patients with high risk AML, however the combination therapy did not enhance clinical responses in AML and was limited to patients presenting with baseline mTORC1 activation as measured by baseline rpS6 phosphorylation. (Kasner et al., 2018; Perl et al., 2009).

Everolimus

Everolimus (RAD001), a derivative of rapamycin, is an allosteric inhibitor of mTORC1 showing promise for several cancer types. Everolimus was granted FDA approval for progressive, well-differentiated non-functional, neuroendocrine tumors of gastrointestinal or lung origin with unresectable, locally advanced or metastatic disease (Hasskarl, 2018). Everolimus interacts with FKBP12, affecting downstream effectors of mTORC1 and ultimately inhibiting cell proliferation (Raimondo et al., 2016; Yang et al., 2013). However, rapamycin-induced targeting of mTORC1 has not been effective inhibiting PI3K/AKT/mTOR activity, which may relate to a negative feedback loop promoting paradoxical hyperactivation of AKT, insensitivity to rapamycin, and IGF-1-mediated feedback loops (Tamburini et al., 2008; Wan et al., 2007).

A Phase 1b study by Park *et al*. evaluated the efficacy and tolerance of everolimus combined with conventional chemotherapy (daunorubicin plus cytarabine) in 28 younger (<65 years old) AML patients at first relapse (Park et al., 2013). Karyotyping revealed that six patients (21.4%) had poor cytogenetic indicators, 19 patients (67.9%) with intermediate risk and three (10.7%) with good prognostic cytogenetic indicators. Mutational analysis identified FLT3-ITD or NPM1 mutation in each of two patients and co-existence of FLT3-ITD and NPM mutation in three patients (10.7%). Everolimus strongly inhibited mTORC1 signaling measured by decreased p-p70S6K at T389. Clinical outcomes revealed that 19 patients (67.9%) achieved CR. Notably, three out of four patients with FLT3-ITD achieved CR. Overall, this study showed that a weekly dose of everolimus (70mg) in combination with conventional therapy was tolerable and had acceptable toxicity in younger AML patients at relapse.

Another Phase 1b study by Tiong *et al*. evaluated the efficacy and tolerability of everolimus in combination with low dose cytarabine (LDAC) in elderly AML (Tiong et al., 2018). Twenty-four AML patients diagnosed with *de novo* AML (n=15) or secondary AML (n=9) were included. Mutational analysis by multiplexed mass spectrometry detected mutation of NRAS/KRAS (n=4), NPM1 (n=3), IDH1/2 (n=3), DNMT3A (n=2), FLT3 D835 (n=2), MPL (n=1), and FLT3-ITD (n=1). Overall response rate (ORR) was achieved in six patients (25%) with four CR or CR with incomplete hematological recovery (CRi) (16.7%), one PR (4.2%), and one morphologic leukemia-free state (4.2%). Furthermore, two patients (8.3%) had >50% reduction in marrow leukemic blasts without blood count recovery. However, there was no clear association between mutational profile and response despite two responding patients carrying a *RAS* mutation. The combination of everolimus with LDAC neither revealed an efficacy signal nor potentially increased toxicity. The authors suggested combining mTOR-directed therapies with other novel agents for the treatment of AML.

Table 2.1 PI3K and mTORi approved by FDA for human cancers

Compound	Generic name	Year	Target	Disease/condition	Reference
Copiktra®	duvelisib	2018	PI3K-δ PI3K-γ	relapsed or refractory CLL, SLL, FL	(Rodrigues et al., 2019)
Aliqopa®	copanlisib	2017	PI3K-α PI3K-δ	relapsed FL	(Markham, 2017)
Zydelig®	idelalisib	2014	PI3K-δ	relapsed CLL in combination with rituximab, relapsed FL and SLL	(Miller et al., 2015)
Piqray®	alpelisib	2019	PI3K-α	in combination with fulvestrant; hormone receptor (HR)-positive, human epidermal growth factor receptor 2 (HER2)-negative, PIK3CA-mutated, advanced or metastatic breast cancer	(Markham, 2019)
Afinitor®	everolimus	2009	mTOR	progressive, well-differentiated non-functional, NET of GI or lung origin with unresectable, locally advanced or metastatic disease	(Hasskarl, 2018)
Torisel®	temsirolimus	2007	mTOR	advanced renal cell carcinoma	(Kwitkowski et al., 2010)
Rapamune®	sirolimus	1999	mTOR	LAM, kidney transplant	(Roskoski, 2019)

CLL= chronic lymphocytic leukemia, SLL= small lymphocytic lymphoma, FL= follicular lymphoma, HER= human epidermal growth factor receptor, NET= neuroendocrine tumors, GI= gastrointestinal, LAM= lymphangioleiomyomatosis

Table 2.2 Phase 1 / 2 clinical trials using PI3K/AKT/mTORi

Investigational agent	Condition	Phase	Status	Subjects	Study period	Trial number
gedatolisib	Therapy-related AML and MDS	2	Terminated	10	2015-2018	NCT02438761
buparlisib	Advanced Leukemias	1	Completed	16	2012-2016	NCT01396499
idelalisib	CLL, NHL, AML, MM	1	Completed	192	2008-2012	NCT00710528
Personalized kinase inhibitor therapy (dasatinib, idelalisib, ruxolitinib, ponatinib, sorafenib, sunitinib) + chemotherapy +/- monoclonal antibody treatment: (cyclophosphamide, cytarabine, doxorubicin, idarubicin, methotrexate, vincristine, rituximab)	ALL, AML	1	Recruiting	24	2016-2019	NCT02779283
dactolisib	ALL, AML, CLL with crisis of blast cells	1	Unknown	23	2017-2017	NCT01756118
MK-2206	Relapsed or refractory AML	2	Completed	19	2010-2018	NCT01253447
afuresertib	Hematological malignancies	1/2	Completed	73	2009-2012	NCT00881946
uprosertib + trametinib	Recurrent or untreated adult AML	2	Terminated	24	2013-2018	NCT01907815
everolimus + midostaurin	AML, MDS	1	Active, not recruiting	29	2009-	NCT00819546
everolimus + nilotinib	AML	1/2	Completed	40	2008-2012	NCT00762632
everolimus + cytarabine/daunorubicin	AML	1	Completed	31	2010-2012	NCT01074086
everolimus + cytarabine	AML	1	Unknown	40	2008-	NCT00636922
everolimus + cytarabine/daunorubicin	Relapsed AML	1	Unknown	21	2007-	NCT00544999
sirolimus + MEC	AML, myeloid leukemias, leukemia, CML	1	Completed	16	2007-2010	NCT00780104
sirolimus + MEC	AML	NA	Completed	36	2010-2016	NCT01184898

sirolimus + idaurubicin/cytarabine	AML, PEL	1	Completed	55	2013-2019	NCT01822015
sirolimus + azacitidine	(Recurrent) AML, de novo MDS, MDS with isolated del(5q) previously treated MDS	2	Active, not recruiting	57	2013-	NCT01869114
sirolimus + decitabine	Relapsed or refractory AML	1	Completed	13	2009-2012	NCT00861874

AML= acute myeloid leukemia, MDS= myelodysplastic syndromes, CLL= chronic lymphocytic leukemia, NHL= non-Hodgkin lymphoma, MM= multiple myeloma, ALL= acute lymphocytic leukemia, PEL= pure erythroid leukemia, CML= chronic myeloid leukemia, MEC= mitoxantrone/etoposide/cytarabine

Table 2.3 Response criteria in AML

Response	Criteria
Complete remission (CR)	Bone marrow blasts <5%; absence of circulating blasts and blasts with Auer rods; absence of extramedullary disease; ANC ≥1.0 × 10^9/L (1000/μL); platelet count ≥100 × 10^9/L (100.000/μL)
CR with incomplete hematological recovery (CRi)	All CR criteria except for residual neutropenia (<1.0 × 10^9/L [1000/μL]) or thrombocytopenia (<100 × 10^9/L [100.000/μL])
Partial remission (PR)	All hematologic criteria of CR; decrease of bone marrow blast percentage to 5% - 25%; and decrease of pre-treatment bone marrow blast percentage by ≥50%

ANC= absolute neutrophil count

2.5 Clinical strategies to overcome resistance to PI3K/AKT/mTORi in AML

In the past, PI3K/AKT/mTORi have been tried mostly combined with cytotoxic chemotherapeutics to improve efficacy and reduce drug-related toxicity. However, combination with targeted therapies may be more effective and cooperatively inhibit PI3K/AKT/mTOR signaling while preventing escape via alternative pathways. Several new, targeted agents are currently under clinical investigation for AML therapy, including drugs targeting epigenetic regulators, kinases, monoclonal antibodies, Bcl-2, and metabolism (Figure 2.4). Here, we will provide the rationale for clinically investigating potential drug combinations using PI3K/AKT/mTORi as a novel targeted therapeutic strategy for AML.

2.5.1 PI3K/AKT/mTORi in combination with epigenetic targeting

The importance of epigenetics in AML pathology was demonstrated by the identification of recurrent mutations in genes encoding epigenetic regulators, such as DNMT3A, Tet methylcytosine dioxygenase 2 (TET2), and IDH1/2 (Cancer Genome Atlas Research Network et al., 2013). In addition to mutations in epigenetic regulators, oncogenic fusion proteins can dysregulate epigenetic modifications, driving abnormal transcriptional programs in AML (Alcalay et al., 2003; Martens and Stunnenberg, 2010). Several targeted epigenetic therapies have been explored for AML – for example, hypomethylating agents (HMA), histone deacetylase (HDAC) inhibitors, and IDH1/2 inhibitors. However, as monotherapy these inhibitors do not seem to be effective and treatment failure is common (Bewersdorf et al., 2019; Choe et al., 2020; Gardin and Dombret, 2017; San José-Enériz et al., 2019). To potentiate the efficacy of epigenetic therapy, combination strategies with cytotoxic chemotherapy or other targeted drugs are currently being extensively studied.

Epigenetic modifiers participate in the PI3K/AKT/mTOR pathway, contributing to the oncogenicity of PI3K in cancer. The cooperation of the PI3K/AKT/mTOR pathway with epigenetic reprogramming involves modulation of DNA methylation and histone methylation to promote transcriptional competence (Spangle et al., 2017; Q. Yang et al., 2019). Because of this collaboration, combination strategies with PI3K/AKT/mTORi and epigenetic therapies have been exploited. There is emerging evidence demonstrating synergism when these classes of agents are combined, involving AKT inactivation, FoxO3a-mediated upregulation of pro-apoptotic targets Bim and Puma, and Mcl-1 downregulation (Long et al., 2020; Nishioka et al., 2008; Rahmani et al., 2014; Thépot et al., 2011). PI3K/AKT/mTORi may potentiate epigenetic therapies inducing LSC death by enhanced activation of ROS, to damage DNA (Li et al., 2015; Rahmani et al., 2014). In addition to enhanced anti-leukemic effects, there is preclinical evidence suggesting that DNMT or HDAC inhibitors can overcome acquired resistance to PI3K/AKT/mTORi (Gupta et al., 2009; Qian et al., 2015).
To our knowledge, there are two clinical studies that have evaluated the combination of mTORi with a hypomethylating agent, reported by Liesveld *et al.* and Tan *et al.* Liesveld *et al.* evaluated decitabine

followed by sirolimus in an open label, single arm, Phase 1 dose escalation study in relapsed/refractory AML (Liesveld et al., 2013). Decitabine is a DNA-hypomethylating agent that has been reported to markedly improve CR rates compared to cytarabine, but failed to significantly improve OS rates (Kantarjian et al., 2012; Malik and Cashen, 2014). Thirteen patients were subjected to therapy of which 12 were included for safety evaluation. Complex cytogenetics were present in most patients and only one patient carried the FLT3-ITD mutation at diagnosis. Overall, the administration of decitabine followed by sirolimus was well tolerated and among the evaluable patients, but only one patient achieved CR. Four patients (31%) demonstrated disease progression, 5 (38%) had stable blast percentage, and 4 (31%) demonstrated reduced blast percentage after one cycle. Usually multiple cycles are required to achieve clinical response, but this was not possible in many of the patients due to persistent cytopenias and need for more palliative approaches. Furthermore, the response to inhibition of PI3K/AKT/mTOR signaling was inconsistent, reflecting on the heterogeneous nature of AML. More potent PI3K/AKT/mTORi may be more effective in these studies.

Tan *et al.* evaluated the MTD and efficacy of everolimus, a more potent mTORi than sirolimus, in combination with azacitidine subcutaneously in an open-label, Phase 1b/2 study in relapsed/refractory AML. Forty patients with relapsed (n = 27), primary refractory (n = 11) or elderly patients unfit for intensive chemotherapy (n = 2) were enrolled, of which 37 were retained for evaluation of toxicity (Tan et al., 2017). Similar to Liesveld *et al*., azacitidine and everolimus were given sequentially to maximize mTORiy effect and avoid potential mTOR-induced cell cycle inhibition, which may attenuate azacitidine activity. Mutational analysis revealed IDH1/2 mutations in 15/35 (43%) and FLT3-ITD mutation in 7/37 (19%) patients. Notably, three patients with relapsed FLT3-ITD had >80% bone marrow blast reductions following sequential therapy, of which two underwent allogeneic stem cell transplantation but subsequently relapsed and died. Overall, the combination of everolimus and azacitidine was well tolerated with an ORR of 22.5% and mean survival of 8.5 months. Collectively, these findings support the clinical investigation of PI3K/AKT/mTORi in combination with targeted epigenetic therapies in AML patients.

2.5.2 PI3K/AKT/mTORi in combination with Bcl-2 inhibitors

Bcl-2, encoded by the human *BCL2* gene is the founding member of the Bcl-2 family of proteins, which are divided into pro-apoptotic and anti-apoptotic members. The anti-apoptotic proteins include Bcl-2, Bcl-XL, Bcl-w, Mcl-1, and A1 that share three or four sequence homology in the Bcl-2 homology (BH) domain. These proteins can directly interact with pro-apoptotic BH3-only proteins Bim, Puma, Bad, Bid, Bik, Bmf, Hrk and Noxa, which share homology in the BH3 domain (Huang and Strasser, 2000). Apoptotic stimuli upregulate BH3-only proteins Bax and Bak that leads to permeabilization of the mitochondrial outer membrane and releases cytochrome c into the cytosol for activation of caspases that dismantle cellular structures (Hata et al., 2015; Kuwana and Newmeyer, 2003; Willis et al., 2005).

Bcl-2 is often overexpressed in AML patients, both at diagnosis as well as at relapse, and can render resistance to cytotoxic chemotherapeutics (Andreeff et al., 1999; J.-D. Zhou et al., 2019). A major finding by Lagadinou *et al*. identified high levels of Bcl-2 as a feature of LSC to maintain mitochondrial integrity for survival (Lagadinou et al., 2013). LSC were characterized by low levels of ROS and displayed overexpression of Bcl-2. Importantly, it was demonstrated that small molecule Bcl-2 inhibitors reduced oxidative phosphorylation and selectively killed quiescent LSC. Thus, targeting Bcl-2 may provide a promising therapeutic strategy to effectively target chemoresistant LSC population. BH3 mimetic venetoclax (ABT-199) is a specific inhibitor of Bcl-2 and has been approved by the FDA for the treatment of CLL. Venetoclax binds to Bcl-2 and prevents pro-apoptotic proteins Bak and Bax from binding to Bcl-2. As venetoclax showed potential both *in vitro* and xenograft models, its efficacy was evaluated for AML (Pan et al., 2014; Souers et al., 2013). Konopleva *et al*. evaluated the efficacy of venetoclax as monotherapy in a Phase 2 study in 32 patients with high-risk relapsed/refractory AML or unfit for intensive chemotherapy (Konopleva et al., 2016). Although venetoclax had acceptable tolerability, the ORR was 19%, of whom 6% achieved CR and 13% achieved CRi. Unfortunately, the clinical response of venetoclax was short-lived as all patients relapsed, suggesting the rapid development of venetoclax resistance. Myoblast dependence on Mcl-1 and Bcl-xL were identified as key players in the intrinsic resistance to venetoclax in AML (Bose et al., 2017; Konopleva et al., 2016). In contrast to CLL, which is relatively homogenously dependent on Bcl-2, AML seems more heterogeneous and depends on multiple pro-apoptotic proteins (Lin et al., 2016; Xiang et al., 2010). Significant efforts have been made to overcome this resistance by combining venetoclax with DNA damaging agents such as daunorubicin and cytarabine, which reduce Mcl-1 levels and enhance venetoclax activity (Konopleva and Letai, 2018; Teh et al., 2018, p. 1). Hypomethylating agent azacitidine was also shown to reduce Mcl-1 protein levels, and synergistically induced apoptosis in AML cells (Tsao et al., 2012). The FDA approved venetoclax in combination with HMAs or LDAC for the treatment of AML patients who are previously untreated and older or unfit for chemotherapy (DiNardo et al., 2019, 2018; Wei et al., 2019).

In addition to cytotoxic chemotherapy and hypomethylating agents, PI3K/AKT/mTORi may also overcome venetoclax resistance and potentiate LSC targeting. The combination of PI3K/AKT/mTORi with Bcl-2 inhibitors has been examined in several preclinical cancer models (Pugazhenthi et al., 2000; Wang et al., 1999). Results demonstrated that PI3K/AKT/mTORi downregulate Mcl-1, in part through GSK3 activation, and upregulate Bim, Bad, Bax and Bak. Although PI3K/AKT/mTOR inhibition downregulated Mcl-1, it did not trigger apoptosis, presumably by increased Bim binding to Bcl-2 and Bcl-XL. Co-targeting Bcl-2 released Bim from Bcl-2 and Bcl-xL and induced Bax and Bak-dependent apoptosis in AML LSC, whilst sparing normal hematopoietic progenitor cells (Bose et al., 2012; Rahmani et al., 2018, 2013; Su et al., 2018; Vachhani et al., 2014). These data support the rationale for the evaluation of the combination of PI3K/AKT/mTORi and Bcl-2 inhibitors in AML. Currently, there is one study exploring the combination of pan-PI3Ki copalisib and venetoclax in relapsed/refractory NHL (NCT03886649) (Choudhary et al., 2015).

2.5.3 PI3K/AKT/mTORi in combination with kinase inhibitors

Previously we discussed other signaling pathways that can integrate with the PI3K/AKT/mTOR pathway, which can potentially reduce the activity of PI3K/AKT/mTORi. Parallel pathway inhibition may improve sensitivity to PI3K/AKT/mTORi and enhance anti-leukemic effects in AML cells. For example, upregulation of PIM was shown to cause resistance to PI3K/AKT/mTORi in AML through a mechanism that involves modulation of mTORC1 activity (Okada et al., 2018; Song et al., 2018). While pan-PIM inhibitor AZD1897 showed limited activity as monotherapy in AML cell lines and primary samples, including FLT3-ITD+ cells, combination of AZD1897 with AKTi AZD5363 displayed synergistic anti-leukemic activity (Meja et al., 2014). This was associated with enhanced inhibition of mTORC1 signaling activity and Mcl-1 levels. Importantly, this combination strategy affected both bulk cells and LSC subsets.

There are two studies in which PIM inhibitors and PI3Ki have been evaluated as combination therapy for hematological malignancies. Novartis Pharmaceuticals evaluated the safety and effectiveness of pan-PIM inhibitor LGH447 and PI3Kα inhibitor BYL719 in patients with relapsed/refractory MM in a Phase 1b/2 study, but the trial never made it to Phase 2 (NCT02144038). Incyte Corporation is currently examining the combination of NCB053914 (pan-PIM inhibitor) with INCB050465 (PI3Kδ inhibitor) in relapsed/refractory diffuse large B-cell lymphoma (DLBCL) in a Phase 1b study (NCT03688152) (Koblish et al., 2018).

Co-targeting the PI3K/AKT/mTOR and MAPK/ERK pathways is another combination strategy that has been evaluated. In AML, the FLT3-ITD mutation is an important mechanism that feeds growth signals into main oncogenic signaling pathways such as PI3K/AKT/mTOR and MAPK/ERK. As crosstalk exists between PI3K/AKT/mTOR and MAPK/ERK pathways, inactivation of both pathways may interrupt oncogenic signals in AML (Carneiro et al., 2015; Jain et al., 2014). This may be particularly beneficial in RAS mutated cases. In fact, several reports have shown *in vitro* enhanced induction of apoptosis when PI3K/AKT/mTORi were combined with MAPK/ERK inhibitors (Sandhöfer et al., 2015). Inhibition of MEK suppressed p-Erk level but caused feedback activation of the PI3K/AKT/mTOR pathway defined by increased p-mTOR and Mcl-1 levels which could be abrogated by co-targeting PI3K/AKT/mTOR (Liu et al., 2010). The MEK inhibitor also resulted in increased expression of Bim and Bcl-2, which could not be abrogated by adding the PI3K/AKT/mTORi. It has been suggested that the increased Bim was bound to Bcl-2 which prevented induction of cell death and that inhibition of Bcl-2 might further sensitize AML cells to apoptotic cell death by the combination of the MEK and PI3K/AKT/mTORi (Su et al., 2018). Indeed, simultaneous inhibition of PI3K, mTOR, and MAPK/ERK synergistically induced cell death in AML cells, which was further enhanced by the addition of venetoclax, while sparing the normal hematopoietic progenitor cells (Liu et al., 2010; Su et al., 2018). This triple-drug combination may potentiate the efficacy of venetoclax to target quiescent LSC. There is one Phase 1b study that examined the MTD for the combination of PI3Kα inhibitor BYL719 and allosteric MEK1/2 inhibitor MEK162 in patients with advanced solid tumors and in adult patients with

AML or high risk MDS carrying RAS or BRAF mutations (NCT01449058). However, the preliminary safety and efficacy findings warrant further exploration as adverse effects were common and stable disease lasting >6 weeks was noted as best response for 31% of patients [284].

Furthermore, dual inhibition of FLT3 activation and downstream targeting of PI3K/AKT/mTOR may have synergistic activity in FLT3 mutated cases. Patients with FLT3-ITD tend to have a high risk of relapse and shorter OS compared to patients without the mutation (Daver et al., 2019). In the last few years, several FLT3 TKI have been developed, which can be divided into first-generation pan-kinase inhibitors such as sorafenib and midostaurin, and next generation inhibitors such as quizartinib and gilteritinib, which are more potent and specific for FLT3 (Antar et al., 2020). Although FLT3i were able to induce response in AML patients with FLT3 mutations, these responses were often not durable, and resistance developed rapidly (Lam and Leung, 2020; Larrosa-Garcia and Baer, 2017). FLT3i are currently evaluated in combination with chemotherapy or hypomethylating agents in various settings, to overcome resistance and prolong OS respectively (Lam and Leung, 2020; Perl et al., 2019; Schlenk et al., 2019). The PI3K/AKT/mTOR pathway is a promising target to overcome resistance to FLT3i. Upregulation of PI3K/AKT/mTOR pathway was shown in FLT3i-resistant FLT3-ITD+ AML cells despite inhibition of FLT3 activation by FLT3i, suggesting that the resistant cells become FLT3 independent (Lindblad et al., 2016; Piloto et al., 2007). Inhibition of PI3K/AKT/mTOR *in vitro* improved sensitivity to FLT3i and enhanced inhibition of growth and apoptosis. PI3K/AKT/mTORi may also potentially suppress FLT3-ITD-induced LSC survival. It has been reported that FLT3-ITD upregulates Mcl-1 to promote survival of AML LSC, which was abrogated by the TKI midostaurin (PKC-412) that targets multiple receptors (including FLT3 and c-Kit) (Yoshimoto et al., 2009b). As PI3K/AKT/mTORi can induce inhibition of Mcl-1, combination of PI3K/AKT/mTORi with FLT3i may potentiate inhibition of LSC survival. Currently, there is one Phase 1 study evaluating the combination of mTORi everolimus with midostaurin in patients with relapsed/refractory or poor prognosis AML or MDS (NCT00819546).

2.5.4 PI3K/AKT/mTORi in combination with DNA repair inhibitors

In a previous section we briefly highlighted the importance of increased ROS in AML, which can promote genomic instability and contributes to chemotherapy resistance. In particular, there is increasing evidence associating FLT3 mutations with DNA damage, specifically through increased ROS, resulting in double strand breaks (DSBs) and impaired DNA repair (Rebechi and Pratz, 2017; Seedhouse et al., 2006). Targeting DNA damage repair mechanisms may provide a novel therapeutic opportunity in AML that may reduce repair errors and genomic instability (Gregory et al., 2016). Genomic stability is maintained by the DDR, a highly orchestrated signaling cascade that results from the induction and detection of DNA damage. At the heart of the DDR are members of the PIKK family comprising ataxia telangiectasia mutated (ATM), ataxia telangiectasia and Rad3-related protein (ATR), and DNA-PK, which upon sensing of DNA damage, in particular DSBs, phosphorylate a large

number of substrates to effectively repair DNA (Menolfi and Zha, 2020). Although DSB repair in normal mammalian cells is primarily dominated by homologous recombination (HR) and DNA-PK-dependent NHEJ, FLT3-ITD directs DSB repair towards an error-prone, alt-NHEJ pathway, which is mediated by poly(ADP-ribose) polymerase-1 (PARP-1) and DNA Lig IIIα (Fan et al., 2010; Scully et al., 2019).

In this regard, PARP inhibitors present a putative therapeutic strategy for AML. PARP1, an important protein of the DDR pathway, senses single strand breaks (SSBs) and has a crucial role for base excision repair (BER). Inhibition of PARP1 leads to accumulation of SSBs which then become DSBs that make cells more dependent on HR (Caron et al., 2019; Chen, 2011). However, in cells with defective HR, such as those with BRCA deficiency, PARP1 inhibition induced synthetic lethality (Lord et al., 2015; Lord and Ashworth, 2017). This concept of synthetic lethality using PARP inhibitors has been effectively examined in BRCA1-defective solid tumors, but was also exploited for the treatment hematological malignancies like AML (Audeh et al., 2010; Tutt et al., 2010; Zhao and So, 2016). Indeed, several *in vitro* studies in AML reported that PARP inhibitors induced cell cycle arrest and apoptosis, and combination with chemotherapy may induce synthetic lethality (Gafencu et al., 2017; Gaymes et al., 2009; Ng et al., 2019).

There is ongoing research evaluating the combination of PARP inhibitors with other agents to extend the therapeutic potential of these inhibitors beyond tumors with mutations of BRCA or other HR deficiencies. As the PI3K/AKT/mTOR pathway contributes to the DDR, combination of PI3K/AKT/mTORi with PARP inhibitors was exploited in several solid tumor models (Huang et al., 2020; Kumar et al., 2010). Inhibition of the PI3K/AKT/mTOR pathway in ovarian, breast, and prostate cancers revealed impaired expression of BRCA1/2 and reduced cellular capacity to conduct HR (De et al., 2014; González-Billalabeitia et al., 2014; Ibrahim et al., 2012; Wang et al., 2016). Consistent with the reduction in the expression of BRCA1/2, PI3K/AKT/mTORi sensitized cells to PARP inhibition and synergistically suppressed cell growth. Although these findings support the rationale for the combination of PI3K/AKT/mTORi with PARP inhibitors, this combination strategy is yet to be evaluated in AML.

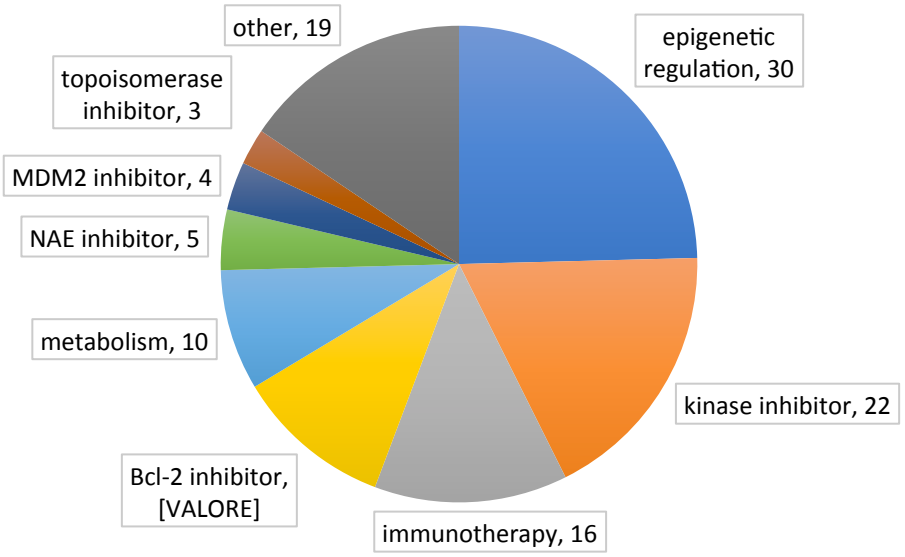

Figure 2.4 Pie chart presenting the classification of interventions for AML therapy evaluated in clinical trials

Data was obtained from ClinicalTrials.gov and filtered for 'recruiting' and 'active, not recruiting' status in adult and elderly AML and study phase (1b-3) with start date from 1st January 2018 Numbers present frequency within 88 studies. *other= frequency <3 include dihydroorotate dehydrogenase (DHODH) inhibitor, proteasome inhibitor, p53 activator, hedgehog signaling inhibitor, CDK inhibitor, E-selectin inhibitor, nuclein export inhibitor, menin-MLL binding interaction inhibitor, CXCR4 antagonist, proteasome inhibitor, corticosteroid, thrombopoietin receptor agonist, and isoprenyl transferase inhibitor. MDM2= mouse double minute 2 homolog, NAE= NEDD8-activating enzyme, Bcl-2= B-cell lymphoma 2.

2.6 Hypothesis and aims

FLT3 is mutated in approximately 25% of all AML cases with normal karyotype and in spite of the development of potent and selective FLT3i, few patients display prolonged remission with targeted monotherapy, highlighting a substantial unmet need for effective treatment. Emerging evidence has shed light on the critical role of the BM environment protecting AML cells from apoptosis and development of resistance to TKI. A major druggable target downstream of constitutively activated FLT3 kinase is the PI3K/AKT/mTOR pathway, with many mechanistic reports of the importance of its inhibition in the treatment of hematologic malignancies. In AML, the PI3K/AKT/mTOR pathway is thought to provide environmental pro-survival support to chemoresistant AML LSC, which are capable of sustaining disease and give rise to relapse. Combination therapy is a promising strategy to overcome BM niche-mediated chemoresistance and potentially restore sensitivity to TKI therapy. It was hypothesized that combination with PI3Ki may strengthen the efficacy of FLT3i in *FLT3*-ITD AML in a pre-clinical setting.

Aims:

- To uncover the phenotype of FLT3-ITD versus FLT3 wildtype AML cell lines following treatment with FLT3i or PI3K/AKT/mTORi.
- To evaluate the efficacy of combination therapy of FLT3i with PI3K/AKT/mTORi in FLT3-ITD AML cell lines and primary AML patient blasts.
- To assess the contribution of stroma and/or exogenous PGF on the efficacy of targeted combination treatment.
- To elucidate persistent cytokines and phosphoproteins as putative novel targets for FLT3-ITD AML therapy.

Chapter 3: Material and Methods

3.1 Materials

3.1.1 Tissue culture

3.1.1.1 Tissue culture reagents

Product	Supplier	Catalog number
1% L-glutamine	Thermo Fisher Scientific	25030081
DMEM	Thermo Fisher Scientific	21969035
RPMI 1640	Thermo Fisher Scientific	21875091
Foetal Bovine Serum (FBS)	Thermo Fisher Scientific	10500064
0.25% Trypsin-EDTA (1x)	Thermo Fisher Scientific	25200072
Trypan blue	Sigma-Aldrich	302643
Resazurin sodium salt	Sigma-Aldrich	R7017
Dimethyl sulphoxide (DMSO)	Sigma-Aldrich	D2650
Phosphate buffered saline (PBS)	Thermo Fisher Scientific	BR0014
DNase I Solution (1 mg/mL)	STEMCELL Technologies	7900
Iscove Modified Dulbecco Media (IMDM)	STEMCELL Technologies	21056023
StemSpan™ SFEM II	Thermo Fisher Scientific	9655
Recombinant human IL-3	200-03	PeproTech
Recombinant human TPO	300-18	PeproTech
Recombinant human G-CSF	300-23	PeproTech
Recombinant Human SCF	300-07	PeproTech
Recombinant Human FLT-3 ligand	300-19	PeproTech
Trifluoroacetic acid	T6508	Sigma-Aldrich
BAY 80-6946	S2802	Selleckchem
PF-04691502	S2743	Selleckchem
cytarabine	S1648	Selleckchem
quizartinib	S1526	Selleckchem

3.1.1.2 Tissue culture solutions

3.1.1.2.1 10x Trypan blue (0.4%)

	Volume
Trypan Blue	400 mg
Phosphate-buffered saline (PBS)	to 10 mL
Filter sterilize through 0.45µm filter before use	

3.1.1.2.2 Freezing solution for cell lines

	Volume
10% (v/v) DMSO	1 mL
50% Fetal Bovine Serum (FBS)	5 mL
Cell culture media	to 10 mL

3.1.1.2.3 Thawing solution of patient samples (DAMP solution)

	Volume
DNase I solution (1 mg/mL)	2 mL
Magnesium chloride ($MgCl_2$) (1M)	1.25 mL
Trisodium Citrate (0.155M)	53 mL
20% (v/v) Human Serum Albumin	100 mL
Dulbecco's PBS (Mg^{2+}/Cl^- free)	to 500 mL

3.1.1.2.4 Serum-free expansion media with high growth factor

	Volume
StemSpan™ medium	10 mL
Interleukin 3 (IL-3) (100 µg/mL)	10 ng/mL
Thrombopoietin (TPO) (100 µg/mL)	10 ng/mL
Granulocyte colony-stimulating factor (G-CSF) (100 µg/mL)	10 ng/mL

3.1.1.2.5 Serum-free expansion media with physiological growth factor

	Volume
StemSpan™ medium	10 mL
Interleukin 3 (IL-3) (100 µg/mL)	1 ng/mL
Thrombopoietin (TPO) (100 µg/mL)	1 ng/mL
Granulocyte colony-stimulating factor (G-CSF) (100 µg/mL)	1 ng/mL

3.1.2 Resazurin assay

3.1.2.1 Resazurin assay solutions

3.1.2.1.1 25mM Resazurin solution

	Volume
Resazurin sodium salt	0.313 g
PBS	to 50 mL
Filter sterilize through 0.45µm filter before use	

3.1.3 Flow cytometry

3.1.3.1 Flow cytometry reagents

Product	Supplier	Catalog number
UltraComp eBeads™ Plus Compensation Beads	Thermo Fisher Scientific	01-3333-41
Ribonuclease A from bovine pancreas	Sigma-Aldrich	R5500
Hank's Balanced Salt Solution (HBSS) (10X)	Thermo Fisher Scientific	14065056
CountBright™ Absolute Counting Beads	Thermo Fisher Scientific	C36950
Phosphate buffered saline (PBS)	Thermo Fisher Scientific	BR0014
Formaldehyde solution	Sigma-Aldrich	47608

3.1.3.2 Flow cytometry solutions

3.1.3.2.1 Propidium Iodide (PI) staining solution

	Volume
Propidium iodide (PI) (1 mg/mL)	200 µL
RNase solution (1 mg/mL)	500 µL
PBS	to 10 mL

3.1.3.2.2 Annexin V/DAPI staining solution

	Volume (per test)
4′,6-diamidino-2-phenylindole (DAPI) (1 mg/mL)	0.1 µL
Annexin V FITC	1 µL
Hanks' Balanced Salt Solution (HBSS)	to 100 µL

3.1.3.2.3 Fixing solution

	Volume (per test)
Formaldehyde solution (≥36.0%)	1 mL
dH_20	to 10 mL

3.1.3.2.4 Flow cytometry antibody panel used in co-culture experiments

Antibody	Fluorophore	Volume (per test)

hCD34	FITC	1 µL
hCD38	PE-Cy7	1 µL
hCD33	AmCyan	1 µL
hCD45	APC-Cy7	1 µL
mCD45.1*	PerCP-Cy5.5	1 µL
Annexin V	PE	1 µL
DAPI (1 mg/mL)	PacBlue	0.1 µL
Hank's Balanced Salt Solution (HBSS)		to 100 µL

*only in PDX samples

3.1.3.3 Flow cytometry antibodies

Product	Supplier	Catalog number
FITC Annexin V	BD Biosciences	556419
APC-Cy7 Mouse Anti-Human CD45	BD Biosciences	557833
Propidium iodide solution	Sigma-Aldrich	P4864
DAPI Solution	BD Biosciences	564907
APC anti-mouse/human CD11b Antibody	Biolegend	101212
PE Mouse Anti-Human CD13	BD Biosciences	555394
BV510 Mouse Anti-Human CD33	BD Biosciences	744351
FITC Mouse Anti-Human CD34	BD Biosciences	555821
PE-Cy™7 Mouse Anti-Human CD38	BD Biosciences	560677
PerCP/Cyanine5.5 anti-mouse CD45.1 Antibody	Biolegend	110728
APC-Cy™7 Mouse Anti-Human CD45	BD Biosciences	557833
PE Annexin V	BD Biosciences	556421

3.1.3.4 Intracellular staining

Primary Antibody	Specie	Supplier	Catalog number	Dilution
Phospho-p44/42 MAPK (Erk1/2) (Thr202/Tyr204) (197G2)	Rabbit	CST	4377S	1:200
Phospho-S6 Ribosomal Protein (Ser235/236) (D57.2.2E) XP®	Rabbit	CST	4858S	1:50
Phospho-Akt (Ser473) (D9E) XP®	Rabbit	CST	4060S	1:100
Goat anti-Rabbit IgG (H+L) Highly Cross-Adsorbed Secondary Antibody, Alexa Fluor 488	Rabbit	Thermo Fisher Scientific	A-11034	1:1000

3.1.4 Western blotting

3.1.4.1 Western blotting reagents

Product	Supplier	Catalog number
Sodium dodecyl sulphate (SDS)	Sigma-Aldrich	D6750
Trizma base	Sigma-Aldrich	T6066
2-Mercaptoethanol	Sigma-Aldrich	M6250
Ethylenediaminetetraacetic acid (EDTA)	Sigma-Aldrich	E9884
Sodium fluoride	Sigma-Aldrich	S7920
Gel Loading Dye, Purple (6X)	New England BioLabs	B7024S
Sodium chloride	Merck-Millipore	106404
Phosphate buffered saline (PBS)	Thermo Fisher Scientific	BR0014
NuPAGE™ 4 to 12%, Bis-Tris, 1.0 mm, Mini Protein Gel, 10-well	Thermo Fisher Scientific	NP0321BOX
NuPAGE™ 4 to 12%, Bis-Tris, 1.5 mm, Mini Protein Gel, 15-well	Thermo Fisher Scientific	NP0336BOX
NuPAGE™ 4 to 12%, Bis-Tris, 1.0 mm, Mini Protein Gel, 12-well	Thermo Fisher Scientific	NP0322PK2
SuperSignal™ West Pico PLUS Chemiluminescent Substrate	Thermo Fisher Scientific	34577
Nitrocellulose Membrane, 0.45 **µ**m, 30 cm x 3.5 m	Thermo Fisher Scientific	88018
PageRuler™ Plus Prestained Protein Ladder, 10 to 250 kDa	Thermo Fisher Scientific	26619
NuPAGE™ Sample Reducing Agent (10X)	Thermo Fisher Scientific	NP0009
PhosSTOP™	Sigma-Aldrich	4906837001
cOmplete™ ULTRA Tablets, Mini, EASYpack Protease Inhibitor Cocktail	Sigma-Aldrich	5892970001
MOPS SDS Running buffer (20x)	Thermo Fisher Scientific	NP0001
Tween™ 20	Sigma-Aldrich	P2287
Bovine Serum Albumin Fraction V	Sigma-Aldrich	10735086001
10x ReBlot Plus Strong	Merck-Millipore	2504
Pierce Coomassie Plus (Bradford) Assay Kit	Thermo Fisher Scientific	23236
NuPAGE™ LDS Sample Buffer (4X)	Thermo Fisher Scientific	NP0007
Ponceau S solution	Sigma-Aldrich	P7170
Whatman 3mm CHR	GE Healthcare Life Sciences	3030-917

3.1.4.2 Western blotting solutions

3.1.4.2.1 Protein extraction buffer

	Volume
20mM Tris (pH 7.4)	20 µL
2mM ethylenediaminetetraacetic acid (EDTA)	20 µL
1% Triton X	10 µL
1mM dithiothreitol (DTT)	10 µL
1M sodiumfluoride (NaF)	10 µL
100 mM diisopropyl fluorophosphate (DIFP)	0.1 µL
10x PhosSTOP™	100 µL
10x Protease Inhibitor Cocktail	100 µL
Deionized H_2O (dH2O)	to 1 mL

3.1.4.2.2 Sample preparation for gel loading

	Volume
Lysate	40 µg
Invitrogen™ NuPAGE™ Sample Reducing Agent (10x)	1x
NuPAGE™ LDS Sample Buffer (4X)	1x
dH_2O	to 15-25 µL

3.1.4.2.3 1x MOPS running buffer

	Volume
20x MOPS ((3-(N-morpholino) propanesulfonic acid) SDS running buffer	50 mL
dH_2O	to 1L

3.1.4.2.4 10x transfer buffer

	Volume
Tris base (250 mM)	30.3 g
Glycine (1.9 M)	144.0 g
dH_2O	to 1L

3.1.4.2.5 1x transfer buffer

	Volume
10x transfer buffer	100 mL
methanol	100 mL
dH_2O	to 1L

3.1.4.2.6 10x Tris-Buffered Saline (TBS) pH 7.6

	Volume
Tris base	60.6 g
NaCl (sodium chloride)	87.6 g
dH_2O	to 1L
pH adjustment to 7.6	

3.1.4.2.7 1x TBS

	Volume
10x TBS	100 mL
Tween-20	1 mL
dH_2O	to 1L

3.1.4.2.8 Bovine Serum Albumin (BSA) 5% (w/v) blocking solution

	Volume
BSA Fraction V	2.5 g
1x TBS	to 50 mL

3.1.4.3 Western blotting antibodies

3.1.4.3.1 Primary antibodies used for western blotting

Primary Antibody	Specie	Supplier	Catalog number	Dilution
Phospho-p44/42 MAPK (Erk1/2) (Thr202/Tyr204) (197G2)	Rabbit	CST	4377S	1:1000
p44/42 MAPK (Erk1/2) (137F5)	Rabbit	CST	4695S	1:1000
S6 Ribosomal Protein (54D2)	Mouse	CST	2317S	1:1000
Phospho-S6 Ribosomal Protein (Ser235/236) (D57.2.2E) XP®	Rabbit	CST	4858S	1:1000
Phospho-Akt (Ser473) (D9E) XP®	Rabbit	CST	4060S	1:1000
Akt (pan) (C67E7)	Rabbit	CST	4691S	1:1000
β-Actin (8H10D10)	Mouse	CST	3700S	1:2000

3.1.4.3.2 Secondary antibodies used for western blotting

Product	Supplier	Catalog number	Dilution
Anti-rabbit IgG, HRP-linked Antibody	CST	7074S	1:1000
Anti-mouse IgG, HRP-linked Antibody	CST	7076S	1:1000
Polyclonal goat anti-mouse antibody HRP	Agilent	PO447	1:10,000
Polyclonal goat anti-rabbit antibody HRP	Agilent	PO448	1:10,000

3.1.5 Polymerase chain reaction (PCR)

3.1.5.1 PCR reagents

Product	Supplier	Catalog number
Ethylenediaminetetraacetic acid (EDTA)	Sigma-Aldrich	E9884
Nuclease-Free Water	Qiagen	129115
SYBR™ Safe DNA Gel Stain	Thermo Fisher Scientific	S33102
Agarose	Sigma-Aldrich	A9539
GelPilot® 50 bp Ladder	Qiagen	239025
DNeasy® Blood & Tissue Kit	Qiagen	69504
RNeasy® Plus Mini Kit	Qiagen	74136
PowerUp™ SYBR™ Green Master Mix	Thermo Fisher Scientific	A25743
SuperScript™ IV Reverse Transcriptase	Thermo Fisher Scientific	18090200
RNaseOUT™ Recombinant Ribonuclease Inhibitor	Thermo Fisher Scientific	10777019
Nucleotide Triphosphate (dNTPs) Mix (10mM)	Thermo Fisher Scientific	18427088
Random Hexamers (50µM)	Thermo Fisher Scientific	N8080127
MicroAmp™ Optical 384-Well Reaction Plate with Barcode	Thermo Fisher Scientific	4343814
GoTaq® G2 DNA Polymerase kit	Promega	M7841

3.1.5.2 PCR solutions

3.1.5.2.1 10x Tris-acetate-EDTA (TAE)

	Volume
Tris base	48.5 g
glacial acetic acid	11.4 mL
0.5M EDTA (pH 8.0)	20 mL
dH_2O	to 1L

3.1.5.2.2 1x TAE

	Volume
10x TAE	100 mL
dH_2O	to 1L

3.1.5.2.3 First strand cDNA synthesis mastermix

	Volume
0.5-1 µg RNA	200 µL
Random hexamers (50 µM)	1 µL
Deoxynucleotide triphosphate (dNTPs) (10 mM)	1 µL
nuclease-free H_2O	to 13 µL

3.1.5.2.4 Reverse transcription mastermix

	Volume
Reaction buffer (5x)	4 µL
Dithiothreitol (DTT)	1 µL
RNase inhibitor	1 µL
SuperScript IV reverse transcriptase	1 µL

3.1.5.2.5 Quantitative real time polymerase chain reaction (RT-qPCR) mastermix

	Volume
Forward primer (10 µM)	0.4 µL
Reverse primer (10 µM)	0.4 µL
SYBR Green	5 µL
cDNA	2 µL
Nuclease-free H_2O	2.2 µL

3.1.5.2.6 PCR amplification of gDNA mastermix

	Volume
Green GoTaq® reaction buffer	5 µL
Deoxynucleotide triphosphate (dNTPs) (10 mM)	0.5 µL
Forward primer (10 µM)	0.5 µL
Reverse primer (10 µM)	0.5 µL
GoTaq® DNA polymerase	0.125 µL
Nuclease-free H_2O	17.375 µL

3.1.5.2.7 PCR primers

Gene	Forward primer sequence (5' to 3')	Reverse primer sequence (5' to 3')
FLT3-ITD	GGTGACCGGCTCCTCAGATA	CGGCAACCTGGATTGAGACT
NFKB1	GCTTAGGAGGGAGAGCCCA	GGTATGGGCCATCTGCTGTT
RPS6KB1	CAGGGAAGCTGAGGACATGG	TTCTGGCCCTCTGTTCACAC
MAP2K1	AATGCCCAAGAAGAAGCCGA	AGCTCTAGCTCCTCCAGCTT
NRAS	TCTGTCCAAAGCAGAGGCAG	TTTTCCCAACACCACCTGCT
GAPDH	GTCAACGGATTTGGTCGTATT	TGTAGTTGAGGTCAATGAAGGG
ACTB	CACAGAGCCTCGCCTTT	GCCGCGATATCATCATCCAT

3.1.6 Cytokine profiling

3.1.6.1 Cytokine profiling reagents

Product	Supplier	Catalog number
Cytokine 25-Plex Human ProcartaPlex™ Panel 1B	Thermo Fisher Scientific	EPX250-12166-901
Magnetic 96-Well Separator	Thermo Fisher Scientific	A14179

3.2 Methods

3.2.1 Drug reconstitution

Arabinoside cytosine (AraC, cytarabine), PF-04691502, and quizartinib (AC220) was reconstituted into stock dilution of 10 mM in DMSO. BAY 80-6946 (copanlisib) was reconstituted into stock dilution of 1 mM in 10% trifluoroacetic acid (TFA) (v/v). Drugs were stored at -20 degrees Celsius (°C).

3.2.2 Cell culture

3.2.2.1 Culture of cell lines

Several cell lines were used in this work and are listed in Table 3.1 below. THP-1, MOLM-13 and MV4-11 were cultured in RPMI 1640 medium supplemented with 10% (v/v) fetal bovine serum (FBS) and 2mM L-glutamine. Cells were passaged every 2-3 days, replating cells at 1 to $2x10^5$ per mL cell density until passage 19. Murine bone marrow-derived stromal cell line MS-5 was cultured in Dulbecco's Modified Eagle Medium (DMEM) medium supplemented with 10% (v/v) FBS and 2 mM L-glutamine. Cells were passaged 1:2 or 1:3 every 2-3 days

until passage 19. Cells were maintained at 37°C, 5% CO_2 in a humidified incubator. All cell lines used in this work were authenticated by sequencing.

Table 3.1 Cell line origin and molecular characteristics

THP-1	Cell line established from the peripheral blood of a 1-year-old boy with acute monocytic leukemia at relapse; cells carry MLL-AF9 fusion.
MOLM-13	Cell line established from the peripheral blood of a 20-year-old man with AML FAB M5a at relapse; cells carry internal tandem duplication of FLT3 and MLL-AF9 fusion.
MV4-11	Cell line established from the blast cells of a 10-year-old boy with biphenotypic B-myelomonocytic leukemia (AML FAB M5); cells carry internal tandem duplication of FLT3 and MLL-AF4 fusion.
MS-5	Cell line established from C3H/HeNSlc mice strain by irradiation of the adherent cells in long-term bone marrow cultures.

3.2.2.2 Cryopreservation of cell lines

For cryopreservation of cell lines, viable cells were counted by Trypan Blue dye exclusion and $5x10^6$ cells per cryovial were resuspended in 1 mL of pre-warmed freezing medium, constituted of 50% (v/v) FBS, 40% (v/v) cell type-specific culture medium and 10% (v/v) dimethyl sulphoxide (DMSO). Cryovials were transferred into a controlled rate freezing container and stored at -80 °C overnight. The cryovials were stored in a liquid nitrogen tank from the next day.

3.2.2.3 Recovery of cell lines

To recover cell lines, the cryovial from the liquid nitrogen storage was thawed by placing in a 37°C water bath. Thawed cells were resuspended in 5 mL pre-warmed cell medium and spun down at 200*g* for 5 mins to remove DMSO. The cell pellet was resuspended in the appropriate cell type-specific culture medium and transferred to an appropriate cell culture vessel.

3.2.2.4 Primary patient and patient-derived xenograft (PDX) collection

Primary cells were collected at diagnosis from AML patients following informed consent. All experimental procedures were performed in compliance with the guidelines of the European (86/609/EEC) and the Italian laws (D.L.116/92), and approved by the local ethic committee with protocols 4331/CE/AML study. PBMC were purified from a bag of whole blood obtained from the Transfusional Center of the Policlinico, Modena, using Ficoll-Paque® Plus. The

non-AML sample was obtained with written informed consent, in accordance with the declaration of Helsinki and with Greater Glasgow and Clyde NHS Trust Ethics Committee approval. Patient-derived xenograft (PDX) were generated thanks to Shaun Patterson. To briefly explain how the PDX model was established, primary patient samples were injected in irradiated immunodeficient NOD rag gamma 3GS (NRG-3GS) or NOD scid gamma (NSG) mice strain. Mice were monitored physiologically for signs of disease and disease development was monitored by analysis of peripheral venous blood post-transplantation. Following established development of disease, AML cells were harvested from the spleen and long bones of the hind legs. In this thesis work, only spleen cells were used. The use of these samples was ethically approved by the Paul O'Gorman Leukaemia Research Centre Cell Bank Approval Committee. The samples used in this thesis are listed in Table 3.2.

Table 3.2 Overview of patient samples used, including gender, age, diagnosis, karyotype, FLT3/NPM1 status and other mutations if known

	Sex	Age	Diagnosis	Karyotype	FLT3	NPM1	Other
PDX							
8.3d (AML020)	M	67	AML NOS	del(20q)	ITD	wt	IDH1
9.2h (AML009)	M	33	AML M4	normal	ITD	mut	
Primary							
AML003	M	45	AML	normal	ITD	mut	
AML004	F	36	AML	normal	ITD	mut	
AML005	M	73	AML M5	FISH negative/ karyotype not available	ITD	mut, type A	
AML006	F	55	AML	normal	ITD	mut	
AML008	F	49	AML M4	normal	ITD	mut	
AML009	M	33	AML	NA	ITD	mut	
AML023	F	78	AML	46, XX	ITD	mut	IDH1
AML027	F	27	AML	FISH negative/ karyotype not available	ITD	mut, type non-A	
AML032	F	72	AML	46, XX	ITD	mut, type A	IDH2

3.2.2.5 Recovery of primary patient and PDX cells

Frozen primary patient and PDX cells, were thawed at 37°C in a water bath and the cell suspension was gently mixed with 1 mL pre-warmed DAMP solution (Section 3.1.1.2.3.). Gradually, an additional 9 mL of DAMP solution was added dropwise over a 10-min period

with constant agitation to prevent clumping of cells. The solution was centrifuged at 150*g* for 10 mins and supernatant was discarded. Cells were washed a second time with 10 mL DAMP followed by a wash with 5 mL 2% (v/v) FBS in PBS. Finally, the cell pellet was resuspended in serum-free expansion medium (SFEM) with high growth factor to maximize cell recovery post-thaw (Section 3.1.1.2.4). Cell number and viability was assessed by trypan blue exclusion cell count and cells were transferred to an appropriate cell culture vessel for 4 hrs incubation at 37°C, 5% CO_2 in a humidified incubator.

3.2.2.6 Culture of primary patient and PDX cells

Primary and PDX cells that were incubated for 4 hrs at 37°C, 5% CO_2 in a humidified incubator were collected and washed in 2% (v/v) FBS in PBS. Cells were filtered through a 70μM filter to obtain a homogenous cell suspension. Cell number and viability was assessed by trypan blue exclusion cell count and cell were resuspended in either SFEM or SFEM with physiological growth factor (Section 3.1.1.2.5) at a cell density between 3-5x10^5 cells/ mL. Cells were plated either on plastic or in co-culture with MS-5 stromal cells. MS-5 cells were seeded the day before at appropriate density in multi-well cell culture plates to reach approximately 70% confluency the next day. Following overnight incubation, MS-5 culture medium was discarded by aspiration and replaced by primary patient and PDX cells. Cells were treated 24 hrs after plating and collected for protein and functional assays as described in the experimental design.

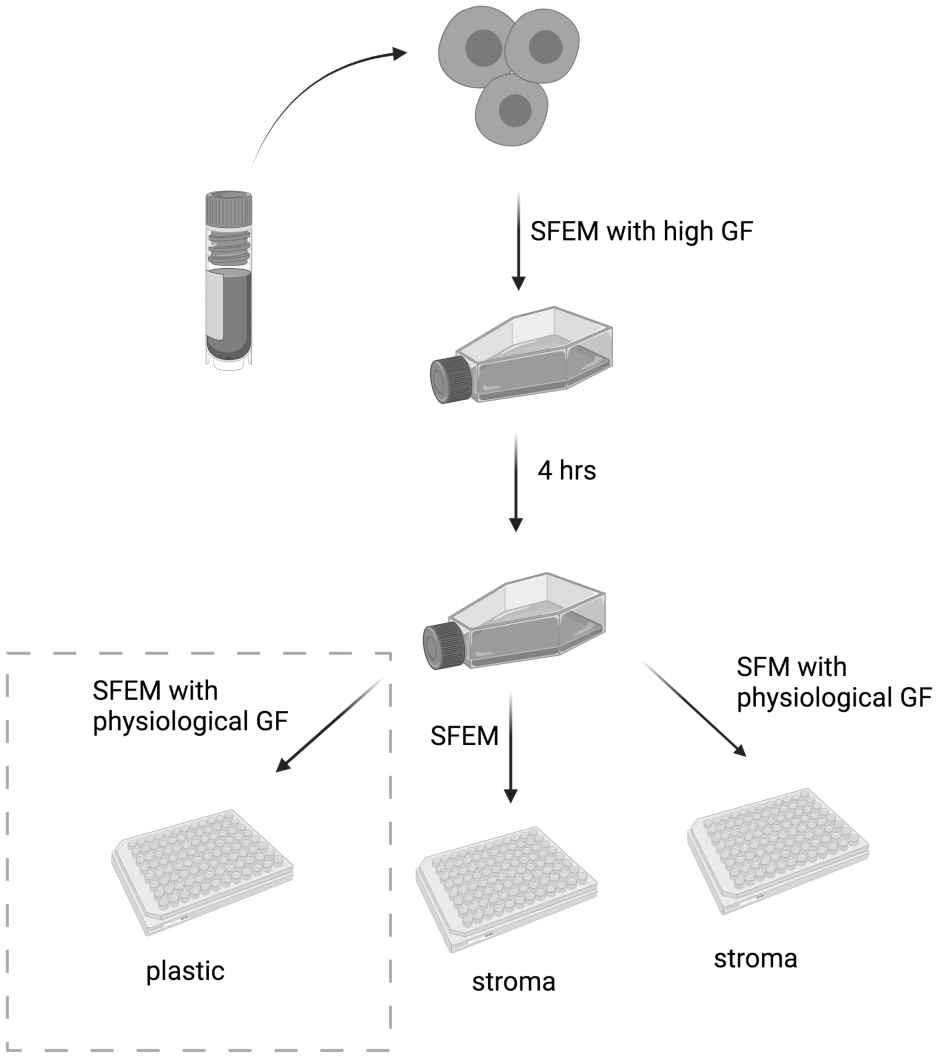

Figure 3.1 Culture of primary patient and patient-derived xenograft (PDX) cells

Schematic illustration of the recovery and culture of primary and PDX cells, where cells are resuspended in serum-free expansion media (SFEM) with high growth factors and incubated for 4 hrs at 37°C, 5% CO_2 in a humidified incubator to recover post-thaw. Following recovery, cells are resuspended in either SFEM or SFEM supplemented with physiological growth factors and cultured on plastic or in co-culture with MS-5 stromal cells, plated the day before. PDX cells were plated in the presence or absence (dashed square) of stroma while primary patient cells were always plated with stroma.

3.2.3 Trypan blue cell counting and viability assessment

Cell counting and viability assessment was performed by trypan blue dye exclusion using a hematocytometer. The assay is based on the principle that viable cells have intact cell membranes that exclude dyes such as trypan blue, whereas dead cells do not. Trypan blue stock (0.4%) (Section 3.1.1.2.1) was diluted 10-fold in PBS before use. The working stock solution was mixed with cell suspension in a ratio of 1:2 (or higher if necessary) and 10 µL of the mix was pipetted in the counting chamber. The following formula was used to calculate

the concentration of cells/mL: concentration = number of cells x 10,000 / number of squares, corrected for the dilution factor. This formula is based on the fact that 1 mm^2 has a volume of 0.1 uL and the depth of the chamber is 0.1 mm.

3.2.4 Resazurin assay

Cell growth was assessed by resazurin assay, which is based on the reduction of oxidized non-fluorescent resazurin to fluorescent resorufin by viable cells. The quantity of resorufin produced is proportional to the number of viable cells. Cells were seeded at $1x10^5$ cells/mL density in appropriate well format.

Following drug treatment, cell suspension was homogenized by pipetting and 100-200 µL volume was transferred in technical triplicates to a clear flat-bottom 96-well plate. At least three minus cell controls (consisting of cell medium of equal volume) and empty wells (blanks) were included on each plate. Resazurin stock (Section 3.1.2.1.1) was diluted 50-fold in pre-warmed serum-free medium (SFM) and 10% (v/v) of working concentration was added to each well and mixed. The plates were incubated for 4 h at 37°C, 5% CO_2 in a humidified incubator to allow for sufficient change in color of the dye. Fluorescence was recorded at 535 nm excitation and 590 nm emission in a plate reader (SpectraMax M5). Cell proliferation relative to vehicle control was calculated by subtracting the minus cell control and blank measurement from the test sample reading.

3.2.5 Flow cytometry

Flow cytometry is a useful tool that enables rapid detection, counting and sorting of significant number of cells at single cell level. The main principle is based on the passage of cells in a liquid stream through a laser beam and when a laser beam hits the cells, scattering of light and emission of fluorescence occurs. The flow cytometer measures multiple physical characteristics of a single cell such as size and granularity (FSC and SSC), which can be used to identify and sort different cell types. Furthermore, flow cytometry can be applied measure cell cycle status, and detect intracellular proteins and surface markers using specific antibodies.

3.2.5.1 Apoptosis assay

Cells were seeded at $1x10^5$ cells/mL density and following drug treatment, cells were harvested by centrifugation for 5 mins at 300 *g*. Cells were washed with Hank's Balanced Salt Solution (HBSS) to remove media and subsequently stained in 100 µL annexin V/DAPI staining solution (Section 3.1.3.2.2) for 15 mins at room temperate in the dark. Following staining, 400 µL HBSS was added to each tube before analysis using the FACSCantoII flow

cytometer (BD Biosciences). An unstained control was included to determine autofluorescence signal or background staining. In addition, single stain controls were included to determine the level of spectral overlap between fluorophores and allows compensation. The percentage of viable and apoptotic cells was quantified using the FlowJo software (Figure 3.2).

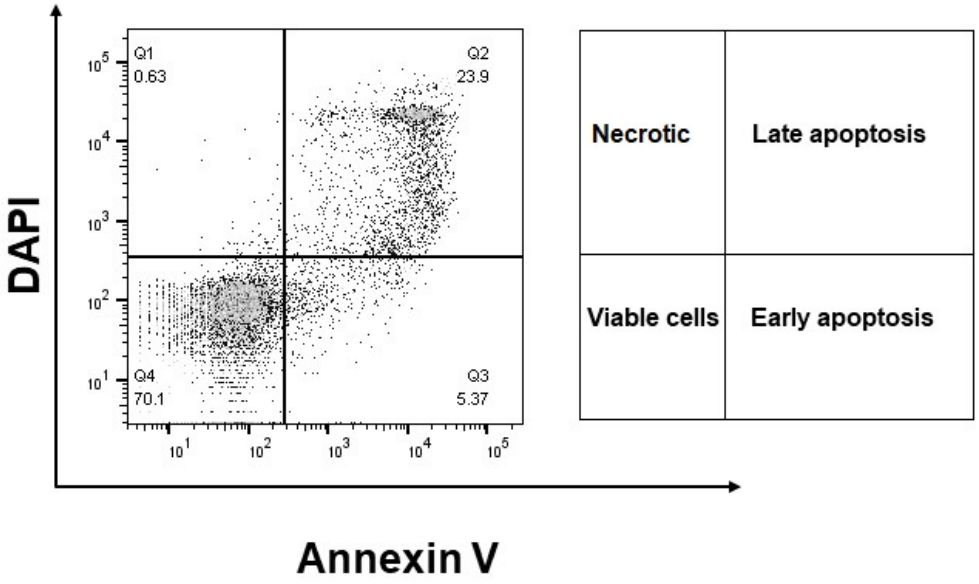

Figure 3.2 Representative example of apoptosis analysis

Apoptosis was assessed using annexinV/DAPI staining. FlowJo software was used to compute the percentage of cells in each quadrant using single stained controls and unstained control to set the gating. Viable cells are negative for both annexinV and DAPI, cells in early apoptosis are annexin positive but DAPI negative, cells in late apoptosis are double positive for annexinV and DAPI, and necrotic cells are annexinV negative and DAPI positive. For calculation of % of apoptosis, the sum of % of cells in early and late apoptosis were calculated.

3.2.5.2 Cell cycle analysis

Flow cytometry was used to assess cell cycle state of cells following drug treatment. Here, propidium iodide (PI) was used, a fluorescent vital dye that binds both deoxyribonucleic acid (DNA) and ribonucleic acid (RNA). To ensure only DNA is stained, cells were treated with ribonuclease.

Cells were seeded at $1x10^5$ cells/mL density and following drug treatment harvested by centrifugation for 5 mins at 300*g*. Cells were washed with PBS to remove medium and fixed by resuspending in 100 µL ice cold 70% (v/v) ethanol in PBS solution. Ethanol allows cells to be fixed and permeabilized. Samples were stored overnight at -20°C and were washed twice

with PBS to remove ethanol. Cells were stained in 250 µL PI staining solution for 30 mins in the dark at 37˚C before being analyzed using the flow cytometer. An unstained control was included to differentiate autofluorescence or background staining. Forward versus and side scatter (FSC vs SSC) plots were made to exclude analysis of cellular debris and dead cells. Data was acquired using BD FACSDiva software. The percentage of cells in each cell phase: G0/G1, S, or G2M was quantified using the FlowJo software (Figure 3.3).

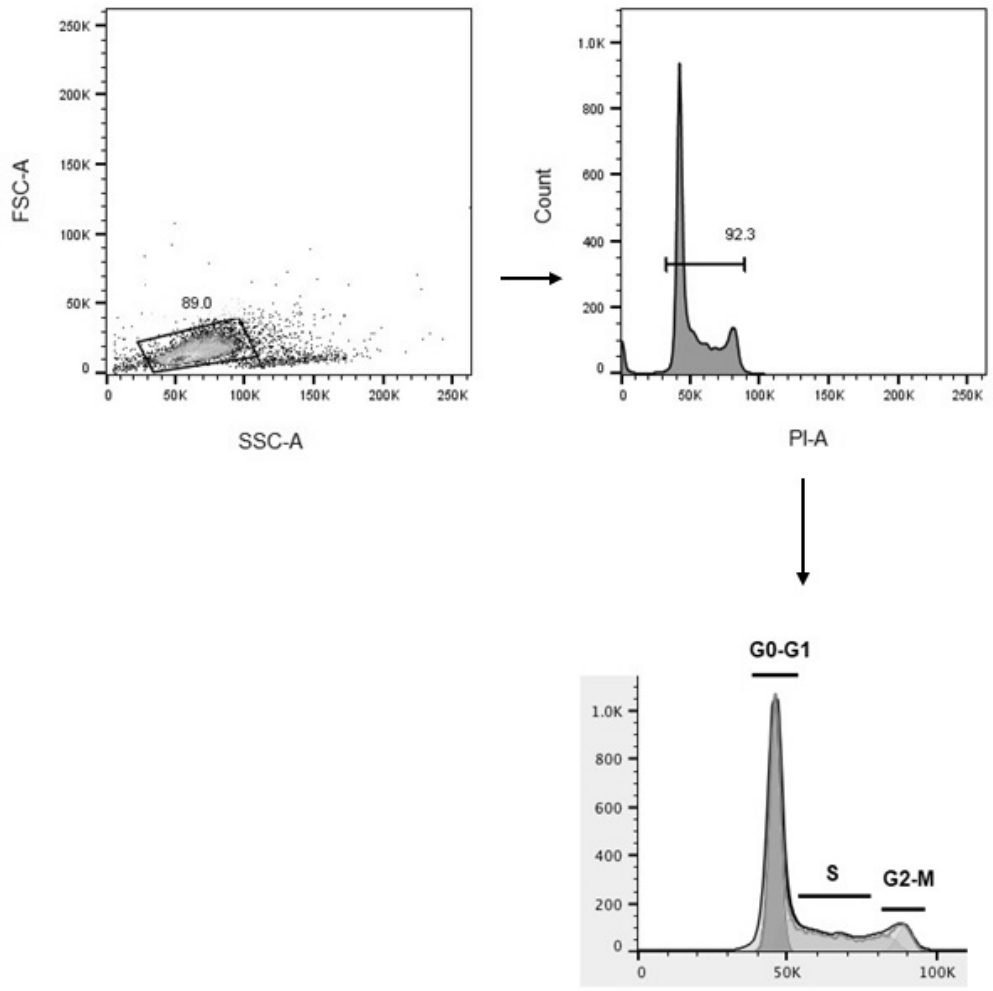

Figure 3.3 Representative example of cell cycle state analysis

Cell cycle status was assessed using propidium iodide (PI)/ ribonuclease staining. Initial gating was placed on the forward versus side scatter (FSC vs SSC) plot. FlowJo software was used to compute the percentage of cells in each phase of the cell cycle.

3.2.5.3 Quantification of protein expression

Quantification of protein expression by flow cytometry was performed both in cell lines and primary patient cells, in which the latter were co-cultured with stromal cells. In the case of primary patient samples, collected cells were washed with PBS and stained for 10 mins in 100 µL 1:100 dilution anti-human CD45 on ice protected from light. After staining for cell surface markers where applicable, pelleted cells were resuspended in 100 µL 4% (v/v) formaldehyde (Section 3.1.3.2.3) and fixed for 15 mins at room temperature. Following fixation, cells were washed twice with PBS and resuspended in their residual volume. Cells were permeabilized by slowly adding 1mL of ice-cold absolute methanol whilst vortexing. The samples were stored overnight at -20˚C and were washed twice with PBS to remove methanol. Following washing, an aliquot of cells was taken as unstained control to set up the voltages and gating. Cells were resuspended in 100 µL of primary antibody dilution (Section 3.1.3.4) diluted in 5% (w/v) BSA in TBS-T and were incubated for 1 hr at room temperature protected from light. Cells were washed twice with PBS and resuspended in 100 µL of diluted fluorochrome-conjugated secondary antibody prepared in 5% (w/v) BSA in TBS-T. After incubation for 30 mins at room temperature protected from light and two washes with PBS, cells were analyzed on the flow cytometer. The percentage of inhibition was calculated using the following formula: (MFI untreated - MFI treated) / (MFI untreated - MFI unstained) *100%, where MFI is the geometric mean fluorescence intensity calculated using the FlowJo software (Figure 3.4).

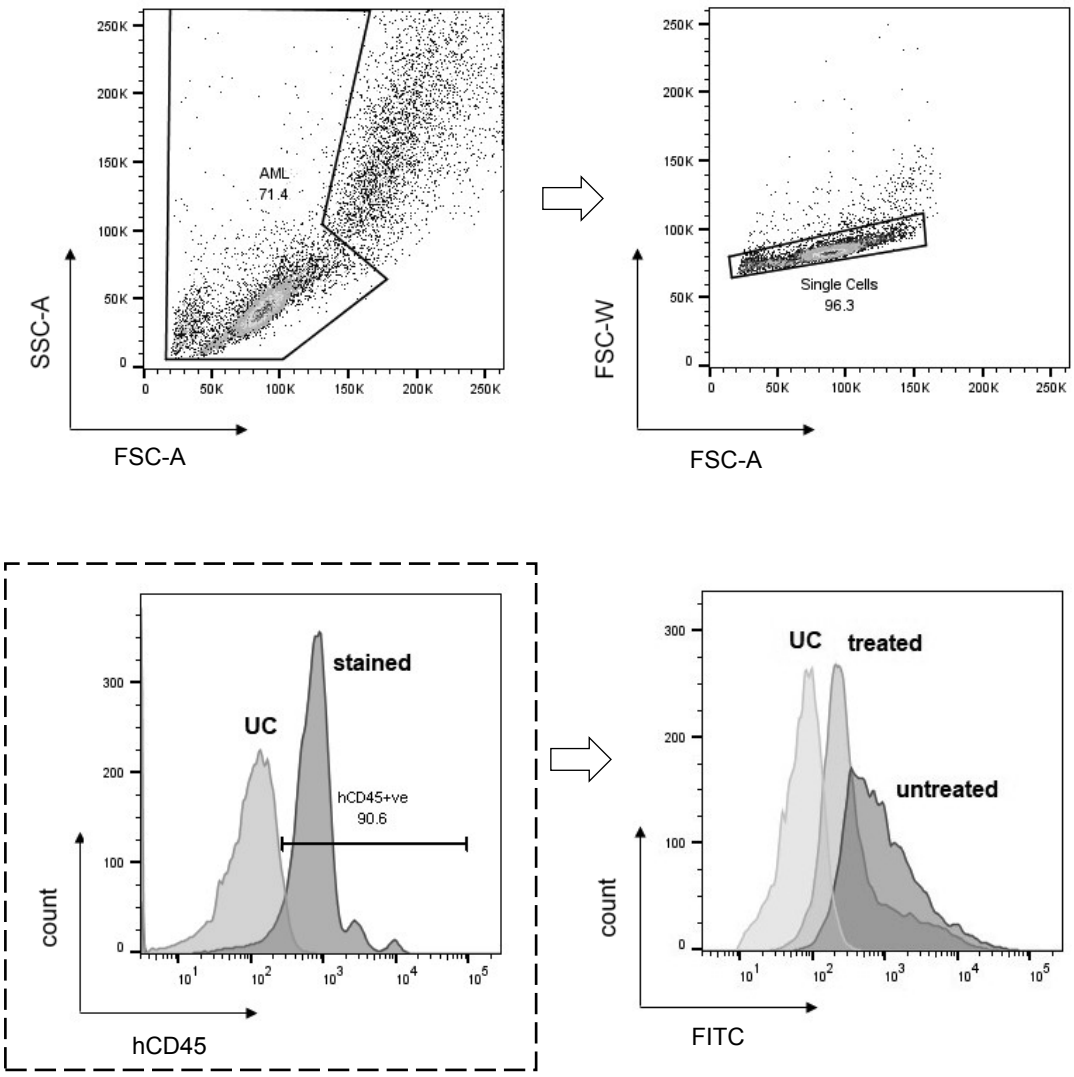

Figure 3.4 Representative example of quantitative protein expression analysis

Representative example of detection and quantification of protein expression by intracellular staining. The example presented is from primary patient cells co-cultured with stromal cells. The cell population of interest was gated on the forward vs side scatter (FSC vs SSC) plot and doublets were excluded from the FSC area vs width plot (FSC-A vs FSC-W). In case of co-cultured primary patient blasts, cells were stained for human CD45 to discriminate the AML blasts from stromal cells (dashed square). The geometric mean fluorescent intensity (MFI) was calculated using the FlowJo software. The percentage of inhibition was calculated from the MFI difference of treated vs untreated cells, respective to unstained control and multiplied by 100.

3.2.5.4 Flow cytometric analysis of primary patient and PDX sample

Cells in suspension were collected by pipetting and adherent cells were collected by washing with PBS followed by trypsinization. Cells were pelleted by centrifugation for 5 mins at 300*g*, washed with PBS and resuspended in 100 µL antibody staining mix (Section 3.1.3.2.4) for 10 mins on ice protected from light. To assess cell count in parallel, 50 µL of CountBright™ Absolute Counting Beads (further explained in Section 3.2.5.5**)** was added prior to analysis.

An unstained control was included to differentiate autofluorescence or background staining. Fluorescence minus one (FMO) controls were used the first time performing the experiment to set up the compensation matrix. FMO controls are used to identify and gate cells in the context of spectral overlap due to the multiple fluorophores in a multi-color panel. Forward versus and side scatter (FSC vs SSC) plots were made to exclude analysis of cellular debris and dead cells. Data was acquired using BD FACSDiva software. The percentage of surface marker expression and viability was quantified using the FlowJo software (Figure 3.5).

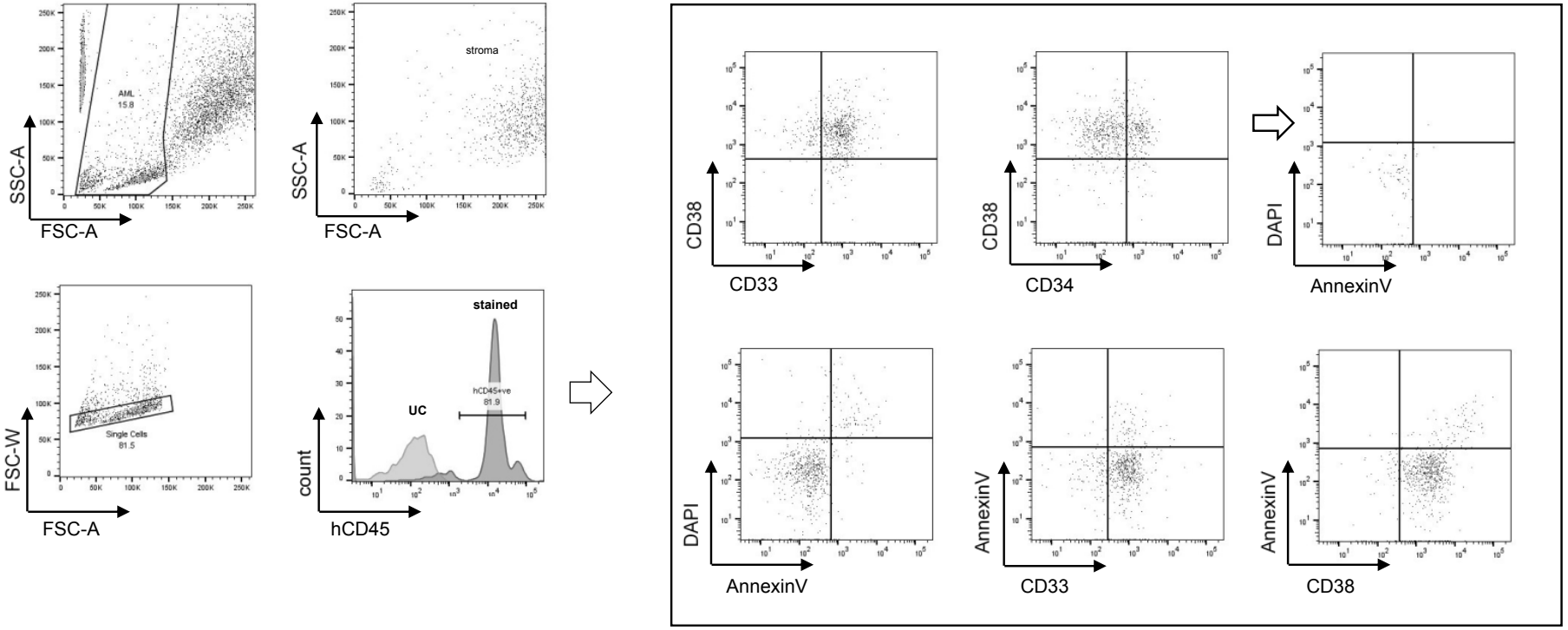

Figure 3.5 Representative example of primary patient and PDX sample analysis

A multi-color antibody panel was used to identify and characterize cell populations of interest. Stromal cells were excluded from the forward vs side scatter (FSC vs SSC) plot by including a stroma only control, based on the finding that they differ in size from AML cells. Doublets were excluded by gating on the FSC-A vs FSC-W plot. In the case of primary-derived xenograft (PDX) cells, murine CD45 positive cells were excluded. Human CD45 positive (hCD45+) population was defined using the unstained control. From the hCD45+ cell population, CD33 vs CD38 (myeloid markers), CD34 vs CD38 (markers of the stem cell-like population), annexinV vs DAPI (viability), CD33 vs annexinV and CD38 vs annexinV plots were created. The unstained control was used to identify the appropriate gating of CD33, CD34, CD38, annexinV and DAPI positive populations. From the stem cell-like population (CD34+CD38-) apoptosis was assessed by annexinV/DAPI staining.

3.2.5.5 Cell growth assay

To assess cell growth of co-cultured primary patient and PDX cells, CountBright™ Absolute Counting Beads (Thermo Fisher Scientific) were used. The bottle containing the beads were vortexed for 30 seconds and 50 µL of beads were transferred in each 5 mL polystyrene round-bottom tube. The tube content was mixed by flicking or vortexing and directly analyzed by flow cytometry. The forward scatter voltage was set low enough to visualize the beads. The bead population was gated using the FSC vs SSC plot and at least 1000 events were recorded (Figure 3.6). The concentration of cells in suspension was calculated with the following formula: (number of cell events / number of bead events) * (assigned bead count of the lot per 50 µL) / (volume of sample in µL) = cell concentration (cells/ µL). Number of cell events in this thesis refers to the viable AML blast population, thus hCD45+ and annexinV- DAPI-.

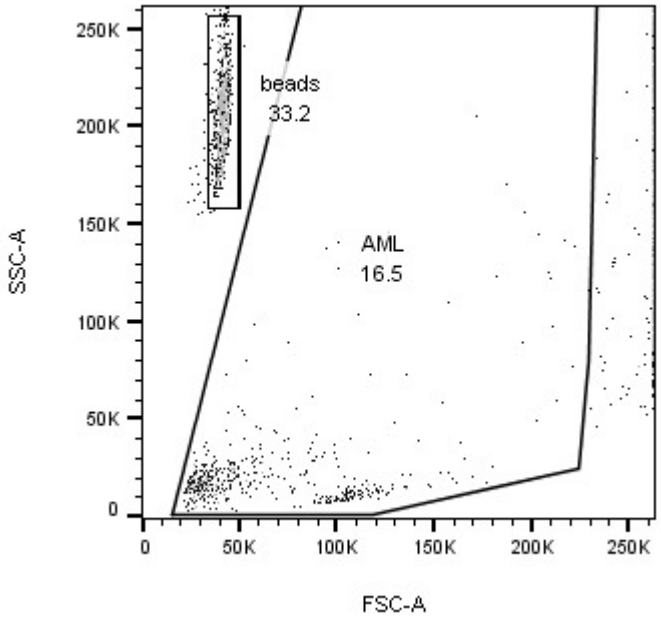

Figure 3.6 Representative example of cell growth assay using counting beads

Cell growth was assessed using CountBright™ Absolute Counting Beads. At least 1000 bead events were recorded by gating on the bead population using the forward vs side scatter (FSC vs SSC) plot. Cell concentration was calculated using the following formula: (number of cell events / number of bead events) * (assigned bead count of the lot per 50 µL) / (volume of sample in µL) = cell concentration (cells/ µL).

3.2.5.6 Fluorescence activated cell sorting (FACS) of primary human CD45+ cells

Cell sorting was performed on primary patient samples co-cultured with MS-5 stromal cells to isolate and collect viable human CD45+ cells. Cell sorting was performed thanks to Jennifer Cassels. Suspension cells were collected by pipetting and adherent cells were

collected by washing with PBS followed by trypsinization. Cells were pelleted by centrifugation for 5 mins at 300*g* and washed with PBS to remove cell culture media. Cells were stained in 100 µL anti-human CD45 antibody in HBSS buffer for 10 mins in the dark on ice. After staining, the volume was adjusted to 500 µL with HBSS buffer and cell suspension was passed through a 70 µm filter prior to sorting with a BD FACS Aria with Diva software. An unstained control was used to set the voltages and identify the appropriate cell population. Gating was performed on human CD45+ population that was viable from the forward and side scatter plot. Doublets were excluded from the analysis by plotting height against the area for forward scatter. Sorted cells were collected in a 15 mL falcon tube containing a few mL of SFEM with physiological growth factors.

3.2.6 Western blotting

3.2.6.1 Protein extraction and quantification

Cells were pelleted by centrifugation for 5 mins at 300*g*, 4˚C, washed once with 1 mL ice-cold PBS and stored at -80˚C until further use. Cells were lysed by adding 25 µL protein extraction buffer (Section 3.1.4.2.1) l freshly supplemented with phosphatase and protease inhibitors per $1x10^6$ cells. The lysate was mixed vigorously by vortexing every 5 mins for a period of 30 mins and subsequently centrifuged for 20 mins at 16,000*g*, 4˚C. The supernatant was transferred into a new 1.5 mL Eppendorf tube. The protein concentration was determined using the Pierce Coomassie Plus (Bradford) Assay kit that includes an albumin standard curve. The cell lysate was diluted 20-fold in dH_2O, 5 µL of each sample was pipetted in technical triplicates in a flat-bottom clear 96-well plate and 250 µL of Bradford reagent was added. The plate was incubated for 10 mins at room temperature on a shaker and absorbance was measured at 595 nm using a plate reader.

3.2.6.2 Gel electrophoresis and immunodetection

Samples were prepared according to Section 3.1.4.2.2 and boiled for 10 mins at 70˚C in a heating block to denature and reduce proteins. After cooling down on ice, samples were briefly centrifuged and loaded on a precast NuPAGE 4-12% Bis-Tris gradient gel. In a separate lane, 5 µL of PageRuler Plus Prestained protein ladder was included. Gels were run between 80-90 mins at 120 V and transferred onto a nitrocellulose membrane using the Mini Blot Module wet transfer device for 60 mins at 10 V. After transfer, membranes were stained with Ponceau S protein stain and cut to detect multiple proteins of interest of different size from the same membrane. Any residual staining was removed by washing with dH_2O and subsequently membranes were blocked for 1 hr in blocking solution at room temperature. After blocking, membranes were incubated overnight in primary antibody

solution diluted in blocking solution at 4˚C. The next day, the membranes were washed three times for 5 mins each wash with TBS-T and incubated with appropriate secondary antibody diluted in blocking solution at room temperature. To remove unbound secondary antibody, the membranes were washed again three times for 5 mins each wash with TBS-T and developed by covering the membrane with SuperSignal West Pico PLUS Chemiluminescent Substrate. Membranes were analyzed using the Odyssey Fc Imaging System. Band intensities were quantified using ImageStudio, the acquisition and analysis software for the Odyssey Fc. Ratio phosphorylated to total protein was calculated following normalization to loading control.

3.2.7 Polymerase chain reaction (PCR)

3.2.7.1 Primer design

Pubmed NCBI gene database was used to design primers sets specific for the target gene of interest. To confirm the specificity of the primers sets for the gene of interest, primers were tested on BLAST. Primers were designed to flank exon junctions to avoid amplification of contaminating genomic DNA. Other parameters applied included primer melting temperature (Tm) of 57 to 63 ˚C, GC content of 50-60% for product stability, and amplicon length < 200 base pairs (bp). The list of primers used in this thesis can be found in Section 3.1.5.2.7.

3.2.7.2 RNA extraction

RNA extraction was performed using the RNeasy® Plus Mini Kit (Qiagen) according to manufacturer's instructions. Briefly, pelleted cells were lysed and homogenized using specific buffers to ensure isolation of intact RNA. For optimal homogenization, lysates were passed through QIAshredder spin column. Genomic DNA (gDNA) was then removed by passing the flowthrough through a gDNA eliminator spin column. The sample was loaded on a RNeasy spin column to which RNA binds and after washing out contaminants, RNA was eluted.

The quantity and quality of RNA was determined using the NanoDrop 1000 Spectophotometer (Labtech). As quality control the ratio of absorbance at 260 and 280 nm was measured as purity indicator. A ratio of 2.0 is generally accepted as pure RNA.

3.2.7.3 cDNA synthesis

First strand cDNA synthesis was performed by preparing a mastermix containing 0.5-1 µg RNA, random hexamers, and deoxynucleotide triphosphate (dNTPs) (Section 3.1.5.2.3). The mix was heated at 65°C for 5 mins on the thermocycler (ProFlex PCR System) and incubated on ice for at least 1 min. Following brief centrifugation, the reverse transcription

mastermix was added, consisting of reaction buffer, dithiothreitol (DTT), RNase inhibitor and reverse transcriptase (Section 3.1.5.2.4). A no reverse transcriptase (noRT) control was prepared to monitor gDNA contamination. The samples were subjected to the following program in the thermocycler: 23°C for 10 mins, 50°C for 10 mins and 80°C for 10 mins. After incubating on ice, samples were briefly centrifuged, and the final volume was adjusted to 100 µL using nuclease-free H_2O. Samples were stored at -20°C.

3.2.7.4 Quantitative real time PCR (RT-qPCR)

The basic principle of RT-qPCR is the detection and quantification of messenger RNA (mRNA) expression. For each reaction, a RT-qPCR mastermix (Section 3.1.5.2.5) was prepared and loaded in triplicate on a MicroAmp optical 96-well reaction plate. Primers encoding for housekeeping genes *GAPDH* and *ACTB* were included to normalize mRNA expression between different samples. Beside a noRT control a no template control (NTC) was included for each primer pair to monitor contamination and primer-dimer formation. The plate was mixed briefly by vortexing and centrifuged for 30 sec at 300*g*. The qPCR thermal cycling conditions were as shown in Table 3.3 (7900HT Fast Real-Time PCR System, Thermo Fisher Scientific). After the run completed, the fluorescence data was analyzed using the Applied Biosystem's SDS software to calculate the cycle threshold (Ct) values. To determine the expression fold change, first the average Ct value of the two housekeeping genes was subtracted from the average Ct value of target gene to calculate the ΔCt value. Then, the differences between ΔCt values for each experimental and control condition (i.e., no drug control) were calculated to obtain the ΔΔCt value. The expression fold change of the target gene when treated relative to untreated control was calculated using the $2^{-\Delta\Delta Ct}$ equation.

Table 3.3 Quantitative real time polymerase chain reaction (RT-qPCR) thermal cycling conditions

Step	Temperature (˚C)	Duration (mins)	Cycles
1	50	2:00	1
2	95	0:10	1
3	95	0:15	40
4	60	1:00	

3.2.7.5 PCR amplification of gDNA

Extraction of gDNA was performed using the DNeasy® Blood and Tissue Kit according to manufacturer's instructions. Briefly, pelleted cells were lysed and loaded onto a DNeasy spin column to which DNA is bound. Specific washing buffers were used to remove contaminants and enzyme inhibitors after which DNA was eluted and quantified using a nanodrop spectrophotometer. DNA purity was determined by the 260/280 absorbance ratio where a ratio of 1.8 is generally considered pure DNA.

For PCR, a mastermix was prepared using the GoTaq® G2 DNA Polymerase kit (Promega), dNTPs and target-specific primers (Section 3.1.5.2.6). 1 µL gDNA was added to the mastermix per reaction and thermal cycling conditions shown in Table 3.4 was programmed on the thermocycler. The PCR product was run on a 3% (w/v) agarose gel made with 1x TAE buffer (Section 2.1.5.2.2) plus 1:10,000 SYBR™ Safe DNA Gel Stain (Thermo Fisher Scientific) for 60 mins at 100 V. In a separate lane, 6 µL DNA ladder was loaded. The gel was imaged using the Odyssey Fc Imaging System.

Table 3.4 PCR amplification of FLT3-ITD DNA thermal cycling conditions

Step	Temperature (˚C)	Duration (mins)	Cycles
1	95	2:00	1
2	95	0:30	30
3	62	0:30	
4	72	0:30	
5	72	2:00	1

3.2.8 Reverse Phase Protein Array (RPPA)

RPPA is a high-throughput antibody-based proteomic tool, which enables simultaneous quantification of multiple proteins in a sample. One great advantage over western blotting is the little amount of protein required. Its principle is based on the spotting of protein lysates onto a nitrocellulose-coated glass slide and detection and quantification of proteins using specific primary antibodies that bind to the protein of interest.

Cells were pelleted by centrifugation for 5 mins at 300*g* (4°C) to remove culture media and subsequently washed with PBS. Pellets were stored at -80°C. Protein lysis and quantification, spotting of protein lysates, and protein quantification was kindly performed by Dr. Valentina Serafin's laboratory staff.

3.2.9 Cytokine profiling

Cytokine profiling was performed to detect and measure the levels of secreted cytokines using the Luminex® Multiplex Assay. The Luminex® Multiplex Assay is a bead-based immunoassay that enables rapid high-throughput measurement of multiple analytes in a biological sample. The technology utilizes fluorescent magnetic beads that correspond to a unique spot on the fluorescent spectrum, or 'bead region'. The beads are coated with a capture antibody specific for one analyte of interest. The captured analyte from a biological sample such as cell culture supernatant, is detected using biotinylated detection antibody and conjugated reported dye streptavidin-conjugated R-phycoerythrin (SA-RPE). A Luminex® instrument is used to measure both the magnetic beads and the corresponding analyte of interest, and SA-RPE fluorescence to quantify the amount of analyte bound.

Cells were plated and treated in technical duplicates. To collect cell culture supernatant, cell suspension from co-cultured AML blasts was collected by pipetting. The cell suspension was centrifuged for 5 mins at 300*g* and supernatant was transferred to a new Eppendorf tube. Supernatant was stored at -80°C. Frozen samples were thawed on ice, mixed well by vortexing, followed by centrifugation at 10,000*g* for 10 mins to remove particulates. Cytokine profiling was performed using the Cytokine 25-Plex Human ProcartaPlex™ Panel 1B (Thermo Fisher Scientific) according to manufacturer's instruction. The MAGPIX® System (Luminex® xMAP® Technology) was used to read the plate. ProcartaPlex™ Analyst software was used for data analysis.

3.2.10 Statistical analysis

In all figures, the data is either shown as individual values or as mean. Error bars represent the standard deviation (SD). Statistical analysis was performed using the GraphPad Prism software. To compare multiple related groups, paired one-way ANOVA with Dunnett's or Tukey's multiple comparisons test was performed. Dunnett's test was perfomed to compare the mean difference between multiple experimental groups against a control group mean (vehicle control) whereas Tukey's test was performed to compare all groups (monotherapy *versus* combination therapy).

To compare multiple groups that have been divided into two independent variables, two-way ANOVA was used followed by Tukey's or Holm-Šidák's multiple comparisons test. A p-value of <0.05 was considered significant.

Combination index (CI) was calculated to assess whether combination of two drugs has a synergistic effect. In this thesis work, where indicated, two methods were used to calculate synergy: Chou-Talalay and Bliss Independence. Chou-Talalay method is based on the

median-effect equation derived from the mass-action law principle. CompuSyn software was used to calculate synergy scores where CI<1 indicates synergism, CI=1 additive effect, and CI>1 antagonism. The Bliss Independence model uses a probabilistic interpretation and stipulates that drugs acts independently, but each of them contribute to a common result. The Bliss Independence score was calculated using SynergyFinder 2.0 or the formula: $CI = (E_A + E_B - E_A \times E_B)/E_{AB}$ where E_A is the effect of drug A, E_B the effect of drug B and E_{AB} the combined effect of drug A and B. CI <0, =0, and >0 indicates synergism, additive effect, and antagonism, respectively.

Chapter 4: Phenotypic profiling of FLT3-ITD versus FLT3 wildtype AML cell lines following treatment with FLT3 or PI3K/AKT/mTOR inhibitors

AML is a genetically heterogeneous clonal malignancy, characterized by recurrent genetic abnormalities involving *FLT3, NPM1, DNMT3A*, and *IDH* among others, leading to the proliferation and aberrant differentiation of immature clonal myeloid cells and impaired normal hematopoiesis (Arber et al., 2016; Döhner et al., 2017; Kumar, 2011; Saultz and Garzon, 2016). Mutations in *FLT3*, detected in approximately one-third of newly diagnosed patients, represent the most common genetic alteration, and is associated with increased risk of relapse and poorer survival (Daver et al., 2019; Döhner et al., 2017). The FLT3 tyrosine kinase receptor represents a putative therapeutic target and accordingly several small molecule inhibitors targeted against FLT3 have been developed and reached clinical investigation (Daver et al., 2019; Grafone et al., 2012). In physiological conditions, FLT3 is activated by its ligand, driving several downstream signaling pathways such as PI3K/AKT/mTOR and Ras/Raf/MEK/ERK (Takahashi, 2011). Mutations of *FLT3* are caused either by ITD or point mutations of the TKD, of which *FLT3-ITD* mutations are more prevalent (Mead et al., 2007). Oncogenic activation of FLT3 by ITD mutation leads to ligand-independent activation of FLT3 and its downstream signaling pathways. In contrast to FLT3 wildtype, FLT3-ITD induces aberrant activation of STAT5 (Choudhary et al., 2007).

FLT3i can be characterized as first generation and second-generation inhibitors. While first generation FLT3i refer to multi-kinase inhibitors, second generation FLT3i, including quizartinib, have more specificity and higher potency against FLT3. Quizartinib was clinically evaluated for the treatment of relapsed and refractory FLT3-ITD AML in Phase I/II/III trials in which quizartinib showed clinical efficacy with a median overall survival of approximately 6 months (Cortes et al., 2019, 2018, 2013). Despite favorable clinical outcomes using FLT3i for the treatment of FLT3-ITD AML, the duration of composite complete remission (CRc) was 12.1 weeks, due to rapid development of drug resistance (Cortes et al., 2019; Gebru and Wang, 2020; Lam and Leung, 2020). Several mechanisms of acquired resistance to FLT3i have been proposed including emerging mutations, activation of alternative signaling pathways and microenvironmental protection (Ghiaur and Levis, 2017; Lam and Leung, 2020; Smith, 2020). To potentiate the clinical outcome of quizartinib, combination strategies are under study combining FLT3i with conventional chemotherapy and other targeted therapies, such as venetoclax and azacitidine (Swaminathan et al., 2021; Yilmaz et al.,

2020). Because PI3K/AKT/mTOR is often hyperactivated in FLT3-ITD AML, it was hypothesized that combination of PI3K/AKT/mTORi with FLT3 targeted therapy might improve clinical outcomes.

The PI3K/AKT/mTOR pathway has a key role in various cellular processes and is frequently deregulated in human cancers, which led to the discovery of multiple small molecule inhibitors targeted against key nodes of the pathway, some of which have been granted FDA approval (J. Yang et al., 2019). However, PI3K/AKT/mTORi have been unsuccessful in clinical trials in AML with adverse clinical outcome due to compensatory signaling, causing pathway reactivation (Darici et al., 2020; Nepstad et al., 2020). Combination treatment with PI3K/AKT/mTORi may potentiate the efficacy of FLT3i and display prolonged beneficial clinical outcome and prevent relapse. As such, aberrant activation of the PI3K/AKT/mTOR pathway is reported in AML blasts resistant to FLT3i (Lindblad et al., 2016) and concomitant inhibition of the PI3K/AKT/mTOR pathway and FLT3 displayed synergistic anti-leukemic effects in preclinical studies (Mohi et al., 2004; Wang et al., 2015; Weisberg et al., 2013). A Phase I study evaluating midostaurin plus everolimus is currently ongoing, but not recruiting (NCT00819546).

In this chapter it was aimed to uncover the phenotypic profile of FLT3-ITD versus FLT3 wildtype cells following treatment with the FLT3i, quizartinib, or PI3K/AKT/mTORi BAY-806946 and PF-04691502. BAY-806946 is a pan-PI3Ki, predominantly against PI3K-α and PI3K-δ isoforms, which has been used clinically in the treatment of adults with relapsed follicular lymphoma (Markham, 2017). PF-04691502 is a potent and selective inhibitor of PI3K (α/β/δ/γ) and mTOR that exhibited potent anticancer activity in advanced cancers, such as endometrial cancer and B-cell NHL (B-NHL) (Blunt et al., 2015; Fang et al., 2013; Latuske et al., 2017). Preliminary screen of a panel of reported inhibitors evaluated in our lab on FLT3-ITD AML confirmed that these inhibitors possess significant cytotoxic activity (Darici et al., 2021).

4.1 Confirmation of FLT3-ITD mutational status of AML cell lines

In this thesis work, two FLT3-ITD positive AML cell lines, namely MOLM-13 and MV4-11 have been used. To confirm ITD mutation of *FLT3* gene, a single multiplex polymerase chain reaction (PCR) assay was performed on genomic DNA. Following amplification, the PCR products were separated by gel electrophoresis. THP-1 cells were included as *FLT3* wildtype control. As shown in Figure 4.1, the PCR product from the *FLT3-ITD* AML cell lines were greater in size than the *FLT3* wildtype cell line. These results confirm the expected 21 base pairs (bp) insertion (MOLM-13) and 30 bp insertion (MV4-11) (Table 4.1) (Quentmeier et al., 2003). While MV4-11 express exclusively the mutated allele, MOLM-13 express both mutated and wildtype allele, which is the reason a second band is detected for the latter.

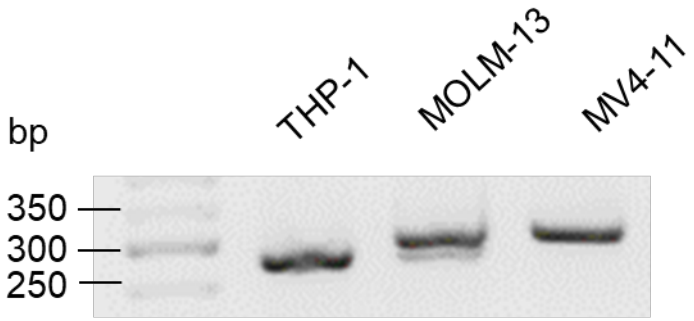

Figure 4.1 Detection of FLT3-ITD in AML cell lines

Human AML-derived cell lines MOLM-13 and MV4-11 express *FLT3-ITD* as assessed by PCR. AML cell line THP-1 was included as *FLT3* wildtype control.

Table 4.1 FLT3 status of AML cell lines

Cell line	FLT3 status	Notes
THP-1	WT/WT	
MOLM-13	WT/ITD	21 bp insertion
MV4-11	ITD/ITD	30 bp insertion

4.2 FLT3 or PI3K/AKT/mTOR inhibitors inhibit growth of AML cell lines

The growth inhibitory activity of quizartinib (FLT3i), BAY-806946 (pan-PI3Ki), PF-04691502 (dual PI3K/mTORi), as well as cytarabine (cytosine arabinoside, AraC; standard chemotherapy), was examined on both FLT3 wildtype (THP-1) and FLT3-ITD (MOLM-13 and MV4-11) AML cell lines. Growth inhibitory effect was assessed at 24, 48 and 72 hrs by resazurin-based metabolic assay and IC50 concentrations determined from the cell growth curves (Figure 4.2-4.4; Table 4.2).

Quizartinib induced growth inhibition in both FLT3-ITD AML cells with IC50 values of 0.7 (MOLM-13) and 0.6 nM (MV4-11) following 48 hrs drug treatment, respectively, but had no effect on the growth on THP-1 cells in the concentration range tested. This suggests that quizartinib-induced growth inhibition is selective for FLT3-ITD AML. Both BAY-806946 and PF-04691502 treatment caused growth inhibition in all three cell lines, irrespective of FLT3 status. As such, IC50 values obtained following 48 hrs BAY-806946 treatment were 117.5 nM (THP-1), 145.9 nM (MOLM-13), and 59.2 nM (MV4-11), respectively. PF-04691502 induced growth inhibition with IC50 values of 508.3 nM (THP-1), 160.9 nM (MOLM-13), and 195.4 nM (MV4-11). AraC was also evaluated as a standard chemotherapy drug that is currently used for AML treatment. AraC also exerted growth inhibition in all three cell lines with IC50 values of 2500 nM (THP-1), 245.2 nM (MOLM-13), and 12.5 nM (MV4-11). Comparison of IC50 concentrations shows that MOLM-13 and MV4-11 have the same sensitivity to quizartinib. MV4-11 seems more sensitive to AraC and BAY-806946 compared to THP-1 or MOLM-13. THP-1 is the least sensitive to AraC, however because only a single FLT3 wildtype cell line was evaluated it cannot be stated whether this difference is associated to the FLT3 status. It is worth noting that growth inhibition was not further enhanced by extending drug treatment time based on comparable IC50 concentrations obtained at 48 hrs versus 72 hrs.

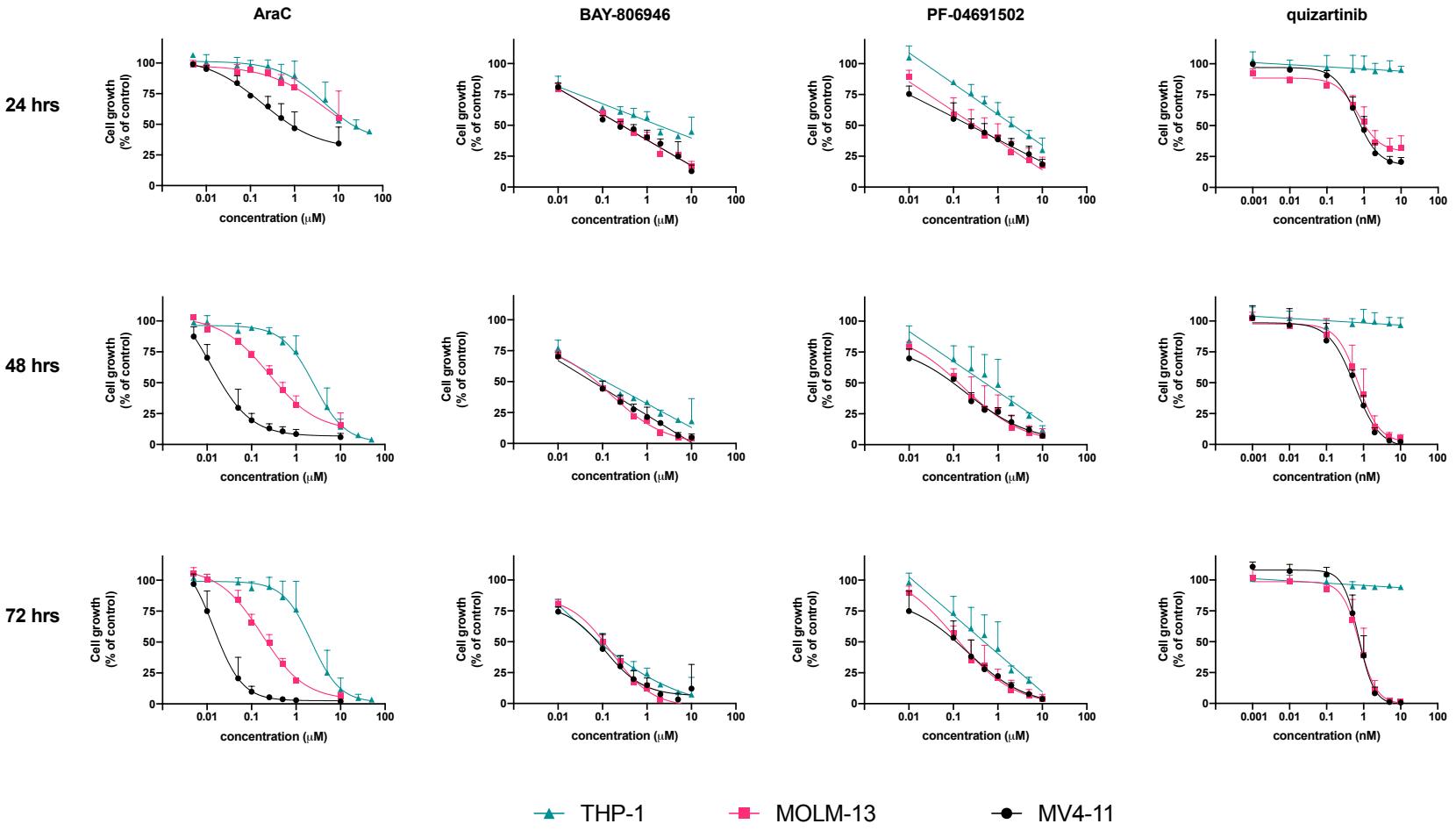

Figure 4.2 FLT3i or PI3K/AKT/mTORi induce growth inhibition in AML cell lines

THP-1 (FLT3 wildtype), MOLM-13 and MV4-11 (FLT3-ITD) cells were exposed to increasing concentrations of AraC (standard chemotherapy), BAY-806946 (pan-PI3Ki), PF-04691502 (dual PI3K/mTORi) or quizartinib (FLT3i). Growth inhibition was assessed at 24, 48 or 72 hrs by resazurin-based metabolic assay. Cell growth curves represent the averages of three independent replicates. Error bars represent average ± SD for each drug concentration. Published in (Darici et al., 2021).

Table 4.2 Summary of IC50 values of FLT3 wildtype (THP-1) and FLT3-ITD (MOLM-13 and MV4-11) AML cell lines treated with FLT3i, PI3K/AKT/mTORi, or standard chemotherapy.

Stated IC50 values (nM) for quizartinib (FLT3i), BAY-806946 and PF-04691502 (PI3K/AKT/mTORi), or cytosine arabinoside (AraC; standard chemotherapy) represent average of three independent replicates. Published in (Darici et al., 2021).

Cell line	Compound	24 hrs	48 hrs	72 hrs
THP-1	AraC	4400	2500	2200
	BAY-806946	1801.3	117.5	17.98
	PF-04691502	2252.6	508.3	497.8
	quizartinib	not reached*	not reached*	not reached*
MOLM-13	AraC	5200	245.2	169.3
	BAY-806946	273.2	145.9	155.9
	PF-04691502	304.8	160.9	111.1
	quizartinib	0.7	0.7	0.8
MV4-11	AraC	186.7	12.5	14.33
	BAY-806946	267.3	59.2	110.9
	PF-04691502	233.9	195.4	206.8
	quizartinib	0.6	0.6	0.7

* ‘not reached’ > 10,000nM quizartinib

4.3 PI3K/AKT/mTOR inhibitors induce G1 cell cycle arrest in AML cell lines

The above results suggested that quizartinib exerts growth inhibition on FLT3-ITD AML cell lines specifically, whilst BAY-806946 and PF-04691502 exert growth inhibition in both FLT3-ITD and FLT3 wildtype AML cell lines irrespective of FLT3 status. This effect was observed between 24 and 72 hrs drug treatment. The observed reduction of cell growth following drug treatment can be a manifestation of the balance between cell cycle arrest and cell death. Therefore, cell cycle status and apoptosis were assessed by flow cytometry (Section 4.4). THP-1, MOLM-13 and MV4-11 cells were treated with increasing concentrations of AraC, BAY-806946, PF-04691502 or quizartinib around the respective IC50 concentration for 24 or 48 hrs. In all three cell lines, increasing drug concentration caused accumulation of cells in the G1 phase of the cell cycle as measured by PI staining, suggesting G1-phase arrest. This was observed as early as 24 hrs after drug treatment. The G1 to (S+G2M) ratio was plotted as a measure of the proportion of cells in the G1 phase of the cell cycle.

In THP-1, no significant difference in this ratio respective to vehicle control was detected following 24 hrs drug treatment even at the highest drug concentrations tested (Figure 4.3). Following 48 hrs treatment with 2 μM BAY-806946, a statistically significant difference to vehicle control was observed ($p \leq 0.0001$). In MOLM-13, BAY-806946 and PF-04691502, but not quizartinib, induced G1 cell cycle arrest (Figure 4.4). For example, treatment with 1 μM PF-04691502 (48 hrs) led to 9.71 times increased G1 to (S+G2M) ratio, which was significantly different from vehicle control (1.33; $p=0.0052$). In MV4-11, 1 μM PF-04691502 (48 hrs) led to a ratio of 7.44 respective to 0.41 ratio observed with vehicle control ($p=0.0011$) (Figure 4.5). Quizartinib was also evaluated on THP-1 to demonstrate that there is no off-target effect. Indeed, quizartinib did not induce cell cycle arrest in FLT3 wildtype cells (Figure 4.3).

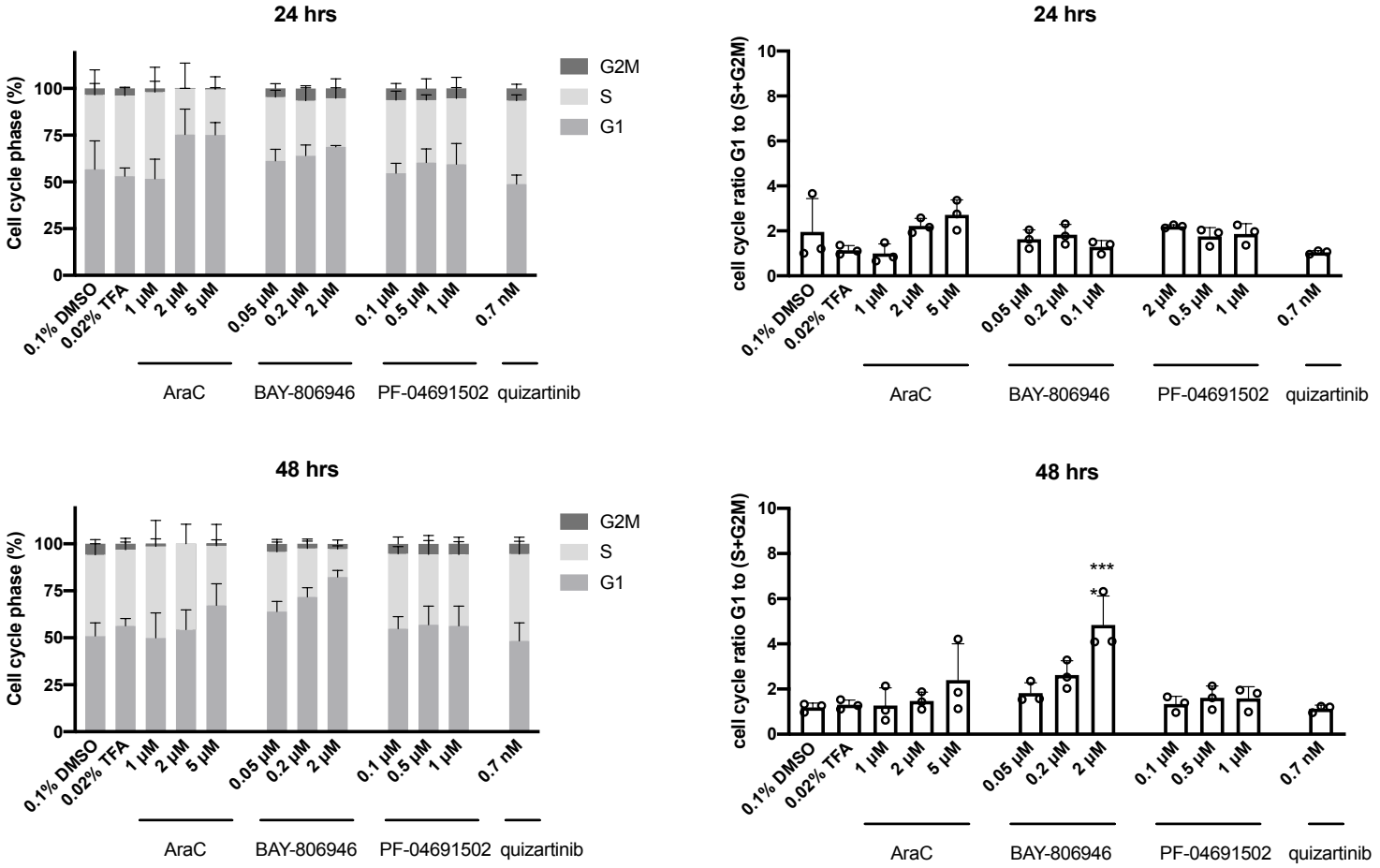

Figure 4.3 PI3K/AKT/mTORi induce G1 cell cycle arrest in THP-1 cells

THP-1 (FLT3 wildtype) cells were exposed to increasing concentrations of AraC, BAY-806946, PF-04691502, and quizartinib for 24 or 48 hrs. THP-1 cells were treated with quizartinib to show there is no detectable off-target effect. Cell cycle state was measured by staining with propidium iodide, detected by flow cytometry. Each bar in the left graph represents the average fraction ± SD in each cell cycle phase and bars in graphs on the right represent the ratio of G1 to (S+G2M) of three independent replicates. Statistical analysis was performed by one-way ANOVA followed by Dunnett's multiple comparisons test (*p ≤ 0.05, **p ≤ 0.01, ***p ≤ 0.001, ****p ≤ 0.0001). Published in (Darici et al., 2021).

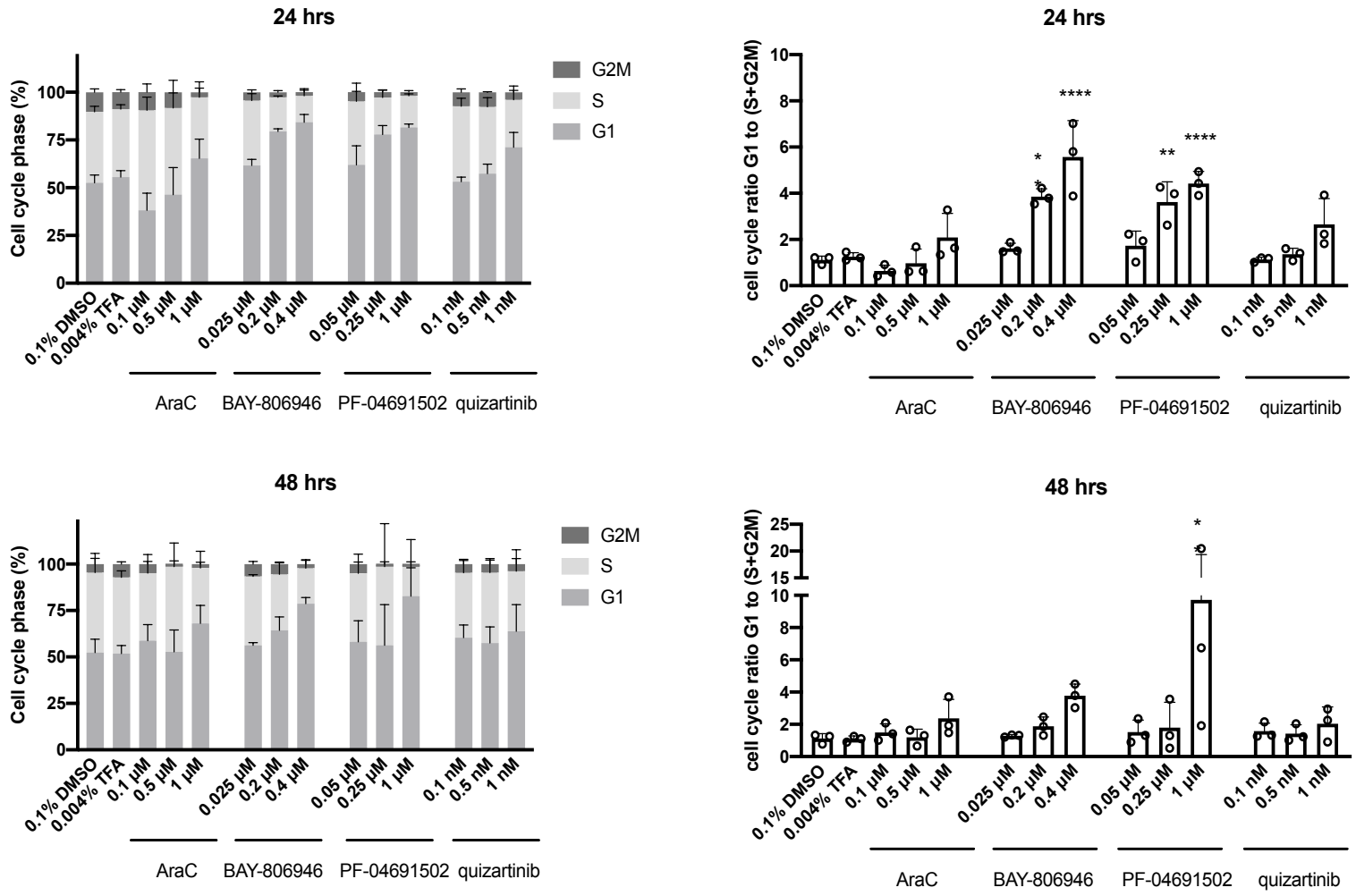

Figure 4.4 PI3K/AKT/mTORi induce G1 cell cycle arrest in MOLM-13 cells

MOLM-13 (FLT3-ITD) cells were exposed to increasing concentrations of AraC, BAY-806946, PF-04691502, and quizartinib for 24 or 48 hrs. Cell cycle state was measured by staining with propidium iodide, detected by flow cytometry. Each bar in the left graph represents the average fraction ± SD in each cell cycle phase and bars in graphs on the right represent the ratio of G1 to (S+G2M) of three independent replicates. Statistical analysis was performed by one-way ANOVA followed by Dunnett's multiple comparisons test (*p ≤ 0.05, **p ≤ 0.01, ***p ≤ 0.001, ****p ≤ 0.0001). Published in (Darici et al., 2021).

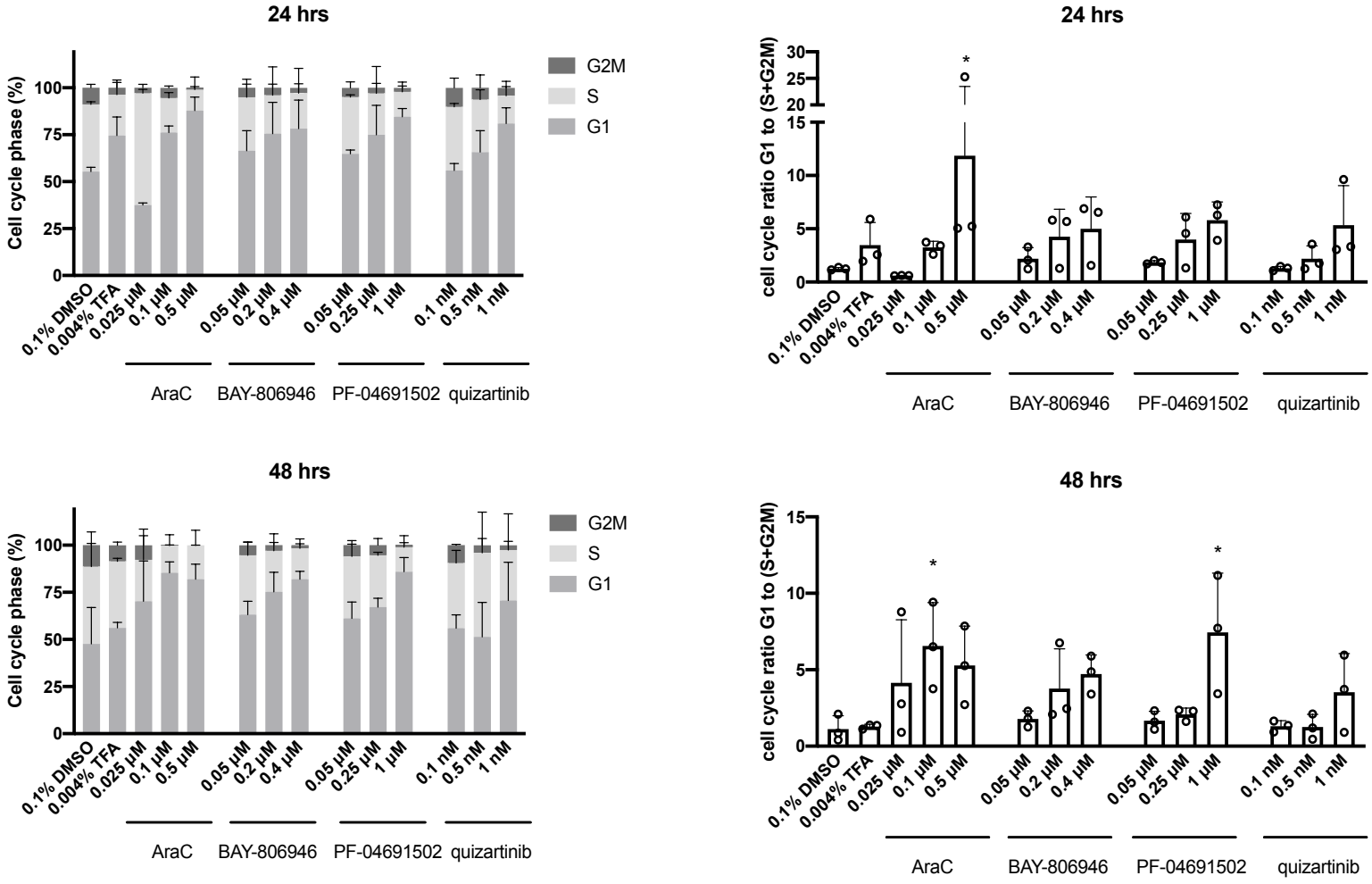

Figure 4.5 PI3K/AKT/mTORi induce G1 cell cycle arrest in MV4-11 cells

MV4-11 (FLT3-ITD) cells were exposed to increasing range of concentrations of AraC, BAY-806946, PF-04691502, and quizartinib for 24 or 48 hrs. Cell cycle state was measured by staining with propidium iodide, detected by flow cytometry. Each bar in the left graph represents the average fraction ± SD in each cell cycle phase and bars in graphs on the right represent the ratio of G1 to (S+G2M) of three independent replicates. Statistical analysis was performed by one-way ANOVA followed by Dunnett's multiple comparisons test (*p ≤ 0.05). Published in (Darici et al., 2021).

4.4 FLT3 or PI3K/AKT/mTOR inhibitors induce apoptosis in AML cell lines

Cells response to drug treatment signals growth arrest to allow DNA damage repair or other rescue mechanisms. However, if the damage cannot be repaired, this can cause the cell to undergo apoptosis. Based on the results above that suggest that PI3K/AKT/mTORi induce G1 cell cycle arrest, it was also assessed whether quizartinib, BAY-806946 and PF-04691502 induce apoptosis in THP-1, MOLM-13 and MV4-11 cells. As a positive control, AraC was included since it is well known that it induces cell death by apoptosis.

Cells were treated for 24 or 48 hrs and apoptosis was measured by annexinV/DAPI staining, detected by flow cytometry (Figures 4.6-4.8). In THP-1 cells, following 24 hrs of AraC treatment more than 50% of cells underwent apoptosis, which was further increased at higher concentrations. This confirmed that AraC is indeed cytotoxic. Treatment with quizartinib did not induce off-target cytotoxicity in FLT3 wildtype THP-1 cells. Between the two PI3K/AKT/mTORi evaluated, BAY-806946 had greater cytotoxic effects, where the highest concentration tested (2 μM) induced more than 50% apoptosis compared to vehicle control. In MOLM-13 and MV4-11 cells, only the highest test concentration of BAY-806946 and PF-04691502 induced apoptotic effects that were significantly different from vehicle control after 48 hrs drug treatment. Quizartinib induced a significant apoptotic effect in MV4-11 at 1 nM concentration following 48 hrs drug treatment. Collectively, these results suggest BAY-806946, PF-04691502 and quizartinib induce apoptosis, but not as efficiently as standard chemotherapy.

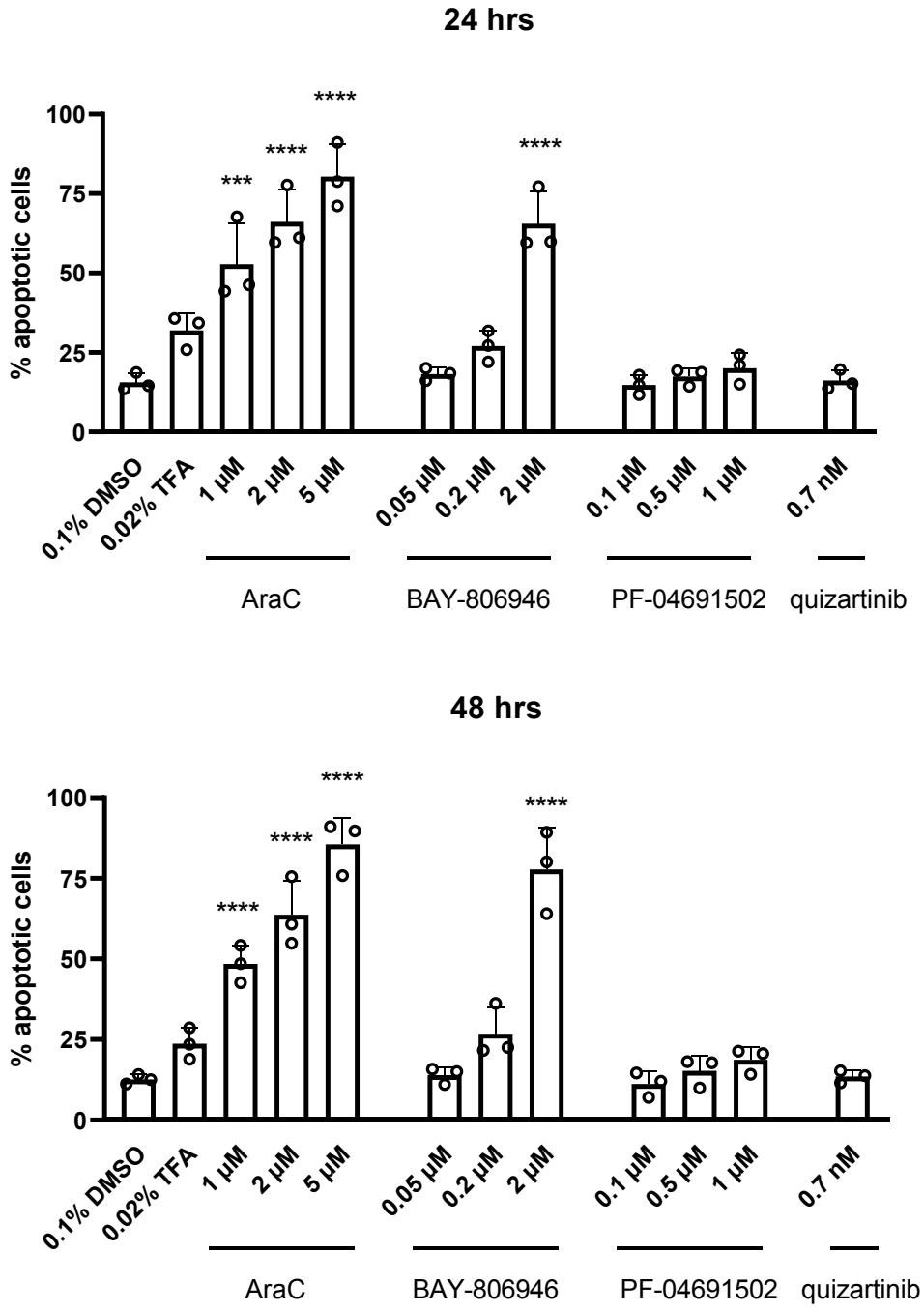

Figure 4.6 PI3K/AKT/mTORi induce apoptosis in THP-1 cells but not as efficiently as chemotherapy

THP-1 (FLT3 wildtype) cells were exposed to increasing concentrations of AraC, BAY-806946, PF-04691502, and quizartinib for 24 or 48 hrs. THP-1 cells were treated with quizartinib to show there is no detectable off-target effect. Apoptosis was measured by annexinV/DAPI staining, detected by flow cytometry. Each bar represents the average ± SD percentages of apoptotic cells of three independent replicates. Statistical analysis was performed by one-way ANOVA followed by Dunnett's multiple comparisons (*$p \leq 0.05$, **$p \leq 0.01$, ***$p \leq 0.001$, ****$p \leq 0.0001$). Published in (Darici et al., 2021).

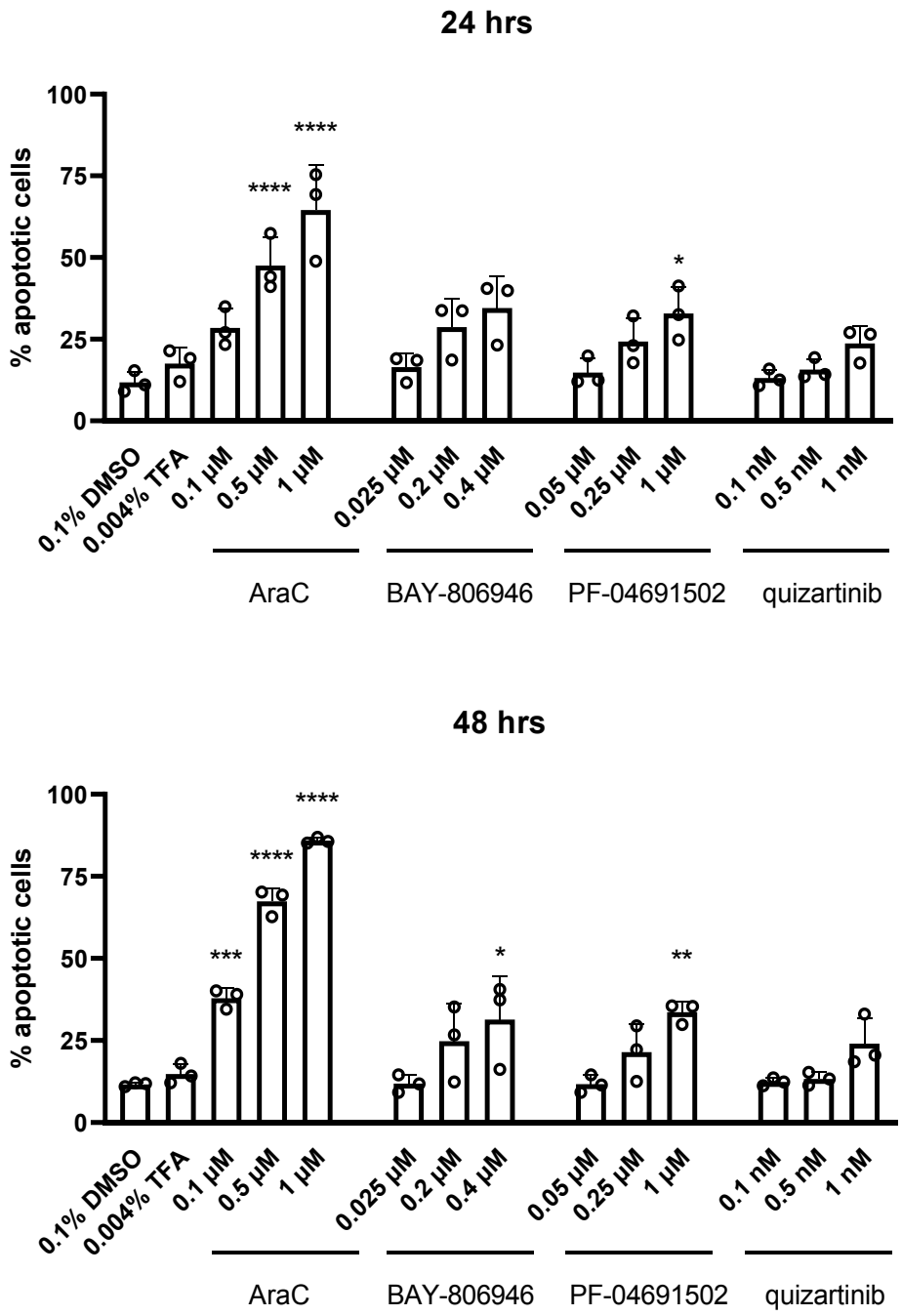

Figure 4.7 PI3K/AKT/mTORi induce apoptosis in MOLM-13 cells but not as efficiently as chemotherapy

MOLM-13 (FLT3-ITD) cells were exposed to increasing concentrations of AraC, BAY-806946, PF-04691502, and quizartinib for 24 or 48 hrs. Apoptosis was measured by annexinV/DAPI staining, detected by flow cytometry. Each bar represents the average ± SD percentages of apoptotic cells of three independent replicates. Statistical analysis was performed by one-way ANOVA followed by Dunnett's multiple comparisons (*p ≤ 0.05, **p ≤ 0.01, ***p ≤ 0.001, ****p ≤ 0.0001). Published in (Darici et al., 2021).

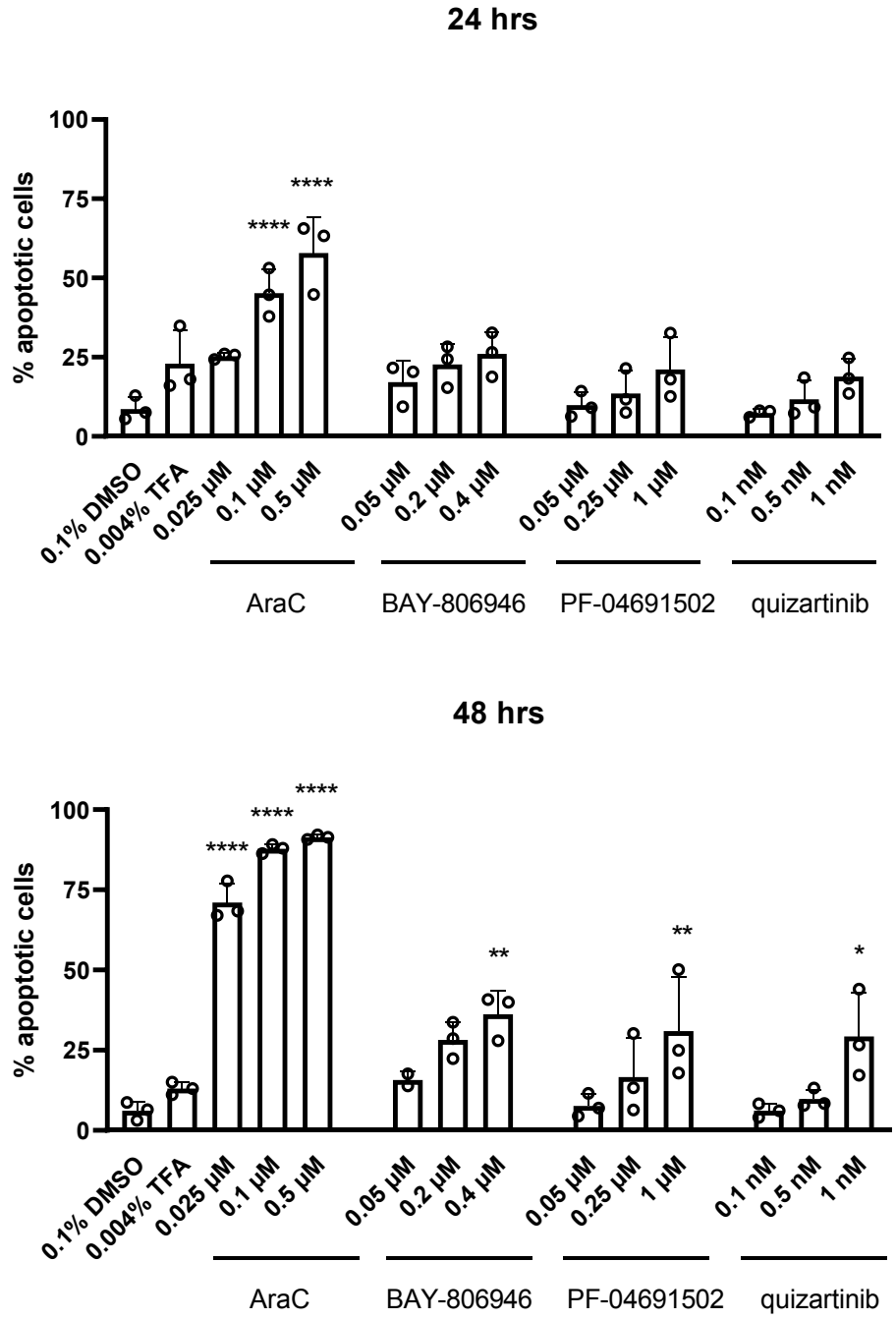

Figure 4.8 FLT3i or PI3K/AKT/mTORi induce apoptosis in MV4-11 cells but not as efficiently as chemotherapy

MV4-11 (FLT3-ITD) cells were exposed to increasing concentrations of AraC, BAY-806946, PF-04691502, and quizartinib for 24 or 48 hrs. Apoptosis was measured by annexinV/DAPI staining, detected by flow cytometry. Each bar represents the average ± SD percentages of apoptotic cells of three independent replicates. Statistical analysis was performed by one-way ANOVA followed by Dunnett's multiple comparisons (*p ≤ 0.05, **p ≤ 0.01, ***p ≤ 0.001, ****p ≤ 0.0001). Published in (Darici et al., 2021).

4.5 On-target inhibition confirmed at the protein expression level in AML cell lines

Following identification of IC50 drug concentrations, it was sought to confirm that the drugs indeed inhibited their target at the protein expression level by western blotting. MOLM-13 and THP-1 cells were treated for 2 hrs at the respective IC50 drug concentration and inhibition of PI3K/AKT/mTOR and FLT3-ITD signaling was determined by detection of phosphorylated AKT (at S473), phosphorylated rpS6 (at S235/236) and phosphorylated ERK [Threonine 202/ Tyrosine 204 (T202/Y204)] (Liao and Hung, 2010; Roskoski, 2012; Ruvinsky and Meyuhas, 2006). The time point was selected based on a study in which it was shown that 2 hrs quizartinib treatment effectively inhibited phosphorylation of AKT and ERK in MV4-11 (FLT3-ITD) cells (Aikawa et al., 2020).

Results obtained in MOLM-13 cells show that treatment with BAY-806946 or PF-04691502 significantly inhibited phosphorylation of AKT (p=0.0004; p=0.0001) and mTOR (p=0.0006; p=0.0002) respective to control, but not phosphorylation of ERK (Figure 4.9). Quizartinib treatment only inhibited phosphorylation of rpS6 at the tested concentration (p=0.0068).

In THP-1, BAY-806946 significantly inhibited phosphorylation of AKT ($p<0.0001$), ERK (p=0.02) and rpS6 ($p<0.0001$) respective to control. Similarly, PF-04691502 also inhibited phosphorylation of AKT ($p<0.0001$) and rpS6 ($p<0.0001$), but not ERK (Figure 4.10). THP-1 (FLT3 wildtype) cells were also treated with quizartinib to confirm that quizartinib selectively inhibits FLT3-ITD downstream signaling. Interestingly, higher basal activation level of AKT was observed in THP-1 cells compared to MOLM-13, which could be attributed to the NRAS mutation (Muñoz-Maldonado et al., 2019).

In this experiment instead of a vehicle control, a NDC was included. It is conceivable that the vehicle diluent may have some cytotoxic effect at higher concentrations, which may alter protein phosphorylation levels. To demonstrate that the vehicle does not affect phosphorylation levels of detected proteins, cells were exposed to DMSO (0.0012%; PF-04691502 and quizartinib vehicle, at highest concentration evaluated) and TFA (0.0011%; BAY-806946 vehicle) for 2 hrs. Whereas marginal differences were observed for phosphorylated rpS6 respective to NDC, differences were large for phosphorylated AKT and ERK levels. However, since this is based on a single measurement, it could be that the average of repeated measurements is statistically indifferent from NDC (Figure 4.11).

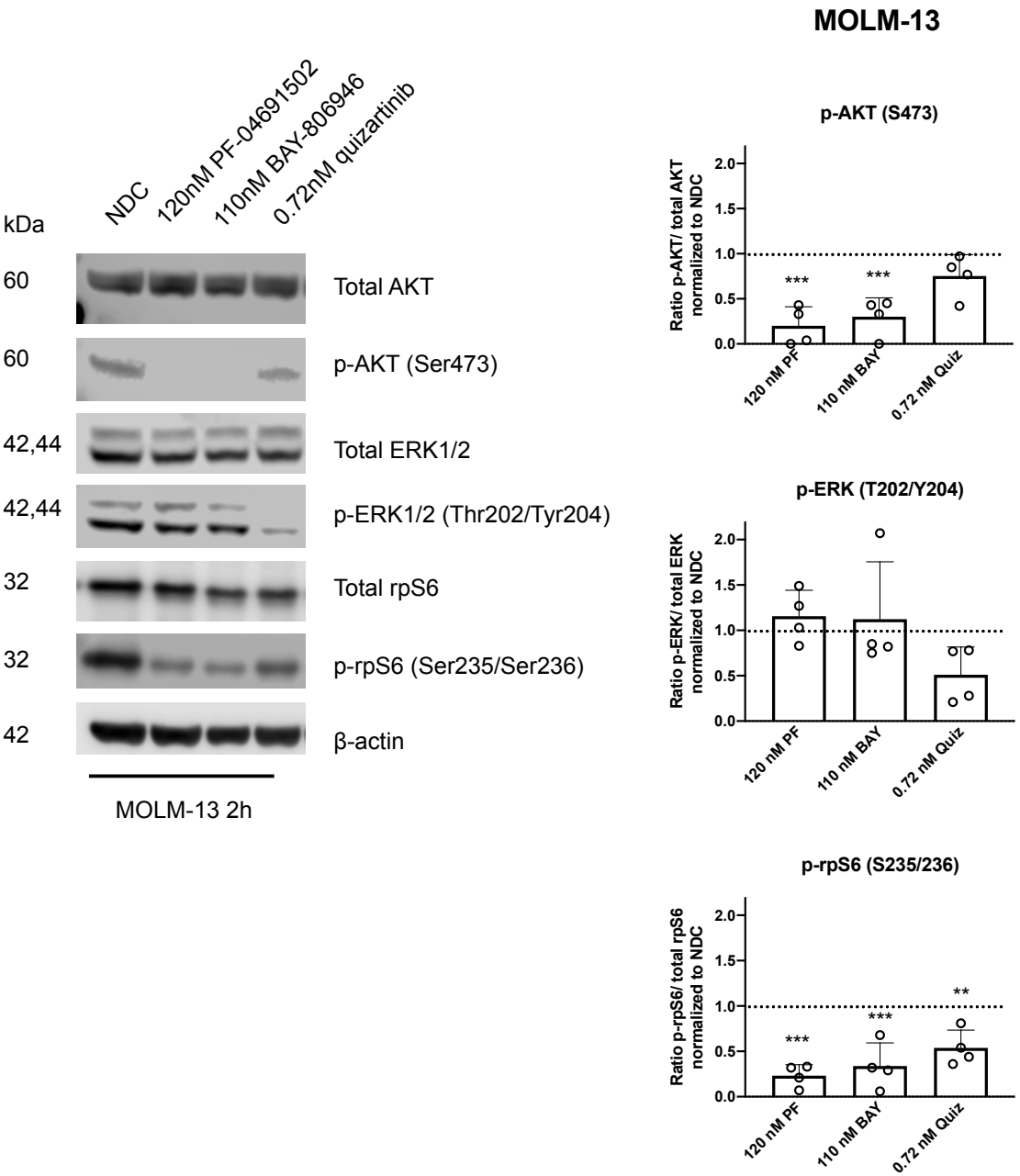

Figure 4.9 Inhibition of FLT3-ITD or PI3K/AKT/mTOR signaling pathway following treatment with FLT3i or PI3K/AKT/mTORi in MOLM-13 cells

MOLM-13 (FLT3-ITD) cells were treated at the indicated concentrations for 2 hrs. Western blot analysis was performed on cell lysates using antibodies against indicated (phospho) proteins. One representative western blot is shown. Bar graphs represent the ratio phosphorylated/total proteins normalized to no drug control (NDC) of four independent replicates ± SD. Statistical analysis was performed by one-way ANOVA followed by Dunnett's multiple comparisons test (**p ≤ 0.01, ***p ≤ 0.001).

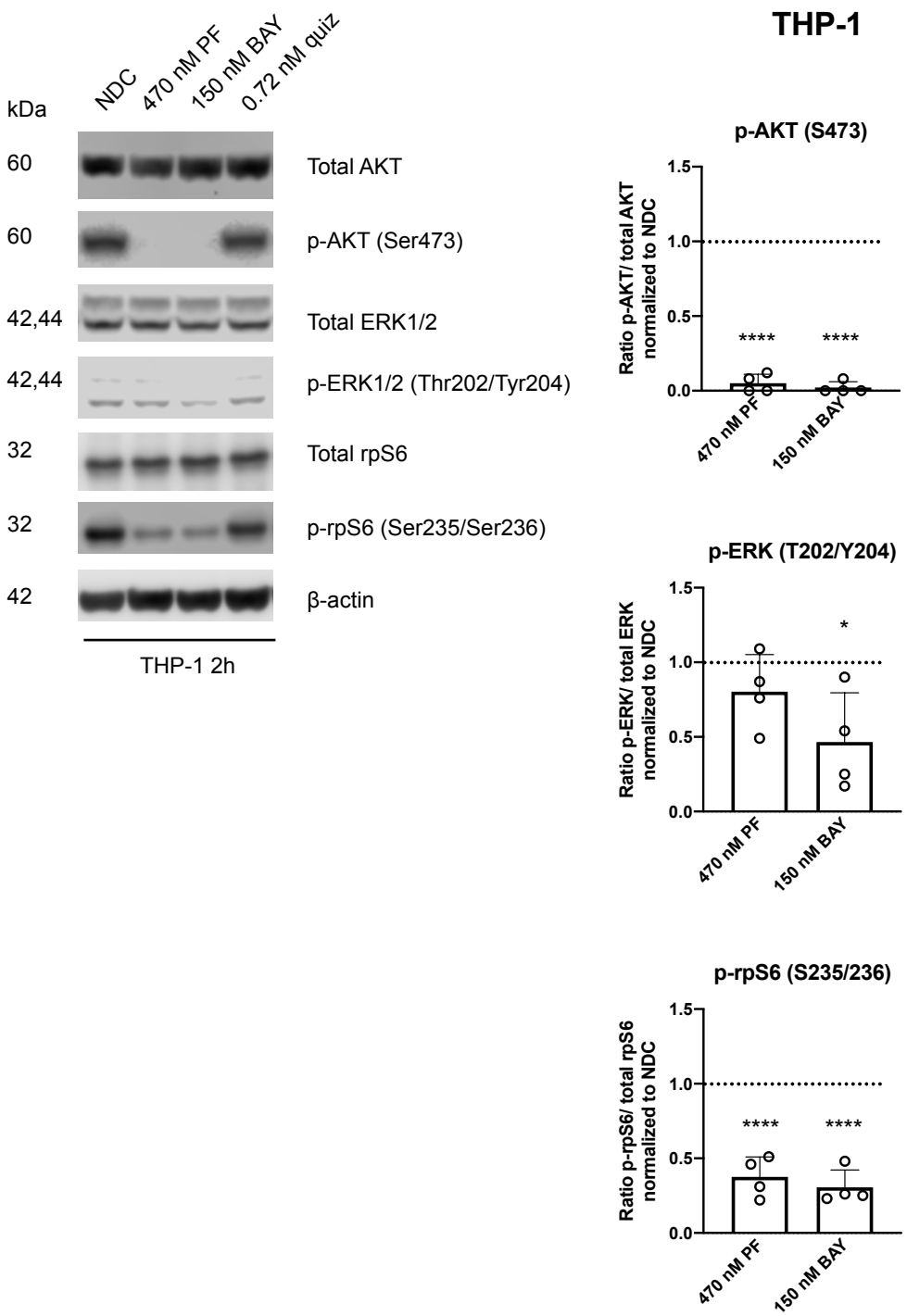

Figure 4.10 Inhibition of FLT3-ITD or PI3K/AKT/mTOR signaling pathway following treatment with FLT3i or PI3K/AKT/mTORi in THP-1 cells

THP-1 (FLT3 wildtype) cells were treated at the indicated concentrations for 2 hrs. Western blot analysis was performed on cell lysates using antibodies against indicated (phospho) proteins. THP-1 cells were treated with quizartinib once to show there is no detectable off-target effect. One representative western blot is shown. Bar graphs represent the ratio phosphorylated/total proteins normalized to no drug control (NDC) of four independent replicates ± SD. Statistical analysis was performed by one-way ANOVA followed by Dunnett's multiple comparisons test (*p ≤ 0.05, ****p ≤ 0.0001).

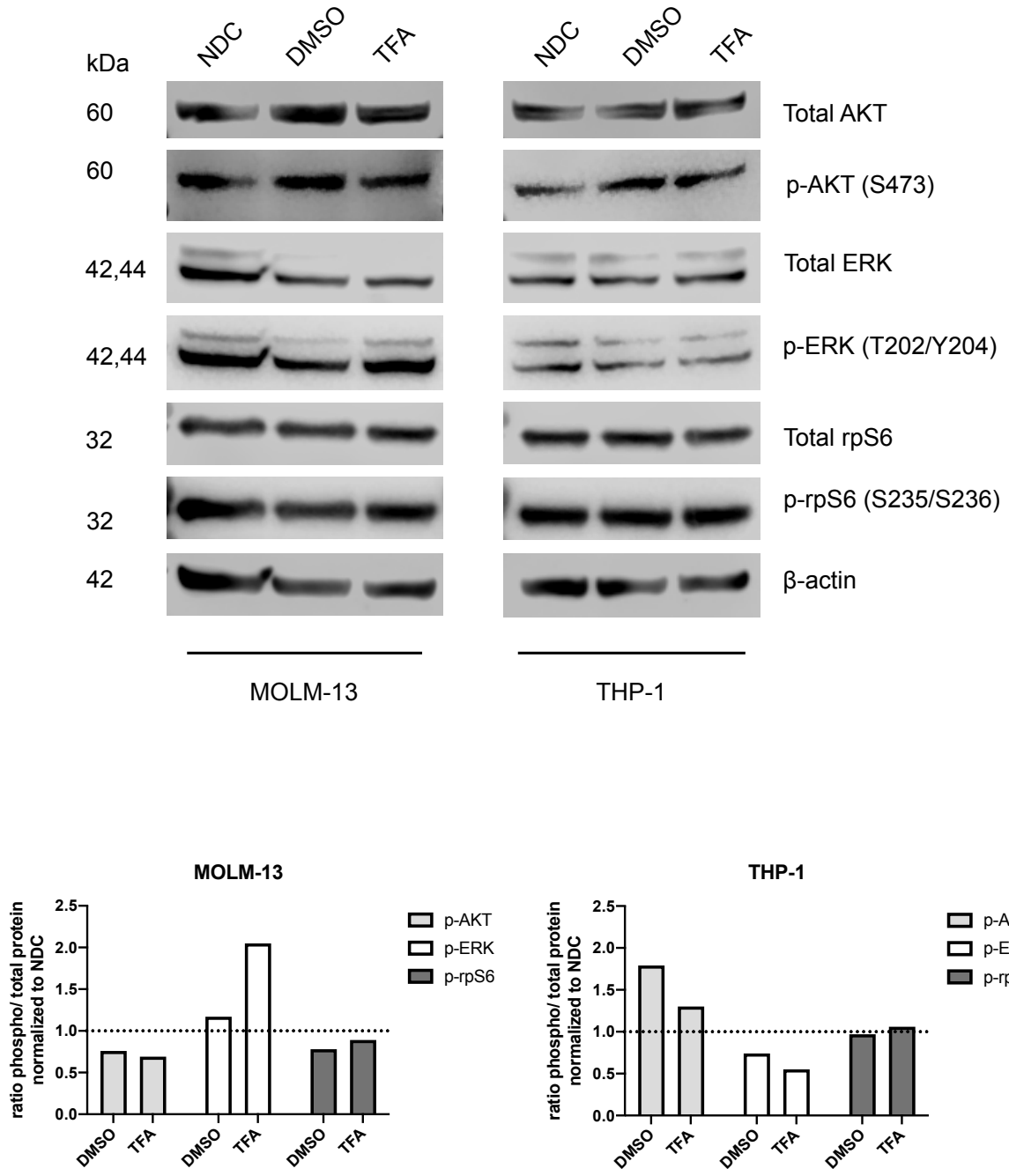

Figure 4.11 Exposure to vehicle controls affect protein expression levels

MOLM-13 and THP-1 cells were exposed to vehicle controls DMSO (0.0012%) and TFA (0.0011%) for 2 hrs (n=1). Western blot analysis was performed on cell lysates using antibodies against indicated proteins. Bar graphs represent quantification of western blot shown.

4.6 Inhibition of FLT3-ITD or PI3K/AKT/mTOR-related genes in AML cell lines

To assess whether FLT3 or PI3K/AKT/mTOR inhibition causes changes at the gene expression level, the mRNA expression of targets of pathway activity, *NRAS*, *RPS6KB1*, *MAPK1*, and *NFKB1* were measured by RT-qPCR. MOLM-13 and THP-1 cells were treated with PF-04691502 or quizartinib for 24 hrs. It was aimed to measure changes at the gene expression at the concentration at which anti-leukemic sequelae is known to happen but at time point before cell death is not yet induced. As 1 μM PF-04691502 was known to cause cell death at 48 hrs in MOLM-13, 24 hrs timepoint was chosen. Cells were treated at the respective IC50 concentration. mRNA expression of the measured targets following treatment with PF-04691502 or quizartinib for 24 hrs in both MOLM-13 and THP-1 was indifferent from untreated (Figure 4.12). There was no statistically significant difference observed respective to NDC ($p>0.05$).

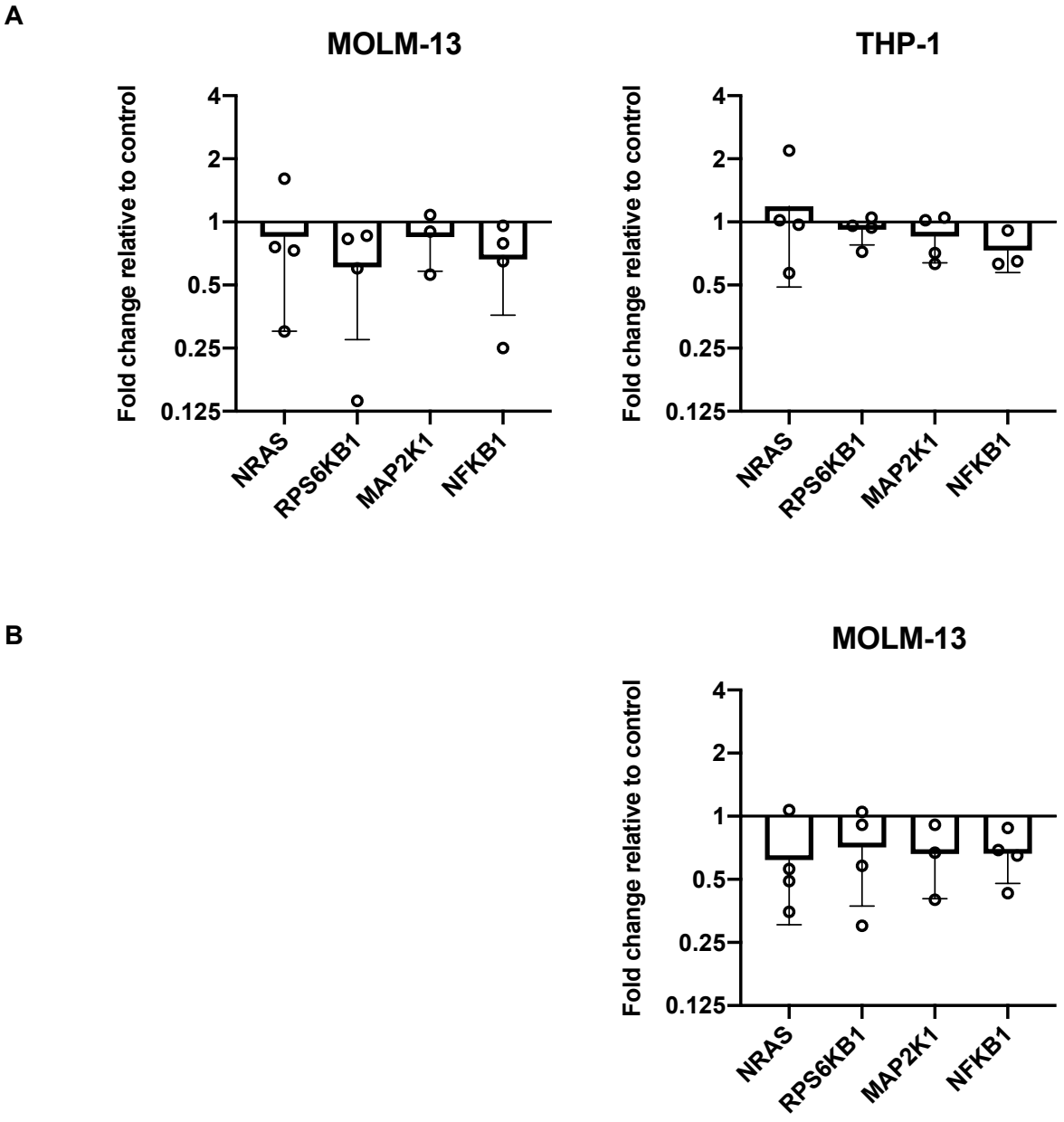

Figure 4.12 Expression levels of FLT3-ITD and PI3K/AKT/mTOR target genes are not affected by treatment with PF-04691502 or quizartinib

MOLM-13 (FLT3-ITD) and THP-1 (FLT3 wildtype) cells were treated with **A)** PF-04691502 (120 nM and 470 nM) or **B)** quizartinib (0.72 nM) for 24 hrs. mRNA expression of *NRAS*, *RPS6KB1*, *MAPK1*, and *NFKB1* were determined relative to control (0.1% DMSO) using the average of two housekeeping genes as reference genes. Only FLT3-ITD positive cell line MOLM-13 was treated with FLT3i quizartinib. Bar graphs represent relative gene expression ± SD of three independent replicates. Statistical analysis was performed by two-way ANOVA followed by Holm-Šidák's multiple comparisons test.

4.7 Discussion

FLT3 receptor mutations have been reported in approximately 30% of AML patients with normal karyotype (Stirewalt and Radich, 2003). Internal tandem duplications are the most common FLT3 mutations leading to constitutive receptor activation that is associated with high leukemic burden and poor prognosis (Arber et al., 2016). Therefore, targeting FLT3 is regarded an attractive strategy for AML treatment. However, despite favorable anti-leukemic effects observed in preclinical studies, clinical outcomes using FLT3i as monotherapy have been disappointing so far due to a lack of durable efficacy and disease relapse caused by drug resistance (Fletcher et al., 2020). Increasing efforts are underway to improve clinical outcomes by combining FLT3is with other therapeutic agents. The PI3K/AKT/mTOR signaling pathway is regarded as a putative target in human cancers due to its prominent role in numerous cellular processes including hematopoiesis and is often hyperactivated in FLT3-ITD, which led to the development of numerous small molecule inhibitors targeting key nodes of this pathway. However, the use of these inhibitors for AML has been hampered by pathway reactivation. There is evidence supporting the rationale of combining FLT3is with PI3K/AKT/mTORi that may induce synergistic effects, but this combination remains to be fully exploited (Darici et al., 2021; Mohi et al., 2004; Wang et al., 2015; Weisberg et al., 2013).

In this chapter it was aimed to uncover the phenotypic profile of FLT3-ITD (MOLM-13 and MV4-11) versus FLT3 wildtype (THP-1) cells following treatment with the FLT3i, quizartinib, or PI3K/AKT/mTORi BAY-806946 and PF-04691502. We know that MOLM-13 has both wildtype and ITD alleles, whereas MV4-11 are homozygous for the FLT3-ITD mutation. These differences may be associated with varying sensitivity to drug treatment. To compare the efficacy of FLT3i and PI3K/AKT/mTORi on FLT3-ITD versus FLT3 wildtype cells, first the growth inhibitory activity of the inhibitors was examined by resazurin-based metabolic assay from which the drug IC50 concentrations were determined. In this thesis work, FLT3i quizartinib, and PI3K/AKT/mTORi BAY-806946 and PF-04691502 were evaluated. Standard chemotherapy AraC was included as a reference drug. Quizartinib is an example of second-generation FLT3is, respectively, whereas BAY-806946 is a pan PI3Ki and PF-04691502 a dual PI3K/mTORi. Only the FLT3-ITD cells (MOLM-13 and MV4-11) were sensitive to quizartinib and did not induce growth inhibition in the FLT3 wildtype THP-1 cells. This suggests that the antileukemic effect induced by quizartinib was selective for FLT3-ITD AML. PI3K/AKT/mTORi and standard chemotherapy reduced cell growth, irrespective of FLT3 status, but with varying sensitivity.

Sensitivity to small molecule inhibitors and/or chemotherapy could be attributed to various factors, including but not limited to genetic background. For instance, THP-1 and MOLM-13 carry MLL-AF9 fusion whereas MV4-11 carries MLL-AF4 fusion. A study by Sandhöfer et al., in which the effectiveness of PI3K/AKT/mTORi in cell lines and primary patient cells was analyzed revealed high sensitivity in cells carrying a MLL rearrangement (Sandhöfer et al., 2015). In addition to MLL fusion, THP-1 is reported to carry mutations in NRAS and TP53, which could be associated to decreased sensitivity to PI3K/AKT/mTORi and/or chemotherapy (Mazumdar et al., 2014).

It was further sought to confirm the selectivity of the drugs by confirmation of target inhibition at the protein expression level (by western blotting) and gene expression (by RT-qPCR). Results showed that FLT3i and PI3K/AKT/mTORi, inhibit their target at the protein expression level, but do not affect pathway activity at the gene expression level. In FLT3-ITD expressing MOLM-13 cells, basal activation of AKT, rpS6 and ERK1/2 was observed which is consistent with constitutively active MAPK and PI3K/AKT/mTOR signaling. Results confirmed that quizartinib is selective against FLT3-ITD AML, as downstream signaling target rpS6 was inhibited following treatment in MOLM-13 cells but not in THP-1. In contrast to a previous report by Aikawa *et al*., at the tested concentration and time point, quizartinib did not inhibit phosphorylation of AKT and ERK (Aikawa et al., 2020). It was also confirmed that BAY-806946 and PF-04691502 selectively inhibited PI3K/AKT/mTOR signaling. Unexpectedly, BAY-806946 inhibited ERK in THP-1 cells, which may be an off-target effect.

Next the underlying mechanism of growth inhibition was investigated by measuring cell cycle state and apoptosis. It has been reported that pharmacological inhibition of PI3K/AKT/mTOR pathway prevents G1 cell cycle progression into S (G1 cell cycle arrest) and induced expression of CDK inhibitor p27 (Chang et al., 2003). PI3K/AKT/mTORi have also been reported to potentially induce apoptosis, however PI3K inhibition *in vitro* is rarely cytotoxic, but more often cytostatic (Bertacchini et al., 2018; Okkenhaug et al., 2016; Xu et al., 2003). Two studies evaluated quizartinib *in vitro* in FLT3-ITD AML cell lines and demonstrated that quizartinib potentially induces apoptosis following 48 hrs drug treatment (Gunawardane et al., 2013; Kampa-Schittenhelm et al., 2013). Furthermore, PARP cleavage, an indicator of apoptosis, was observed as early as 8 hours following quizartinib treatment (Gunawardane et al., 2013). Indeed, concentration-dependent increase of apoptosis following 24 hrs quizartinib treatment was found, but this effect was not as efficient compared to chemotherapy. Cell death by apoptosis was reported at concentrations exceeding 1 nM test concentration, which could explain why quizartinib induced modest apoptosis.

In summary, the sensitivity of FLT3-ITD AML versus FLT3 wildtype AML cells to BAY-806946, PF-04691502 and quizartinib treatment has been demonstrated. BAY-806946 and PF-04691502 exerted growth inhibition caused by G1 cell cycle arrest and apoptosis, and this effect was irrespective of FLT3 status. Quizartinib selectively inhibited cell growth in FLT3-ITD AML and this effect was mainly caused by apoptosis. The observed drug-induced apoptotic effect was however not as efficient as chemotherapy. In the next chapter, the efficacy of combination treatment consisting of quizartinib with BAY-806946 or PF-04691502 in FLT3-ITD AML cell lines was evaluated.

Chapter 5: Evaluating the efficacy of combination therapy of FLT3 inhibitor with PI3K/AKT/mTOR inhibitors in FLT3-ITD AML cell lines

In the previous chapter the phenotypic profile of FLT3-ITD versus FLT3 wildtype AML cell lines following treatment with FLT3i or PI3K/AKT/mTORi was uncovered. Based on the results obtained, in this chapter, it was aimed to investigate whether the efficacy of the FLT3i quizartinib could be enhanced with PI3Ki BAY-806946 (pan-PI3Ki) or PF-04691502 (dual PI3K/mTORi) in human FLT3-ITD AML cell lines.

5.1 Combination of quizartinib with BAY-806946 or PF-04691502 synergistically inhibits FLT3-ITD AML cell growth

To investigate whether the efficacy of quizartinib could be enhanced with BAY-806946 or PF-04691502 in FLT3-ITD AML cell lines, first it was assessed whether drug combination displays enhanced growth inhibition compared to monotherapy. In this regard, MOLM-13 cells were exposed to increasing concentrations of the inhibitors around their respective IC50 drug concentration (c.f. Figure 4.2). These concentrations ranged from ¼, ½, 1, 2, 4x respective IC50 (referred to as “combo” 1-5), where 1x respective IC50 concentrations were 110 nM (BAY-806946), 60 nM (PF-04691502), and 0.72 nM (quizartinib). The inhibitors were added simultaneously and cells were treated for 48 hrs.

Combination of quizartinib with either BAY-806946 or PF-04691502 exerted enhanced growth inhibition in MOLM-13 cells and this effect was statistically significant compared to quizartinib treatment alone [combo 2: $p<0.0001$ (BAY); $p<0.0001$ (PF)] (Figure 5.1 and 5.3). It is worth noting that this is true even at the lowest test concentrations at which the inhibitors were combined (referred to as “combo 1”). Furthermore, in the heatmaps displaying the percentage of growth inhibition of all 25 drug combinations, it is apparent that enhanced growth inhibition is observed at higher concentrations of both inhibitors. It was further questioned whether the observed effect of combination treatment while statistically different from monotherapy, was also synergistic. The Chou-Talalay and Bliss Independence methods were used to determine synergy. Combination index (CI) derived from the Chou-Talalay method is based on the median-effect equation, and defines synergy (CI<1), additive

effect (CI=1), and antagonism (CI>1) (Chou, 2010). CI by Bliss Independence method assumes two drugs elicit their effects independently and compares the observed combination response with the predicted combination response (Zhao et al., 2014). Indeed, combination of quizartinib with either BAY-806946 or PF-04691502 elicits a synergistic growth inhibition in MOLM-13 cells (Figure 5.2 and 5.4). The most synergistic area using the Bliss Independence method seems to overlap with the synergistic area determined using the Chou-Talalay method. These results collectively demonstrated that treatment with either BAY-806946 or PF-04691502 enhances the growth inhibition of quizartinib in FLT3-ITD AML cell lines, and that this effect is truly synergistic.

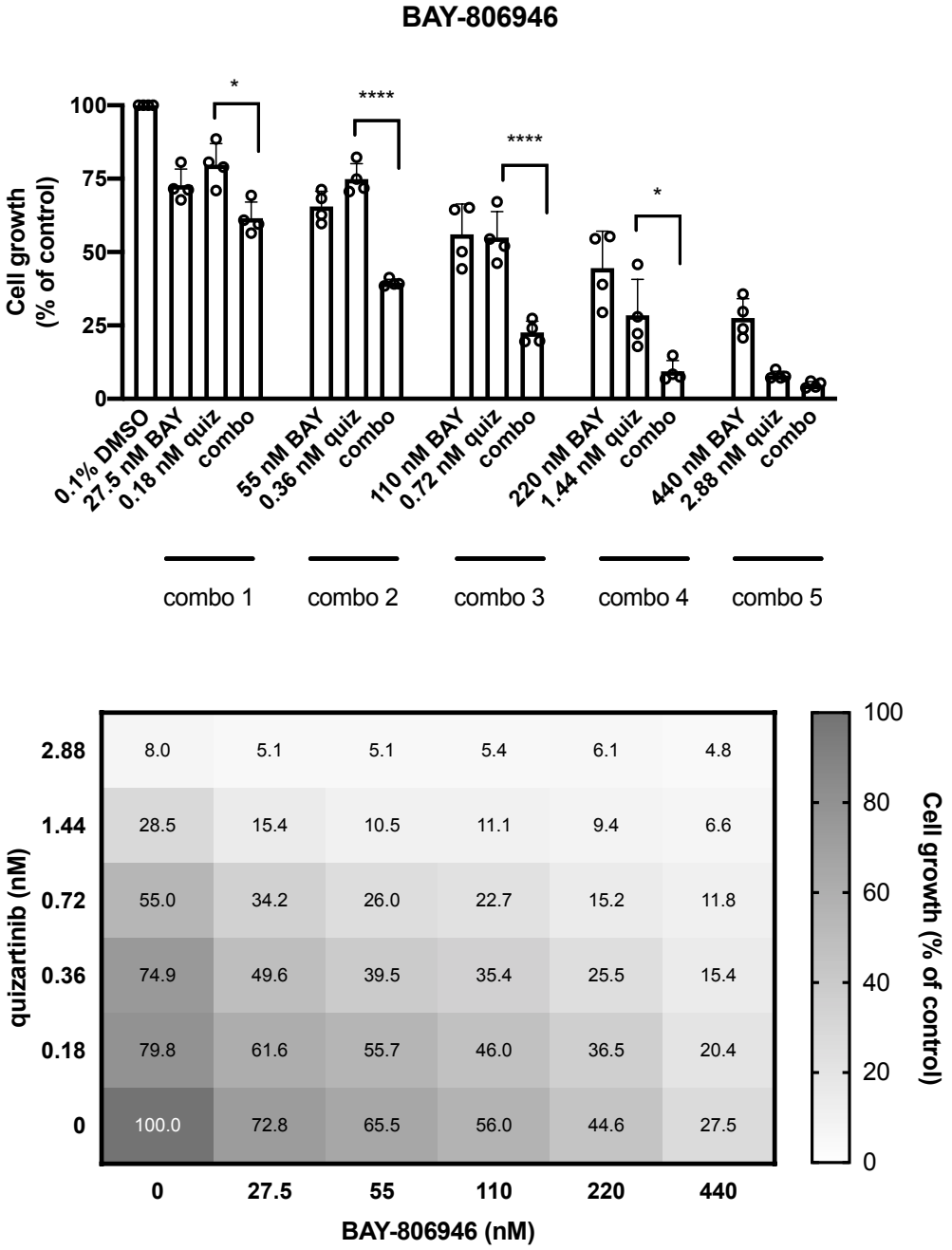

Figure 5.1 Combination of quizartinib with BAY-806946 inhibits cell growth in FLT3-ITD cell lines

MOLM-13 (FLT3-ITD) cells were exposed to increasing concentrations of quizartinib (quiz) and BAY-806946 (BAY) around their respective drug IC50 concentrations for 48 hrs, either alone or in combination. 1x IC50 were 110 nM (BAY) and 0.72 nM (quiz). Growth inhibition was measured by resazurin-based cell metabolism assay. Heatmap and bar graph represent the average percentage of inhibition of cell growth (normalized to vehicle control) of four independent replicates. Bar graphs represent average ± SD for each drug concentration. Statistical analysis was performed by one-way ANOVA followed by Tukey's multiple comparisons. (*$p \leq 0.05$, ****$p \leq 0.0001$).

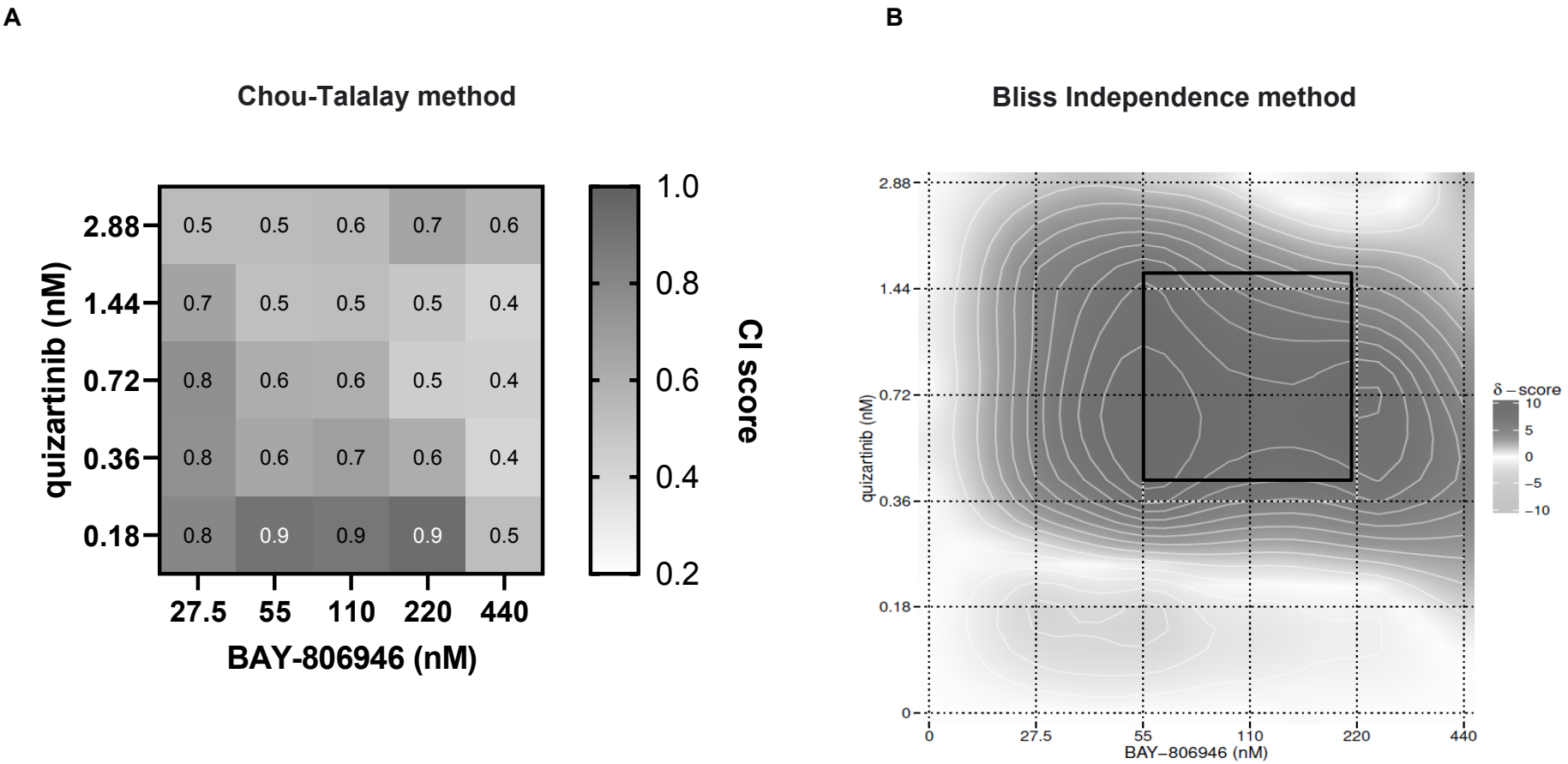

Figure 5.2 Cell growth inhibition induced by combination of quizartinib with BAY-806946 in FLT3-ITD cell lines is synergistic

MOLM-13 (FLT3-ITD) cells were exposed to increasing concentrations of quizartinib (quiz) and BAY-806946 (BAY) around their respective drug IC50 concentrations for 48 hrs, either alone or in combination. 1x IC50 were 110 nM (BAY) and 0.72 nM (quiz). Growth inhibition was measured by resazurin-based cell metabolism assay. Combination index (CI) was calculated by **A)** Chou-Talalay and **B)** Bliss Independence methods. CI by Chou-Talalay method was calculated using CompuSyn software where CI<1 indicates synergism, CI=1 additive effect, and CI>1 antagonism. CI by Bliss independence method was calculated using SynergyFinder (version 2.0). In the synergy heatmap, synergistic (dark) and antagonistic (light) concentration regions are highlighted.

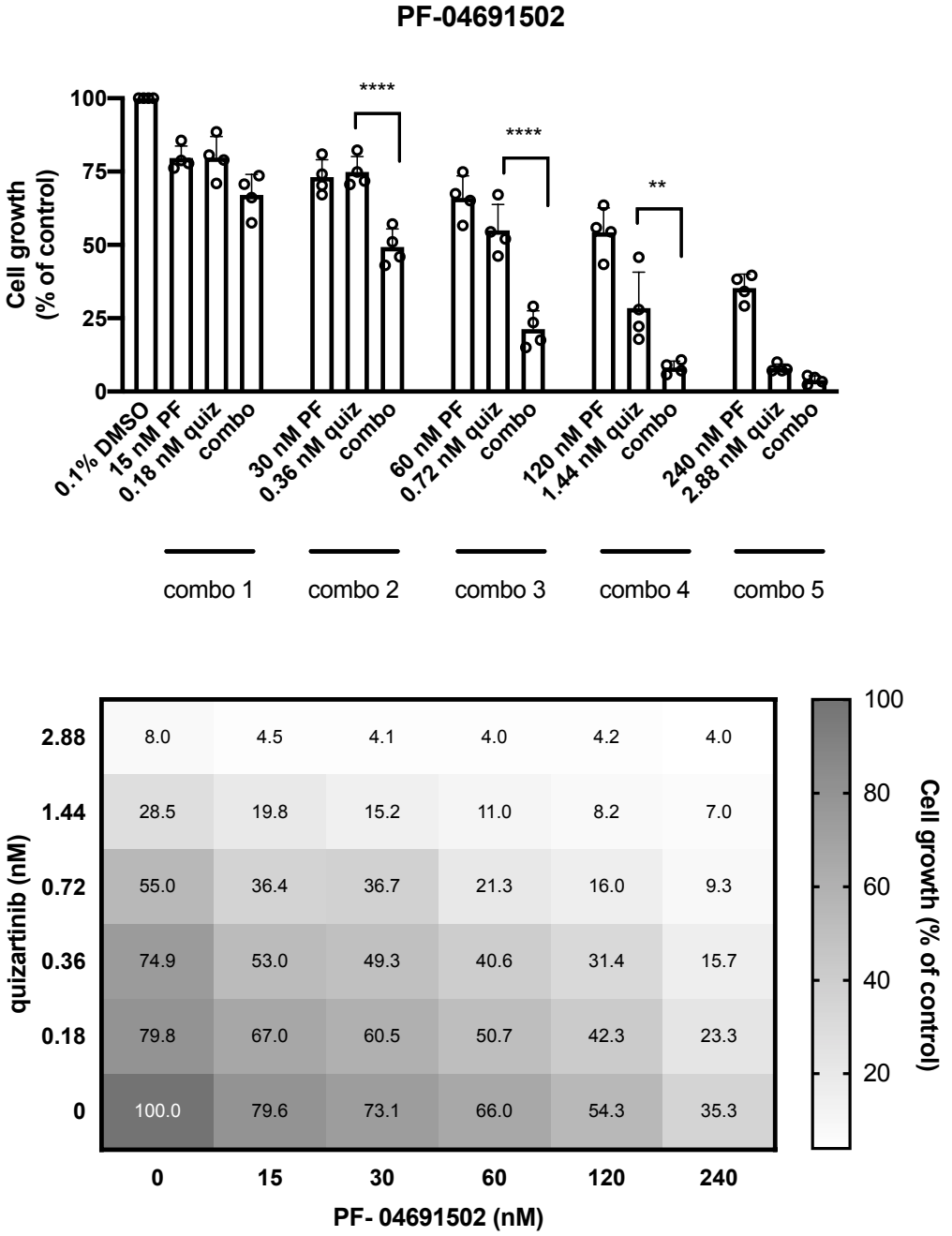

Figure 5.3 Combination of quizartinib with PF-04691502 inhibits cell growth in FLT3-ITD cell lines

MOLM-13 (FLT3-ITD) cells were exposed to increasing concentrations of quizartinib (quiz) and PF-04691502 (PF) around their respective drug IC50 concentrations for 48 hrs, either alone or in combination. 1x IC50 were 60 nM (PF) and 0.72 nM (quiz). Growth inhibition was measured by resazurin-based cell metabolism assay. Heatmap and bar graph represent the average percentage of inhibition of cell growth (normalized to vehicle control) of four independent replicates. Bar graphs represent average ± SD for each drug concentration. Statistical analysis was performed by one-way ANOVA followed by Tukey's multiple comparisons. (**p ≤ 0.01, ****p ≤ 0.0001). Published in (Darici et al., 2021).

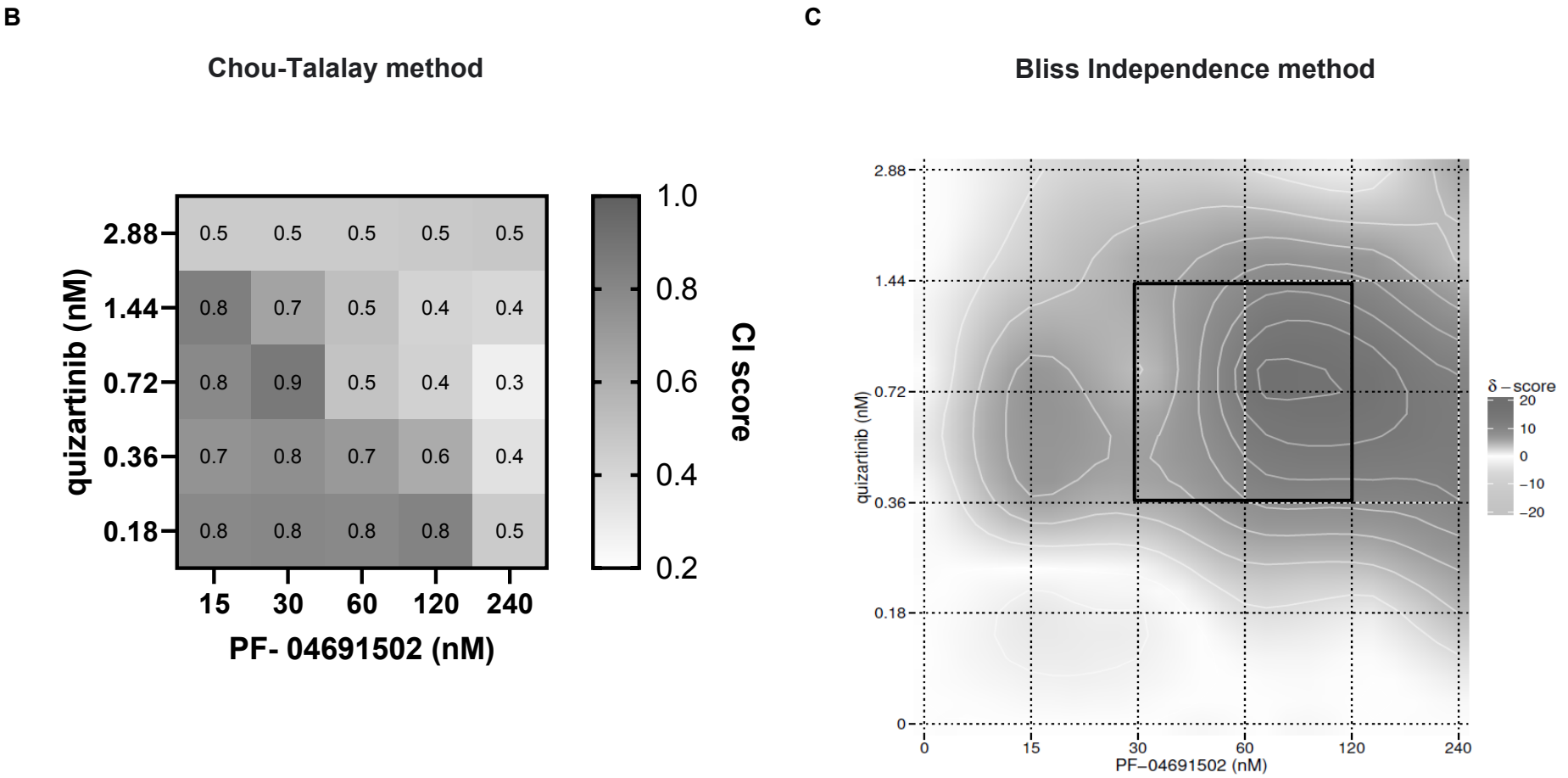

Figure 5.4 Cell growth inhibition induced by combination of quizartinib with PF-04691502 in FLT3-ITD cell lines is synergistic

MOLM-13 (FLT3-ITD) cells were exposed to increasing concentrations of quizartinib (quiz) and PF-04691502 (PF) around their respective drug IC50 concentrations for 48 hrs, either alone or in combination. 1x IC50 were 60 nM (PF) and 0.72 nM (quiz). Growth inhibition was measured by resazurin-based cell metabolism assay. Combination index (CI) was calculated by **A)** Chou-Talalay and **B)** Bliss Independence methods. CI by Chou-Talalay method was calculated using CompuSyn software where CI<1 indicates synergism, CI=1 additive effect, and CI>1 antagonism. CI by Bliss independence method was calculated using SynergyFinder (version 2.0). In the synergy heatmap, synergistic (dark) and antagonistic (light) concentration regions are highlighted. Published in (Darici et al., 2021).

5.2 Combination of quizartinib with BAY-806946 or PF-04691502 exerts enhanced cytostatic and cytotoxic effects

To further exploit whether the enhanced growth inhibition following combination of FLT3i and PI3K/AKT/mTORi was through increased cytostatic and/or cytotoxic effects, cell cycle status (measured by PI staining) and apoptosis (measured by annexinV/DAPI staining) was assessed by cytometry.

MOLM-13 cells were treated with increasing concentrations of quizartinib and BAY-806946 or PF-04691502 alone or in combination for 48 hrs. Assessment of cell cycle status suggests enhanced G1-phase arrest when cells were treated with combination treatment respective to quizartinib treatment alone. For instance, combination of 0.72 nM quizartinib and 110 nM BAY-806946 caused 4.82 times increased G1 to (S+G2M) ratio, which was markedly different from monotherapy with quizartinib (1.88; $p>0.05$) (Figure 5.5). Combination index determined by Bliss Independence method indicates that this effect was synergistic (CI=0.53). As for combination with PF-04691502, treatment with 1.44 nM quizartinib and 120 nM PF-04691502 displayed 2.45 times increased G1 to (S+G2M) ratio compared to quizartinib alone (5.28, $p=0.0102$) (Figure 5.6). Also this effect was found to be synergistic, based on a CI score of 0.89. Combination of the highest test concentrations of the FLT3i and PI3K/AKT/mTORi caused most accumulation of cells in the sub-G0 area, comprised of cell fragments, often resulting from apoptosis. For this reason, in the bar charts, the cell cycle status of “combo 5” (4x respective IC50s) is not shown as this combination caused highest levels of frank toxicity.

Beside cell cycle status, apoptosis was also measured and results indicate a significant incremental uplift of apoptotic levels upon combination treatment with quizartinib with BAY-806946 or PF-04691502 for 48 hrs. As such, combination of quizartinib and BAY-806946 induced a significant increase of apoptosis compared to quizartinib monotherapy, which was observed for combinations #3 ($p<0.0001$), #4 ($p<0.0001$) and #5 ($p=0.0049$) (Figure 5.7 A-B). This effect was synergistic for combinations #3 (CI=0.55) and #4 (CI=0.89), but not for #5 (CI=1.06). Combination of quizartinib and PF-04691502, similarly induced a significant increase of apoptotic levels for combinations #4 ($p<0.0001$), #5 ($p=0.0018$) (Figure 5.7 A). This effect was determined to be synergistic for all three combinations (CI: #3=0.21, #4=0.68, #5=0.98). In summary, these results indicate that combination treatment of quizartinib with either BAY-806946 or PF-04691502 displays enhanced efficacy as compared to monotherapy and that this effect is synergistic.

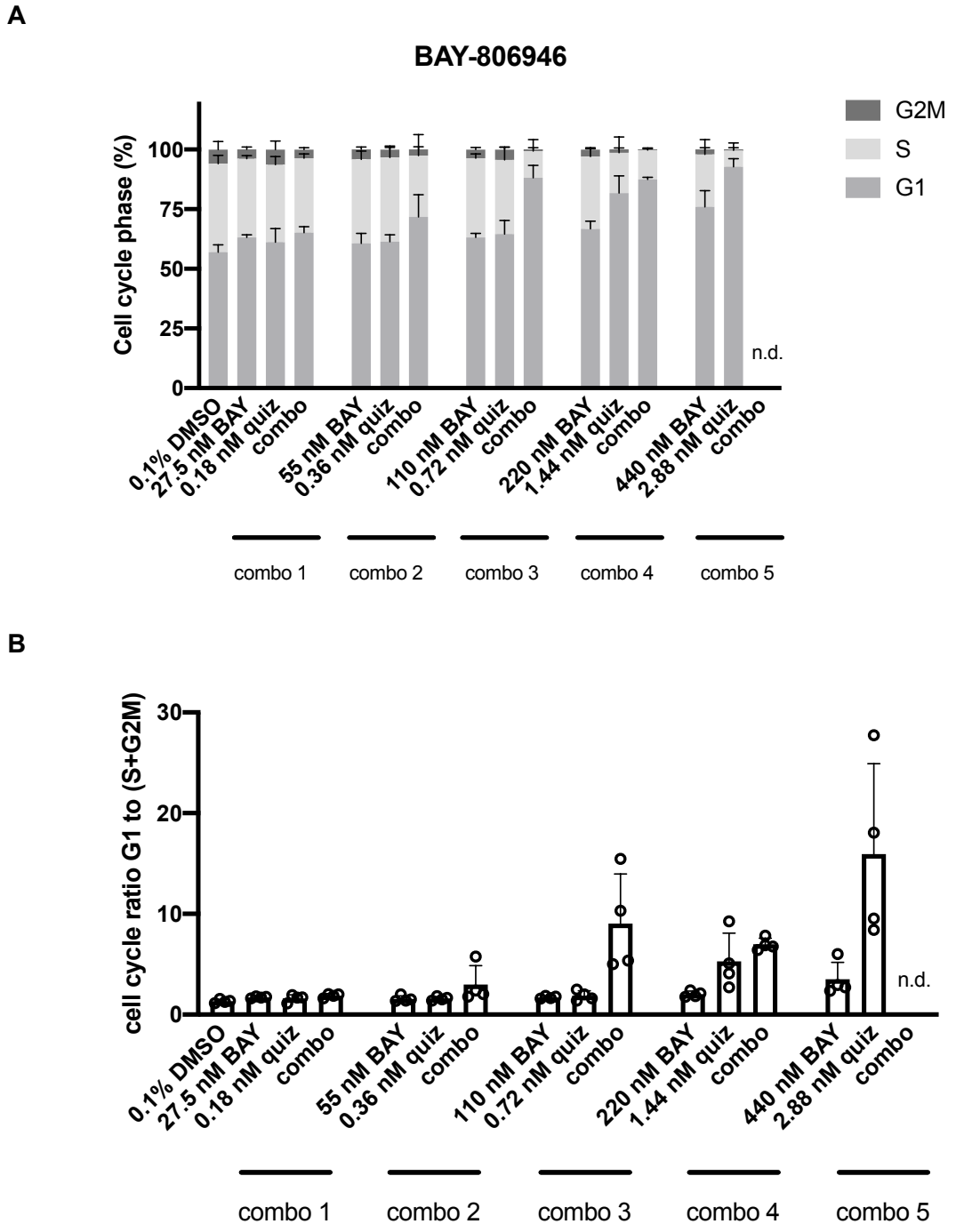

Figure 5.5 Combination of quizartinib with BAY-806946 induces enhanced G1 cell cycle arrest in FLT3-ITD AML cell lines

MOLM-13 (FLT3-ITD) cells were exposed to increasing concentrations of quizartinib (quiz) and BAY-806946 (BAY) around their respective IC50 concentrations for 48 hrs either alone or in combination. 1x IC50 were 110 nM (BAY) and 0.72 nM (quiz). Cell cycle state was measured by staining with propidium iodide, detected by flow cytometry. **A)** Stacked bar graphs represents the average fraction in each cell cycle phase ± SD and bars in **B)** represent the ratio of G1 to (S+G2M) of four independent replicates ± SD. The highest drug concentration combination was toxic and therefore not included (n.d.). Statistical analysis was performed by one-way ANOVA followed by Tukey's multiple comparisons test.

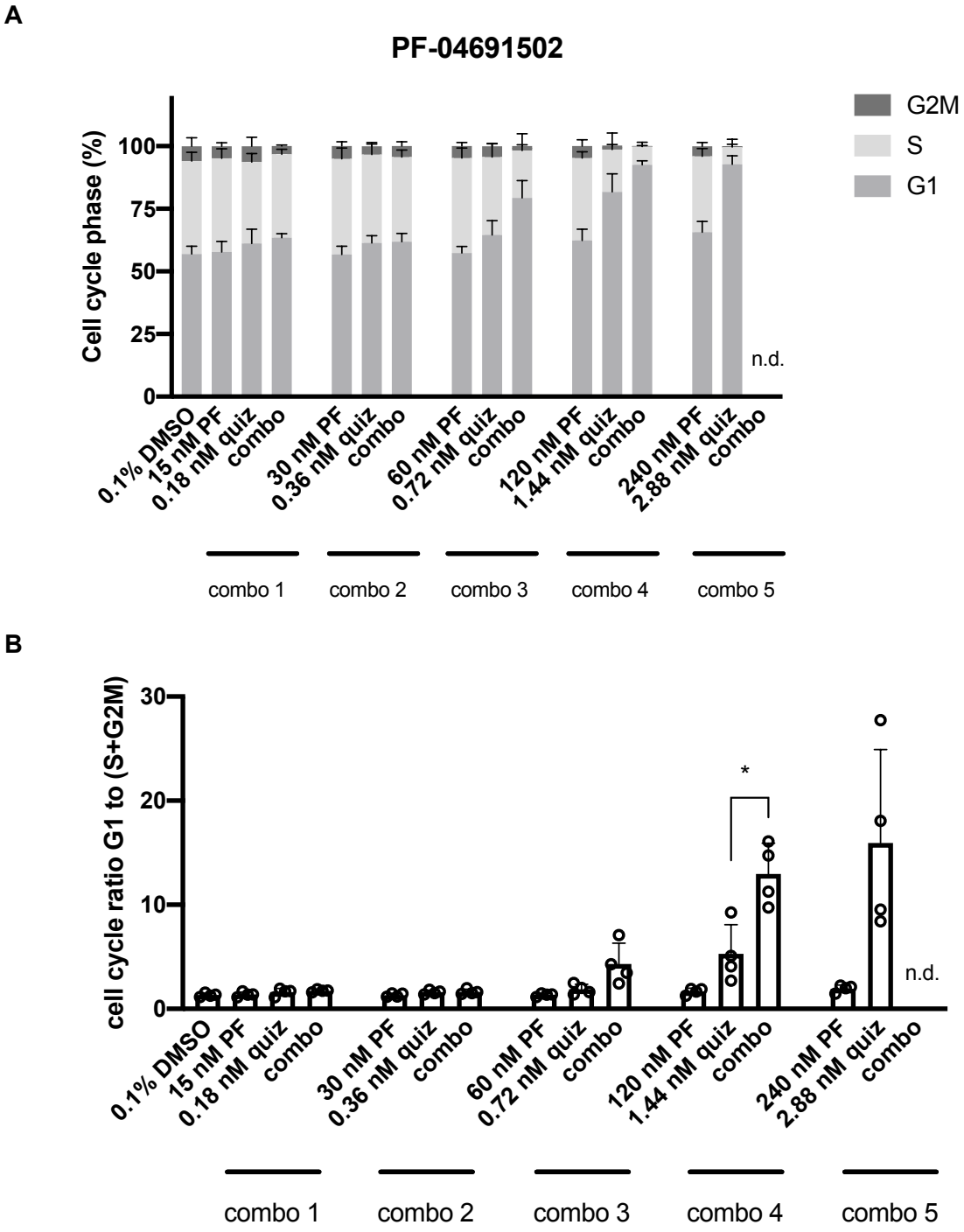

Figure 5.6 Combination of quizartinib with PF-04691502 induces enhanced G1 cell cycle arrest in FLT3-ITD AML cell lines

MOLM-13 (FLT3-ITD) cells were exposed to increasing concentrations of quizartinib (quiz) and PF-04691502 (PF) around their respective IC50 concentrations for 48 hrs either alone or in combination. 1x IC50 were 60 nM (PF) and 0.72 nM (quiz). Cell cycle state was measured by staining with propidium iodide, detected by flow cytometry. **A)** Stacked bar graphs represents the average fraction in each cell cycle phase ± SD and bars in **B)** represent the ratio of G1 to (S+G2M) of four independent replicates ± SD. The highest drug concentration combination was toxic and therefore not included (n.d.). Statistical analysis was performed by one-way ANOVA followed by Tukey's multiple comparisons test. (*p ≤ 0.05). Published in (Darici et al., 2021).

A

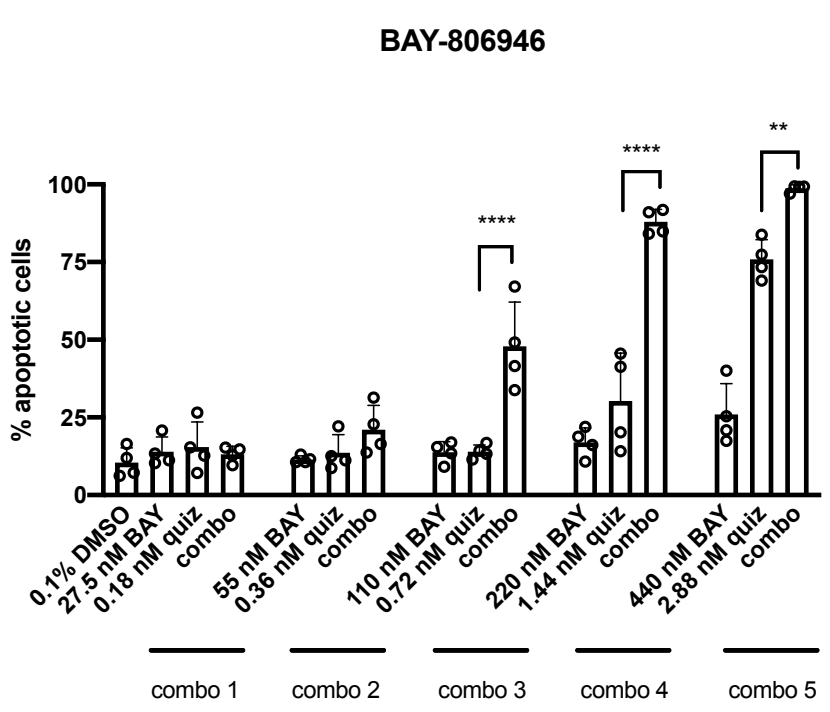
BAY-806946
% apoptotic cells
100
75
50
25
0
****
****
**
0.1% DMSO
27.5 nM BAY
0.18 nM quiz
combo
55 nM BAY
0.36 nM quiz
combo
110 nM BAY
0.72 nM quiz
combo
220 nM BAY
1.44 nM quiz
combo
440 nM BAY
2.88 nM quiz
combo
combo 1
combo 2
combo 3
combo 4
combo 5

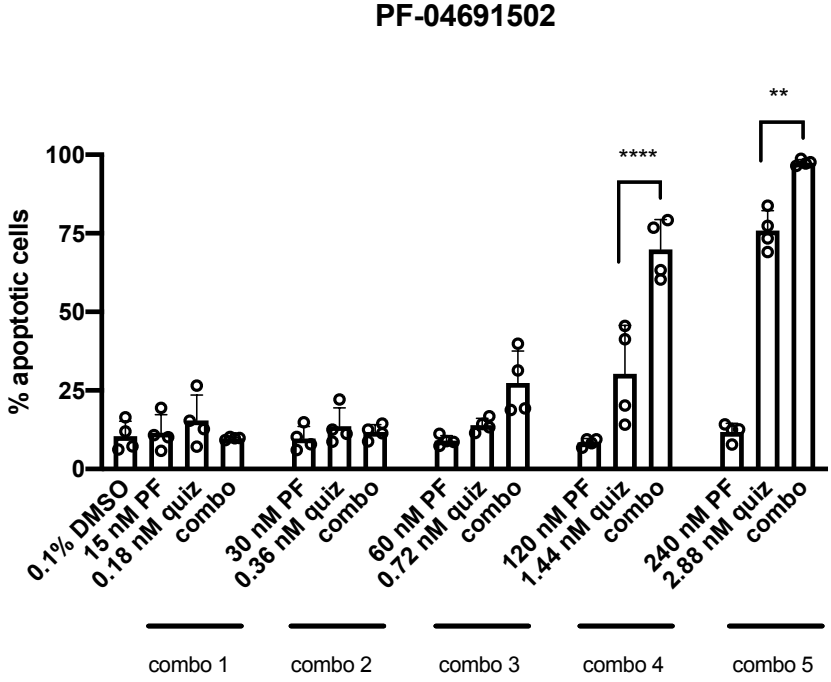
PF-04691502
% apoptotic cells
100
75
50
25
0
****
**
0.1% DMSO
15 nM PF
0.18 nM quiz
combo
30 nM PF
0.36 nM quiz
combo
60 nM PF
0.72 nM quiz
combo
120 nM PF
1.44 nM quiz
combo
240 nM PF
2.88 nM quiz
combo
combo 1
combo 2
combo 3
combo 4
combo 5

B

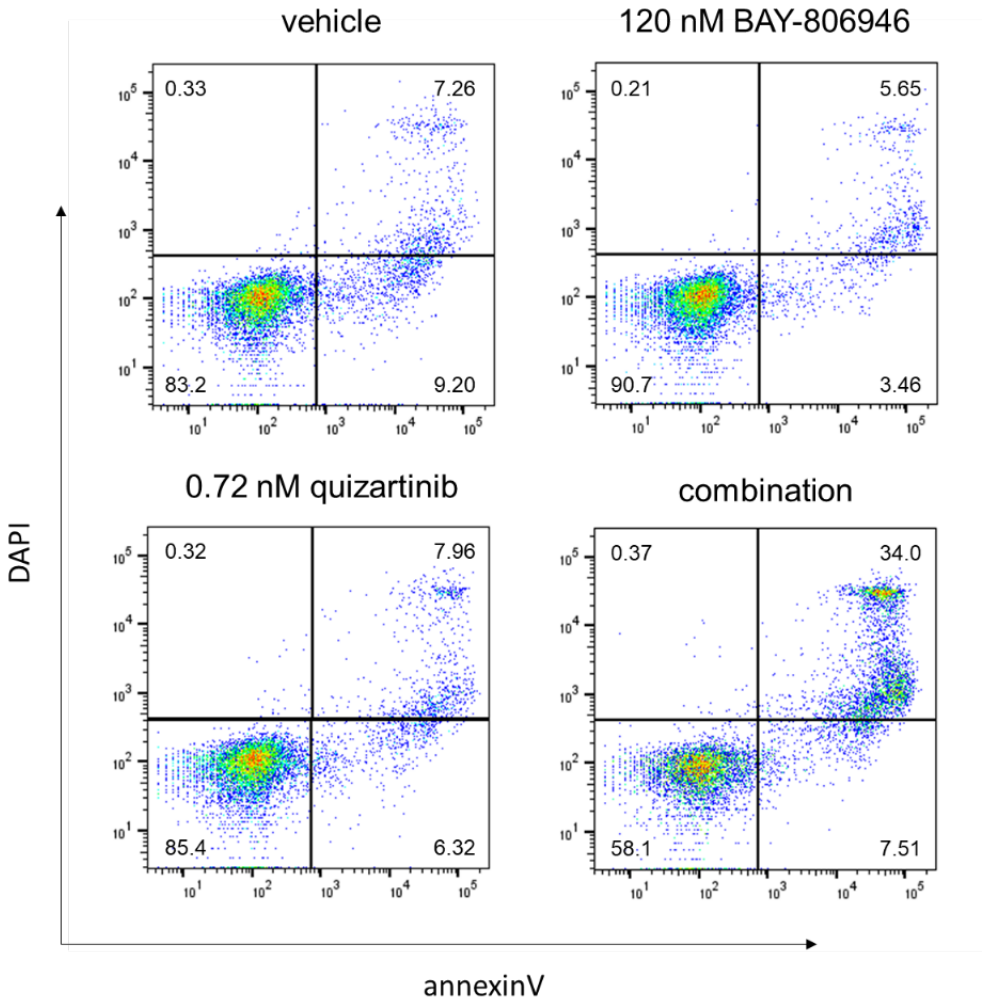

Figure 5.7 Combination of quizartinib with BAY-806946 or PF-04691502 exerts enhanced apoptotic effects

MOLM-13 (FLT3-ITD) cells were exposed to increasing concentration of quizartinib (quiz), BAY-806946 (BAY) or PF-04691502 (PF), around their respective IC50 concentrations for 48 hrs, either alone or in combination. 1x IC50 were 110 nM (BAY), 60 nM (PF) and 0.72 nM (quiz). Apoptosis was measured by annexinV/DAPI staining, detected by flow cytometry. **A)** Each bar represents the average percentages of apoptotic cells ± SD of four independent replicates. Statistical analysis was performed by one-way ANOVA followed by Tukey's multiple comparisons test. (**p ≤ 0.01, ****p ≤ 0.0001). **B)** Dot plots representing an example of apoptosis measurement following treatment with quizartinib and BAY-806946 alone or in combination. Published in (Darici et al., 2021).

5.3 Combination of quizartinib with BAY-806946 or PF-04691502 displays prolonged inhibition of mTOR signaling

Besides exploring the efficacy of quizartinib in combination with BAY-806946 or PF-04691502, it was sought to investigate whether combination treatment enhances signaling pathway inhibition at the protein expression level by western blot. As pathway reactivation by feedback mechanisms is a major drawback for FLT3i and PI3K/AKT/mTORi, the pathway activity was assessed following short-term (2 hrs) and long-term (24 hrs) drug exposure. Levels of phosphorylated AKT (S473), rpS6 (S235/236) and ERK (T202/Y204) respective to total protein was determined as an indication of PI3K/AKT/mTOR and FLT3-ITD activation status. The lowest concentration of both inhibitors that induced a synergistic drug response was chosen for combination treatment on MOLM-13 cells.

Results confirm that after 2 hrs of treatment, both BAY-806946 and PF-04691502 inhibit phosphorylation of AKT at S473 (BAY-806946: 0.3-fold difference; PF-04691502: 0.2-fold difference) and rpS6 at S235/236 (BAY-806946: 0.3-fold difference; PF-04691502: 0.2-fold difference). Further, quizartinib – but not the PI3Ki, inhibited phosphorylation of ERK at T202/Y204 (0.51-fold difference) (Figure 5.8 A-B). While it was anticipated that combination treatment might further enhance signaling blockade, inhibition of AKT and ERK following combination treatment was within the effect seen with either monotherapies. Combination treatment appeared to enhance inhibition of rpS6 respective to monotherapy, but this was not significantly different.

Surprisingly, following 24 hrs of treatment, quizartinib (2.5-fold difference) and BAY-806946 (1.6-fold difference) led to upregulation of p-AKT, which was abrogated by drug combination (0.9-fold difference). PF-04691502 sustained inhibition of AKT activity (0.3-fold difference), but this was not further enhanced by combination with quizartinib (0.8-fold difference). With regards to ERK activity, only quizartinib inhibited p-ERK (0.6-fold difference), but combination treatment with either PI3Ki did not strengthen this effect. Both PI3Ki (BAY-806946: 0.3-fold difference; PF-04691502: 0.3-fold difference) and quizartinib (0.3-fold difference) effectively inhibited phosphorylation of rpS6, which was stronger with drug combination (0.1-fold difference for both PI3Ki). However, this effect was not significantly different from either monotherapy.

For western blotting, instead of vehicle, an untreated control (NDC) was included. To demonstrate that the vehicle does not affect phosphorylation levels of detected proteins, cells were exposed to DMSO (0.0012% (v/v); PF-04691502 and quizartinib vehicle, at

highest concentration evaluated) and TFA (0.0011% (v/v); BAY-806946 vehicle) alone in combination for 2 or 24 hrs. Large variations were found when cells were exposed to the vehicle controls respective to NDC, which may negate any observed effects following drug treatment. It is possible that the vehicles at the evaluated concentration affects phosphorylation levels of the proteins detected, but since this is based on a single measurement, repeated measurements should be performed to confirm this (Figure 5.9).

Based on indications that rebound signaling occurs following long-term drug treatment, it was sought to elucidate persistent protein targets following combination treatment by RPPA analysis. Phosphoproteomic profiling by RPPA is a powerful tool that enables high-throughput detection and quantification of numerous downstream effectors of several signaling pathways. RPPA analysis may give some understanding of the underlying mechanism of pathway reactivation.

MOLM-13 cells were treated with either BAY-806946 or quizartinib alone or in combination. AKT activity was determined by phosphorylation status of its downstream target GSK-3α/β that is phosphorylated at two residues, S21 and S9, respectively (McCubrey et al., 2014). While either monotherapies did not alter levels of phosphorylated GSK-3α/β, combination treatment caused a reduction (0.9-fold difference) respective to vehicle control (Figure 5.10). Rebound activation of PI3K signaling was detected by phosphorylation of IRS-1 (S612) (Andreozzi et al., 2004). Surprisingly, whilst quizartinib reduced phosphorylation of IRS-1 (0.8-fold difference), combination treatment paradoxically caused an upregulation (1.1-fold difference) respective to vehicle control.

mTOR activity was assessed by phosphorylation status of its downstream targets rpS6 (S240/244) and 4E-BP1 (S65); and p-mTOR (S2448) which is key to its activity (Abraham and Eng, 2008; Gingras et al., 1999; Holz and Blenis, 2005; Hutchinson et al., 2011; Sekulić et al., 2000). With regards to rpS6, both BAY-806946 (0.3-fold difference) and quizartinib (0.3-fold difference) inhibited p-rpS6, which was enhanced with drug combination (0.2-fold difference). Similarly, drug combination displayed stronger inhibition of p-4E-BP1 and p-mTOR respective to either monotherapies. These results suggest that combination of BAY-806946 with quizartinib potentiates inhibition of mTOR, which is in line with western blot results.

Further, levels of phosphorylated STAT5 (Y694) and ERK (T202/Y204) were detected indicative of FLT3-ITD activation status. Whereas quizartinib was shown to inhibit p-ERK up to 24 hrs of treatment by western blot, this effect was not observed in the RPPA analysis. Combination treatment caused upregulation of p-ERK and p-STAT5 levels respective to vehicle control. Lastly, cleaved PARP levels – a hallmark of apoptosis, were measured to

confirm that drug combination indeed induces apoptosis in MOLM-13 cells (Kaufmann et al., 1993). Combination treatment induced a 2-fold increase of cleaved PARP respective to vehicle control, whereas this was only marginal with either monotherapies (BAY-806946: 1.2-fold difference; quizartinib: 1.1-fold difference). This is in line with results showing that combination treatment synergistically induces cytotoxic in FLT3-ITD AML cell lines measured by flow cytometry.

In summary, these results demonstrated that combination treatment of BAY-806946 or PF-04691502 with quizartinib enhances inhibition of mTOR which is sustained up to 24 hrs following drug treatment. However, concomitant combination treatment is unable to sustain inhibition of downstream signaling of FLT3-ITD, leading to upregulation of AKT, STAT5 and ERK signaling.

A

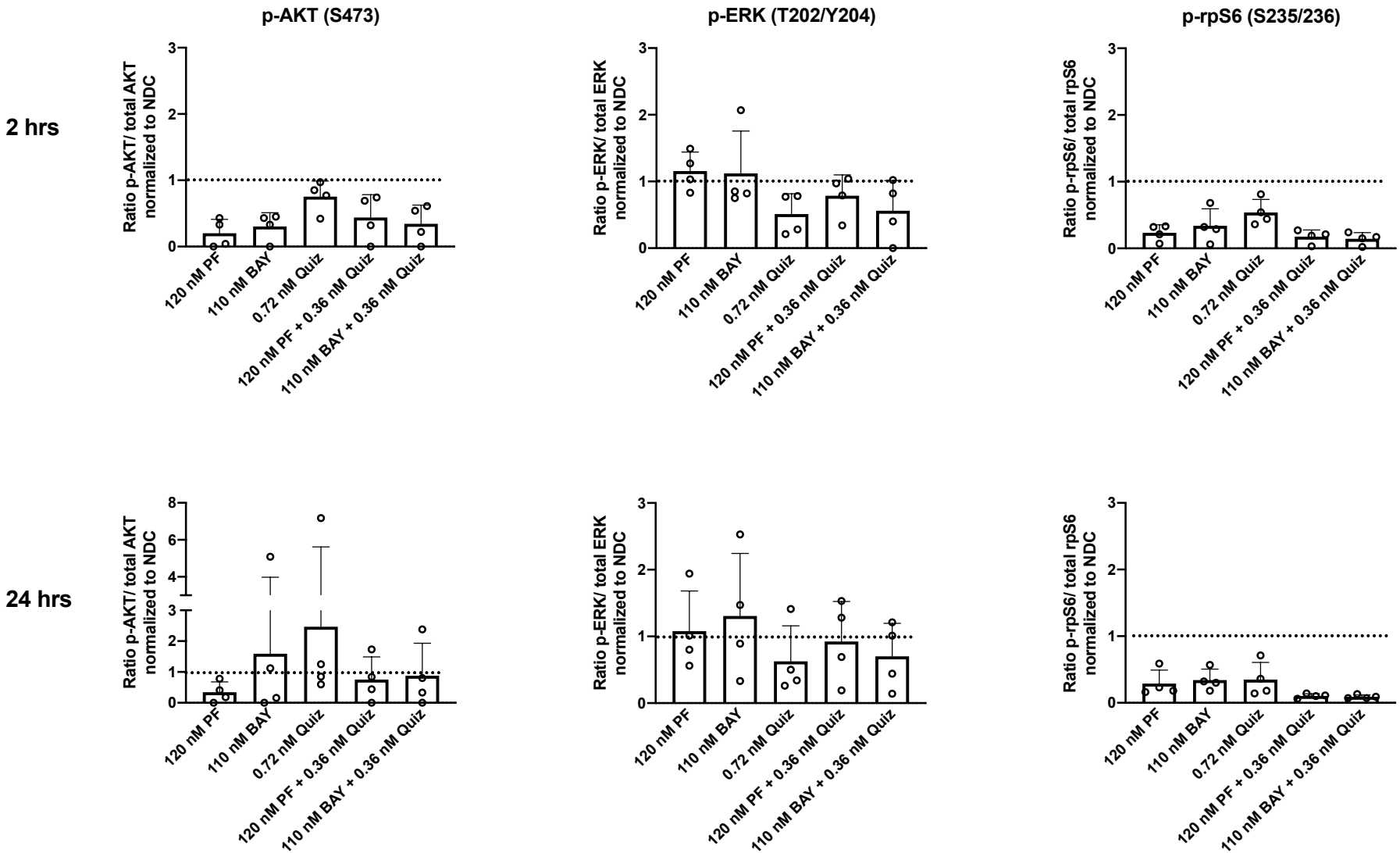
p-AKT (S473)
p-ERK (T202/Y204)
p-rpS6 (S235/236)
2 hrs
24 hrs
Ratio p-AKT/ total AKT normalized to NDC
Ratio p-ERK/ total ERK normalized to NDC
Ratio p-rpS6/ total rpS6 normalized to NDC
120 nM PF
110 nM BAY
0.72 nM Quiz
120 nM PF + 0.36 nM Quiz
110 nM BAY + 0.36 nM Quiz

B

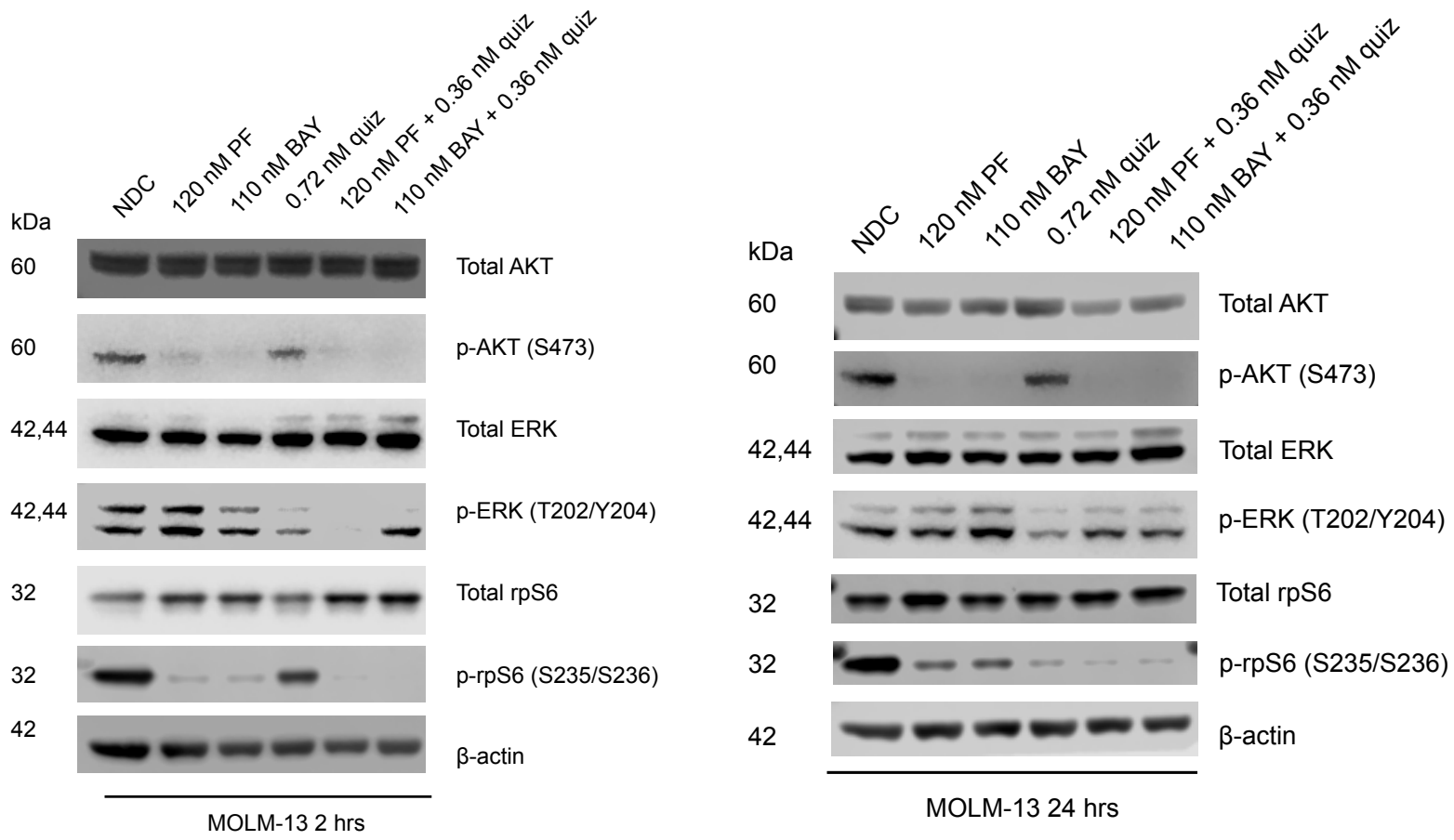

Figure 5.8 Long-term treatment with combination of quizartinib and BAY-806946 leads to rebound activation of AKT, but sustains inhibition of mTOR in FLT3-ITD AML cell lines

A) MOLM-13 (FLT3-ITD) cells were treated with quizartinib (quiz), BAY-806946 (BAY) and PF-04691502 (PF) alone or in combination at the indicated concentrations for 2 or 24 hrs. Western blot analysis was performed on cell lysates using antibodies against indicated proteins. Bar graphs represent the average quantification of four independent replicates ± SD. Statistical analysis was performed by one-way ANOVA followed by Tukey's multiple comparisons test. **B)** One representative western blot for each time point is shown.

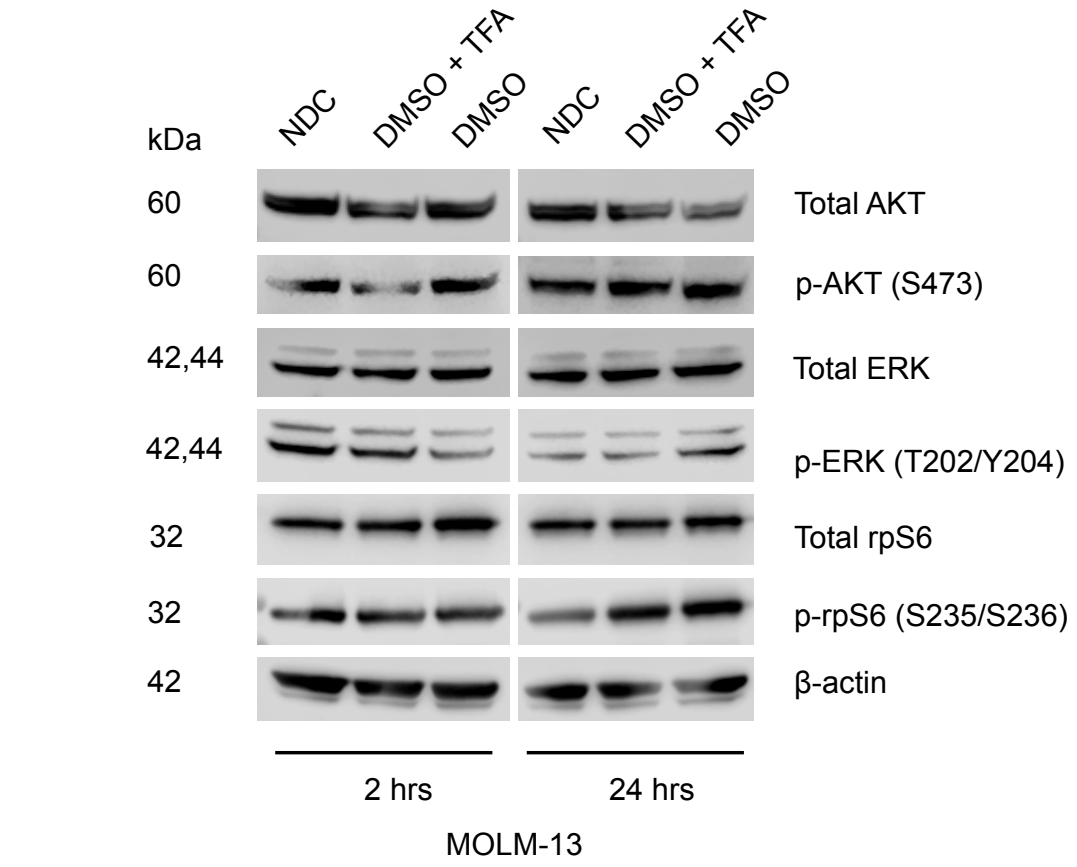

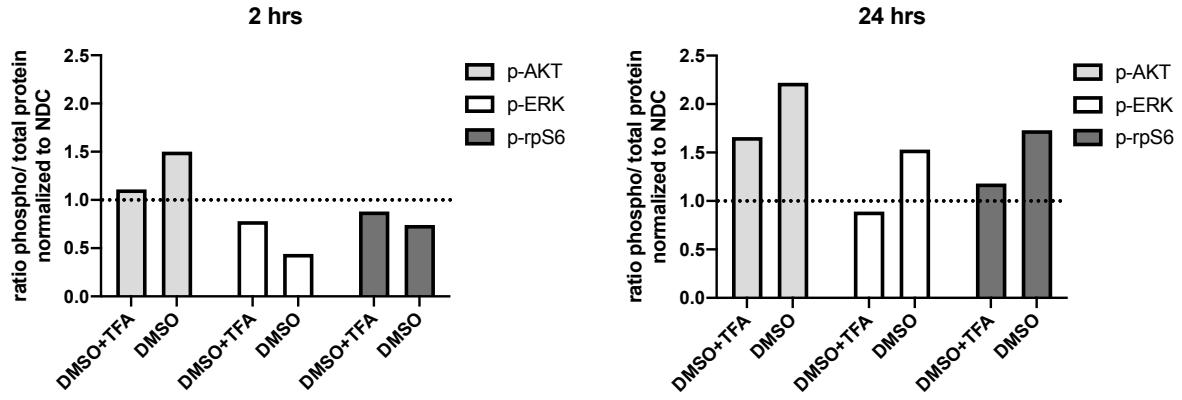

Figure 5.9 Vehicle control affects phosphorylation levels of detected proteins in FLT3-ITD AML cell lines

To demonstrate that the vehicle controls do not affect protein expression levels respective to no drug control, MOLM-13 cells were exposed to vehicle controls DMSO (0.0012%), TFA (0.0011%) or combination for 2 or 24 hrs in a single measurement. Western blot analysis was performed on cell lysates using antibodies against indicated proteins. Bar graphs represent the quantification of the western blot shown.

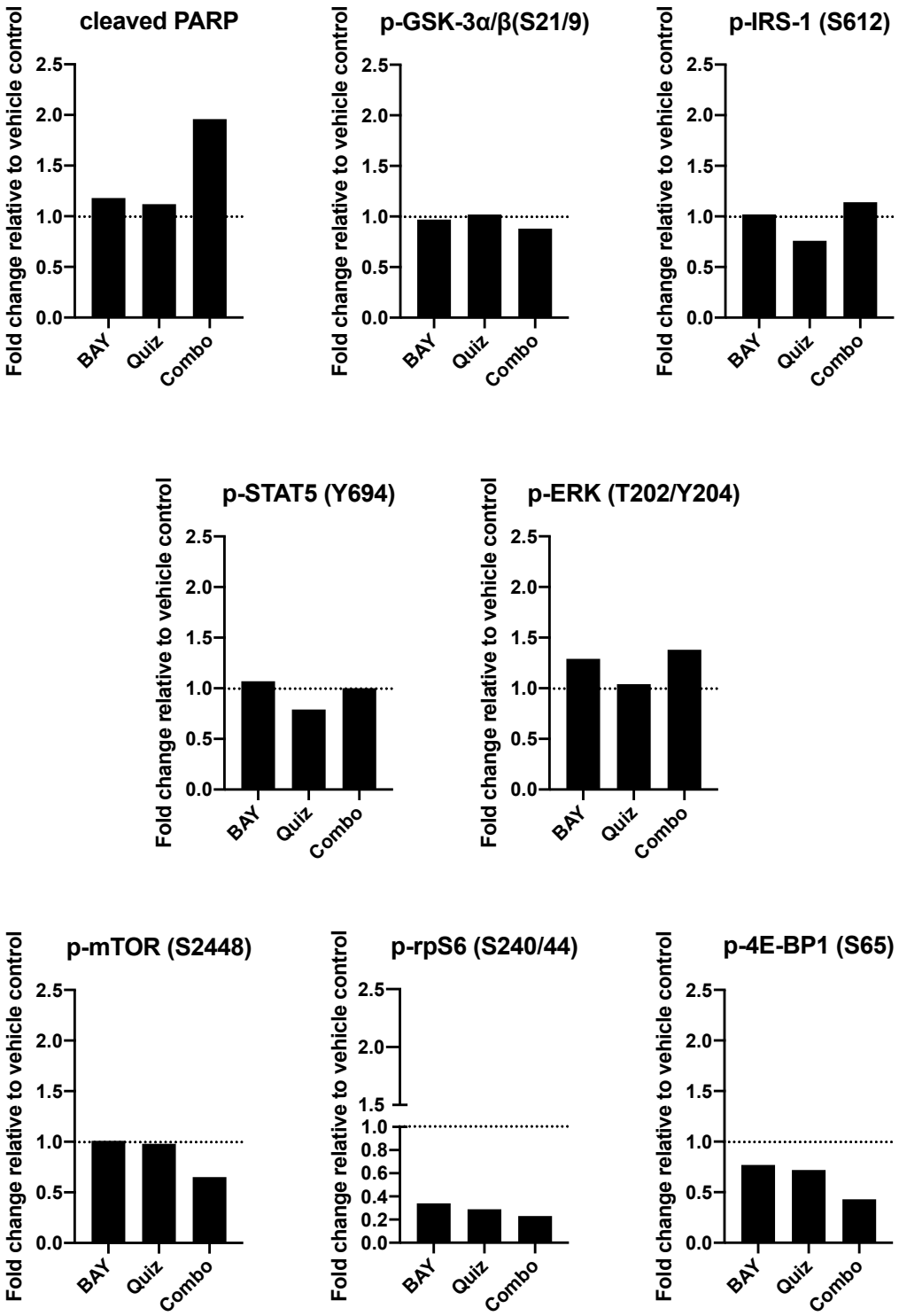

Figure 5.10 Rebound activation of AKT following combination treatment may involve upregulation of STAT5 and/or IRS-1 activity in FLT3-ITD AML cell lines

MOLM-13 (FLT3-ITD) cells were treated with quizartinib (quiz) (0.72 nM) and BAY-806946 (BAY) (110 nM) alone or in combination (0.36 nM quiz + 110 nM BAY) for 24 hrs. The expression of the proteins indicated was analyzed by reverse phase protein array (RPPA). Bar graphs depict the fold change relative to vehicle control of a single measurement.

5.4 Discussion

Acquired resistance mechanisms leading to disease relapse with selective FLT3i monotherapy has resulted in a need to evaluate combination approaches with chemotherapeutic agents or targeted therapies. Upregulation of PI3K/AKT/mTOR was shown in FLT3i-resistant FLT3-ITD AML cells, and concomitant inhibition of PI3K/AKT/mTOR potentiated the antileukemic effects of FLT3i i*n vitro* (Darici et al., 2021; Lindblad et al., 2016; Piloto et al., 2007). The main aim of this pre-clinical research was to validate whether combination of quizartinib with PI3K/AKT/mTORi was worthy of translation into the clinic. First, the efficacy of selected inhibitors was profiled in FLT3-ITD AML cell lines (c.f. Chapter 4). The main observations were that FLT3i or PI3K/AKT/mTORi induce growth inhibition as monotherapies, and in the case of PI3K/AKT/mTORi this was mainly through cell cycle arrest. In this chapter it was further investigated whether the combination of quizartinib with either BAY-806946 or PF-04691502 can potentiate the efficacy of quizartinib in FLT3-ITD AML cell line, MOLM-13.

First, it was assessed whether combination treatment enhances growth inhibition compared to monotherapy. Indeed, combination of quizartinib with either BAY-806946 or PF-04691502 displayed enhanced inhibition of cell growth and this effect was synergistic. From the obtained observations, a number of drug combinations were selected to further assess cell cycle status and apoptosis. Whereas the PI3K/AKT/mTORi as monotherapy were mainly cytostatic and only moderately apoptotic, combination treatment of quizartinib with either PI3K/AKT/mTORi synergistically induced G1 cell cycle arrest and apoptosis.

Further, it was also determined whether combination treatment enhances signaling pathway inhibition at the protein expression level whilst avoiding pathway reactivation by negative feedback mechanisms. It was expected that combination treatment would potentiate inhibition of FLT3-ITD and PI3K/AKT/mTOR signaling. Whilst combination treatment potentiated inhibition of mTOR signaling which was sustained up to 24 hrs, reactivation of ERK and AKT was observed. In an attempt to unveil the underlying mechanism of pathway reactivation following combination treatment, RPPA analysis was performed to identify persistent protein targets. In line with western blot results, either monotherapies induced inhibition of mTOR activity, which was enhanced with drug combination. Also, in agreement with cytotoxicity results detected by flow cytometry, drug combination induced apoptosis, measured by increased level of cleaved PARP. Combination treatment had a negligible effect inhibiting AKT downstream target GSK-3α/β and caused a moderate increase of p-IRS-1 levels, suggesting inefficient inhibition of the PI3K/AKT axis that may involve IRS-

mediated feedback activation. In fact, combination treatment counteracted FLT3-ITD signaling inhibition, observed by upregulation of ERK and STAT5, which might be avoided by modifying the treatment regimen and/or introducing a STAT5-directed targeted treatment.

There are several studies that confirm adaptive feedback mechanism in FLT3-ITD AML that in response to FLT3 TKI caused reactivation of STAT5, ERK, and PI3K/AKT/mTOR signaling (Bruner et al., 2017; Lindblad et al., 2016; Patel et al., 2020). Large body of evidence had demonstrated that combination treatment with cytotoxic agents such as induction chemotherapy and/or other targeted therapies may potentiate the efficacy of quizartinib. For instance, combination of quizartinib with dasatinib, a second-generation TKI, abolished STAT5 activation and overcame stromal protection in FLT3-ITD AML cells (Patel et al., 2020). Another combination includes combination of FLT3i with venetoclax (Bcl-2 inhibitor), which abrogated MAPK reactivation in FLT3 TKI resistant cells (Zhu et al., 2021). Combination of quizartinib with BET inhibitors has also been explored in FLT3-ITD AML (Lee et al., 2021). BET inhibitors can suppress pro-survival proteins Bcl-2 and Myc and in combination with quizartinib, synergistic cytotoxicity was demonstrated *ex vivo*. Whilst quizartinib and crenolanib are still in late-stage of clinical development for the treatment of newly diagnosed and refractory/relapsed AML, FLT3i midostaurin, and gilteritinib have been granted FDA approval in combination with chemotherapy (Perl et al., 2019; Stone et al., 2017). Currently, a triple combination consisting of quizartinib with decitabine and venetoclax is under clinical investigation (Phase 1/2) for relapsed/refractory FLT3-ITD AML (NCT03661307) (Yilmaz et al., 2021, 2020). The combination of FLT3i and PI3K/AKT/mTORi tested here may similarly be potentiated by addition of a third targeted therapy that prevents STAT5 activation.

An important consideration is intermittent dosing regimen may be more tolerable and effective (Lai et al., 2019). This approach that may not only reduce the minimal cytotoxic concentration, but also sustain FLT3-ITD and PI3K/AKT/mTOR signaling inhibition (Luedtke et al., 2020). To evaluate quizartinib with BAY-806946 or PF-04691502 by means of sequential drug treatment, *in vitro* studies are required to determine the optimal order of drug administration, treatment time between addition of the two inhibitors and the drug concentration. Since quizartinib only partially inhibited ERK and PI3K/AKT/mTOR signaling which was not further enhanced by simultaneous addition of BAY-806946 or PF-04691502, it is hypothesized that adding the PI3Ki second may prevent PI3K/AKT/mTOR rebound activation.

Based on the enhanced cytotoxic effect observed by combining FLT3 TKI with PI3K/AKT/mTORi in cell lines, it was aimed to evaluate the combination treatment on FLT3-

ITD AML primary patient blast to elevate this research in a more clinically relevant setting. *Ex vivo* assays hold great advantage to study primary or acquired resistance mechanisms as well as AML treatment options (Cucchi et al., 2020; Sontakke et al., 2014). However, many pre-clinical findings failed to successfully translate into a clinical setting due to genetic and clonal heterogeneity in addition to the protective role of the BM microenvironment *in vivo*. Although cell lines offer several advantages over primary cells such as that they have an indefinite lifespan, cost-effective and easy to use, they are biologically distinct from primary cells. Primary cells require stromal support for survival, without which AML primary cells rapidly undergo differentiation and apoptosis in *ex vivo* cultures (Azadniv et al., 2020; Garrido et al., 2001). Furthermore, cell lines originate from selected patients and are often dependent on a driver mutation (van Alphen et al., 2020). Over long periods of culturing, they can acquire cytogenetic aberrations (Kasai et al., 2016). Because cell lines exhibit altered physiological properties they are not representative of the *in vivo* state unlike primary cells. Thus, *ex vivo* assays using primary cells are needed to demonstrate that the drug combination is also effective in a more clinically relevant setting.

Chapter 6: Combination of quizartinib and BAY-806946 induces cytotoxicity *ex vivo* in primary human FLT3-ITD AML

Treatment of FLT3-ITD AML remains challenging despite the development of potent and selective FLT3i. Drug resistance remains an important determinant of FLT3-ITD AML treatment failure. Despite the development of potent next-generation FLT3i, the relapse rate remains high, as the remissions are often short-lived (Cortes et al., 2019, 2018). Extensive research has identified molecular mechanisms of resistance to FLT3i that can be classified in primary or secondary resistance mechanisms (Eguchi et al., 2020; Friedman, 2022; Scholl et al., 2020).

Primary resistance mechanisms may arise from cellular mechanisms including co-occurring FLT3-TKD mutations within the FLT3-ITD allele, mutations other than *FLT3*, activation of alternative signaling pathways in leukemic cells or the bone marrow niche involved in leukemic cell survival (Kumar et al., 2018; Piloto et al., 2007; Yang et al., 2014; Zeng et al., 2009). Often FLT3-ITD AML cells also express wildtype FLT3, and since wildtype FLT3 is relatively resistant to FLT3i, secretion of FL by the BM niche attenuates anti-leukemic effects induced by FLT3i (Sato et al., 2011).

Secondary resistance mechanisms or acquired resistance to FLT3i are caused by additional mutations in FLT3 ("on-target" resistance) or apart from FLT3 ("off-target" resistance) (Daver et al., 2021). On-target resistance includes emergence of secondary TKD mutations in patients that have received treatment with type II FLT3i such as quizartinib. Quizartinib selective targets FLT3-ITD without affecting FLT3-TKD mutations (Chen et al., 2016; Levis et al., 2005). Therefore, secondary mutations at D835 and Y842 residues in the activation loop as well as the gatekeeper residue F691 in the kinase domain can confer resistance to FLT3i (Man et al., 2012; Smith et al., 2015, 2012). Off-target resistance to FLT3i can be caused by clonal evolution when the *FLT3*-ITD mutant clone is lost at relapse after FLT3i-based therapies (Alotaibi et al., 2021). Gain-of-function mutations in genes other than FLT3 may also lead to the development of clinical resistance to FLT3i. Recently, distinct patterns of resistance in patients with FLT3-ITD AML treated with different FLT3i were studied before and after relapse. Common mutations included *NRAS*, *IDH* and less frequently, wilms tumor 1 (*WT1*) (Alotaibi et al., 2021; McMahon et al., 2019). Other studies have reported the overexpression of PIM, receptor tyrosine kinase AXL, and upregulation of the PI3K/AKT/mTOR pathway in FLT3-ITD AML resistant to FLT3i therapy (Dumas et al., 2019;

Lindblad et al., 2016; Park et al., 2015; Perl et al., 2019). Unraveling mechanisms of resistance might facilitate formulation of strategies to prevent emergence of resistance and essentially avoid disease relapse.

It has been well established that the BM microenvironment that harbor LSC, confers resistance to chemotherapy as well as targeted therapies through leukemia-stroma interactions, release of extracellular soluble mediators such as cytokines, and adhesion molecules (Bolandi et al., 2021; van Gils et al., 2021). Indeed, several studies have demonstrated that stromal cells prevent FLT3-ITD AML cells from undergoing apoptosis following FLT3i treatment (Dumas et al., 2019; Patel et al., 2020; Sexauer et al., 2012). While FLT3 inhibition is able to rapidly eradicate circulating FLT3-ITD AML cells in the peripheral blood, BM cells often show little noticeable response (Borthakur et al., 2011; Weisberg et al., 2012). This highlights the importance of capturing facets of the BM niche to closely mimic human responses, thereby minimizing discrepancies between preclinical and clinical studies. *Ex vivo* studies have enabled creation of a cell culture environment that resembles the BM niche that has proven useful to better predict physiological response. *Ex vivo* models can be divided in three categories: culture with recombinant growth factors, 2D co-culture, and 3D co-culture. Stromal co-culture promotes AML cell viability, proliferation and colony formation through the release of soluble factors and cell contact-mediated pathways (Cucchi et al., 2020; Dhami et al., 2016; Ladikou et al., 2020; Xia et al., 2015). Indeed, direct contact of AML cells with stromal cell lines has proven to protect AML cells against apoptosis induced by chemotherapy as well as FLT3i (Dumas et al., 2019; Kim et al., 2020).

In the previous chapter, it was demonstrated that combination of quizartinib with BAY-806946 or PF-04691502 synergistically induced cytotoxicity in FLT3-ITD AML cell lines. Based on these promising results, it was aimed to assess the efficacy of the drug combination *ex vivo* using primary patient cells. To mimic BM niche-like microenvironment and support the growth of AML cells, primary patient cells were co-cultured with stromal cell line MS-5 and exogenous physiological growth factors (PGF) (IL-3, G-CSF and TPO) (Griessinger et al., 2014). The clinical activity of PI3Ki has been extensively reviewed and it has been reported that pan-PI3Ki are clinically more challenging because of a broad toxicity profile. PF-04691502 is a dual pan-PI3Ki/mTORi, but BAY-806946 is a pan-PI3Ki with predominantly activity against PI3K-α and PI3K-δ isoforms, and is therefore more specific. For this reason, from a clinical point of view, it was chosen to evaluate BAY-806946 in combination with quizartinib rather than PF-04691502, First, the FLT3-ITD status of primary patient material was determined.

Next, it was assessed whether BAY-806946 could potentiate the efficacy of quizartinib in co-cultured FLT3-ITD AML primary patient cells and thus overcome stromal protection. To obtain an indication of a potential therapeutic window and detect any drug-related toxicity, the drug combination was also evaluated on PBMC from a healthy donor and non-AML cells. Finally, it was aimed to unravel the mechanism by which BAY-806946 potentiates the efficacy of quizartinib and identify persistent phosphoproteins and secreted cytokines by RPPA and Luminex assays, respectively. The clinical success of PI3K and/or FLT3i have been hampered by resistance mechanisms caused by incomplete pathway blockade and negative feedback mechanisms, which leads to rebound activation of upstream RTKs and PI3K signaling pathway activity (Scholl et al., 2020; Wright et al., 2021). AML cells have the capacity to constitutively release extracellular soluble factors that may facilitate the survival of AML cells through a common signaling pathway (Abdul-Aziz et al., 2017; Brenner et al., 2017a; Sepehrizadeh et al., 2014). Comparing the phosphoproteomic profile with the cytokine release profile following combination treatment may identify putative targets to improve current therapeutic strategies for AML.

6.1 FLT3-ITD status of primary patient material

In this thesis work, two FLT3-ITD AML PDX samples and nine FLT3-ITD primary patient samples were evaluated (Table 2.2). Confirmation of FLT3-ITD mutational status was performed by separation of the PCR products by gel electrophoresis. A wildtype FLT3 sample was included as control (Figure 4.16).

The evaluated PDX samples 8.3d and 9.2h originate from primary patient samples AML020 and AML009, respectively. The FLT3-ITD insertion is clearly visible for PDX sample 9.2h, whereas the band for 8.3d appears weak (indicated with a circle). Of the nine FLT3-ITD AML primary patient samples on which the drug combination was evaluated, gDNA from eight patient samples was harvested. Samples AML004, AML005, and AML006 have a higher intensity *FLT3*-ITD band intensity compared to their respective wildtype FLT3 band (~300 bp), suggesting that these patients potentially have a higher FLT3-ITD allelic ratio. AML003, AML008, AML009, and AML027 have a higher intensity wildtype FLT3 band intensity respective to FLT3-ITD, meaning that these patients could have a low FLT3-ITD allelic ratio. It is also worth noting that the insertion size is variable among the different patient samples. In particular, samples AML003, AML006, AML008, and AML027 seem to have the largest insertion size.

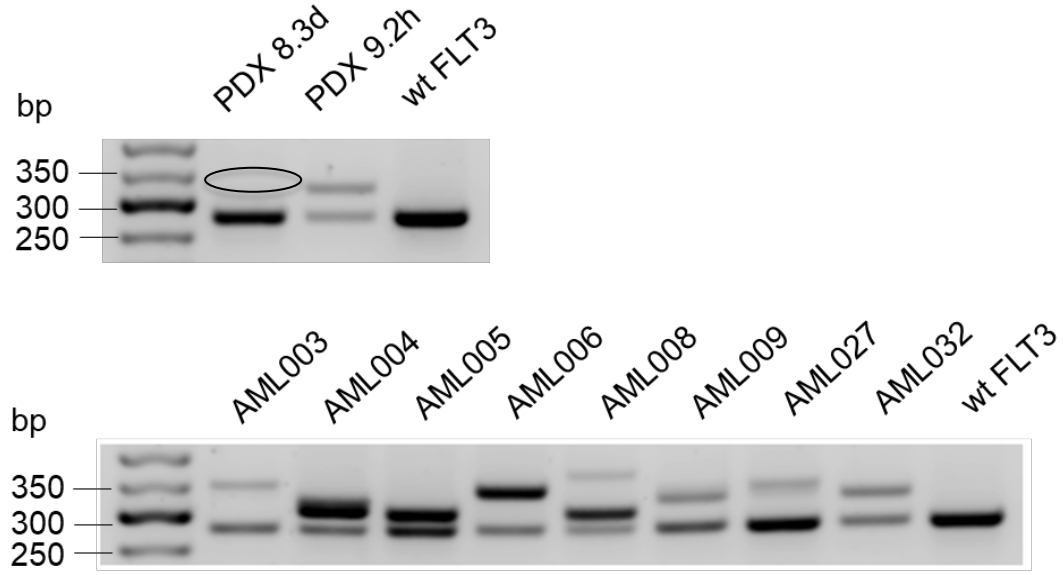

Figure 6.1 Expression of FLT3-ITD in PDX and primary patient AML cell samples

FLT3-ITD mutational status of PDX and primary patient samples used in this thesis was confirmed by PCR. AML cell line THP-1 was included as FLT3 wildtype control. Circle indicates a weak FLT3-ITD insertion.

6.2 BM stromal cells prevent apoptosis in FLT3-ITD AML PDX cells upon FLT3 inhibition

Primary cells are known to exhibit different drug response to cell lines, in part due to different culture conditions and variation in molecular profile among patient samples. Therefore, it is necessary to determine at which concentration quizartinib and BAY-806946 should be combined when evaluating in combination with FLT3-ITD AML primary patient cells. The efficacy of quizartinib was assessed by measurement of cell growth and apoptosis. In a recent report, the Marmiroli lab showed that 500 nM BAY-806946 was effective at inducing apoptosis in AML primary patient cells as measured by cleaved caspase 7 and PARP (Darici et al., 2021). This concentration was selected for evaluation on patients' cells. FLT3-ITD AML PDX cells were cultured either in the absence or presence of murine stromal cell line MS-5 and/or exogenous PGF. FLT3-ITD AML cells without MS-5 in serum-free expansion medium (SFEM) was not evaluated as it was expected that cells would not be viable in this culture condition. It was hypothesized that co-culture with stroma protects FLT3-ITD AML cells against FLT3i-induced cytotoxicity.

Results showed that quizartinib (5 μM) treatment inhibited cell growth in the presence of stroma respective to vehicle control (0.6-fold difference), which was attenuated with addition of PGF (0.7-fold difference) (Figure 6.2). As expected, stroma promoted the viability of FLT3-ITD AML cells observed by elevated levels of apoptosis in vehicle control minus MS-5 versus vehicle control plus MS-5 (Figure 6.3). Stroma also protected FLT3-ITD AML cells against quizartinib-induced apoptosis as observed by drastic reduction of apoptotic levels in cells cultured with MS-5 plus/minus PGF. As such, FLT3-ITD AML cells minus MS-5 displayed 60.7% apoptosis following quizartinib (5 μM) treatment, whereas these levels in co-cultured cells plus/minus PGF were 13.6% and 7.9%, respectively (Figure 6.3). It was predicted that FLT3-ITD AML cells with a lower FLT3-ITD allelic ratio and shorter insertion size would be more sensitive to FLT3i treatment (Liu et al., 2019). Sample 8.3d was shown to have a low FLT3-ITD allelic ratio, but similar insertion size respective to sample 9.2h. Looking more closely at the individual response of the two PDX samples evaluated, it appeared indeed that sample 8.3d is more sensitive to quizartinib than sample 9.2h.

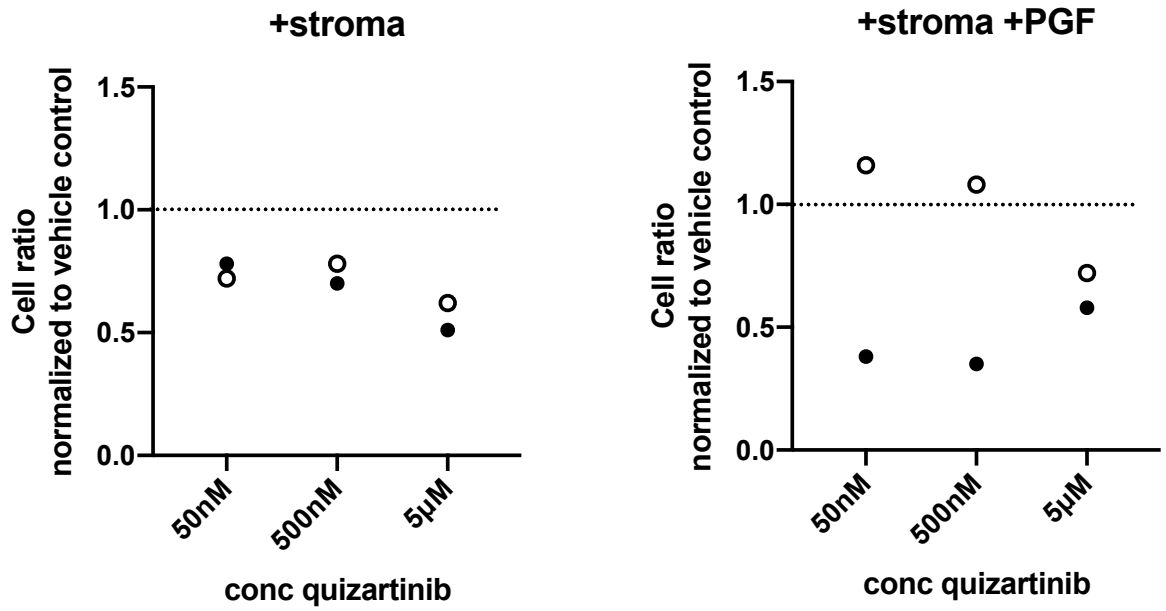

Figure 6.2 Quizartinib treatment exerts growth inhibitory effects in the presence of stroma in FLT3-ITD AML PDX cells

FLT3-ITD AML PDX cells were cultured the presence of stroma in serum-free expansion medium (SFEM) or SFEM supplemented with physiological growth factors (PGF) (IL-3, G-CSF and TPO at 1 ng/mL). Following overnight co-culture, cells were treated with quizartinib at the indicated concentrations. Growth inhibition was assessed in human CD45+ population after 48 hrs using counting beads detected by flow cytometry. Dots represent individual data points of two individual PDX samples normalized to their respective vehicle controls. Flow cytometry was used to measure apoptosis in these cells using annexinV/DAPI as shown in Figure 6.3. Filled and empty circles represent PDX samples 8.3d (low FLT3-ITD allelic ratio) and 9.2h (FLT3-ITD allelic ratio ±1), respectively.

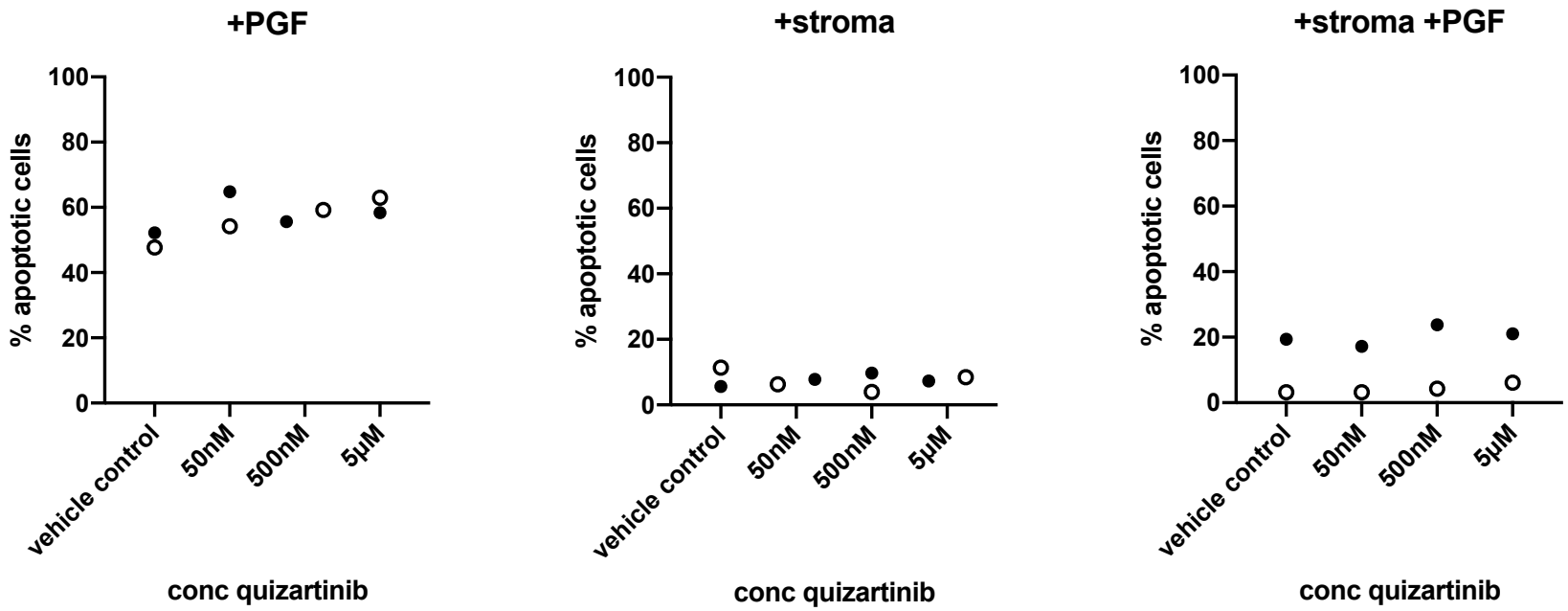

Figure 6.3 Quizartinib-induced apoptotic effects is abrogated in the presence of stroma +/- exogenous physiological growth factors in FLT3-ITD AML PDX cells

FLT3-ITD AML PDX cells were cultured in serum-free expansion medium (SFEM) or SFEM supplemented with physiological growth factors (PGF) (IL-3, G-CSF and TPO at 1 ng/mL) in the absence or presence of stroma. Following overnight co-culture, cells were treated with quizartinib at the indicated concentrations. Apoptosis was assessed in human CD45+ population after 48 hrs by annexinV/DAPI staining, detected by flow cytometry. Dots represent individual data points of two individual PDX samples. Filled and empty circles represent PDX samples 8.3d (low FLT3-ITD allelic ratio) and 9.2h (FLT3-ITD allelic ratio ±1), respectively.

6.3 Combination treatment induces synergistic growth inhibition and cytotoxicity in FLT3-ITD AML primary patient cells *ex vivo*

Next, it was assessed whether BAY-806946 potentiates the efficacy of quizartinib on FLT3-ITD AML primary patient cells *ex vivo*. Primary patient cells from nine different patients with distinct patient and molecular characteristics (Table 3.2) were cultured in the presence of stroma plus/minus PGF. Cells were treated for 48 hrs with 500 nM BAY-806946 or quizartinib as monotherapy, or in combination. Cell growth and cytotoxicity was assessed by flow cytometry.

In cells co-cultured with stroma in SFEM, monotherapy exerted 19.4% (BAY-806946) and 13.7% (quizartinib) inhibition of cell growth respective to vehicle control, which was significantly more pronounced with drug combination (48.3%) (BAY-806946; p=0.0007 and quizartinib; p=0.0209) (Figure 6.4). Similarly, with PGF, the drug combination inhibited cell growth (41.8%), which was enhanced, but not statistically significant, compared to quizartinib (23.4%) and BAY-806946 (29%) treatment alone (Figure 6.4). Combination index as determined by Bliss Independence method confirmed that in SFEM, the effect induced by the combination treatment was synergistic (CI=0.63) but not in the presence of PGF (CI=1.09). It is also worth noting that as hypothesized, drug response was not uniform amongst patient samples.

In cells co-cultured with MS-5 in SFEM, BAY-806946 and quizartinib induced 36.9% and 35.4% apoptosis, respectively, which was further enhanced with combination treatment (49.4%) (Figure 6.5). When PGF were added, BAY-806946 and quizartinib induced 33.1% and 30% apoptosis, respectively, and similarly this effect was greater with the drug combination (41.2%) (Figure 6.5). Furthermore, the apoptotic effect induced by drug combination was significantly different from monotherapy with BAY-806946 or quizartinib both in SFEM (p=0.0008 and p=0.0136) and with PGF (p=0.0032 and p=0.007). However, the combinational effect in either SFEM (CI=1.18) or with PGF (CI=1.17) was not found to be synergistic by combination index. Looking closer at the drug response in individual patient's cells, it is evident that the drug-induced cytotoxicity is variable amongst patient samples (Table 6.1). While in most patient's cells sensitivity to BAY-806946 and quizartinib alone or in combination is attenuated with the addition of PGF, the opposite was observed for samples AML005 and AML027. It is also interesting that the lowest sensitivity was observed in samples AML023 and AML032. As such, sample AML023 was not responsive to either monotherapies, and combination treatment induced only moderate levels of apoptosis

(SFEM: 24.6%; +PGF: 22.8%) and these levels were even lower in sample AML032 (SFEM: 17.3%; +PGF: 15.7%).

Apoptosis was also measured more specifically in the myeloid population (Figure 6.6). CD33 is a common myeloid marker and CD38 is expressed on most AML and myeloma cells. Thus detection of apoptosis in CD33/CD38 positive populations can be used to confirm that indeed leukemic cells are targeted by the combination treatment. Results show that in AML cells co-cultured in SFEM, 39.7% of CD45+ cells were CD33+annexinV+ following combination treatment whereas this was 29.5% with BAY-806946 (p=0.0003) and 28.3% (p=0.0141) with quizartinib treatment. Also, in co-culture with PGF, a significant increase of CD33+annexinV+ population (33.6%) was found respective to monotherapy with BAY-806946 (26.9%, p=0.0076) or quizartinib (24.8%, p=0.0159).

In CD38+annexinV+ population (from CD45+ selection), PGF induced a relatively small protective effect with respect to co-culture in SFEM. As such, in SFEM, CD38+annexinV+ population was 32.6% (BAY-806946, p=0.0013) and 31.3% (quizartinib, p=0.0196) following monotherapy and 44% with combination treatment. With PGF, BAY-806946 and quizartinib showed 28.9% (p=0.0032) and 26.2% (p=0.0106) CD38+annexinV+ cells, respectively which was increased up to 36.8% with the drug combination.

It was additionally aimed to measure cytotoxicity not only in the bulk leukemic cells, but also more specifically in the stem cell-like population, which is often resistant to apoptosis. Because LSC are at the apex generating leukemic progeny, it is essential to assess whether the drug combination is effective targeting LSC. LSCs were initially considered to reside in the CD34+CD38- fraction (Bonnet and Dick, 1997; Lapidot et al., 1994), however this remains controversial, as it has been identified that the leukemia-initiating population display a heterogeneous immunophenotype that is not restricted to the CD34+CD38- cell fraction (Goardon et al., 2011; Horton and Huntly, 2012; Quek et al., 2016). AML LSC may also co-exist in populations that phenotypically resemble more mature cells. For this reason, the CD34+CD38- fraction is referred to as “stem cell-like” population as more accurate functional assays are required to capture the frequency and activity of LSC. Of the nine FLT3-ITD AML primary patient cells evaluated, only three samples showed measurable CD34+CD38- fraction, which was in co-culture with MS-5 plus PGF (Figure 6.7). Results showed that BAY-806946 induced 3.4% apoptosis and quizartinib 2.4%, which was further enhanced to 11% (SD= 6.2) with combination treatment. The effect of the combination treatment was however not significantly different from monotherapy. It should however be considered that the sample size is relatively small and that the patient cells’ drug response was variable amongst the three samples evaluated.

In summary, these results demonstrated that BAY-806946 potentiates the efficacy of quizartinib in FLT3-ITD AML primary patient cells co-cultured with MS-5 stroma cells. Although the growth inhibitory and cytotoxic effect was attenuated with PGF, the drug combination was still able to induce significant apoptosis compared to monotherapy. Drug-induced apoptosis was detected both in the bulk leukemic cells, but to a lesser extent also in the stem cell-like CD34+CD38- subpopulation.

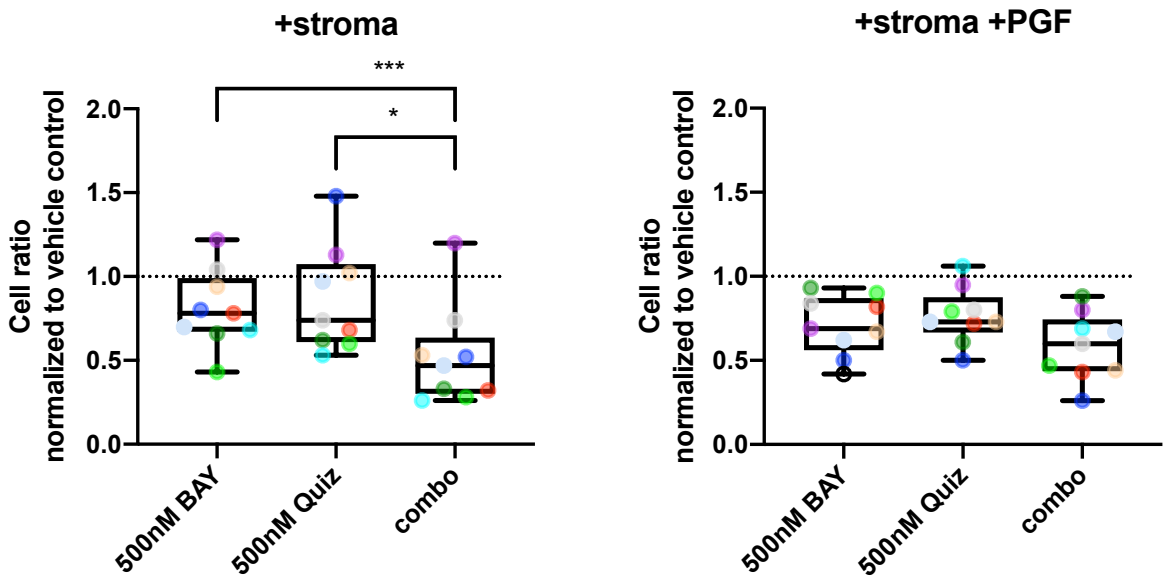

Figure 6.4 Combination treatment induces synergistic growth inhibitory effects in FLT3-ITD AML primary patient cells co-cultured on stroma but is abrogated in the presence of exogenous physiological growth factors

FLT3-ITD AML primary patient cells were cultured in the presence of stroma in serum-free expansion medium (SFEM) or SFEM supplemented with physiological growth factors (PGF) (IL-3, G-CSF and TPO at 1 ng/mL). Following overnight co-culture, cells were treated with quizartinib (Quiz) and BAY-806946 (BAY) alone or in combination at the indicated concentration. Growth inhibition was assessed in human CD45+ population after 48 hrs using counting beads detected by flow cytometry. Box plots depict cell count normalized to vehicle control of 9 individual FLT3-ITD AML primary patients. Statistical significance was calculated by one-way ANOVA (using Geisser-Greenhouse correction) followed by Tukey's multiple comparisons test (*$p \leq 0.05$, ***$p \leq 0.001$). Combination Index was calculated using the Bliss Independence method, where CI<1 indicates synergism, CI=1 independent, and CI>1 antagonism. In SFEM: CI= 0.63 and +PGF: CI= 1.09. Flow cytometry was used to measure apoptosis in these cells using annexinV/DAPI as shown in Figure 6.5.

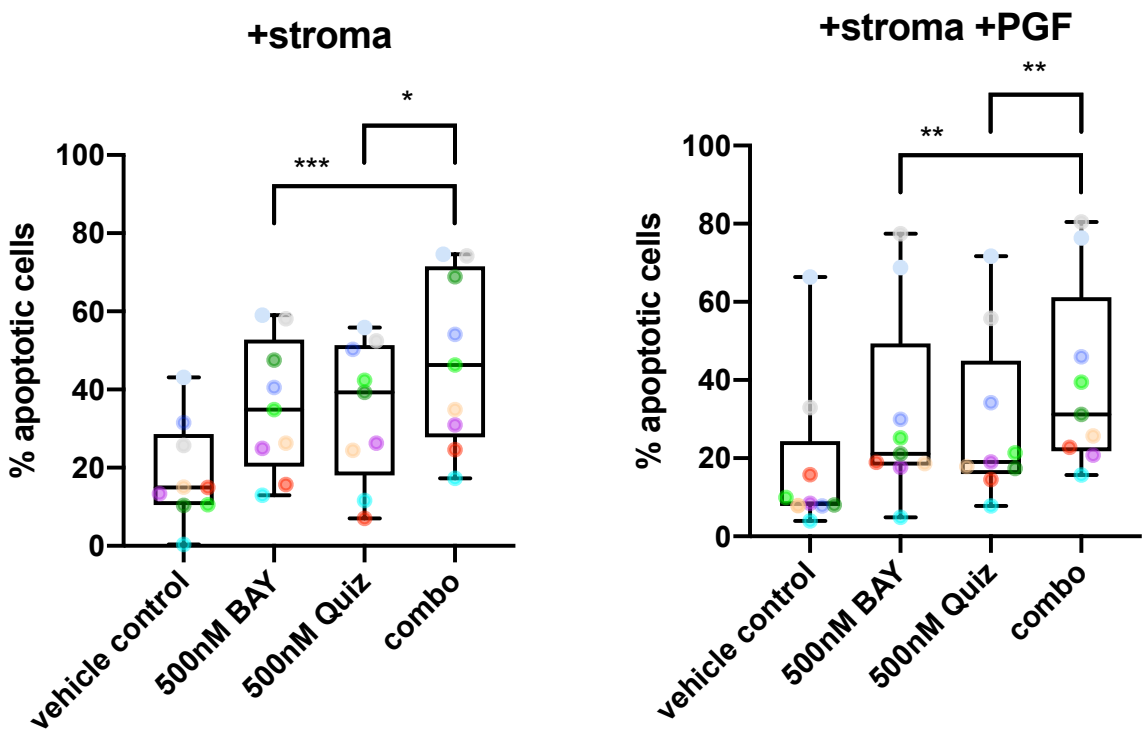

Figure 6.5 Combination treatment induces elevated apoptotic effects in FLT3-ITD AML primary patient cells co-cultured on stroma +/- exogenous physiological growth factors

FLT3-ITD AML primary patient cells were cultured in the presence of stroma in serum-free expansion medium (SFEM) or SFEM supplemented with physiological growth factors (PGF) (IL-3, G-CSF and TPO at 1 ng/mL). Following overnight co-culture, cells were treated with quizartinib (Quiz) and BAY-806946 (BAY) alone or in combination at the indicated concentration. Apoptosis was assessed in human CD45+ population after 48 hrs by annexinV/DAPI, detected by flow cytometry. Box plots depict the percentage of apoptosis in 9 individual FLT3-ITD AML primary patients. Statistical significance was calculated by one-way ANOVA (using Geisser-Greenhouse correction) followed by Tukey's multiple comparisons test (*$p \leq 0.05$, **$p \leq 0.01$, ***$p \leq 0.001$). Combination Index was calculated using the Bliss Independence method, where CI<1 indicates synergism, CI=1 independent, and CI>1 antagonism. In SFEM: CI= 1.18 and +PGF: CI= 1.27.

Table 6.1 Overview of genetic abnormalities, FLT3-ITD allelic ratio, and % apoptosis observed in FLT3-ITD AML primary patient cells co-cultured with stroma plus/minus exogenous physiological growth factors following combination treatment

% apoptotic cells (CD45+ cells)											
+ stroma				+ stroma +PGF							
vehicle control	500 nM BAY	500 nM Quiz	Combo	vehicle control	500 nM BAY	500 nM Quiz	Combo	**Sample #**	**Karyotype**	**Mutations**	**FLT3-ITD allelic ratio***
10.5	34.9	42.4	46.3	10.0	25.2	21.3	39.4	AML003	normal	FLT3-ITD/NPM1	low
10.4	47.5	39.3	68.9	8.1	21.1	17.3	31.2	AML004	normal	FLT3-ITD/NPM1	high
25.7	58.1	52.4	74.2	33.0	77.5	55.8	80.4	AML005	n.d.	FLT3-ITD/NPM1	high
15.0	26.3	24.5	34.9	7.8	18.6	17.9	25.7	AML006	normal	FLT3-ITD/NPM1	high
13.4	24.9	26.3	31.0	8.5	17.7	19.1	20.8	AML008	normal	FLT3-ITD/NPM1	low
31.6	40.5	50.3	54.2	7.8	30.0	34.2	46.0	AML009	normal	FLT3-ITD/NPM1	low
15.0	15.7	7.0	24.6	15.8	19.0	14.6	22.8	AML023	46,XX	FLT3-ITD/NPM1	n.d.
43.1	59.0	55.9	74.6	66.4	68.8	71.7	76.4	AML027	n.d.	FLT3-ITD/NPM1	low
0.4	13.0	11.6	17.3	3.9	4.9	7.8	15.7	AML032	46,XX	FLT3-ITD/NPM1/IDH	high

% apoptotic cells

< 10%

10-25%

25-50%

50-75%

>75%

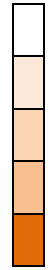

*n.d. not determined; PGF; physiological growth factors; BAY; BAY-806946; Quiz; quizartinib; * as determined in Figure 6.1*

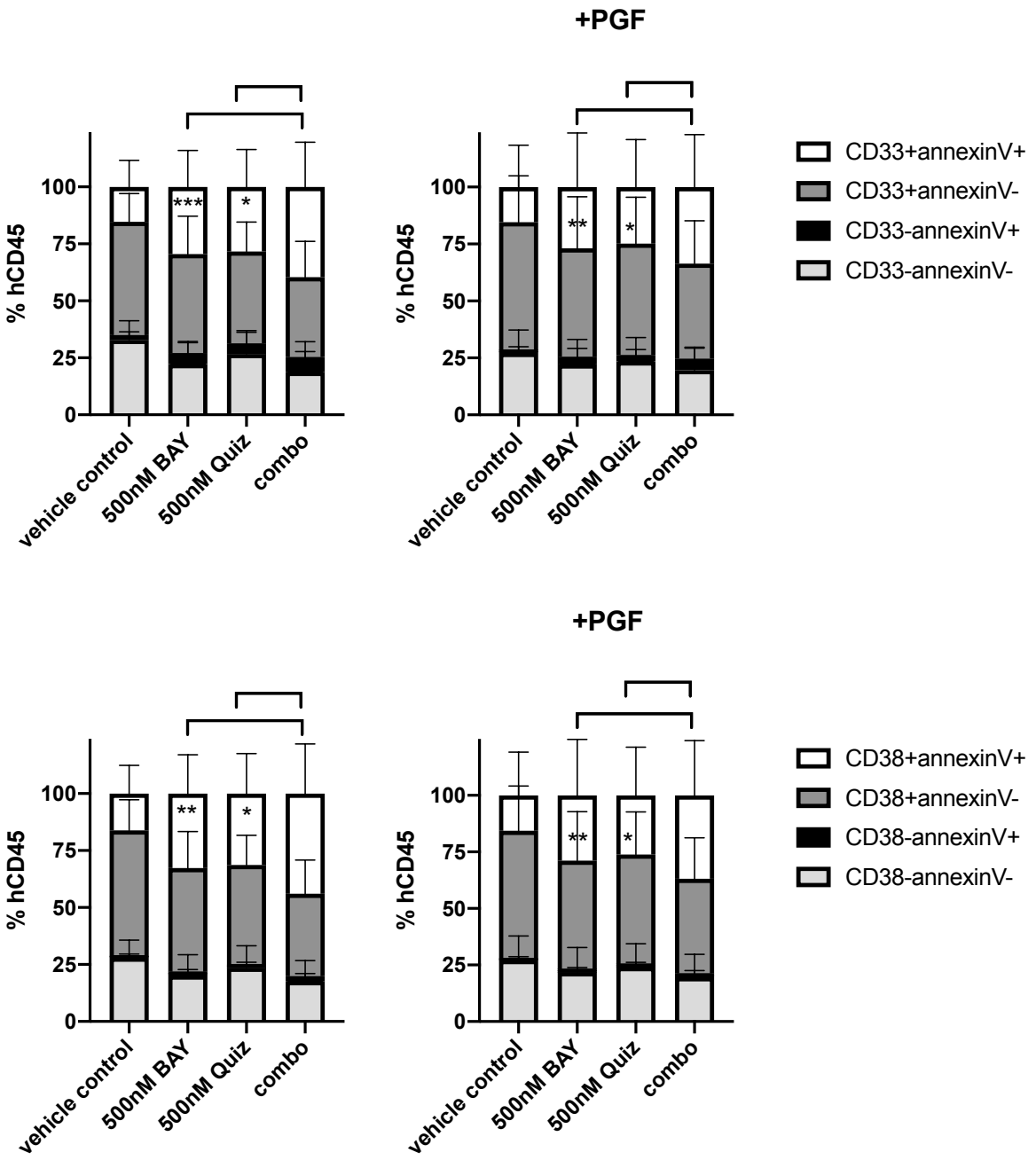

Figure 6.6 Combination treatment induces apoptosis in leukemic cells co-cultured on stroma with or without physiological growth factors

FLT3-ITD AML primary patient cells were cultured in the presence of stroma in serum-free expansion medium (SFEM) or SFEM supplemented with physiological growth factors (PGF) (IL-3, G-CSF and TPO at 1 ng/mL). Following overnight co-culture, cells were treated with quizartinib (Quiz) and BAY-806946 (BAY) alone or in combination at the indicated concentration. After 48 hrs of drug treatment, cells were stained with surface markers including CD45, CD33, CD38 and viability markers annexinV/DAPI, detected by flow cytometry. Stacked bar graphs represent the percentage of CD33/annexinV or CD38/annexinV expression in human CD45+ population in 9 individual FLT3-ITD AML primary patients. In the CD33+/annexinV+ and CD38+/annexinV+ populations, statistical significance between monotherapy with respective to drug combination was calculated by one-way ANOVA (using Geisser-Greenhouse correction) followed by Tukey's multiple comparisons test (*$p \leq 0.05$, **$p \leq 0.01$, ***$p \leq 0.001$).

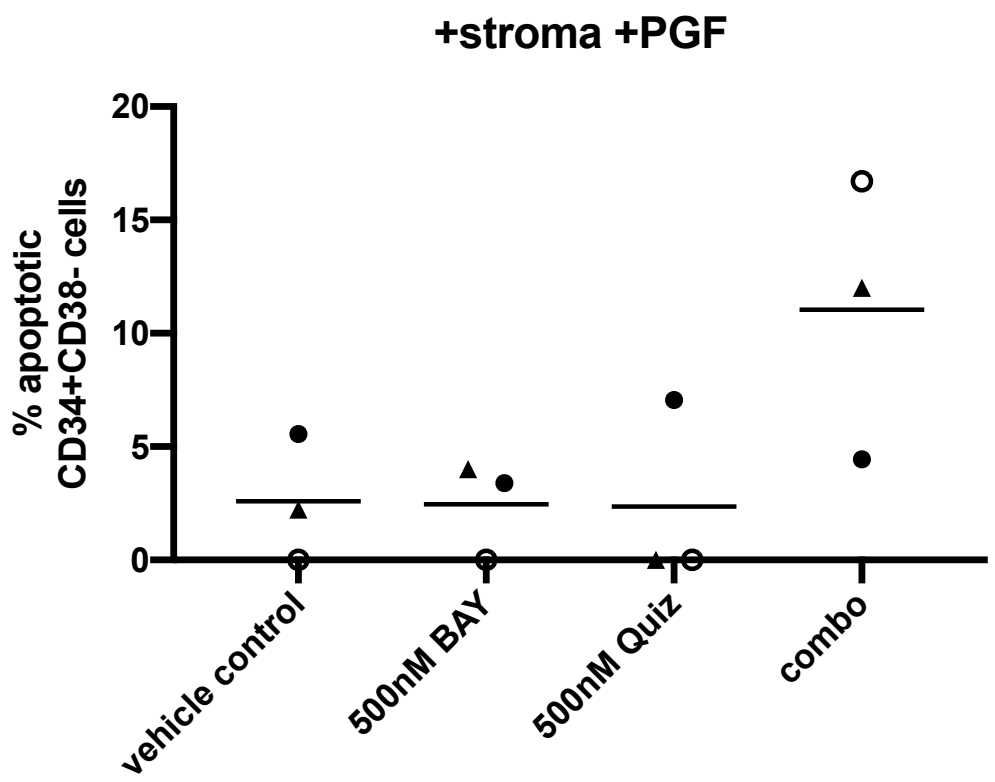

Figure 6.7 Combination treatment induces apoptotic effects in the stem cell-like CD34+CD38- subpopulation of FLT3-ITD AML primary cells co-cultured on stroma with exogenous physiological growth factors

FLT3-ITD AML primary patient cells were cultured in the presence of stroma in serum-free expansion medium (SFEM) supplemented with physiological growth factors (PGF) (IL-3, G-CSF and TPO at 1 ng/mL). Following overnight co-culture, cells were treated with quizartinib (Quiz) and BAY-806946 (BAY) alone or in combination at the indicated concentration. Apoptosis was assessed after 48 hrs by annexinV/DAPI, detected by flow cytometry. Cells were stained with surface markers such as CD45, CD34 and CD38 to measure apoptosis in the CD45+ stem cell-like CD34+CD38- population. CD34+CD38- staining was performed on 9 individual FLT3-ITD AML primary patients, but only 3 patients had a measurable CD34+CD38- population. Box plots depict the mean percentage of apoptosis in these 3 individual FLT3-ITD AML primary patients. Statistical significance was calculated by one-way ANOVA (using Geisser-Greenhouse correction) followed by Tukey's multiple comparisons test.

6.4 Combination treatment spares normal CD34+CD38- cells

To determine if the combination of quizartinib with BAY-806946 induces cytotoxicity specifically for AML, the drug combination was also evaluated on non-AML cells and peripheral blood mononuclear cells (PBMC) from a healthy donor. Here, the non-AML cells are referring to the cells derived from a patient diagnosed with a different hematological malignancy such as lymphoma where unlike AML the CD34+ cells are not considered to be part of the cancer clone, so are 'normal'. Cells were co-cultured with MS-5 stroma cells plus/minus PGF and exposed to quizartinib or BAY-806946 as monotherapy or in combination for 48 hrs.

Results show that in PBMC, quizartinib treatment (500 nM) caused a 0.29-fold decrease of cell growth in SFEM and this effect was similar to that observed with BAY-806946 (500nM) (0.23-fold decrease) (Figure 6.8 A). The drug combination displayed similar growth inhibition (0.32-fold decrease). With PGF, this growth inhibitory effect was however almost completely relieved. The drug combination displayed only 0.1-fold decrease of cell growth. This concentration is below the Cmax of quizartinib (376 ng/mL) following 60mg/day dosing for the treatment of refractory/relapsed FLT3-ITD AML patients.

In non-AML cells, the growth inhibition induced by BAY-806946 was far more pronounced compared to PBMC (Figure 6.8 B). As such, in SFEM, BAY-806946 led to a 0.55-fold decrease of growth compared to vehicle control, whilst cells were not affected by quizartinib treatment (0.03-fold increase). Drug combination showed a 0.48-fold decrease of cell growth, which is most likely caused by BAY-806946. In non-AML cells with PGF, the drug combination had a similar response (0.48-fold decrease) respective to non-AML cells in SFEM (Figure 6.8 B).

Besides the effect on cell growth, the apoptotic effect of the drug combination was also evaluated on PBMC and non-AML cells. In PBMC, both in SFEM or PGF, BAY-806946 and quizartinib alone or in combination were negligible cytotoxic. As such, the drug combination induced only an increase of 4.2% apoptosis in SFEM and 3.4% with PGF respective to vehicle control (Figure 6.9 A). In non-AML cells, both inhibitors induced apoptosis, which was further enhanced with the drug combination (Figure 6.9 B). In SFEM, BAY-806946 induced an increase of 20.6% apoptosis respective to vehicle control, quizartinib 10.2%, and the combination 29.9%. This effect was partly abrogated in the presence of PGF, where apoptotic levels respective to vehicle control were 9.4% (BAY-806946), 5.2% (quizartinib) and 14.3% (combination). Based on these observations, it was assessed whether the combination treatment spares the CD34+CD38- fraction in the non-AML cells (Figure 6.10).

While quizartinib induced only marginal increase of apoptotic levels respective to vehicle control (3.16% in SFEM and 0% with PGF), BAY-806946 induced a 15.9% increase in SFEM, which was abrogated in the presence of PGF. Combination treatment induced only 1.1% increased apoptosis respective to vehicle control in the CD34+CD38- fraction in the presence of PGF. In summary, BAY-806946 induced cytotoxicity to a relative small extent in PBMC but primarily in non-AML cells, which was partly abrogated in the presence of PGF.

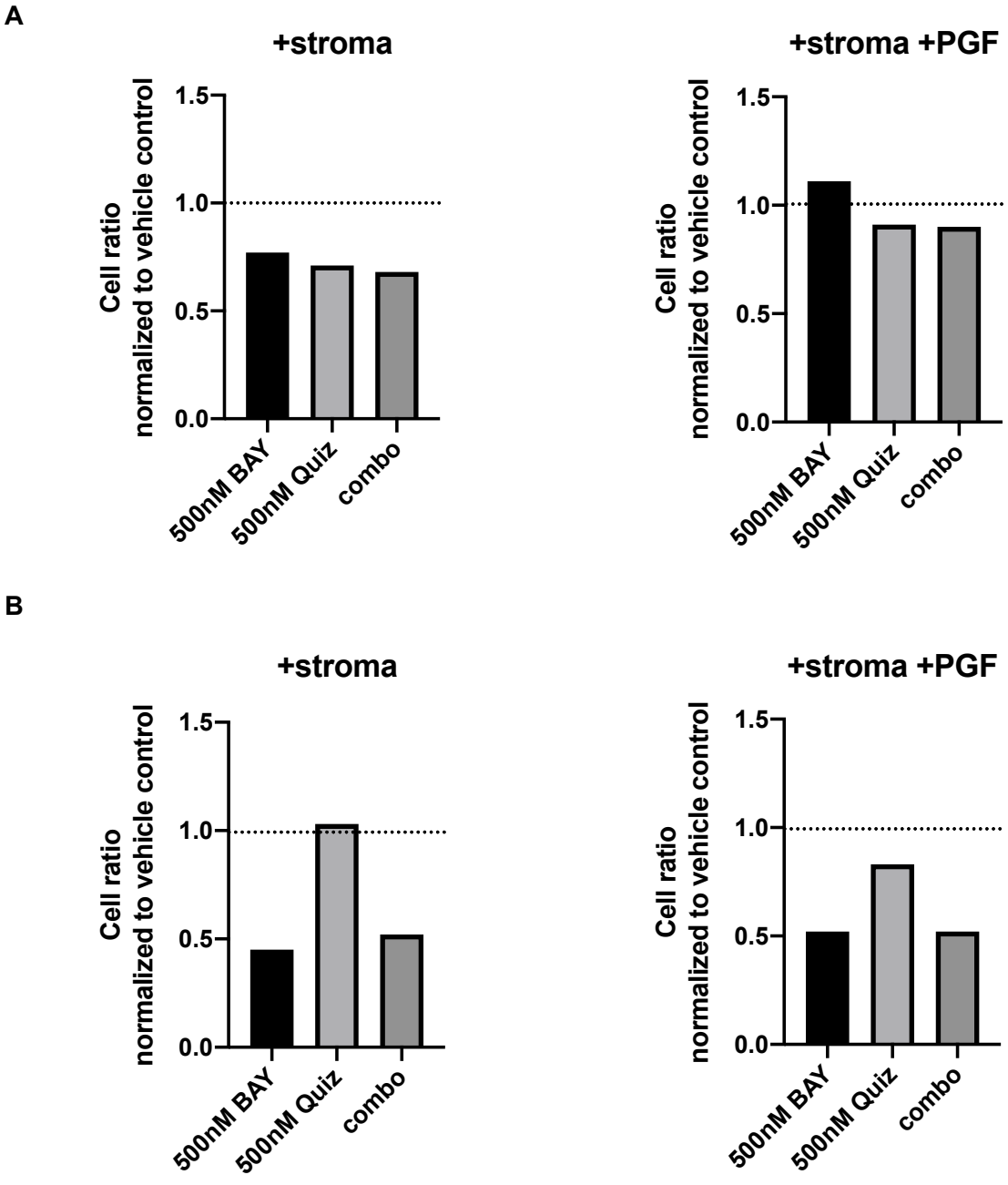

Figure 6.8 BAY-806946 exerts growth inhibitory effects in non-AML CD45+ cells, but spares normal peripheral blood mononuclear cells

A) Peripheral blood mononuclear cells (PBMC) from a healthy donor and **B)** non-AML cells were cultured in the presence of stroma in serum-free expansion medium (SFEM) or SFEM supplemented with physiological growth factors (PGF) (IL-3, G-CSF and TPO at 1 ng/mL). Following overnight co-culture, cells were treated with quizartinib (Quiz) and BAY-806946 (BAY) alone or in combination at the indicated concentration. Growth inhibition was assessed in human CD45+ population after 48 hrs using counting beads detected by flow cytometry. Bars represent cell count normalized to vehicle control of a single donor. Flow cytometry was used to measure apoptosis in a single replicate in these cells using annexinV/DAPI as shown in Figure 6.9.

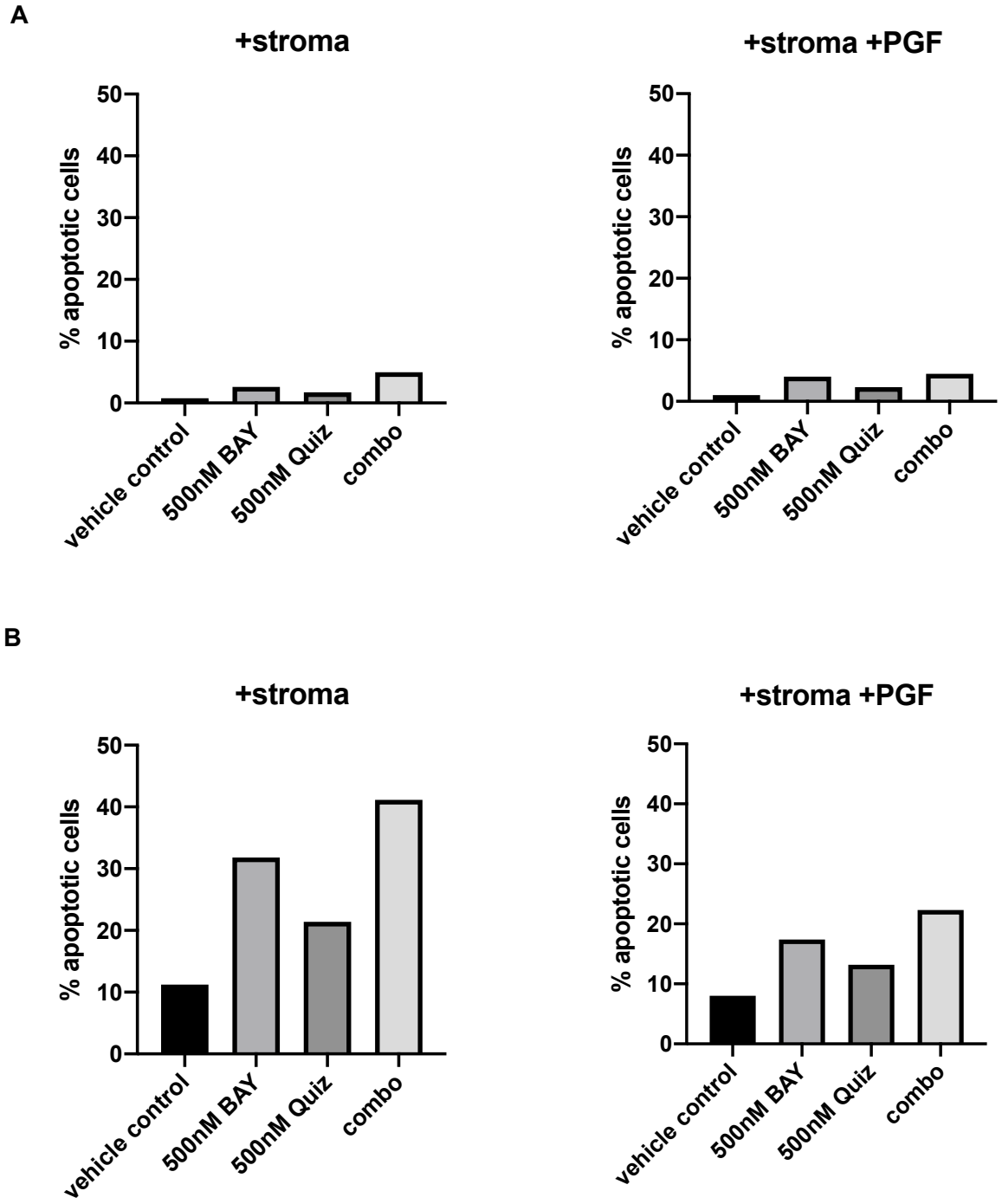

Figure 6.9 Combination treatment induces apoptotic effects in non-AML cells, but spares normal peripheral blood mononuclear cells

A) Peripheral blood mononuclear cells (PBMC) from a healthy donor and **B)** non-AML cells were cultured in the presence of stroma in serum-free expansion medium (SFEM) or SFEM supplemented with physiological growth factors (PGF) (IL-3, G-CSF and TPO at 1 ng/mL). Following overnight co-culture, cells were treated with quizartinib (Quiz) and BAY-806946 (BAY) alone or in combination at the indicated concentration. Apoptosis was assessed in human CD45+ population after 48 hrs by annexinV/DAPI, detected by flow cytometry. Bars represent the percentage of apoptosis of a single donor.

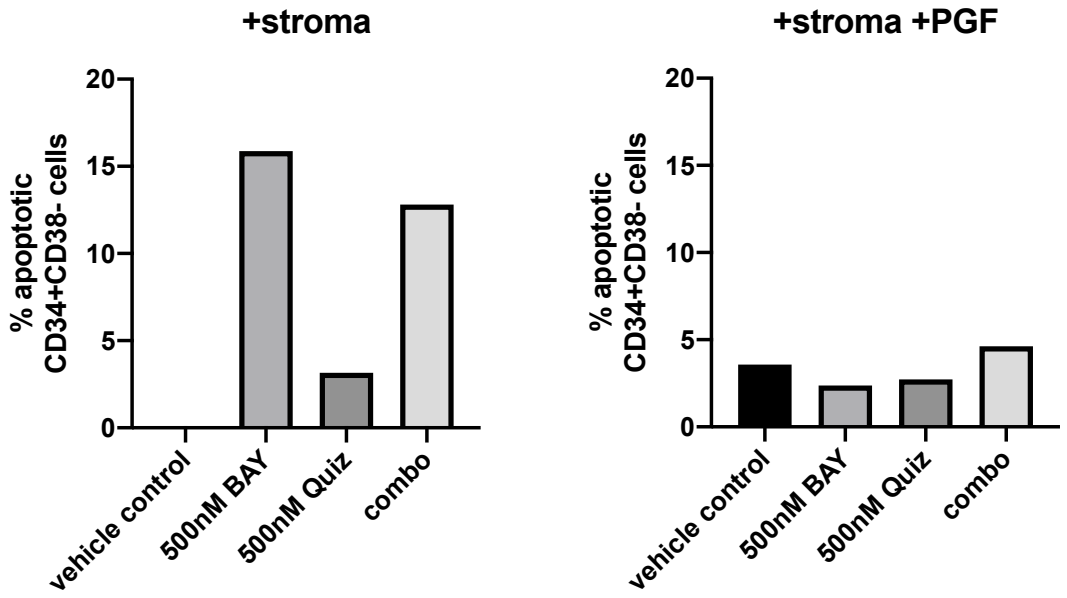

Figure 6.10 BAY-806946 induces apoptotic effects in CD34+CD38- population of non-AML cells in the absence of exogenous physiological growth factors

Non-AML cells were cultured in the presence of stroma in serum-free expansion medium (SFEM) or **B)** SFEM supplemented with physiological growth factors (PGF) (IL-3, G-CSF and TPO at 1 ng/mL). Following overnight co-culture, cells were treated with quizartinib (Quiz) and BAY-806946 (BAY) alone or in combination at the indicated concentration. Apoptosis was assessed after 48 hrs by annexinV/DAPI, detected by flow cytometry. Cells were stained with surface markers such as CD45, CD34 and CD38 to measure apoptosis in the hCD45+ CD34+CD38- population. Bars represent the percentage of apoptosis of a single donor.

6.5 Assessment of the activation status of PI3K/AKT/mTOR and FLT3-ITD signaling upon combination treatment in FLT3-ITD AML primary patient cells

Besides assessing whether BAY-806946 could potentiate the efficacy of quizartinib in FLT3-ITD AML primary patient cells, it was additionally sought to elucidate persistent protein targets following combination treatment by RPPA analysis. Primary patient cells were co-cultured with MS-5 cells in the presence of PGF to more closely resemble the BM microenvironment and cells were treated for 24 hrs with BAY-806946 or quizartinib alone or in combination.

The phosphorylation status of a number of effectors downstream of PI3K/AKT/mTOR and FLT3-ITD was determined, including GSK-3α/β (S9/21), p-mTOR (S2448), p-rpS6 (S240/244), p-4E-BP1 (S65), p-STAT5 (Y694), and p-ERK (T202/Y204). GSK-3α/β is an important component of the Wnt pathway and the PI3K/AKT pathway are entwined by AKT-mediated phosphorylation of GSK-3α at S21 and phosphorylation of GSK-3β at S9 (McCubrey et al., 2014). Phosphorylation of GSK-3α/β was unaffected by quizartinib, but upregulated by BAY-806946 (1.3-fold difference) respective to vehicle control; and this upregulation was also observed with combination treatment (1.2-fold difference) (Figure 6.11). Although it was anticipated that combination treatment would exert enhanced inhibition of AKT (and thus phosphorylation of its downstream targets), upregulation of AKT target GSK-3α/β following combination treatment was in fact observed.

mTOR activity was assessed by phosphorylation of its downstream targets 4E-BP1 (at S65) and p70S6K1 (at S240/244), of which the latter subsequently phosphorylates and activates rpS6 (Gingras et al., 1999; Hutchinson et al., 2011). mTOR is phosphorylated at S2448 by p70S6K as part of a feedback loop (Abraham and Eng, 2008; Holz and Blenis, 2005). Whilst quizartinib inhibited phosphorylation of rpS6 (0.9-fold difference) – but not BAY-806946; the effect observed following combination treatment was within the effect of either monotherapy (0.9-fold difference). Both BAY-806946 (0.9-fold difference) and quizartinib (0.8-fold difference) inhibited phosphorylation of 4E-BP1, but this effect was reversed by drug combination (1.0-fold difference). Combination treatment also upregulated phosphorylation levels of mTOR at S2488 (1.3-fold difference), which could be an indication of upregulation of p70S6K activity. Rebound activation of PI3K signaling was detected by phosphorylation of IRS-1 (S612) (Andreozzi et al., 2004). In spite of indications that PI3K/AKT/mTOR signaling is not effectively inhibited and some downstream effectors are in fact upregulated,

phosphorylation of IRS-1 at S612 was unaffected by either monotherapies or combination treatment. Activity of FLT3-ITD signaling was assessed by phosphorylation of STAT5 at Y694 and ERK at T202/Y204. Unexpectedly, quizartinib was unable to inhibit STAT5 (1.0-fold difference) and combination treatment (1.5-fold difference) led to augmentation of p-STAT5 respective to BAY-806946 monotherapy (1.4-fold difference). ERK activity was reduced with BAY-806946 (0.9-fold difference) – but interestingly not with quizartinib monotherapy or in combination. Besides activation status of PI3K/AKT/mTOR and FLT3-ITD, the expression of cleaved PARP, an apoptosis marker, was measured. Increased level of cleaved PARP was found with BAY-806946 (1.2-fold difference), but not with quizartinib; and although not statistically significant this effect was stronger with drug combination (1.44-fold difference; $p>0.05$; SD=2.5).

In addition to RPPA analysis, activation status of FLT3-ITD and PI3K/AKT/mTOR downstream signaling was confirmed by intracellular staining, detected by flow cytometry. Downstream targets assessed included phosphorylated ERK, AKT and rpS6. Results show that although quizartinib (36.1%) and BAY-806946 (21.8%) inhibit p-ERK, the combination (25.9%) seems to reverse some of this inhibition seen with quizartinib (Figure 6.12). Combination treatment displayed weaker inhibition of ERK compared to quizartinib monotherapy (25.9%) A similar outcome was observed for p-AKT where BAY-806946 induced 17.7% inhibition, quizartinib 25.1% and the combination 21.1% respective to vehicle control. With regards to rpS6, both BAY-806946 (76.6%) and quizartinib (44.7%) inhibited rpS6. While it was anticipated that the combination (56.0%) would further inhibit S6 phosphorylation, in fact the level of inhibition of rpS6 was between that observed with either

These results obtained by RPPA analysis and intracellular staining collectively suggest that simultaneous addition of the inhibitors does not further enhance pathway inhibition, but on the contrary may potentially reverse or antagonize signaling blockade, possibly by mechanisms involving STAT5 upregulation.

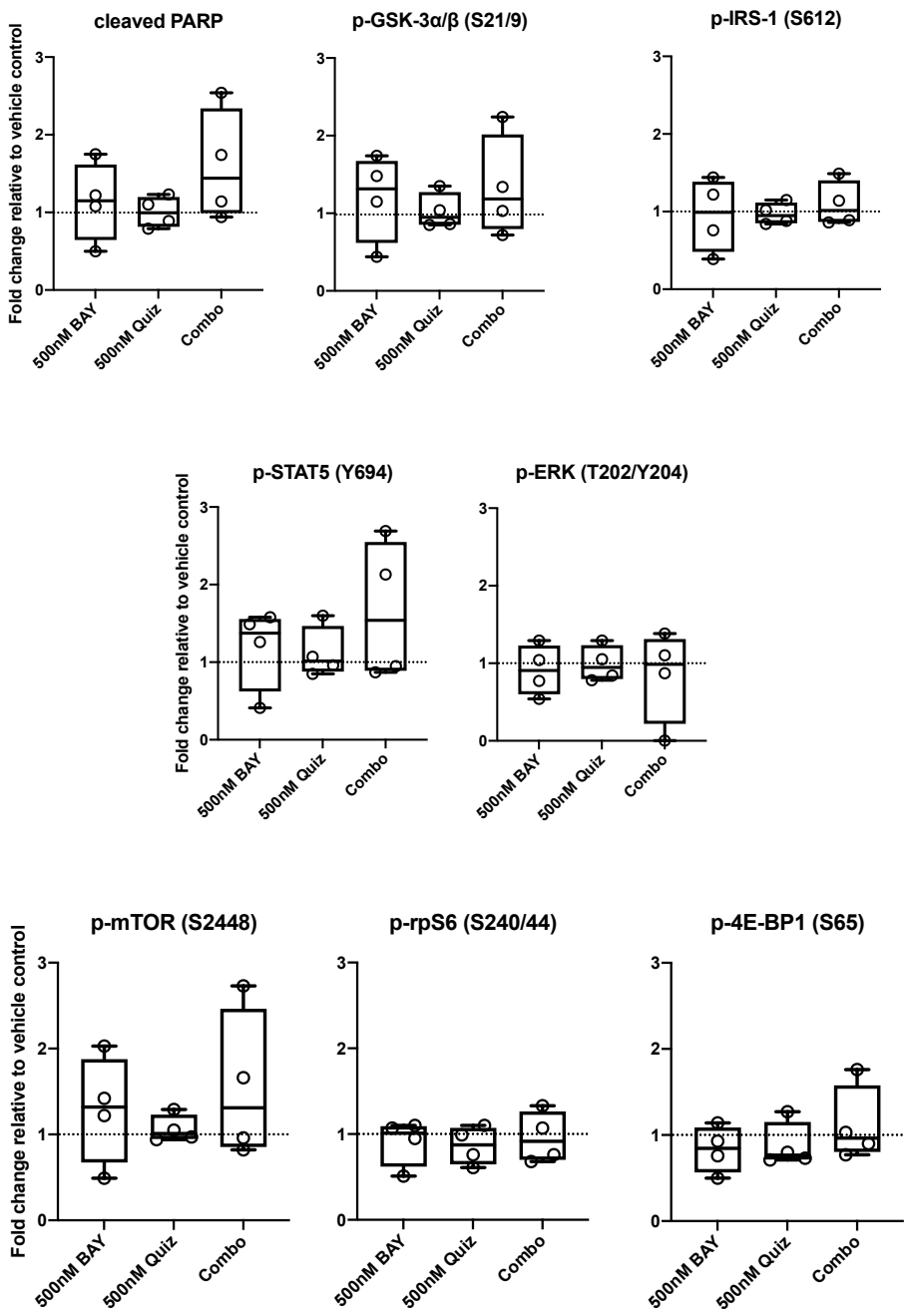

Figure 6.11 Combination of quizartinib and BAY-806946 elicits cleavage of PARP, but is unable to cooperatively inhibit PI3K/AKT/mTOR and FLT3-ITD signaling in FLT3-ITD AML primary patient cells co-cultured +stroma +PGF

FLT3-ITD AML primary patient cells were cultured in the presence of stroma in serum-free expansion medium (SFEM) supplemented with physiological growth factors (PGF) (IL-3, G-CSF and TPO at 1 ng/mL). Following overnight co-culture, cells were treated with quizartinib (Quiz) and BAY-806946 (BAY) alone or in combination at the indicated concentration. After 24 hrs drug treatment, cells were stained with surface marker CD45 and CD45+ cells were collected by fluorescence-activated cell sorting (FACS). Cells were collected following 1 hr recovery in a cell incubator. The expression of the proteins indicated was analyzed by reverse phase protein array (RPPA). Box plots depict the fold change relative to vehicle control of 4 individual FLT3-ITD AML primary patients. Statistical significance was calculated by two-way ANOVA followed by Tukey's multiple comparisons test.

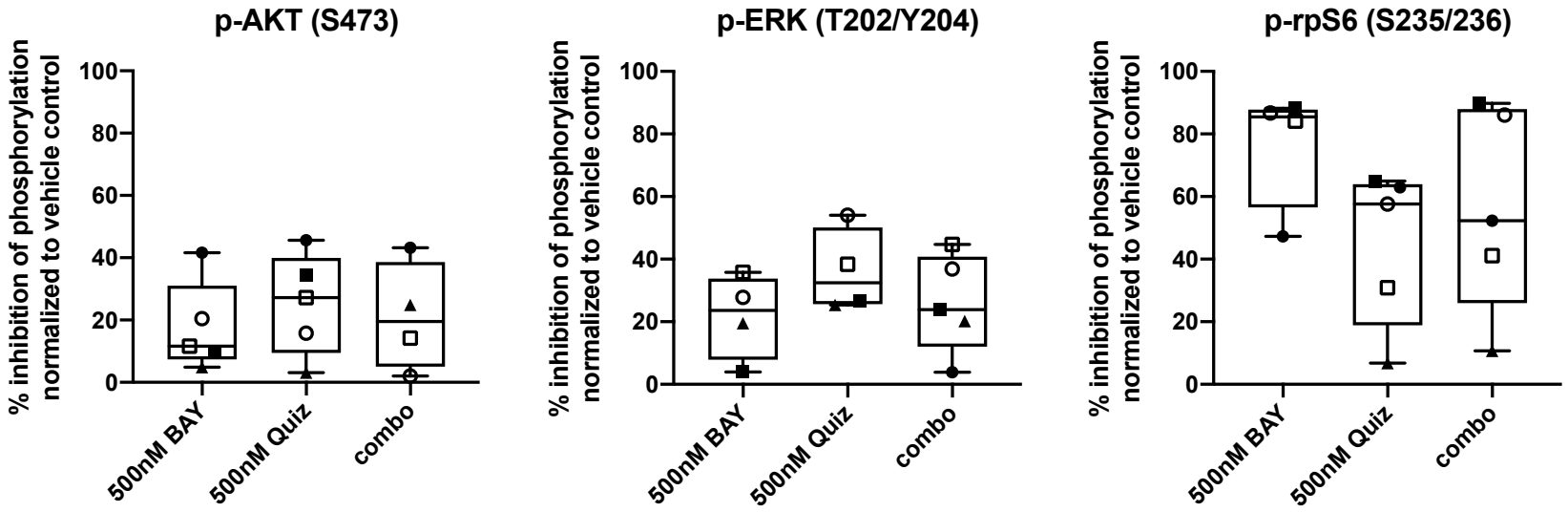

Figure 6.12 Quizartinib and BAY-806946 inhibit PI3K/AKT/mTOR and FLT3-ITD signaling in FLT3-ITD AML primary patient cells but the combination does not act cooperatively at the level of inhibition of the phosphoprotein

FLT3-ITD AML primary patient cells were cultured in the presence of stroma in serum-free expansion medium (SFEM) supplemented with physiological growth factors (PGF) (IL-3, G-CSF and TPO at 1 ng/mL). Following overnight co-culture, cells were treated with quizartinib (quiz) and BAY-806946 (BAY) alone or in combination at the indicated concentration. After 24 hrs drug treatment, cells were stained with surface marker CD45 and subsequently fixed and permeabilized. Protein expression of p-AKT [Serine 473 (S473)], p-rpS6 (S235/236) and p-ERK [Threonine 202/ Tyrosine 204 (T202/Y204)] was detected by intracellular flow cytometric analysis. Samples were gated on human CD45+ population. Box plots depict percentage of protein inhibition normalized to vehicle control of 5 individual FLT3-ITD AML primary patients. Statistical significance was calculated by one-way ANOVA (using Geisser-Greenhouse correction) followed by Tukey's multiple comparisons test.

6.6 Combination treatment and/or addition of exogenous physiological growth factors alters the cytokine release profile of FLT3-ITD AML primary patient cells

Molecules secreted by AML cells are considered to play a role in autocrine and paracrine regulation of AML growth and survival (Behrmann et al., 2018). Considering that co-culture with stromal cells and addition of exogenous PGF was shown to attenuate response to combination treatment in FLT3-ITD AML primary patient cells, it was investigated whether the media conditioned by AML cells is altered in cytokine secretion profile. Cells from nine primary patients and one PDX were co-cultured with MS-5 cells plus/minus PGF and treated for 48 hrs with BAY-806946 and quizartinib alone or in combination. In total, the concentration of 25 different cytokines was measured and the results are summarized in heatmaps (Figure 6.13-6.15) and in tables (Table 6.2 and 6.3).

Of the cytokines chosen for study, only a small number of cytokines were detectable in the culture media using Luminex platform, which were: granulocyte-macrophage colony-stimulating factor (GM-CSF) (2/9), IL-1β (7/9), IL-1RA (8/9), and IL-6 (2/9). Other cytokines were either below detection limit or <1 pg/mL. It should be noted that the cytokine levels were variable amongst patient samples, reflecting the heterogeneity of AML. Results show that IL-RA levels are higher in co-cultured AML cells plus PGF (vehicle control: 132.8 pg/mL) respective to SFEM (vehicle control: 114.9 pg/mL) (Figure 6.13 & 6.14). Furthermore, IL-1RA level following combination treatment was increased respective to vehicle control (in SFEM: 133.1 pg/mL; +PGF: 142.1 pg/mL). In particular sample AML005 showed striking levels of IL-1RA compared to the other evaluated patient samples (Figure 6.14; cross mark). With regards to IL-1β, secretion levels were reduced in the presence of PGF (vehicle control: 0.7 pg/mL) compared to SFEM (vehicle control: 2 pg/mL), and following combination treatment; these levels were further reduced (in SFEM: 1.9 pg/mL; +PGF: 0.5 pg/mL). This effect was particularly pronounced with sample AML009 (Figure 6.14; square shape). A similar pattern was observed with GM-CSF and IL-6 where co-culture in the presence of PGF reduced cytokine levels respective to co-culture in SFEM. Interestingly, in SFEM, both BAY-806946 and quizartinib as monotherapy increased IL-6 levels respective to vehicle control (33.3 pg/mL (BAY), 30.7 pg/mL (quiz) versus 19.4 pg/mL (vehicle), which was further elevated with the drug combination (42 pg/mL). The opposite effect was observed in the presence of PGF where drug treatment decreased IL-6 levels, most strikingly with sample AML009 (Figure 6.14; square shape) Notably, the level of GM-CSF levels was only

measurable in samples AML006 and AML023 (Figure 6.14; diamond shape and plus sign, respectively).

The cytokine secretion profile was also assessed in FLT3-ITD AML PDX cells co-cultured with/without MS-5 and plus/minus PGF following 48 hrs combination treatment. Three secreted cytokines were detectable: GM-CSF, IL-1β and IL-7. However, only marginal differences amongst culture conditions and drug treatments were observed, as the cytokine concentrations were relatively low (<1 pg/mL) (Figure 6.15).

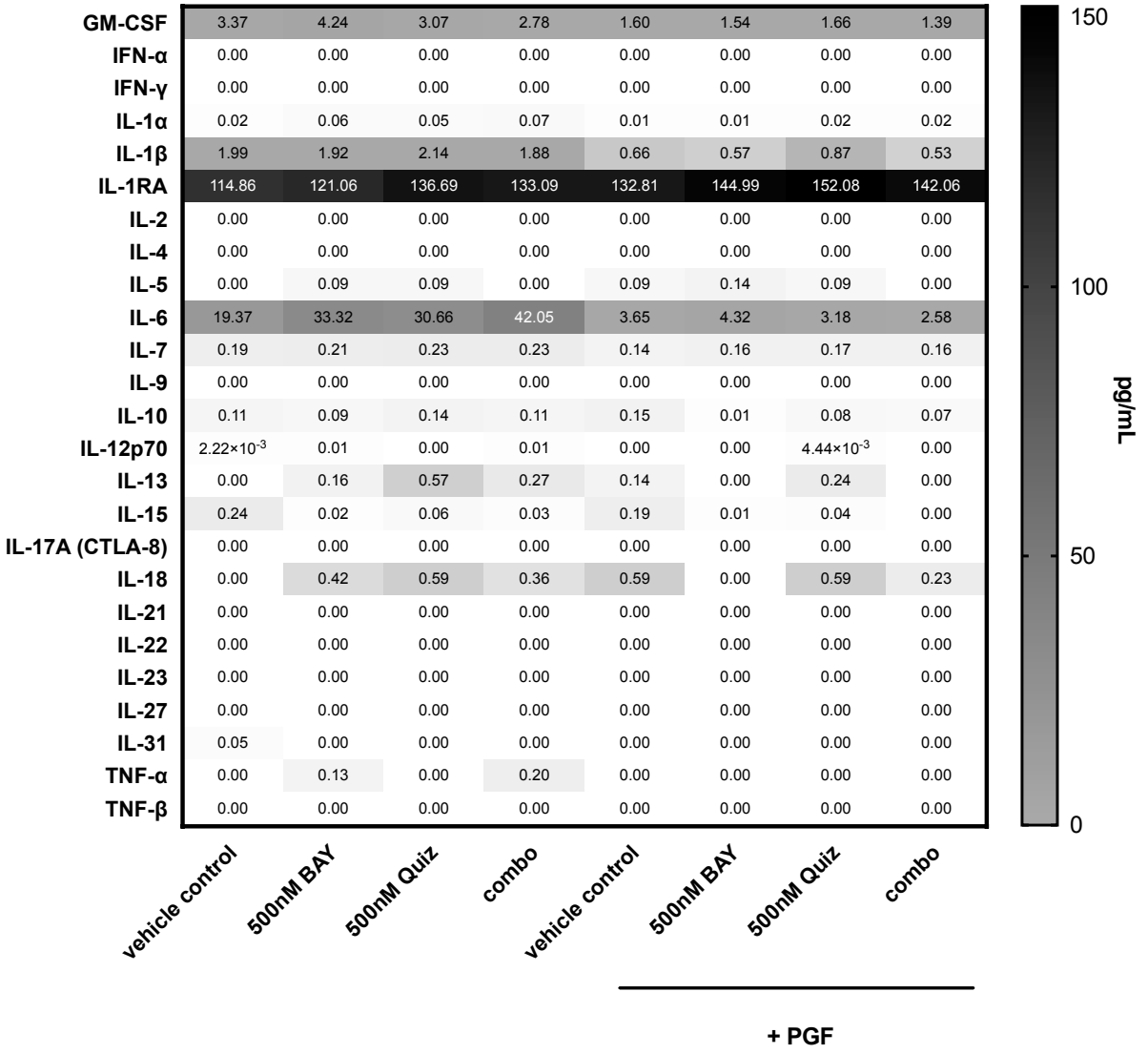

Figure 6.13 Cytokine secretion levels in media harvested from FLT3-ITD AML primary patient cells co-cultured in +stroma or +stroma +PGF following combination treatment

FLT3-ITD AML cells were cultured in the presence of stroma in serum-free expansion medium (SFEM) or SFEM supplemented with physiological growth factors (PGF) (IL-3, G-CSF and TPO at 1 ng/mL). Following overnight co-culture, cells were treated with quizartinib (Quiz) and BAY-806946 (BAY) alone or in combination at the indicated concentration in technical duplicates. After 48 hrs of drug treatment, supernatant was collected for detection and quantification of the indicated cytokines. Heat map represents the mean concentration (pg/mL) of the indicated cytokines measured in nine individual FLT3-ITD AML primary patients.

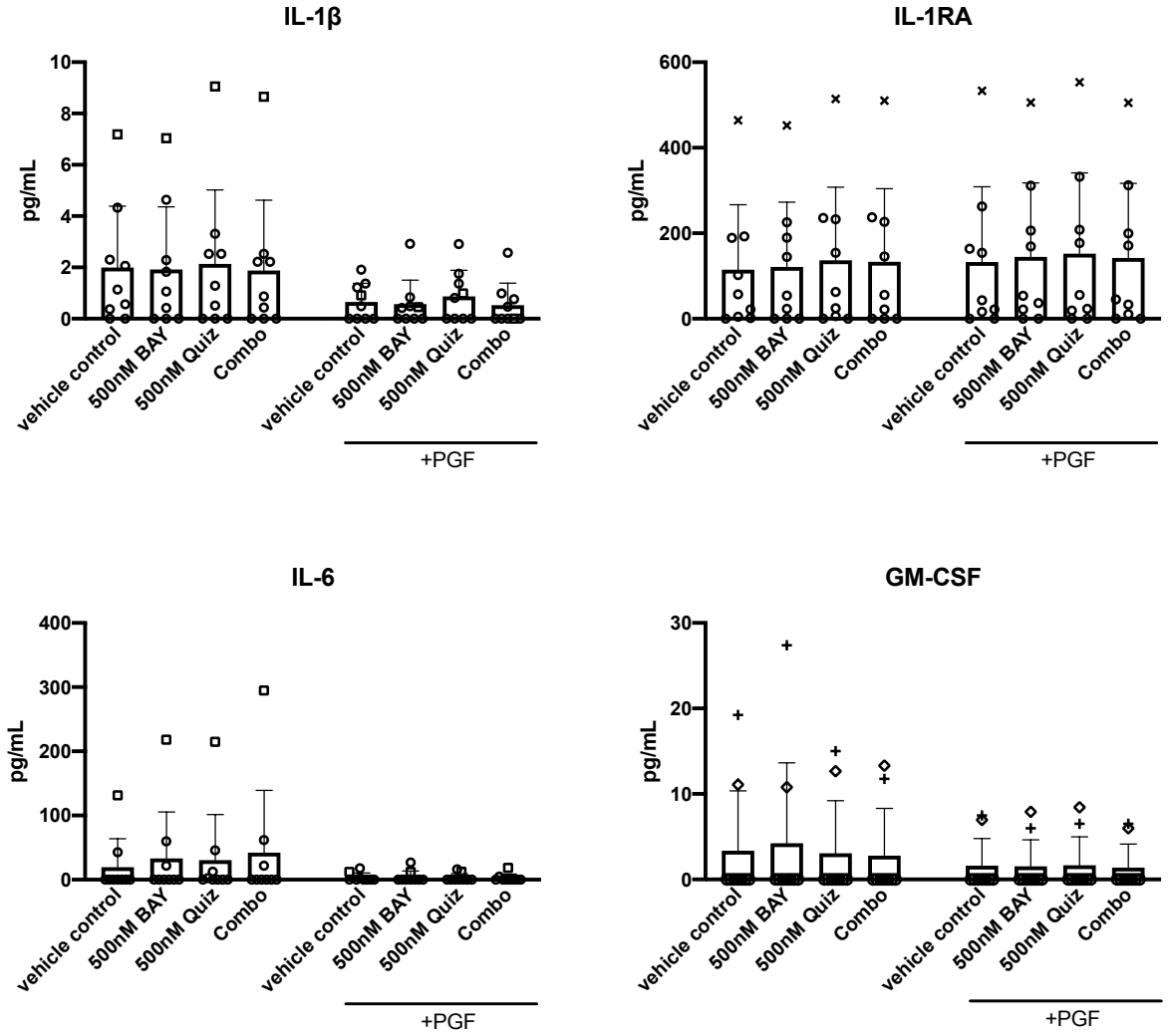

Figure 6.14 FLT3-ITD AML primary patient cells co-cultured with stromal cells display an altered cytokine secretion profile following combination treatment plus/minus exogenous physiological growth factors

FLT3-ITD AML cells were cultured in the presence of stroma in serum-free expansion medium (SFEM) or SFEM supplemented with physiological growth factors (PGF) (IL-3, G-CSF and TPO at 1 ng/mL). Following overnight co-culture, cells were treated with quizartinib (Quiz) and BAY-806946 (BAY) alone or in combination at the indicated concentration in technical duplicates. After 48 hrs of drug treatment, supernatant was collected for detection and quantification of the indicated cytokines. Bars represents the mean concentration of the indicated cytokines measured in nine individual FLT3-ITD AML primary patients. Statistical analysis was performed by one-way ANOVA followed by Tukey's multiple comparisons test. Cross mark= AML005, diamond shape= AML006, square shape= AML009, and plus sign= AML023.

Table 6.2 Cytokine secretion levels for nine FLT3-ITD AML primary patient cells co-cultured with stromal cells in serum-free expansion medium (SFEM) following combination treatment

		vehicle control			BAY-806946			Quizartinib			Combination			
cytokine	**#N**	**Range (pg/mL)**	**Mean conc. (pg/mL)**	**SD**	**Range (pg/mL)**	**Mean conc. (pg/mL)**	**SD**	**Range (pg/mL)**	**Mean conc. (pg/mL)**	**SD**	**Range (pg/mL)**	**Mean conc. (pg/mL)**	**SD**	***p*-value**
GM-CSF	9	0–19.2	3.4	7.0	0–27.4	4.2	9.4	0–15.0	3.1	6.1	0–13.3	2.8	5.5	n.s.
IFN-α	9	0	0.0	0.0	0	0.0	0.0	0	0.0	0.0	0	0.0	0.0	n.s.
IFN-γ	9	0	0.0	0.0	0	0.0	0.0	0	0.0	0.0	0	0.0	0.0	n.s.
IL-1α	9	0–0.1	0.0	0.0	0–0.2	0.1	0.1	0–0.2	0.1	0.1	0–0.2	0.1	0.1	n.s.
IL-1β	9	0–7.2	2.0	2.4	0–7.0	1.9	2.4	0–9.1	2.1	2.9	0–8.7	1.9	2.7	n.s.
IL-1RA	9	0–464.3	114.9	151.7	0–452.3	121.1	151.6	0–514.0	136.7	171.0	0–510.4	133.1	170.9	n.s.
IL-2	9	0	0.0	0.0	0	0.0	0.0	0	0.0	0.0	0	0.0	0.0	n.s.
IL-4	9	0	0.0	0.0	0	0.0	0.0	0	0.0	0.0	0	0.0	0.0	n.s.
IL-5	9	0	0.0	0.0	0–0.1	0.1	0.3	0–0.9	0.1	0.3	0	0.0	0.0	n.s.
IL-6	9	0–131.4	19.4	44.3	0–218.2	33.3	72.2	0–214.9	30.7	70.7	0–294.7	42.0	97.0	n.s.
IL-7	9	0–0.5	0.2	0.2	0–0.5	0.2	0.2	0–0.6	0.2	0.2	0–0.5	0.2	0.2	n.s.
IL-9	9	0	0.0	0.0	0	0.0	0.0	0	0.0	0.0	0	0.0	0.0	n.s.
IL-10	9	0–0.8	0.1	0.3	0–0.7	0.1	0.2	0–0.7	0.1	0.3	0–0.7	0.1	0.2	n.s.
IL-12p70	9	0	0.0	0.0	0–0.1	0.0	0.0	0	0.0	0.0	0–0.1	0.0	0.0	n.s.
IL-13	9	0	0.0	0.0	0–1.4	0.2	0.5	0–5.1	0.6	1.7	0–2.4	0.3	0.8	n.s.
IL-15	9	0	0.2	0.2	0–0.1	0.0	0.0	0–0.3	0.1	0.1	0–0.2	0.0	0.1	n.s.
IL-17A (CTLA-8)	9	0	0.0	0.0	0	0.0	0.0	0	0.0	0.0	0	0.0	0.0	n.s.
IL-18	9	0	0.0	0.0	0–3.8	0.4	1.3	0–5.3	0.6	1.8	0–3.2	0.4	1.1	n.s.
IL-21	9	0	0.0	0.0	0	0.0	0.0	0	0.0	0.0	0	0.0	0.0	n.s.
IL-22	9	0	0.0	0.0	0	0.0	0.0	0	0.0	0.0	0	0.0	0.0	n.s.
IL-23	9	0	0.0	0.0	0	0.0	0.0	0	0.0	0.0	0	0.0	0.0	n.s.
IL-27	9	0	0.0	0.0	0	0.0	0.0	0	0.0	0.0	0	0.0	0.0	n.s.
IL-31	9	0–0.4	0.0	0.1	0	0.0	0.0	0	0.0	0.0	0	0.0	0.0	n.s.
TNF-α	9	0	0.0	0.0	0–1.2	0.1	0.4	0	0.0	0.0	0–1.8	0.2	0.6	n.s.
TNF-β	9	0	0.0	0.0	0	0.0	0.0	0	0.0	0.0	0	0.0	0.0	n.s.

LOD; limit of detection; n.s.; not significant; PGF; physiological growth factors; p-values (two-way ANOVA) for monotherapy with quizartinib versus combination therapy are represented in the right column.

Table 6.3 Cytokine secretion levels for nine FLT3-ITD AML primary patient cells co-cultured with stromal cells in the presence of exogenous physiological growth factors following combination treatment

		vehicle control			BAY-806946			Quizartinib			Combination			
cytokine	**#N**	**Range (pg/mL)**	**Mean conc. (pg/mL)**	**SD**	**Range (pg/mL)**	**Mean conc. (pg/mL)**	**SD**	**Range (pg/mL)**	**Mean conc. (pg/mL)**	**SD**	**Range (pg/mL)**	**Mean conc. (pg/mL)**	**SD**	***p*-value**
GM-CSF	9	0–7.5	1.6	3.2	0–7.9	1.5	3.1	0–8.4	1.7	3.3	0–6.5	1.4	2.8	n.s.
IFN-α	9	0	0.0	0.0	0	0.0	0.0	0	0.0	0.0	0	0.0	0.0	n.s.
IFN-γ	9	0	0.0	0.0	0	0.0	0.0	0	0.0	0.0	0	0.0	0.0	n.s.
IL-1α	9	0	0.0	0.0	0–0.1	0.0	0.0	0–0.1	0.0	0.0	0–0.1	0.0	0.0	n.s.
IL-1β	9	0–1.9	0.7	0.7	0–2.9	0.6	0.9	0–2.9	0.9	1.0	0–2.6	0.5	0.9	n.s.
IL-1RA	9	0–533.2	132.8	176.0	0–505.8	145.0	173.0	0–553.1	152.1	189.4	0–505.3	142.1	174.6	n.s.
IL-2	9	0	0.0	0.0	0	0.0	0.0	0	0.0	0.0	0	0.0	0.0	n.s.
IL-4	9	0	0.0	0.0	0	0.0	0.0	0	0.0	0.0	0	0.0	0.0	n.s.
IL-5	9	0–0.9	0.1	0.3	0–1.3	0.1	0.4	0–0.9	0.1	0.3	0	0.0	0.0	n.s.
IL-6	9	0–18.0	3.7	6.7	0–26.9	4.3	9.3	0–16.0	3.2	6.4	0–18.4	2.6	6.1	n.s.
IL-7	9	0–0.3	0.1	0.1	0–0.4	0.2	0.2	0–0.4	0.2	0.2	0–0.4	0.2	0.2	n.s.
IL-9	9	0	0.0	0.0	0	0.0	0.0	0	0.0	0.0	0	0.0	0.0	n.s.
IL-10	9	0–0.9	0.2	0.3	0–0.1	0.0	0.0	0–0.7	0.1	0.2	0–0.7	0.1	0.2	n.s.
IL-12p70	9	0	0.0	0.0	0	0.0	0.0	0	0.0	0.0	0	0.0	0.0	n.s.
IL-13	9	0–1.2	0.1	0.4	0	0.0	0.0	0–2.2	0.2	0.7	0	0.0	0.0	n.s.
IL-15	9	0–0.5	0.2	0.2	0–0.1	0.0	0.0	0–0.2	0.0	0.1	0	0.0	0.0	n.s.
IL-17A (CTLA-8)	9	0	0.0	0.0	0	0.0	0.0	0	0.0	0.0	0	0.0	0.0	n.s.
IL-18	9	0–5.3	0.6	1.8	0	0.0	0.0	0–5.3	0.6	1.8	0–2.1	0.2	0.7	n.s.
IL-21	9	0	0.0	0.0	0	0.0	0.0	0	0.0	0.0	0	0.0	0.0	n.s.
IL-22	9	0	0.0	0.0	0	0.0	0.0	0	0.0	0.0	0	0.0	0.0	n.s.
IL-23	9	0	0.0	0.0	0	0.0	0.0	0	0.0	0.0	0	0.0	0.0	n.s.
IL-27	9	0	0.0	0.0	0	0.0	0.0	0	0.0	0.0	0	0.0	0.0	n.s.
IL-31	9	0	0.0	0.0	0	0.0	0.0	0	0.0	0.0	0	0.0	0.0	n.s.
TNF-α	9	0	0.0	0.0	0	0.0	0.0	0	0.0	0.0	0	0.0	0.0	n.s.
TNF-β	9	0	0.0	0.0	0	0.0	0.0	0	0.0	0.0	0	0.0	0.0	n.s.

"0" indicates below limit of detection; n.s.; not significant; PGF; physiological growth factors; p-values (two-way ANOVA) for monotherapy with quizartinib versus combination therapy are represented in the right column.

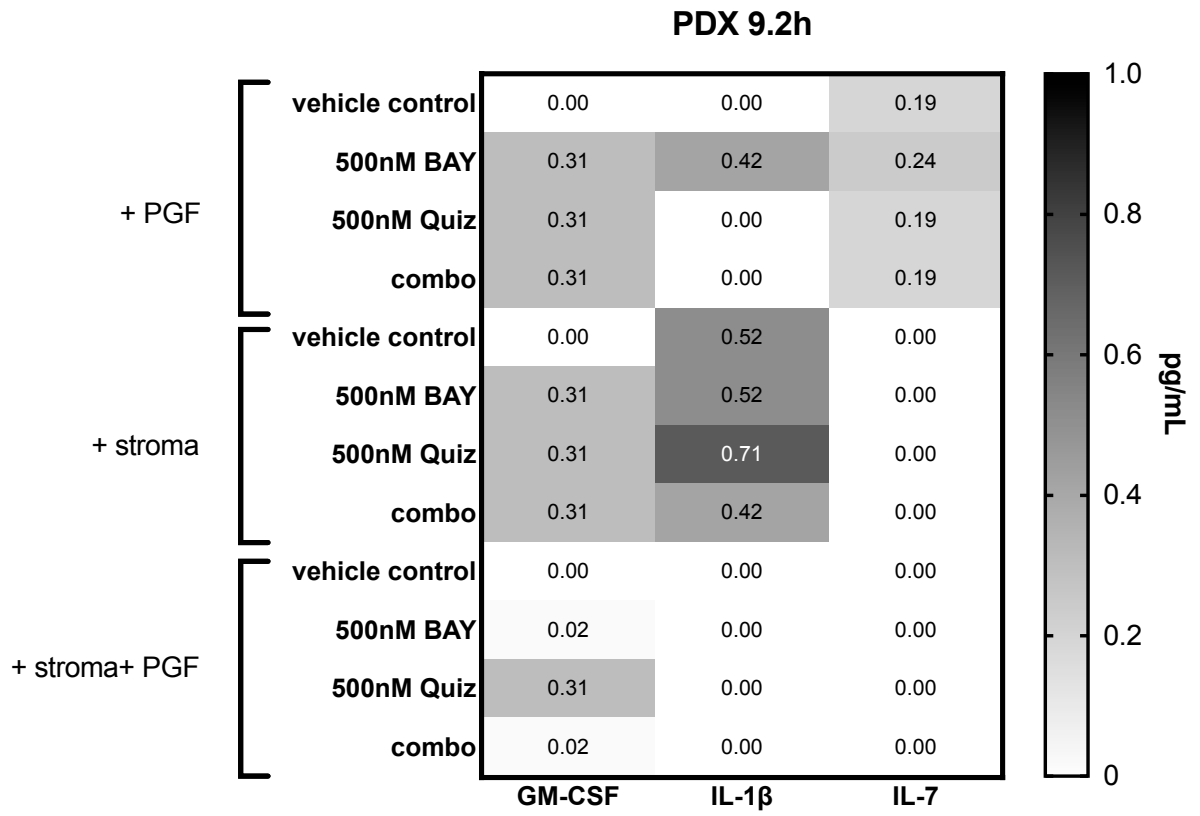

Figure 6.15 Cytokine secretion levels in FLT3-ITD AML PDX cells co-cultured in +PGF, +stroma, +stroma +PGF following combination treatment

FLT3-ITD AML PDX cells were cultured alone or in the presence of stroma in serum-free expansion medium (SFEM) or SFEM supplemented with physiological growth factors (PGF) (IL-3, G-CSF and TPO at 1 ng/mL). Following overnight co-culture, cells were treated with quizartinib (Quiz) and BAY-806946 (BAY) alone or in combination at the indicated concentration in technical duplicates. After 48 hrs of drug treatment, supernatant was collected for detection and quantification of the indicated cytokines. Heat map represents the concentration (pg/mL) of the indicated cytokines measured in a single FLT3-ITD AML PDX sample. Sample 9.2h had a FLT3-ITD allelic ratio ±1 and was sensitive to quizartinib treatment in the presence of PGF but was insensitive in co-culture with stroma (+/- PGF).

6.7 Discussion

The protective BM microenvironment is regarded as an important contributor to therapy failure *in vivo* therefore recapitulating the BM niche *ex vivo* holds great translational value. The most commonly used *ex vivo* approaches include suspension cultures, stromal 2D co-culture and 3D culture systems (Cucchi et al., 2020). Several studies have investigated optimal cytokine combinations that are known to regulate survival and expansion of hematopoietic stem cells based on the physiological function of the BM. In this research, the 2D co-culture system was adapted from a study by Griessinger *et al*. that described a niche-like culture method to maintain LSC *ex vivo* whilst promoting their self-renewal capacity as efficiently as *in vivo* assays (Griessinger et al., 2014). This involved culturing AML on MS-5 stromal cells with the addition of a cytokine cocktail comprised of TPO, IL-3 and G-CSF.

The aim of this chapter was to assess the efficacy of combination therapy consisting of quizartinib and BAY-806946 on FLT3-ITD AML primary patient cells in co-culture with MS-5 stromal cells and exogenous PGF.

First, the *FLT3*-ITD mutational status of patient material was confirmed by PCR. It was shown that amongst patients a great variability of insertion size and band intensity (indicative of FLT3-ITD allelic ratio) is present. To not only detect but also quantify FLT3-ITD mutations, quantitative fragment analysis may be considered that could be correlated to individual patient drug response. The FLT3 mutant to wild-type allelic ratio, ITD length and FLT3-ITD insertion site have been reported to have prognostic importance in newly diagnosed AML. As such, a high allelic ratio and increasing insertion size was associated with shorter OS and disease-free survival (DFS) (Daver et al., 2019; Liu et al., 2019; Stirewalt et al., 2006). While the great majority (70%) of the ITD insertion is localized in the juxtamembrane domain (JMD), ITDs are also detected in the TKD1 (30%). Several studies have shown that ITDs in the TKD1 displayed chemoresistance and significant inferior outcome, as well as altered sensitivity to TKIs (Arreba-Tutusaus et al., 2016; Rücker et al., 2021). A study by Liu *et al.,* demonstrated that longer insertion size was associated with lower sensitivity to FLT3i including quizartinib in *FLT3*-ITD transduced 32D cell strains (Liu et al., 2019). Although a number of studies reported that high FLT3-ITD allelic ratio is associated with poorer prognosis, the impact of allelic burden remains controversial and further studies are needed to elucidate the prognostic value of allelic burden (Döhner et al., 2017; Linch et al., 2014; Yalniz et al., 2019).

Next, the *ex vivo* system was evaluated for its ability to support the survival of FLT3-ITD AML cells, and in parallel to determine the appropriate concentration of the inhibitors for combination treatment. From assessment of the efficacy of quizartinib on FLT3-ITD AML PDX cells cultured in +PGF, +stroma or +PGF +stroma, it was evident that AML primary cells have a better viability in

the presence of stroma and/or PGF. This is in agreement with previous studies that demonstrated that primary cells require stromal support for survival and that addition of physiological cytokines or growth factors are necessary to maintain AML blasts in *ex vivo* culture (Garrido et al., 2001; Rashidi and DiPersio, 2016; Villatoro et al., 2020).

Xenotransplantation of human primary AML cells in immunodeficient animals is regarded as a critical platform for functional assessment of AML biology and to define drug-resistant LSC populations, making PDX models the best *in vivo* preclinical model (Almosailleakh and Schwaller, 2019; Bonnet, 2017). PDX AML cells resemble the primary sample to high extent since they possess similar disease heterogeneity and stability of molecular, genetic and epigenetic landscape. Here, PDX cells were used solely with the purpose of determining the optimal drug concentration for combination therapy, but it should be noted that the drug response observed using PDX cells might differ from *ex vivo* primary cells that haven't been expanded in a murine host. While the PDX model holds great advantage, its use for AML research is limited by poor engraftment rate and time required to detect disease which can take up to six months (Hassan et al., 2020; Mambet et al., 2018). It should be considered that the murine BM niche might be different from that of the human BM niche, which may, in turn, be associated with a different drug response.

After determining the appropriate drug concentrations to evaluate in combination, cell growth and viability following combination treatment was assessed. Results showed that combination treatment efficiently induced growth inhibition and apoptosis in AML cells cultured on MS-5, but this effect was attenuated by addition of the PGF cocktail. The combination results were significantly different from monotherapy, meaning that the drug combination potentially overcomes BM niche-induced protection. Indeed, the cells affected by combination treatment were likely leukemic cells as they were double positive for myeloid blast markers CD33 and CD38. It was expected that patient sample with a low FLT3-ITD allelic ratio would be more sensitive to drug treatment than samples with a high FLT3-ITD allelic ratio, however patient's cells were responsive irrespective of a low allelic ratio. Interestingly, amongst the patient samples where either monotherapy or drug combination induced <25% apoptosis included samples AML023 and AML032 that have a 46,XX karyotype.

In a number of patient samples, detectable CD34+CD38- populations were measured representing the 'LSC-like' population since AML LSC may also be CD34 negative (Kreso and Dick, 2014). Although there was no statistically significant difference due to variable drug response amongst patient samples, there seems to be a trend towards increased apoptosis following combination therapy in the CD34+CD38- cell fraction respective to monotherapy. This may suggest that the combination treatment effectively targets LSC but more accurate functional assays are required to identify LSC. Several methodologies that have been studied to monitor LSC activity include long-

term culture initiating cell (LTC-IC) assay, xenotransplantation assays, and clonal tracking from single-cell transcriptomics (Griessinger et al., 2016; Velten et al., 2021; Zhou and Chng, 2014).

Besides assessing whether combination treatment potentially targets AML LSC-like cells, the specificity of the inhibitors was determined by evaluating the drug combination on PBMC from a healthy donor and non-AML cells. Whilst the drug combination had little effect on the viability of PBMC from a healthy donor, the drug treatment induced growth inhibition and apoptosis in the CD45+ fraction of non-AML cells. This was not surprising as the PI3K/AKT/mTOR pathway has also an active role in normal cellular processes, so this effect might still be on-target but not specific for AML. In the non-AML sample, cytotoxicity following combination treatment was also assessed in the CD34+CD38- fraction that is not considered to be part of the cancer clone. Although combination treatment induced cytotoxicity in the CD34+CD38- fraction of non-AML cells co-cultured on stroma in SFEM, this effect was attenuated in PGF. Thus, in a culture condition more closely mimicking the BM niche, the drug combination was only marginally apoptotic.

Drug-related toxicities is a major obstacle in the clinical development of PI3Ki as the PI3K/AKT/mTOR signaling pathway plays also a critical for normal HSC function. Toxicity from PI3Ki depends on their isoform specificity. As such, pan-PI3K and dual PI3Ki have a broader toxicity profile than isoform-specific PI3Ki (Hanker et al., 2019). Another challenge with PI3Ki is rebound pathway activity caused by negative feedback mechanisms. These negative feedback loops include upregulation of RTK, STAT5, MAPK/ERK signaling (Nepstad et al., 2020; S. Park et al., 2010; Wander et al., 2014). To investigate whether combination of quizartinib with BAY-806946 can surpass rebound signaling, phosphoproteomic analysis was performed that may identify persistent targets.

RPPA analysis showed that BAY-806946 and quizartinib as monotherapy was unable to effectively block PI3K/AKT/mTOR and FLT3-ITD AML signaling and that drug combination potentially has an antagonistic effect. Similar findings were observed with intracellular staining where combination therapy reversed the signaling inhibitory effect of monotherapy. Surprisingly, although PI3K/AKT/mTOR reactivation was shown, IRS-1 phosphorylation level at S612 was not upregulated, indicative of reactivation of PI3K/AKT/mTOR. It may be worth investigating other PI3K/mTOR-binding residues on IRS-1 such as S270, or it is possible that PI3K/AKT/mTOR reactivation occurred through mechanisms independent of IRS-1 (Zhang et al., 2008). One well-known mechanism of resistance to PI3K/AKT/mTORi is the JAK2/STAT5-mediated positive feedback loop that was circumvented by JAK2/STAT5 inhibition in solid cancers (Britschgi et al., 2012; Choudhary et al., 2007; Dumas et al., 2019).. Indeed, it was observed that combination treatment caused upregulation of p-STAT5 at Y694, which may be promoted by exogenous addition of IL-3, G-CSF and TPO, known to activate JAK2/STAT5 (Bacon et al., 1995; Dong et al., 1998; Sung et al., 2019). In an *ex vivo* FLT3-ITD AML model sustained STAT5 phosphorylation

was shown in quizartinib-treated cells, which consequently upregulated AXL expression (Dumas et al., 2019). AXL is a RTK that belongs to the Tyro3-Axl-Mer (TAM) receptor family and is known to activate PI3K/AKT/mTOR in AML. AXL has been recognized to mediate drug resistance in several types of cancers, including FLT3-ITD AML, and has gained increasing interest as a putative therapeutic target (Dumas et al., 2019; Liu et al., 2021; Park et al., 2015). There is ongoing clinical research combining AXLi-directed therapies like the multikinase inhibitor, gilteritinib with other targeted therapies and/or chemotherapy in relapsed or refractory FLT3-ITD AML (Levis and Perl, 2020; Perl et al., 2019). Inefficient blockage of FLT3-ITD signaling was confirmed not only by p-STAT5 but also by p-ERK.

To confirm that combination treatment triggers apoptosis, cleaved PARP expression was determined. In line with results obtained by flow cytometry, combination treatment caused a trend toward increased expression of cleaved PARP. A great addition to these results would be the expression profile of other proteins involved cell death such as the BH3-only Bcl-2 family proteins to understand the mechanism by which combination treatment synergistically induces apoptosis. The activation status of the PI3K/AKT/mTOR and FLT3-ITD signaling was confirmed by intracellular staining. Indeed, it was demonstrated that combination treatment does not further enhance blockade of the FLT3-ITD and PI3K/AKT/mTOR signaling pathways, but may even counteract pathway inhibition, possibly by antagonism. And yet the drug combination acts synergistically for biological outcomes. These results collectively imply that an alternative strategy is needed to achieve effective and sustained PI3K/AKT/mTOR and FLT3-ITD AML signaling. Such a putative strategy to achieve complete and sustained pathway blockade as well as to reduce drug-related toxicity include intermittent treatment schedules (Hanker et al., 2019). However, it should be noted that the best timing and optimal dosing for this assessment is not clear and requires further investigation.

In addition to the phosphoproteomic profile, it was assessed whether combination treatment on FLT3-ITD AML primary cells *ex vivo* alters the cytokine release profile. Conditioned media (SFEM versus PGF) was evaluated for released cytokines, but unexpectedly relative low concentrations were detected and these levels were variable amongst patient samples. Assessment on a larger subset of patient samples and using a broader panel of soluble factors (e.g. chemokines, growth factors and proteases) may obtain a more complex release profile that could identify a subset of patients with a signature mediator release profile. Investigation of the constitutive release of 24 cytokines identified drug-related and/or culture condition-related alteration of cytokine release for IL-1RA, IL1-β, IL-6 and GM-CSF.

Over the recent years, a number of comprehensive studies have reported pro-inflammatory and anti-inflammatory cytokines that exert profound effects on the progression of AML (Chakraborty et al., 2021; Kiyatkin et al., 2006; Sanchez-Correa et al., 2013). Deregulation of the release of

inflammatory cytokines is believed to promote such an environment that promotes leukemic cell proliferation, survival and drug-resistance. As such, in a number of studies it has been demonstrated that AML patients constitutively express cytokines including IL-1, IL-6, IL-8, GM-CSF, G-CSF, tumor necrosis factor α (TNF-α), and SCF, which is thought to stimulate AML cell growth (Carey et al., 2017; Hoang et al., 1989; Kassem et al., 2018; Sanchez-Correa et al., 2013). In a report by Brenner *et al.,* hierarchical clustering was able to subclassify patients based on their constitutive cytokine release profile, which could be associated with overall survival after intensive anti-leukemic therapy (Brenner et al., 2017b). The biological role of the highlighted cytokines from the cytokine release analysis in normal hematopoiesis and AML pathology is discussed in short below.

The IL-1 family plays a central role in the regulation of inflammatory and innate immune responses as well as hematopoiesis. IL-1β is the best characterized of the IL-1 family and is secreted by various cell types of the immune system including monocytes and macrophages (Netea et al., 2009). High expression of IL-1β has been reported in hematological malignancies including AML where its expression was associated with poor patient prognosis and resistant of AML cells to apoptosis (Grauers Wiktorin et al., 2021; Turzanski et al., 2004; Wang et al., 2020). IL-1β has been ascribed a profound role in expansion of myeloid progenitors, whilst paradoxically suppressing the growth of normal progenitors (Carey et al., 2017). The mechanism by which IL-1 promoted cell growth involved elevated p38MAPK phosphorylation and secretion of other inflammatory cytokines and growth factors such as GM-CSF. IL-1β (as well as TNF-α) is reported to potentially promote inflammation by canonical activation of the transcription factor NF-κB that has a critical role in the development of AML (Xu et al., 2009; Zhou et al., 2015). Further research has revealed that AML blasts secrete IL-1β and TNF-α to promote adhesion to the vascular endothelium that may have relevant implications for metastasis and tissue infiltration by leukemic blasts (Stucki et al., 2001). Body of evidence highlighted the therapeutic value of targeting IL-1β in AML, using for example IL-1 receptor antagonist (IL-RA), which negatively regulates IL-1β signaling (Arranz et al., 2017). IL-1RA, another member of the IL-1 family, is an endogenous antagonist of IL-1β and negatively modulates the effects of IL-1β by competitive binding to IL-1R (Schreuder et al., 1997). In the context of AML, patients with high levels of IL-1RA and low levels of IL-1β had reduced risk of leukemic relapse (Grauers Wiktorin et al., 2021).

GM-CSF is a hematopoietic growth factor that promotes the growth, differentiation, and function of myeloid progenitors and generation of dendritic cells (Egea et al., 2010; Fleetwood et al., 2005). It can be produced by a various cell types, including T cells, macrophages, epithelial cells, and endothelial cells in response to proinflammatory stimuli, such as IL-3, IL-6, and TNF-α (Shi et al., 2006). GM-CSF can stimulate the proliferation of leukemic blasts, thereby driving malignant cells into cell cycle. A number of studies have attempted to evaluate GM-CSF concomitant or sequential

with S-phase specific chemotherapeutics such as cytarabine, with the idea that it may sensitize leukemic blasts to chemotherapy-induced cytotoxicity, and thus reduce relapse rate. There are indications that priming with GM-CSF might improve survival and treatment responses of previously untreated AML patients (Büchner et al., 1993; Feng et al., 2018; Rossi et al., 2002).

Pro-inflammatory cytokine IL-6 has pleiotropic functions in immunity, tissue regeneration, and metabolism. Produced mainly by T-cells, monocytes and macrophages; IL-6 expression is induced by inflammatory stimuli like IL-1β and TNF-α (Confalone et al., 2010). Further, IL-6 has a prominent role in hematopoiesis, as it is involved in the survival, self-renewal, or both of hematopoietic stem cells and early progenitors (Bernad et al., 1994). In the context of AML, IL-6 may act as a co-stimulator to enhance CSF-induced clonogenicity of AML blast cells (Beauchemin et al., 1991; Sugiyama et al., 1996). A prognostic significance of IL-6 production in AML blasts has been addressed where high levels of IL-6 was associated with higher percentage of blasts in the peripheral blood and BM; and inferior event-free survival (Stevens et al., 2017; Thomas et al., 1997).

Considering that IL-1β, IL-6, and GM-CSF are reported to promote growth of AML cells, it would be expected that secretion levels of these cytokines would be higher in the presence of PGF – in which cells were shown to be more viable, with respect to AML culture in SFEM. Furthermore, since enhanced growth inhibition following combination therapy was demonstrated in both SFEM and PGF, it was anticipated that combination treatment would reduce IL-1β, IL-6, and GM-CSF levels respective to either monotherapies. However, opposite effects were observed. As such, cytokine secretion analysis revealed that addition of PGF to culture media of FLT3-ITD AML cells co-cultured with stroma decreased basal levels of IL-1β, IL-6, and GM-CSF respective to co-culture in SFEM, whilst a relative small increase was observed for IL-1RA. These alterations were however observed only in a couple of patients' cells, reflecting the heterogeneity of the disease.

IL-1β and IL-6 levels were most pronounced in sample AML009 cultured in SFEM, which was sensitive to either monotherapies and drug combination. Highest levels of IL-1RA were observed in sample AML005, which was the most sensitive to either monotherapy, and where the combination therapy had the most pronounced cytotoxic effect. Since IL-1RA antagonizes the binding of IL-1β to its receptor, increased levels of IL-1RA was expected following drug treatment. This was however only true for BAY-806946 treatment. GM-CSF was detected only in samples AML006 and AML023, of which AML006 was sensitive and AML023 was insensitive to combination treatment. Although not statistically significant, there seems to be a trend towards decreased GM-CSF levels following combination treatment in both culture conditions, which is in line with the expected results. Cytokines are known to activate a plethora of signaling cascades such as NF-κB, p38MAPK, and PI3K/AKT/mTOR signaling (Carey et al., 2017; Hayden and Ghosh, 2014; Kim et al., 2019; Sabio and Davis, 2014). Thus, elucidating the cytokine profile of FLT3-ITD AML patient cells may identify

subgroups of patients that are predicted to be sensitive or resistant to targeted therapies. However, not only should the sample size be increased to unravel such signatures, functional assays are required to confirm these findings. For instance, in addition to measuring the constitutive secretion, expression of these cytokines in FLT3-ITD AML cells could be determined by qPCR and the activity of particular cytokines could be studied by assessing the colony-formation ability of AML cells.

In this work, only a handful of patient samples were selected carrying the FLT3-ITD mutation but as expected the drug response observed was not uniform amongst patient samples. In order to correlate drug response to patient characteristics (e.g., gender and age) and disease characteristics (e.g., previous treatment, mutational profile, diagnosis) a larger set of patient samples should be evaluated. Other aspects to consider include improvement of the *ex vivo* culture model and *in vivo* testing. Co-culture with stromal layer and addition of PGF is one step closer to resembling BM niche conditions, but in reality this microenvironment is far more complex and other component should be considered to further optimize the *ex vivo* model to better predict clinical response. More advanced *ex vivo* models include 3D culture models using hydrogels or scaffold and co-culture with mesenchymal stromal cells and endothelial cells to mimic the vascular niche (Bray et al., 2017; Dhami et al., 2016). Also the effects of hypoxia on cell culture have been addressed. As such, drug responses of primary AML cells co-culture on MS-5 with exogenous growth factors IL-3, G-CSF and TPO in hypoxic condition (3% O_2) was comparable to *in vivo* drug response in mice (Griessinger et al., 2014).

In conclusion, it has been demonstrated *ex vivo* that BAY-806946 has potential to enhance the efficacy of quizartinib on FLT3-ITD AML cells. Combination treatment effectively induced cytotoxicity in FLT3-ITD AML leukemic cells and possibly in LSC. However, both inhibitors alone and in combination induced cytotoxicity in the bulk CD45+ cells of non-AML cells, but that was only marginal in the CD34+CD38- cell fraction. Concomitant targeting of FLT3-ITD and PI3K/AKT/mTOR failed to sustain pathway blockade, leading to rebound signaling, which may be circumvented by intermitted treatment schedules. Finally, combination treatment and/or exogenous PGF altered the cytokine release profile, which may be a useful tool to subclassify patients that are predicted to be responsive to targeted therapies.

Chapter 7: Thesis summary and future directions

This study investigated whether combination with PI3K/AKT/mTORi may potentiate the efficacy of FLT3i in FLT3-ITD AML in a pre-clinical setting. Further to this, validate whether this combination is worthy of translation into the clinic. To this end, first, phenotypic characterization of FLT3-ITD versus FLT3 wildtype AML cell lines following FLT3i or PI3K/AKT/mTORi was performed. Inhibitors tested included selective and potent FLT3i quizartinib, which is currently under clinical investigation in combination with chemotherapy and/or targeted therapies such as Bcl-2 inhibitor (e.g. venetoclax, NCT03735875), or hypomethylating agents (e.g. azacitidine; NCT01892371). The evaluated PI3Ki included BAY-806946 and PF-04691502. BAY-806946 is a pan-PI3Ki with potent p110α and p110δ activities that has been widely explored for the treatment of B-cell malignancies (Krause et al., 2018). PF-04691502 is a dual pan-PI3K/mTORi that has shown promising anti-tumor activity in solid cancers harboring a *PIK3CA* mutation, but clinical investigation for the treatment of recurrent endometrial cancer was terminated due to lack of clinical beneficial response (Fang et al., 2013) (NCT01420081).

It has been demonstrated that quizartinib induced cell growth inhibition, mainly though G1 cell cycle arrest and these anti-leukemic effects were selective for FLT3-ITD AML. BAY-806946 and PF-04691502 also induced growth inhibition irrespective of FLT3 status, yet it seemed that FLT3-ITD AML cell lines were more sensitive to PI3Ki. This is in agreement with a recent report by the Marmiroli lab, which revealed that PI3K/AKT/mTORi display greater anti-leukemic effects in FLT3-ITD AML *in vitro* (Darici et al., 2021). Further, inhibition of PI3K/AKT/mTOR by either BAY-806946 or PF-04691502 was only moderately cytotoxic, instead rather cytostatic. This is also in line with existing literature, underscoring the importance of combination treatment strategies to potentiate cytotoxicity (Okkenhaug et al., 2016). In the FLT3-ITD AML cell line, MOLM-13, constitutively active MAPK and PI3K/AKT/mTOR signaling was inhibited at the protein expression level by either monotherapies. Based on these observations, the efficacy of combination treatment consisting of quizartinib with BAY-806946 or PF-04691502 in FLT3-ITD AML cell lines was next evaluated.

Combination of quizartinib with either BAY-806946 or PF-04691502 synergistically inhibited cell growth, and induced enhanced cytostatic and cytotoxic effects in MOLM-13 cells. Since combination treatment enhanced anti-leukemic effects, it was hypothesized that combination treatment would exert stronger inhibition of FLT3-ITD and PI3K/AKT/mTOR signaling. Whilst combination treatment potentiated inhibition of mTOR, sustained up to 24 hrs, reactivation of AKT and ERK was shown. To uncover persistent protein targets, RPPA analysis was performed, which not only confirmed inefficient blockage of FLT3-ITD and PI3K/AKT/mTOR signaling, but also indicated upregulation of IRS-1 and STAT5. These findings suggest that concomitant inhibition of

FLT3-ITD and PI3K/AKT/mTOR exerts enhanced biological response, but fails to avoid negative feedback mechanisms causing pathway reactivation. Modifying the treatment regimen by sequential drug administration may be more efficient to sustain pathway inhibition. Downstream of FLT3-ITD signaling, STAT5 is known to be involved in resistance to chemotherapy and PI3K/AKT/mTOR inhibition. Combination of TKIs have shown to be effective in suppressing downstream effectors of FLT3-ITD, including STAT5 and MAPK *ex vivo* (Dumas et al., 2019; Patel et al., 2020). Therefore, a TKI combination or dual TK inhibitor such as midostaurin and gilteritinib could be explored in combination with PI3Ki to overcome STAT5-mediated drug resistance. Other targeted therapies such as Bcl-2 inhibitors or PARP inhibitors may also be considered as they have been shown to abrogate STAT5 activation in FLT3-ITD AML (Dellomo et al., 2022; Zhu et al., 2021).

The efficacy of the drug combination was then assessed *ex vivo* using human FLT3-ITD AML primary patient cells, elevating this research in a more clinically relevant setting. To more closely mimic BM niche conditions, primary cells were co-cultured with stromal cells plus/minus exogenous PGF. FLT3-ITD AML PDX cells were shown to have a better viability in the presence of supporting stroma and/or physiological growth factors, and were protected against FLT3 inhibition. These findings confirm the protective effect of the BM niche (Parmar et al., 2011; Patel et al., 2020; Yang et al., 2014, p. 3). Evaluation of combination treatment (consisting of BAY-806946 and quizartinib) on FLT3-ITD AML primary cells cultured with stroma exerted synergistic growth inhibition and apoptosis. Although still enhanced respective to either monotherapies, this effect was attenuated with PGF. The affected cells were indeed leukemic as they were double positive for myeloid markers CD33 and CD38. These results demonstrate that BAY-806946 potentiated the efficacy of quizartinib and was able to overcome stromal protection.

More importantly, it was assessed whether the combination treatment specifically targeted AML LSC, whilst sparing the CD34+CD38- fraction of normal cells. AML LSC represents a rare cell population, which was only measurable in three patient samples. Combination treatment showed a trend towards increased cytotoxicity in the stem cell-like CD34+CD38- cell fraction, however a larger sample size and more accurate assays to detect LSC activity (e.g., LTC-IC) should be considered in future experiments to confirm this. The drug combination was evaluated on PBMC from a healthy donor and non-AML patient as an indication of a potential therapeutic window. Whilst the drug combination exerted negligible cytotoxicity in PBMC, relatively small induction of cytotoxicity was observed in the CD34+CD38- fraction of non-AML cells. This effect was mainly caused by BAY-806946 rather than quizartinib, and was abrogated in the presence of PGF. It was not surprising that BAY-806946 had such an effect on non-AML cells as the PI3K/AKT/mTOR signaling pathway is also active in normal hematopoiesis.

In cell line work, it came to light that although combination treatment enhanced drug-induced cytotoxicity, persistent proteins were upregulated that may relate to PI3K/AKT/mTOR and FLT3-ITD pathway reactivation. To this end, pathway activation status and phosphoproteomic analysis by RPPA was assessed on FLT3-ITD AML primary cells co-cultured with stroma plus PGF. Comparable with cell line work, following 24 hrs drug treatment sustained inhibition of mTOR, but reactivation of ERK and AKT was found. In addition, upregulation of STAT5 was detected; underscoring that further optimization of this combined targeted treatment strategy is needed in future experiments before moving on to *in vivo* testing.

In the final part of this thesis work, it was investigated whether combination treatment and/or culture with PGF alters the cytokine secretion profile of FLT3-ITD AML primary cells. The constitutive release of 25 cytokines was determined of FLT3-ITD AML primary cells (n=9) co-cultured with stroma plus/minus PGF following combination treatment. Only four cytokines were above detection limit: GM-CSF (2/9), IL-1β (7/9), IL-1RA (8/9), and IL-6 (2/9). This was surprising considering that relative higher levels of these cytokines and others were detected in related studies (Brenner et al., 2017b; Kornblau et al., 2010; Reikvam et al., 2019). A wide variation for each individual cytokine was measured, reflecting the patient heterogeneity. Since GM-CSF, IL-1β, and IL-6 have a stimulatory role on AML cell growth, proliferation, differentiation and survival it was expected that secretion levels of these cytokines would be higher with PGF and consequently reduced following drug treatment. This would support the enhanced cytotoxicity observed following combination treatment. Paradoxically, addition of PGF decreased basal levels of IL-1β, IL-6, and GM-CSF respective to co-culture in SFEM. Combination treatment was shown to only reduce secretion of GM-CSF. Since cytokines are known to activate various signaling cascades, cytokine-based stratification may be predictive of patient responsiveness to drug treatment. However, based on the observed discrepancies between biological outcome (i.e. drug-induced cytotoxicity) and cytokine release profile, further studies are required to identify such a cytokine signature. First of all, a larger subset of patients should be evaluated since a wide variation for each released cytokine was found amongst patient samples. Subsequently, upon elucidating putative cytokines, functional studies are required to confirm the pro-inflammatory role of cytokines in FLT3-ITD AML.

In summary, it has been demonstrated that PI3Ki can potentiate the efficacy of FLT3i in FLT3-ITD AML. Using an *ex vivo* model to mimic BM niche conditions consisting of co-culture with stroma and PGF, it has been shown that the drug combination overcomes stromal protection and induces enhanced cytotoxicity. Furthermore, there are indications that the drug treatment may eradicate AML LSC whilst moderately affecting normal cells that require PI3K/AKT/mTOR activity for normal cellular function. A major drawback of concomitant targeting of PI3K/AKT/mTOR and FLT3-ITD was the occurrence of pathway reactivation that might be avoided by optimizing the treatment

schedule or addition of targeted therapies. RPPA and the secreted cytokine assay have shown to be useful tools to elucidate persistent proteins or cytokines. The activation status of additional protein kinases and released cytokines may provide further insight into the FLT3-ITD AML cell responsiveness to combination treatment. This might create new avenues for understanding the mechanism of action of synergy or drug resistance, and potentially predict responsiveness of FLT3-ITD AML patient cells.

List of References:

Abdul-Aziz, A.M., Shafat, M.S., Mehta, T.K., Di Palma, F., Lawes, M.J., Rushworth, S.A., Bowles, K.M., 2017. MIF-Induced Stromal PKCβ/IL8 Is Essential in Human Acute Myeloid Leukemia. Cancer Res. 77, 303–311. https://doi.org/10.1158/0008-5472.CAN-16-1095

Abdul-Aziz, A.M., Shafat, M.S., Sun, Y., Marlein, C.R., Piddock, R.E., Robinson, S.D., Edwards, D.R., Zhou, Z., Collins, A., Bowles, K.M., Rushworth, S.A., 2018. HIF1α drives chemokine factor pro-tumoral signaling pathways in acute myeloid leukemia. Oncogene 37, 2676–2686. https://doi.org/10.1038/s41388-018-0151-1

Abraham, R.T., Eng, C.H., 2008. Mammalian target of rapamycin as a therapeutic target in oncology. Expert Opin. Ther. Targets 12, 209–222. https://doi.org/10.1517/14728222.12.2.209

Aikawa, T., Togashi, N., Iwanaga, K., Okada, H., Nishiya, Y., Inoue, S., Levis, M.J., Isoyama, T., 2020. Quizartinib, a selective FLT3 inhibitor, maintains antileukemic activity in preclinical models of RAS-mediated midostaurin-resistant acute myeloid leukemia cells. Oncotarget 11, 943–955. https://doi.org/10.18632/oncotarget.27489

Akcakanat, A., Meric-Bernstam, F., 2018. MK-2206 window of opportunity study in breast cancer. Ann. Transl. Med. 6. https://doi.org/10.21037/atm.2018.10.32

Alcalay, M., Meani, N., Gelmetti, V., Fantozzi, A., Fagioli, M., Orleth, A., Riganelli, D., Sebastiani, C., Cappelli, E., Casciari, C., Sciurpi, M.T., Mariano, A.R., Minardi, S.P., Luzi, L., Muller, H., Di Fiore, P.P., Frosina, G., Pelicci, P.G., 2003. Acute myeloid leukemia fusion proteins deregulate genes involved in stem cell maintenance and DNA repair. J. Clin. Invest. 112, 1751–1761. https://doi.org/10.1172/JCI17595

Alessi, D.R., Andjelkovic, M., Caudwell, B., Cron, P., Morrice, N., Cohen, P., Hemmings, B.A., 1996. Mechanism of activation of protein kinase B by insulin and IGF-1. EMBO J. 15, 6541–6551.

Alessi, D.R., Kozlowski, M.T., Weng, Q.P., Morrice, N., Avruch, J., 1998. 3-Phosphoinositide-dependent protein kinase 1 (PDK1) phosphorylates and activates the p70 S6 kinase in vivo and in vitro. Curr. Biol. CB 8, 69–81. https://doi.org/10.1016/s0960-9822(98)70037-5

Allegretti, M., Ricciardi, M.R., Licchetta, R., Mirabilii, S., Orecchioni, S., Reggiani, F., Talarico, G., Foà, R., Bertolini, F., Amadori, S., Torrisi, M.R., Tafuri, A., 2015. The pan-class I phosphatidyl-inositol-3 kinase inhibitor NVP-BKM120 demonstrates anti-leukemic activity in acute myeloid leukemia. Sci. Rep. 5. https://doi.org/10.1038/srep18137

Almosailleakh, M., Schwaller, J., 2019. Murine Models of Acute Myeloid Leukaemia. Int. J. Mol. Sci. 20, 453. https://doi.org/10.3390/ijms20020453

Alotaibi, A.S., Yilmaz, M., Kanagal-Shamanna, R., Loghavi, S., Kadia, T.M., DiNardo, C.D., Borthakur, G., Konopleva, M., Pierce, S.A., Wang, S.A., Tang, G., Guerra, V., Samra, B., Pemmaraju, N., Jabbour, E., Short, N.J., Issa, G.C., Ohanian, M., Garcia-Manero, G., Bhalla, K.N., Patel, K.P., Takahashi, K., Andreeff, M., Cortes, J.E., Kantarjian, H.M., Ravandi, F., Daver, N., 2021. Patterns of Resistance Differ in Patients with Acute Myeloid Leukemia Treated with Type I versus Type II FLT3 Inhibitors. Blood Cancer Discov. 2, 125–134. https://doi.org/10.1158/2643-3230.BCD-20-0143

Amaravadi, R., Thompson, C.B., 2005. The survival kinases Akt and Pim as potential pharmacological targets. J. Clin. Invest. 115, 2618–2624. https://doi.org/10.1172/JCI26273

Andreeff, M., Jiang, S., Zhang, X., Konopleva, M., Estrov, Z., Snell, V.E., Xie, Z., Okcu, M.F., Sanchez-Williams, G., Dong, J., Estey, E.H., Champlin, R.C., Kornblau, S.M., Reed, J.C., Zhao, S., 1999. Expression of Bcl-2-related genes in normal and AML progenitors: changes induced by chemotherapy and retinoic acid. Leukemia 13, 1881–1892. https://doi.org/10.1038/sj.leu.2401573

Andreozzi, F., D'Alessandris, C., Federici, M., Laratta, E., Del Guerra, S., Del Prato, S., Marchetti, P., Lauro, R., Perticone, F., Sesti, G., 2004. Activation of the hexosamine pathway leads to phosphorylation of insulin receptor substrate-1 on Ser307 and Ser612 and impairs the phosphatidylinositol 3-kinase/Akt/mammalian target of rapamycin insulin biosynthetic pathway in RIN pancreatic beta-cells. Endocrinology 145, 2845–2857. https://doi.org/10.1210/en.2003-0939

Annageldiyev, C., Tan, S.-F., Thakur, S., Dhanyamraju, P.K., Ramisetti, S.R., Bhadauria, P., Schick, J., Zeng, Z., Sharma, V., Dunton, W., Dovat, S., Desai, D., Zheng, H., Feith, D.J., Loughran, T.P., Amin, S., Sharma, A.K., Claxton, D., Sharma, A., 2020. The PI3K/AKT Pathway Inhibitor ISC-4 Induces Apoptosis and Inhibits Growth of Leukemia in Preclinical Models of Acute Myeloid Leukemia. Front. Oncol. 10.

Antar, A.I., Otrock, Z.K., Jabbour, E., Mohty, M., Bazarbachi, A., 2020. FLT3 inhibitors in acute myeloid leukemia: ten frequently asked questions. Leukemia 34, 682–696. https://doi.org/10.1038/s41375-019-0694-3

Arai, F., Hirao, A., Ohmura, M., Sato, H., Matsuoka, S., Takubo, K., Ito, K., Koh, G.Y., Suda, T., 2004. Tie2/angiopoietin-1 signaling regulates hematopoietic stem cell quiescence in the bone marrow niche. Cell 118, 149–161. https://doi.org/10.1016/j.cell.2004.07.004

Arai, N., Homma, M., Abe, M., Baba, Y., Murai, S., Watanuki, M., Kawaguchi, Y., Fujiwara, S., Kabasawa, N., Tsukamoto, H., Uto, Y., Ariizumi, H., Yanagisawa, K., Hattori, N., Saito, B., Shiozawa, E., Harada, H., Yamochi-Onizuka, T., Nakamaki, T., Takimoto, M., 2019. Impact of CD123 expression, analyzed by immunohistochemistry, on clinical outcomes in patients with acute myeloid leukemia. Int. J. Hematol. 109, 539–544. https://doi.org/10.1007/s12185-019-02616-y

Arber, D.A., Orazi, A., Hasserjian, R., Thiele, J., Borowitz, M.J., Le Beau, M.M., Bloomfield, C.D., Cazzola, M., Vardiman, J.W., 2016. The 2016 revision to the World Health Organization classification of myeloid neoplasms and acute leukemia. Blood 127, 2391–2405. https://doi.org/10.1182/blood-2016-03-643544

Arranz, L., Arriero, M. del M., Villatoro, A., 2017. Interleukin-1β as emerging therapeutic target in hematological malignancies and potentially in their complications. Blood Rev. 31, 306–317. https://doi.org/10.1016/j.blre.2017.05.001

Arreba-Tutusaus, P., Mack, T., Bullinger, L., Schnöder, T., Polanetzki, A., Weinert, S., Ballaschk, A., Wang, Z., Deshpande, A., Armstrong, S., Döhner, K., Fischer, T., Heidel, F., 2016. Impact of FLT3-ITD location on sensitivity to TKI-therapy in vitro and in vivo. Leukemia 30, 1220–1225. https://doi.org/10.1038/leu.2015.292

Audeh, M.W., Carmichael, J., Penson, R.T., Friedlander, M., Powell, B., Bell-McGuinn, K.M., Scott, C., Weitzel, J.N., Oaknin, A., Loman, N., Lu, K., Schmutzler, R.K., Matulonis, U., Wickens, M., Tutt, A., 2010. Oral poly(ADP-ribose) polymerase inhibitor olaparib in patients with BRCA1 or BRCA2 mutations and recurrent ovarian cancer: a proof-of-concept trial. Lancet Lond. Engl. 376, 245–251. https://doi.org/10.1016/S0140-6736(10)60893-8

Azadniv, M., Myers, J.R., McMurray, H.R., Guo, N., Rock, P., Coppage, M.L., Ashton, J., Becker, M.W., Calvi, L.M., Liesveld, J.L., 2020. Bone marrow mesenchymal stromal cells from acute myelogenous leukemia patients demonstrate adipogenic differentiation propensity with implications for leukemia cell support. Leukemia 34, 391–403. https://doi.org/10.1038/s41375-019-0568-8

Aziz, A.U.R., Farid, S., Qin, K., Wang, H., Liu, B., 2018. PIM Kinases and Their Relevance to the PI3K/AKT/mTOR Pathway in the Regulation of Ovarian Cancer. Biomolecules 8. https://doi.org/10.3390/biom8010007

Bachas, C., Schuurhuis, G.J., Assaraf, Y.G., Kwidama, Z.J., Kelder, A., Wouters, F., Snel, A.N., Kaspers, G.J.L., Cloos, J., 2012. The role of minor subpopulations within the leukemic blast compartment of AML patients at initial diagnosis in the development of relapse. Leukemia 26, 1313–1320. https://doi.org/10.1038/leu.2011.383

Bacon, C.M., Tortolani, P.J., Shimosaka, A., Rees, R.C., Longo, D.L., O'Shea, J.J., 1995. Thrombopoietin (TPO) induces tyrosine phosphorylation and activation of STAT5 and STAT3. FEBS Lett. 370, 63–68. https://doi.org/10.1016/0014-5793(95)00796-c

Bakker, A.B.H., van den Oudenrijn, S., Bakker, A.Q., Feller, N., van Meijer, M., Bia, J.A., Jongeneelen, M.A.C., Visser, T.J., Bijl, N., Geuijen, C.A.W., Marissen, W.E., Radosevic, K., Throsby, M., Schuurhuis, G.J., Ossenkoppele, G.J., de Kruif, J., Goudsmit, J., Kruisbeek, A.M., 2004. C-type lectin-like molecule-1: a novel myeloid cell surface marker associated with acute myeloid leukemia. Cancer Res. 64, 8443–8450. https://doi.org/10.1158/0008-5472.CAN-04-1659

Beauchemin, V., Villeneuve, L., Rodriguez-Cimadevilla, J.C., Rajotte, D., Kenney, J.S., Clark, S.C., Hoang, T., 1991. Interleukin-6 production by the blast cells of acute myeloblastic leukemia:

regulation by endogenous interleukin-1 and biological implications. J. Cell. Physiol. 148, 353–361. https://doi.org/10.1002/jcp.1041480305
Behrmann, L., Wellbrock, J., Fiedler, W., 2018. Acute Myeloid Leukemia and the Bone Marrow Niche—Take a Closer Look. Front. Oncol. 8, 444. https://doi.org/10.3389/fonc.2018.00444
Bellezza, I., Giambanco, I., Minelli, A., Donato, R., 2018. Nrf2-Keap1 signaling in oxidative and reductive stress. Biochim. Biophys. Acta Mol. Cell Res. 1865, 721–733. https://doi.org/10.1016/j.bbamcr.2018.02.010
Bendall, L.J., Bradstock, K.F., Gottlieb, D.J., 2000. Expression of CD44 variant exons in acute myeloid leukemia is more common and more complex than that observed in normal blood, bone marrow or CD34+ cells. Leukemia 14, 1239–1246. https://doi.org/10.1038/sj.leu.2401830
Benito, J., Ramirez, M.S., Millward, N.Z., Velez, J., Harutyunyan, K.G., Lu, H., Shi, Y.-X., Matre, P., Jacamo, R., Ma, H., Konoplev, S., McQueen, T., Volgin, A., Protopopova, M., Mu, H., Lee, J., Bhattacharya, P.K., Marszalek, J.R., Davis, R.E., Bankson, J.A., Cortes, J.E., Hart, C.P., Andreeff, M., Konopleva, M., 2016. Hypoxia-Activated Prodrug TH-302 Targets Hypoxic Bone Marrow Niches in Preclinical Leukemia Models. Clin. Cancer Res. Off. J. Am. Assoc. Cancer Res. 22, 1687–1698. https://doi.org/10.1158/1078-0432.CCR-14-3378
Bernad, A., Kopf, M., Kulbacki, R., Weich, N., Koehler, G., Gutierrez-Ramos, J.C., 1994. Interleukin-6 is required in vivo for the regulation of stem cells and committed progenitors of the hematopoietic system. Immunity 1, 725–731. https://doi.org/10.1016/s1074-7613(94)80014-6
Bernasconi, P., Borsani, O., 2019. Targeting Leukemia Stem Cell-Niche Dynamics: A New Challenge in AML Treatment. J. Oncol. 2019, e8323592. https://doi.org/10.1155/2019/8323592
Bernt, K.M., Zhu, N., Sinha, A.U., Vempati, S., Faber, J., Krivtsov, A.V., Feng, Z., Punt, N., Daigle, A., Bullinger, L., Pollock, R.M., Richon, V.M., Kung, A.L., Armstrong, S.A., 2011. MLL-rearranged leukemia is dependent on aberrant H3K79 methylation by DOT1L. Cancer Cell 20, 66–78. https://doi.org/10.1016/j.ccr.2011.06.010
Bertacchini, J., Frasson, C., Chiarini, F., D'Avella, D., Accordi, B., Anselmi, L., Barozzi, P., Forghieri, F., Luppi, M., Martelli, A.M., Basso, G., Najmaldin, S., Khosravi, A., Rahim, F., Marmiroli, S., 2018. Dual inhibition of PI3K/mTOR signaling in chemoresistant AML primary cells. Adv. Biol. Regul. 68, 2–9. https://doi.org/10.1016/j.jbior.2018.03.001
Bertacchini, J., Guida, M., Accordi, B., Mediani, L., Martelli, A.M., Barozzi, P., Petricoin, E., Liotta, L., Milani, G., Giordan, M., Luppi, M., Forghieri, F., De Pol, A., Cocco, L., Basso, G., Marmiroli, S., 2014. Feedbacks and adaptive capabilities of the PI3K/Akt/mTOR axis in acute myeloid leukemia revealed by pathway selective inhibition and phosphoproteome analysis. Leukemia 28, 2197–2205. https://doi.org/10.1038/leu.2014.123
Bewersdorf, J.P., Shallis, R., Stahl, M., Zeidan, A.M., 2019. Epigenetic therapy combinations in acute myeloid leukemia: what are the options? Ther. Adv. Hematol. 10. https://doi.org/10.1177/2040620718816698
Birkenkamp, K.U., Geugien, M., Lemmink, H.H., Kruijer, W., Vellenga, E., 2001. Regulation of constitutive STAT5 phosphorylation in acute myeloid leukemia blasts. Leukemia 15, 1923–1931. https://doi.org/10.1038/sj.leu.2402317
Birkenkamp, K.U., Geugien, M., Schepers, H., Westra, J., Lemmink, H.H., Vellenga, E., 2004. Constitutive NF-kappaB DNA-binding activity in AML is frequently mediated by a Ras/PI3-K/PKB-dependent pathway. Leukemia 18, 103–112. https://doi.org/10.1038/sj.leu.2403145
Blagden, S.P., Hamilton, A.L., Mileshkin, L., Wong, S., Michael, A., Hall, M., Goh, J.C., Lisyanskaya, A.S., DeSilvio, M., Frangou, E., Stronach, E.A., Gopalakrishna, P., Meniawy, T.M., Gabra, H., 2019. Phase IB Dose Escalation and Expansion Study of AKT Inhibitor Afuresertib with Carboplatin and Paclitaxel in Recurrent Platinum-resistant Ovarian Cancer. Clin. Cancer Res. Off. J. Am. Assoc. Cancer Res. 25, 1472–1478. https://doi.org/10.1158/1078-0432.CCR-18-2277
Bleier, L., Dröse, S., 2013. Superoxide generation by complex III: from mechanistic rationales to functional consequences. Biochim. Biophys. Acta 1827, 1320–1331. https://doi.org/10.1016/j.bbabio.2012.12.002

Blunt, M.D., Carter, M.J., Larrayoz, M., Smith, L.D., Aguilar-Hernandez, M., Cox, K.L., Tipton, T., Reynolds, M., Murphy, S., Lemm, E., Dias, S., Duncombe, A., Strefford, J.C., Johnson, P.W.M., Forconi, F., Stevenson, F.K., Packham, G., Cragg, M.S., Steele, A.J., 2015. The PI3K/mTOR inhibitor PF-04691502 induces apoptosis and inhibits microenvironmental signaling in CLL and the Eμ-TCL1 mouse model. Blood 125, 4032–4041. https://doi.org/10.1182/blood-2014-11-610329

Boettcher, S., Manz, M.G., 2017. Regulation of Inflammation- and Infection-Driven Hematopoiesis. Trends Immunol. 38, 345–357. https://doi.org/10.1016/j.it.2017.01.004

Bolandi, S.M., Pakjoo, M., Beigi, P., Kiani, M., Allahgholipour, A., Goudarzi, N., Khorashad, J.S., Eiring, A.M., 2021. A Role for the Bone Marrow Microenvironment in Drug Resistance of Acute Myeloid Leukemia. Cells 10, 2833. https://doi.org/10.3390/cells10112833

Bonnet, D., 2017. Acute myeloid leukemia including favorable-risk group samples engraft in NSG mice: just be patient. Haematologica 102, 805–806. https://doi.org/10.3324/haematol.2017.165159

Bonnet, D., Dick, J.E., 1997. Human acute myeloid leukemia is organized as a hierarchy that originates from a primitive hematopoietic cell. Nat. Med. 3, 730–737. https://doi.org/10.1038/nm0797-730

Borthakur, G., Kantarjian, H., Ravandi, F., Zhang, W., Konopleva, M., Wright, J.J., Faderl, S., Verstovsek, S., Mathews, S., Andreeff, M., Cortes, J.E., 2011. Phase I study of sorafenib in patients with refractory or relapsed acute leukemias. Haematologica 96, 62–68. https://doi.org/10.3324/haematol.2010.030452

Bose, P., Gandhi, V., Konopleva, M., 2017. Pathways and mechanisms of venetoclax resistance. Leuk. Lymphoma 58, 1–17. https://doi.org/10.1080/10428194.2017.1283032

Bose, P., Rahmani, M., Grant, S., 2012. Coordinate PI3K pathway and Bcl-2 family disruption in AML. Oncotarget 3, 1499–1500.

Bosman, M.C.J., Schuringa, J.J., Vellenga, E., 2016. Constitutive NF-κB activation in AML: Causes and treatment strategies. Crit. Rev. Oncol. Hematol. 98, 35–44. https://doi.org/10.1016/j.critrevonc.2015.10.001

Bourgeais, J., Gouilleux-Gruart, V., Gouilleux, F., 2013. Oxidative metabolism in cancer: A STAT affair? JAK-STAT 2, e25764. https://doi.org/10.4161/jkst.25764

Brandes, R.P., Weissmann, N., Schröder, K., 2014. Nox family NADPH oxidases: Molecular mechanisms of activation. Free Radic. Biol. Med. 76, 208–226. https://doi.org/10.1016/j.freeradbiomed.2014.07.046

Brandts, C.H., Sargin, B., Rode, M., Biermann, C., Lindtner, B., Schwäble, J., Buerger, H., Müller-Tidow, C., Choudhary, C., McMahon, M., Berdel, W.E., Serve, H., 2005. Constitutive activation of Akt by Flt3 internal tandem duplications is necessary for increased survival, proliferation, and myeloid transformation. Cancer Res. 65, 9643–9650. https://doi.org/10.1158/0008-5472.CAN-05-0422

Bras, A.E., de Haas, V., van Stigt, A., Jongen-Lavrencic, M., Beverloo, H.B., te Marvelde, J.G., Zwaan, C.M., van Dongen, J.J.M., Leusen, J.H.W., van der Velden, V.H.J., 2019. CD123 expression levels in 846 acute leukemia patients based on standardized immunophenotyping. Cytometry B Clin. Cytom. 96, 134–142. https://doi.org/10.1002/cyto.b.21745

Bray, L.J., Binner, M., Körner, Y., Bonin, M. von, Bornhäuser, M., Werner, C., 2017. A three-dimensional ex vivo tri-culture model mimics cell-cell interactions between acute myeloid leukemia and the vascular niche. Haematologica 102, 1215–1226. https://doi.org/10.3324/haematol.2016.157883

Brenner, A.K., Nepstad, I., Bruserud, Ø., 2017a. Mesenchymal Stem Cells Support Survival and Proliferation of Primary Human Acute Myeloid Leukemia Cells through Heterogeneous Molecular Mechanisms. Front. Immunol. 8, 106. https://doi.org/10.3389/fimmu.2017.00106

Brenner, A.K., Tvedt, T.H.A., Nepstad, I., Rye, K.P., Hagen, K.M., Reikvam, H., Bruserud, Ø., 2017b. Patients with acute myeloid leukemia can be subclassified based on the constitutive cytokine release of the leukemic cells; the possible clinical relevance and the importance of cellular iron metabolism. Expert Opin. Ther. Targets 21, 357–369. https://doi.org/10.1080/14728222.2017.1300255

Britschgi, A., Andraos, R., Brinkhaus, H., Klebba, I., Romanet, V., Müller, U., Murakami, M., Radimerski, T., Bentires-Alj, M., 2012. JAK2/STAT5 Inhibition Circumvents Resistance to PI3K/mTOR Blockade: A Rationale for Cotargeting These Pathways in Metastatic Breast Cancer. Cancer Cell 22, 796–811. https://doi.org/10.1016/j.ccr.2012.10.023

Brock, C., Schaefer, M., Reusch, H.P., Czupalla, C., Michalke, M., Spicher, K., Schultz, G., Nürnberg, B., 2003. Roles of Gβγ in membrane recruitment and activation of p110γ/p101 phosphoinositide 3-kinase γ. J. Cell Biol. 160, 89–99. https://doi.org/10.1083/jcb.200210115

Bruner, J.K., Ma, H.S., Li, L., Qin, A.C.R., Rudek, M.A., Jones, R.J., Levis, M.J., Pratz, K.W., Pratilas, C.A., Small, D., 2017. Adaptation to TKI Treatment Reactivates ERK Signaling in Tyrosine Kinase-Driven Leukemias and Other Malignancies. Cancer Res. 77, 5554–5563. https://doi.org/10.1158/0008-5472.CAN-16-2593

Bruno, S., Mancini, M., De Santis, S., Monaldi, C., Cavo, M., Soverini, S., 2021. The Role of Hypoxic Bone Marrow Microenvironment in Acute Myeloid Leukemia and Future Therapeutic Opportunities. Int. J. Mol. Sci. 22, 6857. https://doi.org/10.3390/ijms22136857

Bruserud, Ø., Ryningen, A., Olsnes, A.M., Stordrange, L., Øyan, A.M., Kalland, K.H., Gjertsen, B.T., 2007. Subclassification of patients with acute myelogenous leukemia based on chemokine responsiveness and constitutive chemokine release by their leukemic cells. Haematologica 92, 332–341. https://doi.org/10.3324/haematol.10148

Büchner, T., Hiddemann, W., Wörmann, B., Rottmann, R., Maschmeyer, G., Ludwig, W.D., Zühlsdorf, M., Buntkirchen, K., Sander, A., Aswald, J., 1993. The role of GM-CSF in the treatment of acute myeloid leukemia. Leuk. Lymphoma 11 Suppl 2, 21–24. https://doi.org/10.3109/10428199309064257

Burger, M.T., Pecchi, S., Wagman, A., Ni, Z.-J., Knapp, M., Hendrickson, T., Atallah, G., Pfister, K., Zhang, Y., Bartulis, S., Frazier, K., Ng, S., Smith, A., Verhagen, J., Haznedar, J., Huh, K., Iwanowicz, E., Xin, X., Menezes, D., Merritt, H., Lee, I., Wiesmann, M., Kaufman, S., Crawford, K., Chin, M., Bussiere, D., Shoemaker, K., Zaror, I., Maira, S.-M., Voliva, C.F., 2011. Identification of NVP-BKM120 as a Potent, Selective, Orally Bioavailable Class I PI3 Kinase Inhibitor for Treating Cancer. ACS Med. Chem. Lett. 2, 774–779. https://doi.org/10.1021/ml200156t

Cancer Genome Atlas Research Network, Ley, T.J., Miller, C., Ding, L., Raphael, B.J., Mungall, A.J., Robertson, A.G., Hoadley, K., Triche, T.J., Laird, P.W., Baty, J.D., Fulton, L.L., Fulton, R., Heath, S.E., Kalicki-Veizer, J., Kandoth, C., Klco, J.M., Koboldt, D.C., Kanchi, K.-L., Kulkarni, S., Lamprecht, T.L., Larson, D.E., Lin, L., Lu, C., McLellan, M.D., McMichael, J.F., Payton, J., Schmidt, H., Spencer, D.H., Tomasson, M.H., Wallis, J.W., Wartman, L.D., Watson, M.A., Welch, J., Wendl, M.C., Ally, A., Balasundaram, M., Birol, I., Butterfield, Y., Chiu, R., Chu, A., Chuah, E., Chun, H.-J., Corbett, R., Dhalla, N., Guin, R., He, A., Hirst, C., Hirst, M., Holt, R.A., Jones, S., Karsan, A., Lee, D., Li, H.I., Marra, M.A., Mayo, M., Moore, R.A., Mungall, K., Parker, J., Pleasance, E., Plettner, P., Schein, J., Stoll, D., Swanson, L., Tam, A., Thiessen, N., Varhol, R., Wye, N., Zhao, Y., Gabriel, S., Getz, G., Sougnez, C., Zou, L., Leiserson, M.D.M., Vandin, F., Wu, H.-T., Applebaum, F., Baylin, S.B., Akbani, R., Broom, B.M., Chen, K., Motter, T.C., Nguyen, K., Weinstein, J.N., Zhang, N., Ferguson, M.L., Adams, C., Black, A., Bowen, J., Gastier-Foster, J., Grossman, T., Lichtenberg, T., Wise, L., Davidsen, T., Demchok, J.A., Shaw, K.R.M., Sheth, M., Sofia, H.J., Yang, L., Downing, J.R., Eley, G., 2013. Genomic and epigenomic landscapes of adult de novo acute myeloid leukemia. N. Engl. J. Med. 368, 2059–2074. https://doi.org/10.1056/NEJMoa1301689

Carey, A., Edwards, D.K., Eide, C.A., Newell, L., Traer, E., Medeiros, B.C., Pollyea, D.A., Deininger, M.W., Collins, R.H., Tyner, J.W., Druker, B.J., Bagby, G.C., McWeeney, S.K., Agarwal, A., 2017. Identification of interleukin-1 by functional screening as a key mediator of cellular expansion and disease progression in acute myeloid leukemia. Cell Rep. 18, 3204–3218. https://doi.org/10.1016/j.celrep.2017.03.018

Carlo, M.I., Molina, A.M., Lakhman, Y., Patil, S., Woo, K., DeLuca, J., Lee, C.-H., Hsieh, J.J., Feldman, D.R., Motzer, R.J., Voss, M.H., 2016. A Phase Ib Study of BEZ235, a Dual Inhibitor of Phosphatidylinositol 3-Kinase (PI3K) and Mammalian Target of Rapamycin

(mTOR), in Patients With Advanced Renal Cell Carcinoma. The Oncologist 21, 787–788. https://doi.org/10.1634/theoncologist.2016-0145
Carneiro, B.A., Kaplan, J.B., Altman, J.K., Giles, F.J., Platanias, L.C., 2015. Targeting mTOR signaling pathways and related negative feedback loops for the treatment of acute myeloid leukemia. Cancer Biol. Ther. 16, 648–656. https://doi.org/10.1080/15384047.2015.1026510
Caron, M.-C., Sharma, A.K., O'Sullivan, J., Myler, L.R., Ferreira, M.T., Rodrigue, A., Coulombe, Y., Ethier, C., Gagné, J.-P., Langelier, M.-F., Pascal, J.M., Finkelstein, I.J., Hendzel, M.J., Poirier, G.G., Masson, J.-Y., 2019. Poly(ADP-ribose) polymerase-1 antagonizes DNA resection at double-strand breaks. Nat. Commun. 10. https://doi.org/10.1038/s41467-019-10741-9
Carracedo, A., Pandolfi, P.P., 2008. The PTEN-PI3K pathway: of feedbacks and cross-talks. Oncogene 27, 5527–5541. https://doi.org/10.1038/onc.2008.247
Carriere, A., Romeo, Y., Acosta-Jaquez, H.A., Moreau, J., Bonneil, E., Thibault, P., Fingar, D.C., Roux, P.P., 2011. ERK1/2 phosphorylate Raptor to promote Ras-dependent activation of mTOR complex 1 (mTORC1). J. Biol. Chem. 286, 567–577. https://doi.org/10.1074/jbc.M110.159046
Carter, J.L., Hege, K., Yang, J., Kalpage, H.A., Su, Y., Edwards, H., Hüttemann, M., Taub, J.W., Ge, Y., 2020. Targeting multiple signaling pathways: the new approach to acute myeloid leukemia therapy. Signal Transduct. Target. Ther. 5, 1–29. https://doi.org/10.1038/s41392-020-00361-x
Cen, B., Mahajan, S., Wang, W., Kraft, A.S., 2013. Elevation of receptor tyrosine kinases by small molecule AKT inhibitors in prostate cancer is mediated by Pim-1. Cancer Res. 73, 3402–3411. https://doi.org/10.1158/0008-5472.CAN-12-4619
Chakraborty, S., Shapiro, L.C., de Oliveira, S., Rivera-Pena, B., Verma, A., Shastri, A., 2021. Therapeutic targeting of the inflammasome in myeloid malignancies. Blood Cancer J. 11, 1–10. https://doi.org/10.1038/s41408-021-00547-8
Chang, F., Lee, J.T., Navolanic, P.M., Steelman, L.S., Shelton, J.G., Blalock, W.L., Franklin, R.A., McCubrey, J.A., 2003. Involvement of PI3K/Akt pathway in cell cycle progression, apoptosis, and neoplastic transformation: a target for cancer chemotherapy. Leukemia 17, 590–603. https://doi.org/10.1038/sj.leu.2402824
Chapuis, N., Tamburini, J., Cornillet-Lefebvre, P., Gillot, L., Bardet, V., Willems, L., Park, S., Green, A.S., Ifrah, N., Dreyfus, F., Mayeux, P., Lacombe, C., Bouscary, D., 2010a. Autocrine IGF-1/IGF-1R signaling is responsible for constitutive PI3K/Akt activation in acute myeloid leukemia: therapeutic value of neutralizing anti-IGF-1R antibody. Haematologica 95, 415–423. https://doi.org/10.3324/haematol.2009.010785
Chapuis, N., Tamburini, J., Green, A.S., Vignon, C., Bardet, V., Neyret, A., Pannetier, M., Willems, L., Park, S., Macone, A., Maira, S.-M., Ifrah, N., Dreyfus, F., Herault, O., Lacombe, C., Mayeux, P., Bouscary, D., 2010b. Dual Inhibition of PI3K and mTORC1/2 Signaling by NVP-BEZ235 as a New Therapeutic Strategy for Acute Myeloid Leukemia. Clin. Cancer Res. 16, 5424–5435. https://doi.org/10.1158/1078-0432.CCR-10-1102
Chatterjee, S., Browning, E.A., Hong, N., DeBolt, K., Sorokina, E.M., Liu, W., Birnbaum, M.J., Fisher, A.B., 2012. Membrane depolarization is the trigger for PI3K/Akt activation and leads to the generation of ROS. Am. J. Physiol. Heart Circ. Physiol. 302, H105-114. https://doi.org/10.1152/ajpheart.00298.2011
Chauhan, P.S., Ihsan, R., Singh, L.C., Gupta, D.K., Mittal, V., Kapur, S., 2013. Mutation of NPM1 and FLT3 Genes in Acute Myeloid Leukemia and Their Association with Clinical and Immunophenotypic Features. Dis. Markers 35, 581–588. https://doi.org/10.1155/2013/582569
Chávez-González, A., Dorantes-Acosta, E., Moreno-Lorenzana, D., Alvarado-Moreno, A., Arriaga-Pizano, L., Mayani, H., 2014. Expression of CD90, CD96, CD117, and CD123 on different hematopoietic cell populations from pediatric patients with acute myeloid leukemia. Arch. Med. Res. 45, 343–350. https://doi.org/10.1016/j.arcmed.2014.04.001
Chen, A., 2011. PARP inhibitors: its role in treatment of cancer. Chin. J. Cancer 30, 463–471. https://doi.org/10.5732/cjc.011.10111
Chen, C., Liu, Yu, Liu, R., Ikenoue, T., Guan, K.-L., Liu, Yang, Zheng, P., 2008. TSC-mTOR maintains quiescence and function of hematopoietic stem cells by repressing mitochondrial

biogenesis and reactive oxygen species. J. Exp. Med. 205, 2397–2408. https://doi.org/10.1084/jem.20081297
Chen, F., Ishikawa, Y., Akashi, A., Naoe, T., Kiyoi, H., 2016. Co-expression of wild-type FLT3 attenuates the inhibitory effect of FLT3 inhibitor on FLT3 mutated leukemia cells. Oncotarget 7, 47018–47032. https://doi.org/10.18632/oncotarget.10147
Chen, W., Drakos, E., Grammatikakis, I., Schlette, E.J., Li, J., Leventaki, V., Staikou-Drakopoulou, E., Patsouris, E., Panayiotidis, P., Medeiros, L.J., Rassidakis, G.Z., 2010. mTOR signaling is activated by FLT3 kinase and promotes survival of FLT3-mutated acute myeloid leukemia cells. Mol. Cancer 9, 292. https://doi.org/10.1186/1476-4598-9-292
Cheng, S.W.Y., Fryer, L.G.D., Carling, D., Shepherd, P.R., 2004. Thr2446 is a novel mammalian target of rapamycin (mTOR) phosphorylation site regulated by nutrient status. J. Biol. Chem. 279, 15719–15722. https://doi.org/10.1074/jbc.C300534200
Chiang, G.G., Abraham, R.T., 2005. Phosphorylation of mammalian target of rapamycin (mTOR) at Ser-2448 is mediated by p70S6 kinase. J. Biol. Chem. 280, 25485–25490. https://doi.org/10.1074/jbc.M501707200
Choe, S., Wang, H., DiNardo, C.D., Stein, E.M., de Botton, S., Roboz, G.J., Altman, J.K., Mims, A.S., Watts, J.M., Pollyea, D.A., Fathi, A.T., Tallman, M.S., Kantarjian, H.M., Stone, R.M., Quek, L., Konteatis, Z., Dang, L., Nicolay, B., Nejad, P., Liu, G., Zhang, V., Liu, H., Goldwasser, M., Liu, W., Marks, K., Bowden, C., Biller, S.A., Attar, E.C., Wu, B., 2020. Molecular mechanisms mediating relapse following ivosidenib monotherapy in IDH1-mutant relapsed or refractory AML. Blood Adv. 4, 1894–1905. https://doi.org/10.1182/bloodadvances.2020001503
Chopra, M., Bohlander, S.K., 2019. The cell of origin and the leukemia stem cell in acute myeloid leukemia. Genes. Chromosomes Cancer 58, 850–858. https://doi.org/10.1002/gcc.22805
Chou, T.-C., 2010. Drug combination studies and their synergy quantification using the Chou-Talalay method. Cancer Res. 70, 440–446. https://doi.org/10.1158/0008-5472.CAN-09-1947
Choudhary, C., Brandts, C., Schwable, J., Tickenbrock, L., Sargin, B., Ueker, A., Böhmer, F.-D., Berdel, W.E., Müller-Tidow, C., Serve, H., 2007. Activation mechanisms of STAT5 by oncogenic Flt3-ITD. Blood 110, 370–374. https://doi.org/10.1182/blood-2006-05-024018
Choudhary, G.S., Al-Harbi, S., Mazumder, S., Hill, B.T., Smith, M.R., Bodo, J., Hsi, E.D., Almasan, A., 2015. MCL-1 and BCL-xL-dependent resistance to the BCL-2 inhibitor ABT-199 can be overcome by preventing PI3K/AKT/mTOR activation in lymphoid malignancies. Cell Death Dis. 6, e1593. https://doi.org/10.1038/cddis.2014.525
Chow, S., Minden, M.D., Hedley, D.W., 2006. Constitutive phosphorylation of the S6 ribosomal protein via mTOR and ERK signaling in the peripheral blasts of acute leukemia patients. Exp. Hematol. 34, 1183–1191. https://doi.org/10.1016/j.exphem.2006.05.002
Chu, S.H., Heiser, D., Li, L., Kaplan, I., Collector, M., Huso, D., Sharkis, S.J., Civin, C., Small, D., 2012. FLT3-ITD knockin impairs hematopoietic stem cell quiescence/homeostasis, leading to myeloproliferative neoplasm. Cell Stem Cell 11, 346–358. https://doi.org/10.1016/j.stem.2012.05.027
Colon-Otero, G., Weroha, S.J., Foster, N.R., Haluska, P., Hou, X., Wahner-Hendrickson, A.E., Jatoi, A., Block, M.S., Dinh, T.A., Robertson, M.W., Copland, J.A., 2017. Phase 2 trial of everolimus and letrozole in relapsed estrogen receptor-positive high-grade ovarian cancers. Gynecol. Oncol. 146, 64–68. https://doi.org/10.1016/j.ygyno.2017.04.020
Confalone, E., D'Alessio, G., Furia, A., 2010. IL-6 Induction by TNFα and IL-1β in an Osteoblast-Like Cell Line. Int. J. Biomed. Sci. IJBS 6, 135–140.
Cooper, T.M., Sison, E.A.R., Baker, S.D., Li, L., Ahmed, A., Trippett, T., Gore, L., Macy, M.E., Narendran, A., August, K., Absalon, M.J., Boklan, J., Pollard, J., Magoon, D., Brown, P.A., 2017. A phase 1 study of the CXCR4 antagonist plerixafor in combination with high-dose cytarabine and etoposide in children with relapsed or refractory acute leukemias or myelodysplastic syndrome: A Pediatric Oncology Experimental Therapeutics Investigators' Consortium study (POE 10-03). Pediatr. Blood Cancer 64. https://doi.org/10.1002/pbc.26414
Cortes, J.E., Kantarjian, H., Foran, J.M., Ghirdaladze, D., Zodelava, M., Borthakur, G., Gammon, G., Trone, D., Armstrong, R.C., James, J., Levis, M., 2013. Phase I study of quizartinib

administered daily to patients with relapsed or refractory acute myeloid leukemia irrespective of FMS-like tyrosine kinase 3-internal tandem duplication status. J. Clin. Oncol. Off. J. Am. Soc. Clin. Oncol. 31, 3681–3687. https://doi.org/10.1200/JCO.2013.48.8783

Cortes, J.E., Khaled, S., Martinelli, G., Perl, A.E., Ganguly, S., Russell, N., Krämer, A., Dombret, H., Hogge, D., Jonas, B.A., Leung, A.Y.-H., Mehta, P., Montesinos, P., Radsak, M., Sica, S., Arunachalam, M., Holmes, M., Kobayashi, K., Namuyinga, R., Ge, N., Yver, A., Zhang, Y., Levis, M.J., 2019. Quizartinib versus salvage chemotherapy in relapsed or refractory FLT3-ITD acute myeloid leukaemia (QuANTUM-R): a multicentre, randomised, controlled, open-label, phase 3 trial. Lancet Oncol. 20, 984–997. https://doi.org/10.1016/S1470-2045(19)30150-0

Cortes, J.E., Tallman, M.S., Schiller, G.J., Trone, D., Gammon, G., Goldberg, S.L., Perl, A.E., Marie, J.-P., Martinelli, G., Kantarjian, H.M., Levis, M.J., 2018. Phase 2b study of 2 dosing regimens of quizartinib monotherapy in FLT3-ITD-mutated, relapsed or refractory AML. Blood 132, 598–607. https://doi.org/10.1182/blood-2018-01-821629

Cucchi, D.G.J., Groen, R.W.J., Janssen, J.J.W.M., Cloos, J., 2020. Ex vivo cultures and drug testing of primary acute myeloid leukemia samples: Current techniques and implications for experimental design and outcome. Drug Resist. Updat. 53, 100730. https://doi.org/10.1016/j.drup.2020.100730

Darici, S., Alkhaldi, H., Horne, G., Jørgensen, H.G., Marmiroli, S., Huang, X., 2020. Targeting PI3K/Akt/mTOR in AML: Rationale and Clinical Evidence. J. Clin. Med. 9, 2934. https://doi.org/10.3390/jcm9092934

Darici, S., Zavatti, M., Braglia, L., Accordi, B., Serafin, V., Horne, G.A., Manzoli, L., Palumbo, C., Huang, X., Jørgensen, H.G., Marmiroli, S., 2021. Synergistic cytotoxicity of dual PI3K/mTOR and FLT3 inhibition in FLT3-ITD AML cells. Adv. Biol. Regul. 82, 100830. https://doi.org/10.1016/j.jbior.2021.100830

Daver, N., Schlenk, R.F., Russell, N.H., Levis, M.J., 2019. Targeting FLT3 mutations in AML: review of current knowledge and evidence. Leukemia 33, 299–312. https://doi.org/10.1038/s41375-018-0357-9

Daver, N., Venugopal, S., Ravandi, F., 2021. FLT3 mutated acute myeloid leukemia: 2021 treatment algorithm. Blood Cancer J. 11, 1–9. https://doi.org/10.1038/s41408-021-00495-3

de Beauchamp, L., Himonas, E., Helgason, G.V., 2022. Mitochondrial metabolism as a potential therapeutic target in myeloid leukaemia. Leukemia 36, 1–12. https://doi.org/10.1038/s41375-021-01416-w

De Kouchkovsky, I., Abdul-Hay, M., 2016. “Acute myeloid leukemia: a comprehensive review and 2016 update.” Blood Cancer J. 6, e441. https://doi.org/10.1038/bcj.2016.50

De, P., Sun, Y., Carlson, J.H., Friedman, L.S., Leyland-Jones, B.R., Dey, N., 2014. Doubling down on the PI3K-AKT-mTOR pathway enhances the antitumor efficacy of PARP inhibitor in triple negative breast cancer model beyond BRCA-ness. Neoplasia N. Y. N 16, 43–72. https://doi.org/10.1593/neo.131694

Del Campo, J.M., Birrer, M., Davis, C., Fujiwara, K., Gollerkeri, A., Gore, M., Houk, B., Lau, S., Poveda, A., González-Martín, A., Muller, C., Muro, K., Pierce, K., Suzuki, M., Vermette, J., Oza, A., 2016. A randomized phase II non-comparative study of PF-04691502 and gedatolisib (PF-05212384) in patients with recurrent endometrial cancer. Gynecol. Oncol. 142, 62–69. https://doi.org/10.1016/j.ygyno.2016.04.019

Dellomo, A.J., Abbotts, R., Eberly, C.L., Karbowski, M., Baer, M.R., Kingsbury, T.J., Rassool, F.V., 2022. PARP1 PARylates and stabilizes STAT5 in FLT3-ITD acute myeloid leukemia and other STAT5-activated cancers. Transl. Oncol. 15, 101283. https://doi.org/10.1016/j.tranon.2021.101283

Deng, L., Jiang, L., Lin, X.-H., Tseng, K.-F., Liu, Y., Zhang, X., Dong, R.-H., Lu, Z.-G., Wang, X.-J., 2017. The PI3K/mTOR dual inhibitor BEZ235 suppresses proliferation and migration and reverses multidrug resistance in acute myeloid leukemia. Acta Pharmacol. Sin. 38, 382–391. https://doi.org/10.1038/aps.2016.121

Dengler, F., 2020. Activation of AMPK under Hypoxia: Many Roads Leading to Rome. Int. J. Mol. Sci. 21. https://doi.org/10.3390/ijms21072428

Deynoux, M., Sunter, N., Hérault, O., Mazurier, F., 2016. Hypoxia and Hypoxia-Inducible Factors in Leukemias. Front. Oncol. 6.

Dhami, S.P.S., Kappala, S.S., Thompson, A., Szegezdi, E., 2016. Three-dimensional ex vivo co-culture models of the leukaemic bone marrow niche for functional drug testing. Drug Discov. Today 21, 1464–1471. https://doi.org/10.1016/j.drudis.2016.04.019

Dias, S., Choy, M., Alitalo, K., Rafii, S., 2002. Vascular endothelial growth factor (VEGF)-C signaling through FLT-4 (VEGFR-3) mediates leukemic cell proliferation, survival, and resistance to chemotherapy. Blood 99, 2179–2184. https://doi.org/10.1182/blood.v99.6.2179

DiNardo, C.D., Garcia-Manero, G., Pierce, S., Nazha, A., Bueso-Ramos, C., Jabbour, E., Ravandi, F., Cortes, J., Kantarjian, H., 2016. Interactions and relevance of blast percentage and treatment strategy among younger and older patients with acute myeloid leukemia (AML) and myelodysplastic syndrome (MDS). Am. J. Hematol. 91, 227–232. https://doi.org/10.1002/ajh.24252

DiNardo, C.D., Pratz, K., Pullarkat, V., Jonas, B.A., Arellano, M., Becker, P.S., Frankfurt, O., Konopleva, M., Wei, A.H., Kantarjian, H.M., Xu, T., Hong, W.-J., Chyla, B., Potluri, J., Pollyea, D.A., Letai, A., 2019. Venetoclax combined with decitabine or azacitidine in treatment-naive, elderly patients with acute myeloid leukemia. Blood 133, 7–17. https://doi.org/10.1182/blood-2018-08-868752

DiNardo, C.D., Pratz, K.W., Letai, A., Jonas, B.A., Wei, A.H., Thirman, M., Arellano, M., Frattini, M.G., Kantarjian, H., Popovic, R., Chyla, B., Xu, T., Dunbar, M., Agarwal, S.K., Humerickhouse, R., Mabry, M., Potluri, J., Konopleva, M., Pollyea, D.A., 2018. Safety and preliminary efficacy of venetoclax with decitabine or azacitidine in elderly patients with previously untreated acute myeloid leukaemia: a non-randomised, open-label, phase 1b study. Lancet Oncol. 19, 216–228. https://doi.org/10.1016/S1470-2045(18)30010-X

Ding, L., Saunders, T.L., Enikolopov, G., Morrison, S.J., 2012. Endothelial and perivascular cells maintain haematopoietic stem cells. Nature 481, 457–462. https://doi.org/10.1038/nature10783

Ding, Q., Xia, W., Liu, J.-C., Yang, J.-Y., Lee, D.-F., Xia, J., Bartholomeusz, G., Li, Y., Pan, Y., Li, Z., Bargou, R.C., Qin, J., Lai, C.-C., Tsai, F.-J., Tsai, C.-H., Hung, M.-C., 2005. Erk associates with and primes GSK-3beta for its inactivation resulting in upregulation of beta-catenin. Mol. Cell 19, 159–170. https://doi.org/10.1016/j.molcel.2005.06.009

Döhner, H., Estey, E., Grimwade, D., Amadori, S., Appelbaum, F.R., Büchner, T., Dombret, H., Ebert, B.L., Fenaux, P., Larson, R.A., Levine, R.L., Lo-Coco, F., Naoe, T., Niederwieser, D., Ossenkoppele, G.J., Sanz, M., Sierra, J., Tallman, M.S., Tien, H.-F., Wei, A.H., Löwenberg, B., Bloomfield, C.D., 2017. Diagnosis and management of AML in adults: 2017 ELN recommendations from an international expert panel. Blood 129, 424–447. https://doi.org/10.1182/blood-2016-08-733196

Dong, F., Liu, X., Koning, J.P. de, Touw, I.P., Henninghausen, L., Larner, A., Grimley, P.M., 1998. Stimulation of Stat5 by Granulocyte Colony-Stimulating Factor (G-CSF) Is Modulated by Two Distinct Cytoplasmic Regions of the G-CSF Receptor. J. Immunol. 161, 6503–6509.

Dumas, P.-Y., Naudin, C., Martin-Lannerée, S., Izac, B., Casetti, L., Mansier, O., Rousseau, B., Artus, A., Dufossée, M., Giese, A., Dubus, P., Pigneux, A., Praloran, V., Bidet, A., Villacreces, A., Guitart, A., Milpied, N., Kosmider, O., Vigon, I., Desplat, V., Dusanter-Fourt, I., Pasquet, J.-M., 2019. Hematopoietic niche drives FLT3-ITD acute myeloid leukemia resistance to quizartinib via STAT5-and hypoxia-dependent upregulation of AXL. Haematologica 104, 2017–2027. https://doi.org/10.3324/haematol.2018.205385

Egea, L., Hirata, Y., Kagnoff, M.F., 2010. GM-CSF: a role in immune and inflammatory reactions in the intestine. Expert Rev. Gastroenterol. Hepatol. 4, 723–731. https://doi.org/10.1586/egh.10.73

Eguchi, M., Minami, Y., Kuzume, A., Chi, S., 2020. Mechanisms Underlying Resistance to FLT3 Inhibitors in Acute Myeloid Leukemia. Biomedicines 8, 245. https://doi.org/10.3390/biomedicines8080245

Ehninger, A., Trumpp, A., 2011. The bone marrow stem cell niche grows up: mesenchymal stem cells and macrophages move in. J. Exp. Med. 208, 421–428. https://doi.org/10.1084/jem.20110132

Emerson, S.G., 2007. Thrombopoietin, HSCs, and the osteoblast niche: holding on loosely, but not letting G0. Cell Stem Cell 1, 599–600. https://doi.org/10.1016/j.stem.2007.11.010

Eppert, K., Takenaka, K., Lechman, E.R., Waldron, L., Nilsson, B., van Galen, P., Metzeler, K.H., Poeppl, A., Ling, V., Beyene, J., Canty, A.J., Danska, J.S., Bohlander, S.K., Buske, C., Minden, M.D., Golub, T.R., Jurisica, I., Ebert, B.L., Dick, J.E., 2011. Stem cell gene expression programs influence clinical outcome in human leukemia. Nat. Med. 17, 1086–1093. https://doi.org/10.1038/nm.2415

Fan, J., Li, L., Small, D., Rassool, F., 2010. Cells expressing FLT3/ITD mutations exhibit elevated repair errors generated through alternative NHEJ pathways: implications for genomic instability and therapy. Blood 116, 5298–5305. https://doi.org/10.1182/blood-2010-03-272591

Fang, D.D., Zhang, C.C., Gu, Y., Jani, J.P., Cao, J., Tsaparikos, K., Yuan, J., Thiel, M., Jackson-Fisher, A., Zong, Q., Lappin, P.B., Hayashi, T., Schwab, R.B., Wong, A., John-Baptiste, A., Bagrodia, S., Los, G., Bender, S., Christensen, J., Vanarsdale, T., 2013. Antitumor Efficacy of the Dual PI3K/mTOR Inhibitor PF-04691502 in a Human Xenograft Tumor Model Derived from Colorectal Cancer Stem Cells Harboring a PIK3CA Mutation. PloS One 8, e67258. https://doi.org/10.1371/journal.pone.0067258

Feng, X., Lan, H., Ruan, Y., Li, C., 2018. Impact on acute myeloid leukemia relapse in granulocyte colony-stimulating factor application: a meta-analysis. Hematology 23, 581–589. https://doi.org/10.1080/10245332.2018.1446811

Fleetwood, A.J., Cook, A.D., Hamilton, J.A., 2005. Functions of granulocyte-macrophage colony-stimulating factor. Crit. Rev. Immunol. 25, 405–428. https://doi.org/10.1615/critrevimmunol.v25.i5.50

Fletcher, L., Joshi, S.K., Traer, E., 2020. Profile of Quizartinib for the Treatment of Adult Patients with Relapsed/Refractory FLT3-ITD-Positive Acute Myeloid Leukemia: Evidence to Date. Cancer Manag. Res. 12, 151–163. https://doi.org/10.2147/CMAR.S196568

Florian, S., Sonneck, K., Hauswirth, A.W., Krauth, M.-T., Schernthaner, G.-H., Sperr, W.R., Valent, P., 2006. Detection of molecular targets on the surface of CD34+/CD38-- stem cells in various myeloid malignancies. Leuk. Lymphoma 47, 207–222. https://doi.org/10.1080/10428190500272507

Fong, C.Y., Gilan, O., Lam, E.Y.N., Rubin, A.F., Ftouni, S., Tyler, D., Stanley, K., Sinha, D., Yeh, P., Morison, J., Giotopoulos, G., Lugo, D., Jeffrey, P., Lee, S.C.-W., Carpenter, C., Gregory, R., Ramsay, R.G., Lane, S.W., Abdel-Wahab, O., Kouzarides, T., Johnstone, R.W., Dawson, S.-J., Huntly, B.J.P., Prinjha, R.K., Papenfuss, A.T., Dawson, M.A., 2015. BET inhibitor resistance emerges from leukaemia stem cells. Nature 525, 538–542. https://doi.org/10.1038/nature14888

Forte, D., García-Fernández, M., Sánchez-Aguilera, A., Stavropoulou, V., Fielding, C., Martín-Pérez, D., López, J.A., Costa, A.S.H., Tronci, L., Nikitopoulou, E., Barber, M., Gallipoli, P., Marando, L., Fernández de Castillejo, C.L., Tzankov, A., Dietmann, S., Cavo, M., Catani, L., Curti, A., Vázquez, J., Frezza, C., Huntly, B.J., Schwaller, J., Méndez-Ferrer, S., 2020. Bone Marrow Mesenchymal Stem Cells Support Acute Myeloid Leukemia Bioenergetics and Enhance Antioxidant Defense and Escape from Chemotherapy. Cell Metab. 32, 829-843.e9. https://doi.org/10.1016/j.cmet.2020.09.001

Fransecky, L., Mochmann, L.H., Baldus, C.D., 2015. Outlook on PI3K/AKT/mTOR inhibition in acute leukemia. Mol. Cell. Ther. 3, 2. https://doi.org/10.1186/s40591-015-0040-8

Friedman, R., 2022. The molecular mechanisms behind activation of FLT3 in acute myeloid leukemia and resistance to therapy by selective inhibitors. Biochim. Biophys. Acta BBA - Rev. Cancer 1877, 188666. https://doi.org/10.1016/j.bbcan.2021.188666

Fruman, D.A., Rommel, C., 2014. PI3K and cancer: lessons, challenges and opportunities. Nat. Rev. Drug Discov. 13, 140–156. https://doi.org/10.1038/nrd4204

Fuchs, A., Cella, M., Giurisato, E., Shaw, A.S., Colonna, M., 2004. Cutting Edge: CD96 (Tactile) Promotes NK Cell-Target Cell Adhesion by Interacting with the Poliovirus Receptor (CD155). J. Immunol. 172, 3994–3998. https://doi.org/10.4049/jimmunol.172.7.3994

Gafencu, G.A., Tomuleasa, C.I., Ghiaur, G., 2017. PARP inhibitors in acute myeloid leukaemia therapy: How a synthetic lethality approach can be a valid therapeutic alternative. Med. Hypotheses 104, 30–34. https://doi.org/10.1016/j.mehy.2017.05.015

Galán-Díez, M., Cuesta-Domínguez, Á., Kousteni, S., 2018. The Bone Marrow Microenvironment in Health and Myeloid Malignancy. Cold Spring Harb. Perspect. Med. 8, a031328. https://doi.org/10.1101/cshperspect.a031328

Galán-Díez, M., Kousteni, S., 2017. The osteoblastic niche in hematopoiesis and hematological myeloid malignancies. Curr. Mol. Biol. Rep. 3, 53–62. https://doi.org/10.1007/s40610-017-0055-9

Gallay, N., Dos Santos, C., Cuzin, L., Bousquet, M., Simmonet Gouy, V., Chaussade, C., Attal, M., Payrastre, B., Demur, C., Récher, C., 2009. The level of AKT phosphorylation on threonine 308 but not on serine 473 is associated with high-risk cytogenetics and predicts poor overall survival in acute myeloid leukaemia. Leukemia 23, 1029–1038. https://doi.org/10.1038/leu.2008.395

Gao, Y., Gao, J., Li, M., Zheng, Y., Wang, Y., Zhang, H., Wang, W., Chu, Y., Wang, X., Xu, M., Cheng, T., Ju, Z., Yuan, W., 2016. Rheb1 promotes tumor progression through mTORC1 in MLL-AF9-initiated murine acute myeloid leukemia. J. Hematol. Oncol.J Hematol Oncol 9, 36. https://doi.org/10.1186/s13045-016-0264-3

Gao, Y.-Y., Hu, L.-S., Han, H.-J., Song, C.-Y., Huang, Y.-X., Guo, K.-Y., 2013. [NVP-BEZ235 inhibits proliferation and colony-forming capability of CD34(+)CD38(-) human acute myeloid leukemia stem cells]. Zhongguo Shi Yan Xue Ye Xue Za Zhi 21, 334–338. https://doi.org/10.7534/j.issn.1009-2137.2013.02.015

Gardin, C., Dombret, H., 2017. Hypomethylating Agents as a Therapy for AML. Curr. Hematol. Malig. Rep. 12, 1–10. https://doi.org/10.1007/s11899-017-0363-4

Garrido, S.M., Appelbaum, F.R., Willman, C.L., Banker, D.E., 2001. Acute myeloid leukemia cells are protected from spontaneous and drug-induced apoptosis by direct contact with a human bone marrow stromal cell line (HS-5). Exp. Hematol. 29, 448–457. https://doi.org/10.1016/s0301-472x(01)00612-9

Gaymes, T.J., Shall, S., MacPherson, L.J., Twine, N.A., Lea, N.C., Farzaneh, F., Mufti, G.J., 2009. Inhibitors of poly ADP-ribose polymerase (PARP) induce apoptosis of myeloid leukemic cells: potential for therapy of myeloid leukemia and myelodysplastic syndromes. Haematologica 94, 638–646. https://doi.org/10.3324/haematol.2008.001933

Gebru, M.T., Wang, H.-G., 2020. Therapeutic targeting of FLT3 and associated drug resistance in acute myeloid leukemia. J. Hematol. Oncol.J Hematol Oncol 13, 155. https://doi.org/10.1186/s13045-020-00992-1

Georgiev, H., Ravens, I., Papadogianni, G., Bernhardt, G., 2018. Coming of Age: CD96 Emerges as Modulator of Immune Responses. Front. Immunol. 9.

Ghiaur, G., Levis, M., 2017. Mechanisms of Resistance to FLT3 Inhibitors and the Role of the Bone Marrow Microenvironment. Hematol. Oncol. Clin. North Am. 31, 681–692. https://doi.org/10.1016/j.hoc.2017.04.005

Ghosh, J., Kapur, R., 2017. Role of mTORC1-S6K1 signaling pathway in regulation of hematopoietic stem cell and acute myeloid leukemia. Exp. Hematol. 50, 13–21. https://doi.org/10.1016/j.exphem.2017.02.004

Ghosh, J., Kapur, R., 2016. Regulation of Hematopoietic Stem Cell Self-Renewal and Leukemia Maintenance by the PI3K-mTORC1 Pathway. Curr. Stem Cell Rep. 2, 368–378. https://doi.org/10.1007/s40778-016-0067-z

Ghosh, J., Kobayashi, M., Ramdas, B., Chatterjee, A., Ma, P., Mali, R.S., Carlesso, N., Liu, Y., Plas, D.R., Chan, R.J., Kapur, R., 2016. S6K1 regulates hematopoietic stem cell self-renewal and leukemia maintenance. J. Clin. Invest. 126, 2621–2625. https://doi.org/10.1172/JCI84565

Gibbons, J.J., Abraham, R.T., Yu, K., 2009. Mammalian target of rapamycin: discovery of rapamycin reveals a signaling pathway important for normal and cancer cell growth. Semin. Oncol. 36 Suppl 3, S3–S17. https://doi.org/10.1053/j.seminoncol.2009.10.011

Gilliland, D.G., Griffin, J.D., 2002. The roles of FLT3 in hematopoiesis and leukemia. Blood 100, 1532–1542. https://doi.org/10.1182/blood-2002-02-0492

Gingras, A.C., Gygi, S.P., Raught, B., Polakiewicz, R.D., Abraham, R.T., Hoekstra, M.F., Aebersold, R., Sonenberg, N., 1999. Regulation of 4E-BP1 phosphorylation: a novel two-step mechanism. Genes Dev. 13, 1422–1437. https://doi.org/10.1101/gad.13.11.1422

Goardon, N., Marchi, E., Atzberger, A., Quek, L., Schuh, A., Soneji, S., Woll, P., Mead, A., Alford, K.A., Rout, R., Chaudhury, S., Gilkes, A., Knapper, S., Beldjord, K., Begum, S., Rose, S., Geddes, N., Griffiths, M., Standen, G., Sternberg, A., Cavenagh, J., Hunter, H., Bowen, D., Killick, S., Robinson, L., Price, A., Macintyre, E., Virgo, P., Burnett, A., Craddock, C., Enver, T., Jacobsen, S.E.W., Porcher, C., Vyas, P., 2011. Coexistence of LMPP-like and GMP-like leukemia stem cells in acute myeloid leukemia. Cancer Cell 19, 138–152. https://doi.org/10.1016/j.ccr.2010.12.012

Gonçalves Silva, I., Rüegg, L., Gibbs, B.F., Bardelli, M., Fruehwirth, A., Varani, L., Berger, S.M., Fasler-Kan, E., Sumbayev, V.V., 2016. The immune receptor Tim-3 acts as a trafficker in a Tim-3/galectin-9 autocrine loop in human myeloid leukemia cells. Oncoimmunology 5, e1195535. https://doi.org/10.1080/2162402X.2016.1195535

González-Billalabeitia, E., Seitzer, N., Song, S.J., Song, M.S., Patnaik, A., Liu, X.-S., Epping, M.T., Papa, A., Hobbs, R.M., Chen, M., Lunardi, A., Ng, C., Webster, K.A., Signoretti, S., Loda, M., Asara, J.M., Nardella, C., Clohessy, J.G., Cantley, L.C., Pandolfi, P.P., 2014. Vulnerabilities of PTEN-TP53-deficient prostate cancers to compound PARP-PI3K inhibition. Cancer Discov. 4, 896–904. https://doi.org/10.1158/2159-8290.CD-13-0230

Gopal, A., Graf, S., 2016. Idelalisib for the treatment of non-Hodgkin lymphoma. Expert Opin. Pharmacother. 17, 265–274. https://doi.org/10.1517/14656566.2016.1135130

Grafone, T., Palmisano, M., Nicci, C., Storti, S., 2012. An overview on the role of FLT3-tyrosine kinase receptor in acute myeloid leukemia: biology and treatment. Oncol. Rev. 6, e8. https://doi.org/10.4081/oncol.2012.e8

Grandage, V.L., Gale, R.E., Linch, D.C., Khwaja, A., 2005. PI3-kinase/Akt is constitutively active in primary acute myeloid leukaemia cells and regulates survival and chemoresistance via NF-kappaB, Mapkinase and p53 pathways. Leukemia 19, 586–594. https://doi.org/10.1038/sj.leu.2403653

Grauers Wiktorin, H., Aydin, E., Christenson, K., Issdisai, N., Thorén, F.B., Hellstrand, K., Martner, A., 2021. Impact of IL-1β and the IL-1R antagonist on relapse risk and survival in AML patients undergoing immunotherapy for remission maintenance. OncoImmunology 10, 1944538. https://doi.org/10.1080/2162402X.2021.1944538

Green, A.S., Maciel, T.T., Hospital, M.-A., Yin, C., Mazed, F., Townsend, E.C., Pilorge, S., Lambert, M., Paubelle, E., Jacquel, A., Zylbersztejn, F., Decroocq, J., Poulain, L., Sujobert, P., Jacque, N., Adam, K., So, J.C.C., Kosmider, O., Auberger, P., Hermine, O., Weinstock, D.M., Lacombe, C., Mayeux, P., Vanasse, G.J., Leung, A.Y., Moura, I.C., Bouscary, D., Tamburini, J., 2015. Pim kinases modulate resistance to FLT3 tyrosine kinase inhibitors in FLT3-ITD acute myeloid leukemia. Sci. Adv. 1, e1500221. https://doi.org/10.1126/sciadv.1500221

Gregory, M.A., D'Alessandro, A., Alvarez-Calderon, F., Kim, J., Nemkov, T., Adane, B., Rozhok, A.I., Kumar, A., Kumar, V., Pollyea, D.A., Wempe, M.F., Jordan, C.T., Serkova, N.J., Tan, A.C., Hansen, K.C., DeGregori, J., 2016. ATM/G6PD-driven redox metabolism promotes FLT3 inhibitor resistance in acute myeloid leukemia. Proc. Natl. Acad. Sci. U. S. A. 113, E6669–E6678. https://doi.org/10.1073/pnas.1603876113

Griessinger, E., Anjos-Afonso, F., Pizzitola, I., Rouault-Pierre, K., Vargaftig, J., Taussig, D., Gribben, J., Lassailly, F., Bonnet, D., 2014. A niche-like culture system allowing the maintenance of primary human acute myeloid leukemia-initiating cells: a new tool to decipher their chemoresistance and self-renewal mechanisms. Stem Cells Transl. Med. 3, 520–529. https://doi.org/10.5966/sctm.2013-0166

Griessinger, E., Anjos-Afonso, F., Vargaftig, J., Taussig, D.C., Lassailly, F., Prebet, T., Imbert, V., Nebout, M., Vey, N., Chabannon, C., Filby, A., Bollet-Quivogne, F., Gribben, J.G., Peyron, J.-F., Bonnet, D., 2016. Frequency and Dynamics of Leukemia-Initiating Cells during Short-term Ex Vivo Culture Informs Outcomes in Acute Myeloid Leukemia Patients. Cancer Res. 76, 2082–2086. https://doi.org/10.1158/0008-5472.CAN-15-2063

Grignani, G., Palmerini, E., Ferraresi, V., D'Ambrosio, L., Bertulli, R., Asaftei, S.D., Tamburini, A., Pignochino, Y., Sangiolo, D., Marchesi, E., Capozzi, F., Biagini, R., Gambarotti, M., Fagioli, F., Casali, P.G., Picci, P., Ferrari, S., Aglietta, M., Italian Sarcoma Group, 2015. Sorafenib and everolimus for patients with unresectable high-grade osteosarcoma progressing after

standard treatment: a non-randomised phase 2 clinical trial. Lancet Oncol. 16, 98–107. https://doi.org/10.1016/S1470-2045(14)71136-2
Gunawardane, R.N., Nepomuceno, R.R., Rooks, A.M., Hunt, J.P., Ricono, J.M., Belli, B., Armstrong, R.C., 2013. Transient exposure to quizartinib mediates sustained inhibition of FLT3 signaling while specifically inducing apoptosis in FLT3-activated leukemia cells. Mol. Cancer Ther. 12, 438–447. https://doi.org/10.1158/1535-7163.MCT-12-0305
Gupta, M., Ansell, S.M., Novak, A.J., Kumar, S., Kaufmann, S.H., Witzig, T.E., 2009. Inhibition of histone deacetylase overcomes rapamycin-mediated resistance in diffuse large B-cell lymphoma by inhibiting Akt signaling through mTORC2. Blood 114, 2926–2935. https://doi.org/10.1182/blood-2009-05-220889
Gurska, L., Ames, K., Gritsman, K., 2019. Signaling Pathways in Leukemic Stem Cells. Adv. Exp. Med. Biol. 1143, 1–39. https://doi.org/10.1007/978-981-13-7342-8_1
Gutjahr, J.C., Bayer, E., Yu, X., Laufer, J.M., Höpner, J.P., Tesanovic, S., Härzschel, A., Auer, G., Rieß, T., Salmhofer, A., Szenes, E., Haslauer, T., Durand-Onayli, V., Ramspacher, A., Pennisi, S.P., Artinger, M., Zaborsky, N., Chigaev, A., Aberger, F., Neureiter, D., Pleyer, L., Legler, D.F., Orian-Rousseau, V., Greil, R., Hartmann, T.N., 2021. CD44 engagement enhances acute myeloid leukemia cell adhesion to the bone marrow microenvironment by increasing VLA-4 avidity. Haematologica 106, 2102–2113. https://doi.org/10.3324/haematol.2019.231944
Guzman, M.L., Neering, S.J., Upchurch, D., Grimes, B., Howard, D.S., Rizzieri, D.A., Luger, S.M., Jordan, C.T., 2001. Nuclear factor-kappaB is constitutively activated in primitive human acute myelogenous leukemia cells. Blood 98, 2301–2307. https://doi.org/10.1182/blood.v98.8.2301
Guzman, M.L., Swiderski, C.F., Howard, D.S., Grimes, B.A., Rossi, R.M., Szilvassy, S.J., Jordan, C.T., 2002. Preferential induction of apoptosis for primary human leukemic stem cells. Proc. Natl. Acad. Sci. U. S. A. 99, 16220–16225. https://doi.org/10.1073/pnas.252462599
Gwinn, D.M., Shackelford, D.B., Egan, D.F., Mihaylova, M.M., Mery, A., Vasquez, D.S., Turk, B.E., Shaw, R.J., 2008. AMPK phosphorylation of raptor mediates a metabolic checkpoint. Mol. Cell 30, 214–226. https://doi.org/10.1016/j.molcel.2008.03.003
Han, G., Chen, G., Shen, B., Li, Y., 2013. Tim-3: an activation marker and activation limiter of innate immune cells. Front. Immunol. 4, 449. https://doi.org/10.3389/fimmu.2013.00449
Han, J.W., Pearson, R.B., Dennis, P.B., Thomas, G., 1995. Rapamycin, wortmannin, and the methylxanthine SQ20006 inactivate p70s6k by inducing dephosphorylation of the same subset of sites. J. Biol. Chem. 270, 21396–21403. https://doi.org/10.1074/jbc.270.36.21396
Hanekamp, D., Cloos, J., Schuurhuis, G.J., 2017. Leukemic stem cells: identification and clinical application. Int. J. Hematol. 105, 549–557. https://doi.org/10.1007/s12185-017-2221-5
Hanker, A.B., Kaklamani, V., Arteaga, C.L., 2019. Challenges for the Clinical Development of PI3K Inhibitors: Strategies to Improve Their Impact in Solid Tumors. Cancer Discov. 9, 482–491. https://doi.org/10.1158/2159-8290.CD-18-1175
Hardie, D.G., 2005. New roles for the LKB1-->AMPK pathway. Curr. Opin. Cell Biol. 17, 167–173. https://doi.org/10.1016/j.ceb.2005.01.006
Harris, W.J., Huang, X., Lynch, J.T., Spencer, G.J., Hitchin, J.R., Li, Y., Ciceri, F., Blaser, J.G., Greystoke, B.F., Jordan, A.M., Miller, C.J., Ogilvie, D.J., Somervaille, T.C.P., 2012. The histone demethylase KDM1A sustains the oncogenic potential of MLL-AF9 leukemia stem cells. Cancer Cell 21, 473–487. https://doi.org/10.1016/j.ccr.2012.03.014
Hassan, N., Yang, J., Wang, J.Y., 2020. An Improved Protocol for Establishment of AML Patient-Derived Xenograft Models. STAR Protoc. 1, 100156. https://doi.org/10.1016/j.xpro.2020.100156
Hasskarl, J., 2018. Everolimus. Recent Results Cancer Res. Fortschritte Krebsforsch. Progres Dans Rech. Sur Cancer 211, 101–123. https://doi.org/10.1007/978-3-319-91442-8_8
Hata, A.N., Engelman, J.A., Faber, A.C., 2015. The BCL-2 family: key mediators of the apoptotic response to targeted anti-cancer therapeutics. Cancer Discov. 5, 475–487. https://doi.org/10.1158/2159-8290.CD-15-0011
Haubner, S., Perna, F., Köhnke, T., Schmidt, C., Berman, S., Augsberger, C., Schnorfeil, F.M., Krupka, C., Lichtenegger, F.S., Liu, X., Kerbs, P., Schneider, S., Metzeler, K.H., Spiekermann, K., Hiddemann, W., Greif, P.A., Herold, T., Sadelain, M., Subklewe, M.,

2019. Coexpression profile of leukemic stem cell markers for combinatorial targeted therapy in AML. Leukemia 33, 64–74. https://doi.org/10.1038/s41375-018-0180-3
Hawley, S.A., Davison, M., Woods, A., Davies, S.P., Beri, R.K., Carling, D., Hardie, D.G., 1996. Characterization of the AMP-activated protein kinase kinase from rat liver and identification of threonine 172 as the major site at which it phosphorylates AMP-activated protein kinase. J. Biol. Chem. 271, 27879–27887. https://doi.org/10.1074/jbc.271.44.27879
Hayakawa, F., Towatari, M., Kiyoi, H., Tanimoto, M., Kitamura, T., Saito, H., Naoe, T., 2000. Tandem-duplicated Flt3 constitutively activates STAT5 and MAP kinase and introduces autonomous cell growth in IL-3-dependent cell lines. Oncogene 19, 624–631. https://doi.org/10.1038/sj.onc.1203354
Hayden, M.S., Ghosh, S., 2014. Regulation of NF-κB by TNF Family Cytokines. Semin. Immunol. 26, 253–266. https://doi.org/10.1016/j.smim.2014.05.004
Hazen, A.L., Smith, M.J., Desponts, C., Winter, O., Moser, K., Kerr, W.G., 2009. SHIP is required for a functional hematopoietic stem cell niche. Blood 113, 2924–2933. https://doi.org/10.1182/blood-2008-02-138008
Hemmings, B.A., Restuccia, D.F., 2012. PI3K-PKB/Akt pathway. Cold Spring Harb. Perspect. Biol. 4, a011189. https://doi.org/10.1101/cshperspect.a011189
Ho, T.-C., LaMere, M., Stevens, B.M., Ashton, J.M., Myers, J.R., O'Dwyer, K.M., Liesveld, J.L., Mendler, J.H., Guzman, M., Morrissette, J.D., Zhao, J., Wang, E.S., Wetzler, M., Jordan, C.T., Becker, M.W., 2016. Evolution of acute myelogenous leukemia stem cell properties after treatment and progression. Blood 128, 1671–1678. https://doi.org/10.1182/blood-2016-02-695312
Hoang, T., Levy, B., Onetto, N., Haman, A., Rodriguez-Cimadevilla, J.C., 1989. Tumor necrosis factor alpha stimulates the growth of the clonogenic cells of acute myeloblastic leukemia in synergy with granulocyte/macrophage colony-stimulating factor. J. Exp. Med. 170, 15–26. https://doi.org/10.1084/jem.170.1.15
Hole, P.S., Zabkiewicz, J., Munje, C., Newton, Z., Pearn, L., White, P., Marquez, N., Hills, R.K., Burnett, A.K., Tonks, A., Darley, R.L., 2013. Overproduction of NOX-derived ROS in AML promotes proliferation and is associated with defective oxidative stress signaling. Blood 122, 3322–3330. https://doi.org/10.1182/blood-2013-04-491944
Holz, M.K., Blenis, J., 2005. Identification of S6 kinase 1 as a novel mammalian target of rapamycin (mTOR)-phosphorylating kinase. J. Biol. Chem. 280, 26089–26093. https://doi.org/10.1074/jbc.M504045200
Horton, S.J., Huntly, B.J.P., 2012. Recent advances in acute myeloid leukemia stem cell biology. Haematologica 97, 966–974. https://doi.org/10.3324/haematol.2011.054734
Hosen, N., Park, C.Y., Tatsumi, N., Oji, Y., Sugiyama, H., Gramatzki, M., Krensky, A.M., Weissman, I.L., 2007. CD96 is a leukemic stem cell-specific marker in human acute myeloid leukemia. Proc. Natl. Acad. Sci. U. S. A. 104, 11008–11013. https://doi.org/10.1073/pnas.0704271104
Hou, H.-A., Tien, H.-F., 2020. Genomic landscape in acute myeloid leukemia and its implications in risk classification and targeted therapies. J. Biomed. Sci. 27. https://doi.org/10.1186/s12929-020-00674-7
Houshmand, M., Blanco, T.M., Circosta, P., Yazdi, N., Kazemi, A., Saglio, G., Zarif, M.N., 2019. Bone marrow microenvironment: The guardian of leukemia stem cells. World J. Stem Cells 11, 476–490. https://doi.org/10.4252/wjsc.v11.i8.476
Huang, D.C., Strasser, A., 2000. BH3-Only proteins-essential initiators of apoptotic cell death. Cell 103, 839–842. https://doi.org/10.1016/s0092-8674(00)00187-2
Huang, J., Manning, B.D., 2008. The TSC1-TSC2 complex: a molecular switchboard controlling cell growth. Biochem. J. 412, 179–190. https://doi.org/10.1042/BJ20080281
Huang, J.-C., Cui, Z.-F., Chen, S.-M., Yang, L.-J., Lian, H.-K., Liu, B., Su, Z.-H., Liu, J.-S., Wang, M., Hu, Z.-B., Ouyang, J.-Y., Li, Q.-C., Lu, H., 2018. NVP-BEZ235 synergizes cisplatin sensitivity in osteosarcoma. Oncotarget 9, 10483–10496. https://doi.org/10.18632/oncotarget.23711
Huang, T.-T., Lampert, E.J., Coots, C., Lee, J.-M., 2020. Targeting the PI3K pathway and DNA damage response as a therapeutic strategy in ovarian cancer. Cancer Treat. Rev. 86, 102021. https://doi.org/10.1016/j.ctrv.2020.102021

Huang, X., Wullschleger, S., Shpiro, N., McGuire, V.A., Sakamoto, K., Woods, Y.L., McBurnie, W., Fleming, S., Alessi, D.R., 2008. Important role of the LKB1-AMPK pathway in suppressing tumorigenesis in PTEN-deficient mice. Biochem. J. 412, 211–221. https://doi.org/10.1042/BJ20080557

Humphrey, S.J., Yang, G., Yang, P., Fazakerley, D.J., Stöckli, J., Yang, J.Y., James, D.E., 2013. Dynamic adipocyte phosphoproteome reveals that Akt directly regulates mTORC2. Cell Metab. 17, 1009–1020. https://doi.org/10.1016/j.cmet.2013.04.010

Hutchinson, J.A., Shanware, N.P., Chang, H., Tibbetts, R.S., 2011. Regulation of Ribosomal Protein S6 Phosphorylation by Casein Kinase 1 and Protein Phosphatase 1. J. Biol. Chem. 286, 8688–8696. https://doi.org/10.1074/jbc.M110.141754

Ibrahim, Y.H., García-García, C., Serra, V., He, L., Torres-Lockhart, K., Prat, A., Anton, P., Cozar, P., Guzmán, M., Grueso, J., Rodríguez, O., Calvo, M.T., Aura, C., Díez, O., Rubio, I.T., Pérez, J., Rodón, J., Cortés, J., Ellisen, L.W., Scaltriti, M., Baselga, J., 2012. PI3K inhibition impairs BRCA1/2 expression and sensitizes BRCA-proficient triple-negative breast cancer to PARP inhibition. Cancer Discov. 2, 1036–1047. https://doi.org/10.1158/2159-8290.CD-11-0348

Iezzi, A., Caiola, E., Broggini, M., 2016. Activity of Pan-Class I Isoform PI3K/mTOR Inhibitor PF-05212384 in Combination with Crizotinib in Ovarian Cancer Xenografts and PDX. Transl. Oncol. 9, 458–465. https://doi.org/10.1016/j.tranon.2016.08.011

Imrali, A., Mao, X., Yeste-Velasco, M., Shamash, J., Lu, Y., 2016. Rapamycin inhibits prostate cancer cell growth through cyclin D1 and enhances the cytotoxic efficacy of cisplatin. Am. J. Cancer Res. 6, 1772–1784.

Inoki, K., Zhu, T., Guan, K.-L., 2003. TSC2 mediates cellular energy response to control cell growth and survival. Cell 115, 577–590. https://doi.org/10.1016/s0092-8674(03)00929-2

Itkin, T., Gur-Cohen, S., Spencer, J.A., Schajnovitz, A., Ramasamy, S.K., Kusumbe, A.P., Ledergor, G., Jung, Y., Milo, I., Poulos, M.G., Kalinkovich, A., Ludin, A., Kollet, O., Shakhar, G., Butler, J.M., Rafii, S., Adams, R.H., Scadden, D.T., Lin, C.P., Lapidot, T., 2016. Distinct bone marrow blood vessels differentially regulate hematopoiesis. Nature 532, 323–328. https://doi.org/10.1038/nature17624

Ivanivska, T.S., Sklyarenko, L.M., Zavelevich, M.P., Philchenkov, A.A., Koval, S.V., Polishchuk, A.S., Gluzman, D.F., 2019. Immunophenotypic features of leukemic stem cells and bulk of blasts in acute myeloid leukemia. Exp. Oncol. 41, 207–209. https://doi.org/10.32471/exp-oncology.2312-8852.vol-41-no-3.13492

Jacamo, R., Chen, Y., Wang, Z., Ma, W., Zhang, M., Spaeth, E.L., Wang, Y., Battula, V.L., Mak, P.Y., Schallmoser, K., Ruvolo, P., Schober, W.D., Shpall, E.J., Nguyen, M.H., Strunk, D., Bueso-Ramos, C.E., Konoplev, S., Davis, R.E., Konopleva, M., Andreeff, M., 2014. Reciprocal leukemia-stroma VCAM-1/VLA-4-dependent activation of NF-κB mediates chemoresistance. Blood 123, 2691–2702. https://doi.org/10.1182/blood-2013-06-511527

Jackson, R.J., Hellen, C.U.T., Pestova, T.V., 2010. The mechanism of eukaryotic translation initiation and principles of its regulation. Nat. Rev. Mol. Cell Biol. 11, 113–127. https://doi.org/10.1038/nrm2838

Jain, N., Curran, E., Iyengar, N.M., Diaz-Flores, E., Kunnavakkam, R., Popplewell, L., Kirschbaum, M.H., Karrison, T., Erba, H.P., Green, M., Poire, X., Koval, G., Shannon, K., Reddy, P.L., Joseph, L., Atallah, E.L., Dy, P., Thomas, S.P., Smith, S.E., Doyle, L.A., Stadler, W.M., Larson, R.A., Stock, W., Odenike, O., 2014. Phase II Study of the Oral Mek Inhibitor Selumetinib in Advanced Acute Myeloid Leukemia (AML): A University of Chicago Phase II Consortium Trial. Clin. Cancer Res. Off. J. Am. Assoc. Cancer Res. 20, 490–498. https://doi.org/10.1158/1078-0432.CCR-13-1311

Jan, M., Chao, M.P., Cha, A.C., Alizadeh, A.A., Gentles, A.J., Weissman, I.L., Majeti, R., 2011. Prospective separation of normal and leukemic stem cells based on differential expression of TIM3, a human acute myeloid leukemia stem cell marker. Proc. Natl. Acad. Sci. U. S. A. 108, 5009–5014. https://doi.org/10.1073/pnas.1100551108

Javidi-Sharifi, N., Martinez, J., English, I., Joshi, S.K., Scopim-Ribeiro, R., Viola, S.K., Edwards, D.K., Agarwal, A., Lopez, C., Jorgens, D., Tyner, J.W., Druker, B.J., Traer, E., 2019. FGF2-FGFR1 signaling regulates release of Leukemia-Protective exosomes from bone marrow stromal cells. eLife 8, e40033. https://doi.org/10.7554/eLife.40033

Jayavelu, A.K., Moloney, J.N., Böhmer, F.-D., Cotter, T.G., 2016. NOX-driven ROS formation in cell transformation of FLT3-ITD-positive AML. Exp. Hematol. 44, 1113–1122. https://doi.org/10.1016/j.exphem.2016.08.008

Jin, L., Hope, K.J., Zhai, Q., Smadja-Joffe, F., Dick, J.E., 2006. Targeting of CD44 eradicates human acute myeloid leukemic stem cells. Nat. Med. 12, 1167–1174. https://doi.org/10.1038/nm1483

Jin, L., Jin, M.-H., Nam, A.-R., Park, J.-E., Bang, J.-H., Oh, D.-Y., Bang, Y.-J., 2017. Anti-tumor effects of NVP-BKM120 alone or in combination with MEK162 in biliary tract cancer. Cancer Lett. 411, 162–170. https://doi.org/10.1016/j.canlet.2017.10.002

Jin, L., Lee, E.M., Ramshaw, H.S., Busfield, S.J., Peoppl, A.G., Wilkinson, L., Guthridge, M.A., Thomas, D., Barry, E.F., Boyd, A., Gearing, D.P., Vairo, G., Lopez, A.F., Dick, J.E., Lock, R.B., 2009. Monoclonal antibody-mediated targeting of CD123, IL-3 receptor alpha chain, eliminates human acute myeloid leukemic stem cells. Cell Stem Cell 5, 31–42. https://doi.org/10.1016/j.stem.2009.04.018

Jones, C.L., Stevens, B.M., D'Alessandro, A., Culp-Hill, R., Reisz, J.A., Pei, S., Gustafson, A., Khan, N., DeGregori, J., Pollyea, D.A., Jordan, C.T., 2019. Cysteine depletion targets leukemia stem cells through inhibition of electron transport complex II. Blood 134, 389–394. https://doi.org/10.1182/blood.2019898114

Jordan, C.T., Upchurch, D., Szilvassy, S.J., Guzman, M.L., Howard, D.S., Pettigrew, A.L., Meyerrose, T., Rossi, R., Grimes, B., Rizzieri, D.A., Luger, S.M., Phillips, G.L., 2000. The interleukin-3 receptor alpha chain is a unique marker for human acute myelogenous leukemia stem cells. Leukemia 14, 1777–1784. https://doi.org/10.1038/sj.leu.2401903

Jung, N., Dai, B., Gentles, A.J., Majeti, R., Feinberg, A.P., 2015. An LSC epigenetic signature is largely mutation independent and implicates the HOXA cluster in AML pathogenesis. Nat. Commun. 6, 8489. https://doi.org/10.1038/ncomms9489

Jung, Y., Shiozawa, Y., Wang, J., Patel, L.R., Havens, A.M., Song, J., Krebsbach, P.H., Roodman, G.D., Taichman, R.S., 2011. Annexin-2 is a regulator of stromal cell-derived factor-1/CXCL12 function in the hematopoietic stem cell endosteal niche. Exp. Hematol. 39, 151-166.e1. https://doi.org/10.1016/j.exphem.2010.11.007

Jung, Y., Wang, Jingcheng, Song, J., Shiozawa, Y., Wang, Jianhua, Havens, A., Wang, Z., Sun, Y.-X., Emerson, S.G., Krebsbach, P.H., Taichman, R.S., 2007. Annexin II expressed by osteoblasts and endothelial cells regulates stem cell adhesion, homing, and engraftment following transplantation. Blood 110, 82–90. https://doi.org/10.1182/blood-2006-05-021352

Juric, D., Soria, J.-C., Sharma, S., Banerji, U., Azaro, A., Desai, J., Ringeisen, F.P., Kaag, A., Radhakrishnan, R., Hourcade-Potelleret, F., Maacke, H., Rodon Ahnert, J., 2014. A phase 1b dose-escalation study of BYL719 plus binimetinib (MEK162) in patients with selected advanced solid tumors. J. Clin. Oncol. 32, 9051–9051. https://doi.org/10.1200/jco.2014.32.15_suppl.9051

Juvekar, A., Hu, H., Yadegarynia, S., Lyssiotis, C.A., Ullas, S., Lien, E.C., Bellinger, G., Son, J., Hok, R.C., Seth, P., Daly, M.B., Kim, B., Scully, R., Asara, J.M., Cantley, L.C., Wulf, G.M., 2016. Phosphoinositide 3-kinase inhibitors induce DNA damage through nucleoside depletion. Proc. Natl. Acad. Sci. U. S. A. 113, E4338-4347. https://doi.org/10.1073/pnas.1522223113

Kagoya, Y., Yoshimi, A., Kataoka, K., Nakagawa, M., Kumano, K., Arai, S., Kobayashi, H., Saito, T., Iwakura, Y., Kurokawa, M., 2014. Positive feedback between NF-κB and TNF-α promotes leukemia-initiating cell capacity. J. Clin. Invest. 124, 528–542. https://doi.org/10.1172/JCI68101

Kampa-Schittenhelm, K.M., Heinrich, M.C., Akmut, F., Döhner, H., Döhner, K., Schittenhelm, M.M., 2013. Quizartinib (AC220) is a potent second generation class III tyrosine kinase inhibitor that displays a distinct inhibition profile against mutant-FLT3, -PDGFRA and -KIT isoforms. Mol. Cancer 12, 19. https://doi.org/10.1186/1476-4598-12-19

Kantarjian, H.M., Thomas, X.G., Dmoszynska, A., Wierzbowska, A., Mazur, G., Mayer, J., Gau, J.-P., Chou, W.-C., Buckstein, R., Cermak, J., Kuo, C.-Y., Oriol, A., Ravandi, F., Faderl, S., Delaunay, J., Lysák, D., Minden, M., Arthur, C., 2012. Multicenter, randomized, open-label, phase III trial of decitabine versus patient choice, with physician advice, of either supportive care or low-dose cytarabine for the treatment of older patients with newly diagnosed acute

myeloid leukemia. J. Clin. Oncol. Off. J. Am. Soc. Clin. Oncol. 30, 2670–2677. https://doi.org/10.1200/JCO.2011.38.9429
Karp, J.E., Gojo, I., Pili, R., Gocke, C.D., Greer, J., Guo, C., Qian, D., Morris, L., Tidwell, M., Chen, H., Zwiebel, J., 2004. Targeting vascular endothelial growth factor for relapsed and refractory adult acute myelogenous leukemias: therapy with sequential 1-beta-d-arabinofuranosylcytosine, mitoxantrone, and bevacizumab. Clin. Cancer Res. Off. J. Am. Assoc. Cancer Res. 10, 3577–3585. https://doi.org/10.1158/1078-0432.CCR-03-0627
Kasai, F., Hirayama, N., Ozawa, M., Iemura, M., Kohara, A., 2016. Changes of heterogeneous cell populations in the Ishikawa cell line during long-term culture: Proposal for an in vitro clonal evolution model of tumor cells. Genomics 107, 259–266. https://doi.org/10.1016/j.ygeno.2016.04.003
Kasner, M., Luger, S.M., Jeschke, G.R., Mick, R., Carroll, M., Perl, A.E., 2011. Single-Cell Pharmacodynamic Monitoring of S6 Ribosomal Protein in AML Blasts During Trials Combining Sirolimus and Intensive Chemotherapy: Target Inhibition Enhances Response. Blood 118, 230–230. https://doi.org/10.1182/blood.V118.21.230.230
Kasner, M.T., Mick, R., Jeschke, G.R., Carabasi, M., Filicko-O'Hara, J., Flomenberg, N., Frey, N.V., Hexner, E.O., Luger, S.M., Loren, A.W., Mangan, J.K., Wagner, J.L., Weiss, M., Carroll, M., Perl, A.E., 2018. Sirolimus enhances remission induction in patients with high risk acute myeloid leukemia and mTORC1 target inhibition. Invest. New Drugs 36, 657–666. https://doi.org/10.1007/s10637-018-0585-x
Kassem, N.M., Ayad, A.M., El Husseiny, N.M., El-Demerdash, D.M., Kassem, H.A., Mattar, M.M., 2018. Role of Granulocyte-Macrophage Colony-Stimulating Factor in Acute Myeloid Leukemia/Myelodysplastic Syndromes. J. Glob. Oncol. 1–6. https://doi.org/10.1200/JGO.2017.009332
Katayama, Y., Battista, M., Kao, W.-M., Hidalgo, A., Peired, A.J., Thomas, S.A., Frenette, P.S., 2006. Signals from the sympathetic nervous system regulate hematopoietic stem cell egress from bone marrow. Cell 124, 407–421. https://doi.org/10.1016/j.cell.2005.10.041
Katoh, O., Takahashi, T., Oguri, T., Kuramoto, K., Mihara, K., Kobayashi, M., Hirata, S., Watanabe, H., 1998. Vascular Endothelial Growth Factor Inhibits Apoptotic Death in Hematopoietic Cells after Exposure to Chemotherapeutic Drugs by Inducing MCL1 Acting as an Antiapoptotic Factor. Cancer Res. 58, 5565–5569.
Kaufmann, S.H., Desnoyers, S., Ottaviano, Y., Davidson, N.E., Poirier, G.G., 1993. Specific proteolytic cleavage of poly(ADP-ribose) polymerase: an early marker of chemotherapy-induced apoptosis. Cancer Res. 53, 3976–3985.
Keane, N.A., Reidy, M., Natoni, A., Raab, M.S., O'Dwyer, M., 2015. Targeting the Pim kinases in multiple myeloma. Blood Cancer J. 5, e325. https://doi.org/10.1038/bcj.2015.46
Kennedy, V.E., Smith, C.C., 2020. FLT3 Mutations in Acute Myeloid Leukemia: Key Concepts and Emerging Controversies. Front. Oncol. 10, 612880. https://doi.org/10.3389/fonc.2020.612880
Kharas, M.G., Okabe, R., Ganis, J.J., Gozo, M., Khandan, T., Paktinat, M., Gilliland, D.G., Gritsman, K., 2010. Constitutively active AKT depletes hematopoietic stem cells and induces leukemia in mice. Blood 115, 1406–1415. https://doi.org/10.1182/blood-2009-06-229443
Kikushige, Y., Miyamoto, T., Yuda, J., Jabbarzadeh-Tabrizi, S., Shima, T., Takayanagi, S., Niiro, H., Yurino, A., Miyawaki, K., Takenaka, K., Iwasaki, H., Akashi, K., 2015. A TIM-3/Gal-9 Autocrine Stimulatory Loop Drives Self-Renewal of Human Myeloid Leukemia Stem Cells and Leukemic Progression. Cell Stem Cell 17, 341–352. https://doi.org/10.1016/j.stem.2015.07.011
Kikushige, Y., Shima, T., Takayanagi, S., Urata, S., Miyamoto, T., Iwasaki, H., Takenaka, K., Teshima, T., Tanaka, T., Inagaki, Y., Akashi, K., 2010. TIM-3 is a promising target to selectively kill acute myeloid leukemia stem cells. Cell Stem Cell 7, 708–717. https://doi.org/10.1016/j.stem.2010.11.014
Kikushige, Y., Yoshimoto, G., Miyamoto, T., Iino, T., Mori, Y., Iwasaki, H., Niiro, H., Takenaka, K., Nagafuji, K., Harada, M., Ishikawa, F., Akashi, K., 2008. Human Flt3 is expressed at the hematopoietic stem cell and the granulocyte/macrophage progenitor stages to maintain cell

survival. J. Immunol. Baltim. Md 1950 180, 7358–7367. https://doi.org/10.4049/jimmunol.180.11.7358
Kim, B.-R., Jung, S.-H., Han, A.-R., Park, G., Kim, H.-J., Yuan, B., Battula, V.L., Andreeff, M., Konopleva, M., Chung, Y.-J., Cho, B.-S., 2020. CXCR4 Inhibition Enhances Efficacy of FLT3 Inhibitors in FLT3-Mutated AML Augmented by Suppressed TGF-β Signaling. Cancers 12, 1737. https://doi.org/10.3390/cancers12071737
Kim, D.-H., Sarbassov, D.D., Ali, S.M., King, J.E., Latek, R.R., Erdjument-Bromage, H., Tempst, P., Sabatini, D.M., 2002. mTOR interacts with raptor to form a nutrient-sensitive complex that signals to the cell growth machinery. Cell 110, 163–175. https://doi.org/10.1016/s0092-8674(02)00808-5
Kim, J., Guan, K.-L., 2019. mTOR as a central hub of nutrient signalling and cell growth. Nat. Cell Biol. 21, 63–71. https://doi.org/10.1038/s41556-018-0205-1
Kim, J.H., Kim, W.S., Park, C., 2019. Interleukin-6 mediates resistance to PI3K-pathway-targeted therapy in lymphoma. BMC Cancer 19, 936. https://doi.org/10.1186/s12885-019-6057-7
Kim, K.-T., Baird, K., Ahn, J.-Y., Meltzer, P., Lilly, M., Levis, M., Small, D., 2005. Pim-1 is up-regulated by constitutively activated FLT3 and plays a role in FLT3-mediated cell survival. Blood 105, 1759–1767. https://doi.org/10.1182/blood-2004-05-2006
Kiyatkin, A., Aksamitiene, E., Markevich, N.I., Borisov, N.M., Hoek, J.B., Kholodenko, B.N., 2006. Scaffolding protein Grb2-associated binder 1 sustains epidermal growth factor-induced mitogenic and survival signaling by multiple positive feedback loops. J. Biol. Chem. 281, 19925–19938. https://doi.org/10.1074/jbc.M600482200
Kobayashi, H., Butler, J.M., O'Donnell, R., Kobayashi, M., Ding, B.-S., Bonner, B., Chiu, V.K., Nolan, D.J., Shido, K., Benjamin, L., Rafii, S., 2010. Angiocrine factors from Akt-activated endothelial cells balance self-renewal and differentiation of haematopoietic stem cells. Nat. Cell Biol. 12, 1046–1056. https://doi.org/10.1038/ncb2108
Koblish, H., Li, Y.-L., Shin, N., Hall, L., Wang, Q., Wang, K., Covington, M., Marando, C., Bowman, K., Boer, J., Burke, K., Wynn, R., Margulis, A., Reuther, G.W., Lambert, Q.T., Dostalik Roman, V., Zhang, K., Feng, H., Xue, C.-B., Diamond, S., Hollis, G., Yeleswaram, S., Yao, W., Huber, R., Vaddi, K., Scherle, P., 2018. Preclinical characterization of INCB053914, a novel pan-PIM kinase inhibitor, alone and in combination with anticancer agents, in models of hematologic malignancies. PloS One 13, e0199108. https://doi.org/10.1371/journal.pone.0199108
Kodaki, T., Woscholski, R., Hallberg, B., Rodriguez-Viciana, P., Downward, J., Parker, P.J., 1994. The activation of phosphatidylinositol 3-kinase by Ras. Curr. Biol. CB 4, 798–806. https://doi.org/10.1016/s0960-9822(00)00177-9
Kok, K., Nock, G.E., Verrall, E.A.G., Mitchell, M.P., Hommes, D.W., Peppelenbosch, M.P., Vanhaesebroeck, B., 2009. Regulation of p110delta PI 3-kinase gene expression. PloS One 4, e5145. https://doi.org/10.1371/journal.pone.0005145
Kolos, J.M., Voll, A.M., Bauder, M., Hausch, F., 2018. FKBP Ligands-Where We Are and Where to Go? Front. Pharmacol. 9, 1425. https://doi.org/10.3389/fphar.2018.01425
Konopleva, M., Letai, A., 2018. BCL-2 inhibition in AML: an unexpected bonus? Blood 132, 1007–1012. https://doi.org/10.1182/blood-2018-03-828269
Konopleva, M., Pollyea, D.A., Potluri, J., Chyla, B., Hogdal, L., Busman, T., McKeegan, E., Salem, A.H., Zhu, M., Ricker, J.L., Blum, W., DiNardo, C.D., Kadia, T., Dunbar, M., Kirby, R., Falotico, N., Leverson, J., Humerickhouse, R., Mabry, M., Stone, R., Kantarjian, H., Letai, A., 2016. Efficacy and Biological Correlates of Response in a Phase II Study of Venetoclax Monotherapy in Patients with Acute Myelogenous Leukemia. Cancer Discov. 6, 1106–1117. https://doi.org/10.1158/2159-8290.CD-16-0313
Konopleva, M.Y., Walter, R.B., Faderl, S.H., Jabbour, E.J., Zeng, Z., Borthakur, G., Huang, X., Kadia, T.M., Ruvolo, P.P., Feliu, J.B., Lu, H., Debose, L., Burger, J.A., Andreeff, M., Liu, W., Baggerly, K.A., Kornblau, S.M., Doyle, L.A., Estey, E.H., Kantarjian, H.M., 2014. Preclinical and early clinical evaluation of the oral AKT inhibitor, MK-2206, for the treatment of acute myelogenous leukemia. Clin. Cancer Res. Off. J. Am. Assoc. Cancer Res. 20, 2226–2235. https://doi.org/10.1158/1078-0432.CCR-13-1978
Kornblau, S.M., McCue, D., Singh, N., Chen, W., Estrov, Z., Coombes, K.R., 2010. Recurrent expression signatures of cytokines and chemokines are present and are independently

prognostic in acute myelogenous leukemia and myelodysplasia. Blood 116, 4251–4261. https://doi.org/10.1182/blood-2010-01-262071
Koundouros, N., Poulogiannis, G., 2018. Phosphoinositide 3-Kinase/Akt Signaling and Redox Metabolism in Cancer. Front. Oncol. 8, 160. https://doi.org/10.3389/fonc.2018.00160
Kovacina, K.S., Park, G.Y., Bae, S.S., Guzzetta, A.W., Schaefer, E., Birnbaum, M.J., Roth, R.A., 2003. Identification of a proline-rich Akt substrate as a 14-3-3 binding partner. J. Biol. Chem. 278, 10189–10194. https://doi.org/10.1074/jbc.M210837200
Krause, G., Hassenrück, F., Hallek, M., 2018. Copanlisib for treatment of B-cell malignancies: the development of a PI3K inhibitor with considerable differences to idelalisib. Drug Des. Devel. Ther. 12, 2577–2590. https://doi.org/10.2147/DDDT.S142406
Kreso, A., Dick, J.E., 2014. Evolution of the cancer stem cell model. Cell Stem Cell 14, 275–291. https://doi.org/10.1016/j.stem.2014.02.006
Kumar, A., Fernandez-Capetillo, O., Fernadez-Capetillo, O., Carrera, A.C., 2010. Nuclear phosphoinositide 3-kinase beta controls double-strand break DNA repair. Proc. Natl. Acad. Sci. U. S. A. 107, 7491–7496. https://doi.org/10.1073/pnas.0914242107
Kumar, B., Garcia, M., Weng, L., Jung, X., Murakami, J.L., Hu, X., McDonald, T., Lin, A., Kumar, A.R., DiGiusto, D.L., Stein, A.S., Pullarkat, V.A., Hui, S.K., Carlesso, N., Kuo, Y.-H., Bhatia, R., Marcucci, G., Chen, C.-C., 2018. Acute myeloid leukemia transforms the bone marrow niche into a leukemia-permissive microenvironment through exosome secretion. Leukemia 32, 575–587. https://doi.org/10.1038/leu.2017.259
Kumar, C.C., 2011. Genetic abnormalities and challenges in the treatment of acute myeloid leukemia. Genes Cancer 2, 95–107. https://doi.org/10.1177/1947601911408076
Kunisaki, Y., Bruns, I., Scheiermann, C., Ahmed, J., Pinho, S., Zhang, D., Mizoguchi, T., Wei, Q., Lucas, D., Ito, K., Mar, J.C., Bergman, A., Frenette, P.S., 2013. Arteriolar niches maintain haematopoietic stem cell quiescence. Nature 502, 637–643. https://doi.org/10.1038/nature12612
Kuwana, T., Newmeyer, D.D., 2003. Bcl-2-family proteins and the role of mitochondria in apoptosis. Curr. Opin. Cell Biol. 15, 691–699. https://doi.org/10.1016/j.ceb.2003.10.004
Kwitkowski, V.E., Prowell, T.M., Ibrahim, A., Farrell, A.T., Justice, R., Mitchell, S.S., Sridhara, R., Pazdur, R., 2010. FDA approval summary: temsirolimus as treatment for advanced renal cell carcinoma. The Oncologist 15, 428–435. https://doi.org/10.1634/theoncologist.2009-0178
Ladikou, E.E., Sivaloganathan, H., Pepper, A., Chevassut, T., 2020. Acute Myeloid Leukaemia in Its Niche: the Bone Marrow Microenvironment in Acute Myeloid Leukaemia. Curr. Oncol. Rep. 22, 27. https://doi.org/10.1007/s11912-020-0885-0
Lagadinou, E.D., Sach, A., Callahan, K., Rossi, R.M., Neering, S.J., Minhajuddin, M., Ashton, J.M., Pei, S., Grose, V., O'Dwyer, K.M., Liesveld, J.L., Brookes, P.S., Becker, M.W., Jordan, C.T., 2013. BCL-2 inhibition targets oxidative phosphorylation and selectively eradicates quiescent human leukemia stem cells. Cell Stem Cell 12, 329–341. https://doi.org/10.1016/j.stem.2012.12.013
Lai, C., Doucette, K., Norsworthy, K., 2019. Recent drug approvals for acute myeloid leukemia. J. Hematol. Oncol.J Hematol Oncol 12, 100. https://doi.org/10.1186/s13045-019-0774-x
Lam, S.S.Y., Leung, A.Y.H., 2020. Overcoming Resistance to FLT3 Inhibitors in the Treatment of FLT3-Mutated AML. Int. J. Mol. Sci. 21. https://doi.org/10.3390/ijms21041537
Langdon, S.P., Kay, C., Um, I.H., Dodds, M., Muir, M., Sellar, G., Kan, J., Gourley, C., Harrison, D.J., 2019. Evaluation of the dual mTOR/PI3K inhibitors Gedatolisib (PF-05212384) and PF-04691502 against ovarian cancer xenograft models. Sci. Rep. 9, 18742. https://doi.org/10.1038/s41598-019-55096-9
Lapidot, T., Sirard, C., Vormoor, J., Murdoch, B., Hoang, T., Caceres-Cortes, J., Minden, M., Paterson, B., Caligiuri, M.A., Dick, J.E., 1994. A cell initiating human acute myeloid leukaemia after transplantation into SCID mice. Nature 367, 645–648. https://doi.org/10.1038/367645a0
Laplante, M., Sabatini, D.M., 2009. mTOR signaling at a glance. J. Cell Sci. 122, 3589–3594. https://doi.org/10.1242/jcs.051011

Larrosa-Garcia, M., Baer, M.R., 2017. FLT3 inhibitors in acute myeloid leukemia: Current status and future directions. Mol. Cancer Ther. 16, 991–1001. https://doi.org/10.1158/1535-7163.MCT-16-0876

Latuske, E.-M., Stamm, H., Klokow, M., Vohwinkel, G., Muschhammer, J., Bokemeyer, C., Jücker, M., Kebenko, M., Fiedler, W., Wellbrock, J., 2017. Combined inhibition of GLI and FLT3 signaling leads to effective anti-leukemic effects in human acute myeloid leukemia. Oncotarget 8, 29187–29201. https://doi.org/10.18632/oncotarget.16304

Layani-Bazar, A., Skornick, I., Berrebi, A., Pauker, M.H., Noy, E., Silberman, A., Albeck, M., Longo, D.L., Kalechman, Y., Sredni, B., 2014. Redox modulation of adjacent thiols in VLA-4 by AS101 converts myeloid leukemia cells from a drug-resistant to drug-sensitive state. Cancer Res. 74, 3092–3103. https://doi.org/10.1158/0008-5472.CAN-13-2159

Lee, J.Y., Nakada, D., Yilmaz, O.H., Tothova, Z., Joseph, N.M., Lim, M.S., Gilliland, D.G., Morrison, S.J., 2010. mTOR activation induces tumor suppressors that inhibit leukemogenesis and deplete hematopoietic stem cells after Pten deletion. Cell Stem Cell 7, 593–605. https://doi.org/10.1016/j.stem.2010.09.015

Lee, L., Hizukuri, Y., Severson, P., Powell, B., Zhang, C., Ma, Y., Narahara, M., Sumi, H., Hernandez, D., Rajkhowa, T., Bollag, G., Levis, M., 2021. A novel combination regimen of BET and FLT3 inhibition for FLT3-ITD acute myeloid leukemia. Haematologica 106, 1022–1033. https://doi.org/10.3324/haematol.2020.247346

Legras, S., Günthert, U., Stauder, R., Curt, F., Oliferenko, S., Kluin-Nelemans, H.C., Marie, J.P., Proctor, S., Jasmin, C., Smadja-Joffe, F., 1998. A strong expression of CD44-6v correlates with shorter survival of patients with acute myeloid leukemia. Blood 91, 3401–3413.

Leslie, N.R., Bennett, D., Lindsay, Y.E., Stewart, H., Gray, A., Downes, C.P., 2003. Redox regulation of PI 3-kinase signalling via inactivation of PTEN. EMBO J. 22, 5501–5510. https://doi.org/10.1093/emboj/cdg513

Levis, M., Murphy, K.M., Pham, R., Kim, K.-T., Stine, A., Li, L., McNiece, I., Smith, B.D., Small, D., 2005. Internal tandem duplications of the FLT3 gene are present in leukemia stem cells. Blood 106, 673–680. https://doi.org/10.1182/blood-2004-05-1902

Levis, M., Perl, A.E., 2020. Gilteritinib: potent targeting of FLT3 mutations in AML. Blood Adv. 4, 1178–1191. https://doi.org/10.1182/bloodadvances.2019000174

Li, F., Sethi, G., 2010. Targeting transcription factor NF-kappaB to overcome chemoresistance and radioresistance in cancer therapy. Biochim. Biophys. Acta 1805, 167–180. https://doi.org/10.1016/j.bbcan.2010.01.002

Li, S., Garrett-Bakelman, F.E., Chung, S.S., Sanders, M.A., Hricik, T., Rapaport, F., Patel, J., Dillon, R., Vijay, P., Brown, A.L., Perl, A.E., Cannon, J., Bullinger, L., Luger, S., Becker, M., Lewis, I.D., To, L.B., Delwel, R., Löwenberg, B., Döhner, H., Döhner, K., Guzman, M.L., Hassane, D.C., Roboz, G.J., Grimwade, D., Valk, P.J.M., D'Andrea, R.J., Carroll, M., Park, C.Y., Neuberg, D., Levine, R., Melnick, A.M., Mason, C.E., 2016. Distinct evolution and dynamics of epigenetic and genetic heterogeneity in acute myeloid leukemia. Nat. Med. 22, 792–799. https://doi.org/10.1038/nm.4125

Li, Y., Chen, K., Zhou, Y., Xiao, Y., Deng, M., Jiang, Z., Ye, W., Wang, X., Wei, X., Li, J., Liang, J., Zheng, Z., Yao, Y., Wang, W., Li, P., Xu, B., 2015. A New Strategy to Target Acute Myeloid Leukemia Stem and Progenitor Cells Using Chidamide, a Histone Deacetylase Inhibitor. Curr. Cancer Drug Targets 15, 493–503. https://doi.org/10.2174/1568009615061508051532 30

Liao, Y., Hung, M.-C., 2010. Physiological regulation of Akt activity and stability. Am. J. Transl. Res. 2, 19–42.

Liesveld, J.L., O'Dwyer, K., Walker, A., Becker, M.W., Ifthikharuddin, J.J., Mulford, D., Chen, R., Bechelli, J., Rosell, K., Minhajuddin, M., Jordan, C.T., Phillips, G.L., 2013. A phase I study of decitabine and rapamycin in relapsed/refractory AML. Leuk. Res. 37, 1622–1627. https://doi.org/10.1016/j.leukres.2013.09.002

Lin, K.H., Winter, P.S., Xie, A., Roth, C., Martz, C.A., Stein, E.M., Anderson, G.R., Tingley, J.P., Wood, K.C., 2016. Targeting MCL-1/BCL-XL Forestalls the Acquisition of Resistance to ABT-199 in Acute Myeloid Leukemia. Sci. Rep. 6, 27696. https://doi.org/10.1038/srep27696

Linch, D.C., Hills, R.K., Burnett, A.K., Khwaja, A., Gale, R.E., 2014. Impact of FLT3(ITD) mutant allele level on relapse risk in intermediate-risk acute myeloid leukemia. Blood 124, 273–276. https://doi.org/10.1182/blood-2014-02-554667

Lindblad, O., Cordero, E., Puissant, A., Macaulay, L., Ramos, A., Kabir, N.N., Sun, J., Vallon-Christersson, J., Haraldsson, K., Hemann, M.T., Borg, Å., Levander, F., Stegmaier, K., Pietras, K., Rönnstrand, L., Kazi, J.U., 2016. Aberrant activation of the PI3K/mTOR pathway promotes resistance to sorafenib in AML. Oncogene 35, 5119–5131. https://doi.org/10.1038/onc.2016.41

Liu, H., Diaz-Flores, E., Poiré, X., Odenike, O., Koval, G., Malnassy, G., Ihonor, P., Zhang, Y., Le Beau, M.M., Shannon, K., Stock, W., 2010. Combination of a MEK Inhibitor, AZD6244, and Dual PI3K/mTOR Inhibitor, NVP-BEZ235: An Effective Therapeutic Strategy for Acute Myeloid Leukemia. Blood 116, 3978–3978. https://doi.org/10.1182/blood.V116.21.3978.3978

Liu, P., Cheng, H., Roberts, T.M., Zhao, J.J., 2009. Targeting the phosphoinositide 3-kinase pathway in cancer. Nat. Rev. Drug Discov. 8, 627–644. https://doi.org/10.1038/nrd2926

Liu, Q., Turner, K.M., Alfred Yung, W.K., Chen, K., Zhang, W., 2014. Role of AKT signaling in DNA repair and clinical response to cancer therapy. Neuro-Oncol. 16, 1313–1323. https://doi.org/10.1093/neuonc/nou058

Liu, S.-B., Dong, H.-J., Bao, X.-B., Qiu, Q.-C., Li, H.-Z., Shen, H.-J., Ding, Z.-X., Wang, C., Chu, X.-L., Yu, J.-Q., Tao, T., Li, Z., Tang, X.-W., Chen, S.-N., Wu, D.-P., Li, L., Xue, S.-L., 2019. Impact of FLT3-ITD length on prognosis of acute myeloid leukemia. Haematologica 104, e9–e12. https://doi.org/10.3324/haematol.2018.191809

Liu, Y., Wei, J., Liu, J., Ma, W., Duan, Y., Liu, D., 2021. Novel AXL-targeted agents overcome FLT3 inhibitor resistance in FLT3-ITD+ acute myeloid leukemia cells. Oncol. Lett. 21, 397. https://doi.org/10.3892/ol.2021.12658

Long, J., Jia, M.-Y., Fang, W.-Y., Chen, X.-J., Mu, L.-L., Wang, Z.-Y., Shen, Y., Xiang, R.-F., Wang, L.-N., Wang, L., Jiang, C.-H., Jiang, J.-L., Zhang, W.-J., Sun, Y.-D., Chang, L., Gao, W.-H., Wang, Y., Li, J.-M., Hong, D.-L., Liang, A.-B., Hu, J., 2020. FLT3 inhibition upregulates HDAC8 via FOXO to inactivate p53 and promote maintenance of FLT3-ITD+ acute myeloid leukemia. Blood 135, 1472–1483. https://doi.org/10.1182/blood.2019003538

Lord, C.J., Ashworth, A., 2017. PARP inhibitors: Synthetic lethality in the clinic. Science 355, 1152–1158. https://doi.org/10.1126/science.aam7344

Lord, C.J., Tutt, A.N.J., Ashworth, A., 2015. Synthetic lethality and cancer therapy: lessons learned from the development of PARP inhibitors. Annu. Rev. Med. 66, 455–470. https://doi.org/10.1146/annurev-med-050913-022545

Lu, J.-W., Lin, Y.-M., Lai, Y.-L., Chen, C.-Y., Hu, C.-Y., Tien, H.-F., Ou, D.-L., Lin, L.-I., 2015. MK-2206 induces apoptosis of AML cells and enhances the cytotoxicity of cytarabine. Med. Oncol. Northwood Lond. Engl. 32, 206. https://doi.org/10.1007/s12032-015-0650-7

Luedtke, D.A., Su, Y., Ma, J., Li, X., Buck, S.A., Edwards, H., Polin, L., Kushner, J., Dzinic, S.H., White, K., Lin, H., Taub, J.W., Ge, Y., 2020. Inhibition of CDK9 by voruciclib synergistically enhances cell death induced by the Bcl-2 selective inhibitor venetoclax in preclinical models of acute myeloid leukemia. Signal Transduct. Target. Ther. 5, 1–11. https://doi.org/10.1038/s41392-020-0112-3

Luo, J.-M., Liu, Z.-L., Hao, H.-L., Wang, F.-X., Dong, Z.-R., Ohno, R., 2004. Mutation analysis of SHIP gene in acute leukemia. Zhongguo Shi Yan Xue Ye Xue Za Zhi 12, 420–426.

Lyu, T., Wang, Y., Li, D., Yang, H., Qin, B., Zhang, W., Li, Z., Cheng, C., Zhang, B., Guo, R., Song, Y., 2021. Exosomes from BM-MSCs promote acute myeloid leukemia cell proliferation, invasion and chemoresistance via upregulation of S100A4. Exp. Hematol. Oncol. 10, 24. https://doi.org/10.1186/s40164-021-00220-7

Ma, C.X., Suman, V., Goetz, M.P., Northfelt, D., Burkard, M.E., Ademuyiwa, F., Naughton, M., Margenthaler, J., Aft, R., Gray, R., Tevaarwerk, A., Wilke, L., Haddad, T., Moynihan, T., Loprinzi, C., Hieken, T., Barnell, E.K., Skidmore, Z.L., Feng, Y.-Y., Krysiak, K., Hoog, J., Guo, Z., Nehring, L., Wisinski, K.B., Mardis, E., Hagemann, I.S., Vij, K., Sanati, S., Al-Kateb, H., Griffith, O.L., Griffith, M., Doyle, L., Erlichman, C., Ellis, M.J., 2017. A Phase II Trial of Neoadjuvant MK-2206, an AKT Inhibitor, with Anastrozole in Clinical Stage II or III

PIK3CA-Mutant ER-Positive and HER2-Negative Breast Cancer. Clin. Cancer Res. Off. J. Am. Assoc. Cancer Res. 23, 6823–6832. https://doi.org/10.1158/1078-0432.CCR-17-1260
Ma, L., Chen, Z., Erdjument-Bromage, H., Tempst, P., Pandolfi, P.P., 2005. Phosphorylation and functional inactivation of TSC2 by Erk implications for tuberous sclerosis and cancer pathogenesis. Cell 121, 179–193. https://doi.org/10.1016/j.cell.2005.02.031
Ma, Y., Jin, Z., Yu, K., Liu, Q., 2019. NVP-BEZ235-induced autophagy as a potential therapeutic approach for multiple myeloma. Am. J. Transl. Res. 11, 87–105.
Magee, J.A., Ikenoue, T., Nakada, D., Lee, J.Y., Guan, K.-L., Morrison, S.J., 2012. Temporal changes in PTEN and mTORC2 regulation of hematopoietic stem cell self-renewal and leukemia suppression. Cell Stem Cell 11, 415–428. https://doi.org/10.1016/j.stem.2012.05.026
Maira, S.-M., Pecchi, S., Huang, A., Burger, M., Knapp, M., Sterker, D., Schnell, C., Guthy, D., Nagel, T., Wiesmann, M., Brachmann, S., Fritsch, C., Dorsch, M., Chène, P., Shoemaker, K., De Pover, A., Menezes, D., Martiny-Baron, G., Fabbro, D., Wilson, C.J., Schlegel, R., Hofmann, F., García-Echeverría, C., Sellers, W.R., Voliva, C.F., 2012. Identification and characterization of NVP-BKM120, an orally available pan-class I PI3-kinase inhibitor. Mol. Cancer Ther. 11, 317–328. https://doi.org/10.1158/1535-7163.MCT-11-0474
Malik, P., Cashen, A.F., 2014. Decitabine in the treatment of acute myeloid leukemia in elderly patients. Cancer Manag. Res. 6, 53–61. https://doi.org/10.2147/CMAR.S40600
Mallon, R., Feldberg, L.R., Lucas, J., Chaudhary, I., Dehnhardt, C., Santos, E.D., Chen, Z., dos Santos, O., Ayral-Kaloustian, S., Venkatesan, A., Hollander, I., 2011. Antitumor efficacy of PKI-587, a highly potent dual PI3K/mTOR kinase inhibitor. Clin. Cancer Res. Off. J. Am. Assoc. Cancer Res. 17, 3193–3203. https://doi.org/10.1158/1078-0432.CCR-10-1694
Mambet, C., Chivu-Economescu, M., Matei, L., Necula, L.G., Dragu, D.L., Bleotu, C., Diaconu, C.C., 2018. Murine models based on acute myeloid leukemia-initiating stem cells xenografting. World J. Stem Cells 10, 57–65. https://doi.org/10.4252/wjsc.v10.i6.57
Man, C.H., Fung, T.K., Ho, C., Han, H.H.C., Chow, H.C.H., Ma, A.C.H., Choi, W.W.L., Lok, S., Cheung, A.M.S., Eaves, C., Kwong, Y.L., Leung, A.Y.H., 2012. Sorafenib treatment of FLT3-ITD(+) acute myeloid leukemia: favorable initial outcome and mechanisms of subsequent nonresponsiveness associated with the emergence of a D835 mutation. Blood 119, 5133–5143. https://doi.org/10.1182/blood-2011-06-363960
Manning, B.D., Cantley, L.C., 2003. Rheb fills a GAP between TSC and TOR. Trends Biochem. Sci. 28, 573–576. https://doi.org/10.1016/j.tibs.2003.09.003
Manning, B.D., Toker, A., 2017. AKT/PKB Signaling: Navigating the Network. Cell 169, 381–405. https://doi.org/10.1016/j.cell.2017.04.001
Maranzana, E., Barbero, G., Falasca, A.I., Lenaz, G., Genova, M.L., 2013. Mitochondrial Respiratory Supercomplex Association Limits Production of Reactive Oxygen Species from Complex I. Antioxid. Redox Signal. 19, 1469–1480. https://doi.org/10.1089/ars.2012.4845
Markham, A., 2019. Alpelisib: First Global Approval. Drugs 79, 1249–1253. https://doi.org/10.1007/s40265-019-01161-6
Markham, A., 2017. Copanlisib: First Global Approval. Drugs 77, 2057–2062. https://doi.org/10.1007/s40265-017-0838-6
Martelli, A.M., Evangelisti, C., Chiarini, F., Grimaldi, C., Cappellini, A., Ognibene, A., McCubrey, J.A., 2010. The emerging role of the phosphatidylinositol 3-kinase/Akt/mammalian target of rapamycin signaling network in normal myelopoiesis and leukemogenesis. Biochim. Biophys. Acta 1803, 991–1002. https://doi.org/10.1016/j.bbamcr.2010.04.005
Martelli, A.M., Nyåkern, M., Tabellini, G., Bortul, R., Tazzari, P.L., Evangelisti, C., Cocco, L., 2006. Phosphoinositide 3-kinase/Akt signaling pathway and its therapeutical implications for human acute myeloid leukemia. Leukemia 20, 911–928. https://doi.org/10.1038/sj.leu.2404245
Martens, J.H.A., Stunnenberg, H.G., 2010. The molecular signature of oncofusion proteins in acute myeloid leukemia. FEBS Lett. 584, 2662–2669. https://doi.org/10.1016/j.febslet.2010.04.002
Mazumdar, T., Byers, L.A., Ng, P.K.S., Mills, G.B., Peng, S., Diao, L., Fan, Y.-H., Stemke-Hale, K., Heymach, J.V., Myers, J.N., Glisson, B.S., Johnson, F.M., 2014. A comprehensive evaluation of biomarkers predictive of response to PI3K inhibitors and of resistance

mechanisms in head and neck squamous cell carcinoma. Mol. Cancer Ther. 13, 2738–2750. https://doi.org/10.1158/1535-7163.MCT-13-1090
McCubrey, J.A., Rakus, D., Gizak, A., Steelman, L.S., Abrams, S.L., Lertpiriyapong, K., Fitzgerald, T.L., Yang, L.V., Montalto, G., Cervello, M., Libra, M., Nicoletti, F., Scalisi, A., Torino, F., Fenga, C., Neri, L.M., Marmiroli, S., Cocco, L., Martelli, A.M., 2016. Effects of mutations in Wnt/β-catenin, hedgehog, Notch and PI3K pathways on GSK-3 activity-Diverse effects on cell growth, metabolism and cancer. Biochim. Biophys. Acta 1863, 2942–2976. https://doi.org/10.1016/j.bbamcr.2016.09.004
McCubrey, J.A., Steelman, L.S., Bertrand, F.E., Davis, N.M., Sokolosky, M., Abrams, S.L., Montalto, G., D'Assoro, A.B., Libra, M., Nicoletti, F., Maestro, R., Basecke, J., Rakus, D., Gizak, A., Demidenko, Z., Cocco, L., Martelli, A.M., Cervello, M., 2014. GSK-3 as potential target for therapeutic intervention in cancer. Oncotarget 5, 2881–2911.
McMahon, C.M., Ferng, T., Canaani, J., Wang, E.S., Morrissette, J.J.D., Eastburn, D.J., Pellegrino, M., Durruthy-Durruthy, R., Watt, C.D., Asthana, S., Lasater, E.A., DeFilippis, R., Peretz, C.A.C., McGary, L.H.F., Deihimi, S., Logan, A.C., Luger, S.M., Shah, N.P., Carroll, M., Smith, C.C., Perl, A.E., 2019. Clonal Selection with RAS Pathway Activation Mediates Secondary Clinical Resistance to Selective FLT3 Inhibition in Acute Myeloid Leukemia. Cancer Discov. 9, 1050–1063. https://doi.org/10.1158/2159-8290.CD-18-1453
Mead, A.J., Linch, D.C., Hills, R.K., Wheatley, K., Burnett, A.K., Gale, R.E., 2007. FLT3 tyrosine kinase domain mutations are biologically distinct from and have a significantly more favorable prognosis than FLT3 internal tandem duplications in patients with acute myeloid leukemia. Blood 110, 1262–1270. https://doi.org/10.1182/blood-2006-04-015826
Meja, K., Stengel, C., Sellar, R., Huszar, D., Davies, B.R., Gale, R.E., Linch, D.C., Khwaja, A., 2014. PIM and AKT kinase inhibitors show synergistic cytotoxicity in acute myeloid leukaemia that is associated with convergence on mTOR and MCL1 pathways. Br. J. Haematol. 167, 69–79. https://doi.org/10.1111/bjh.13013
Méndez-Ferrer, S., Michurina, T.V., Ferraro, F., Mazloom, A.R., Macarthur, B.D., Lira, S.A., Scadden, D.T., Ma'ayan, A., Enikolopov, G.N., Frenette, P.S., 2010. Mesenchymal and haematopoietic stem cells form a unique bone marrow niche. Nature 466, 829–834. https://doi.org/10.1038/nature09262
Mendoza, M.C., Er, E.E., Blenis, J., 2011. The Ras-ERK and PI3K-mTOR pathways: cross-talk and compensation. Trends Biochem. Sci. 36, 320–328. https://doi.org/10.1016/j.tibs.2011.03.006
Menolfi, D., Zha, S., 2020. ATM, ATR and DNA-PKcs kinases—the lessons from the mouse models: inhibition ≠ deletion. Cell Biosci. 10, 8. https://doi.org/10.1186/s13578-020-0376-x
Mi, T., Wang, Z., Bunting, K.D., 2018. The Cooperative Relationship between STAT5 and Reactive Oxygen Species in Leukemia: Mechanism and Therapeutic Potential. Cancers 10. https://doi.org/10.3390/cancers10100359
Milella, M., Falcone, I., Conciatori, F., Cesta Incani, U., Del Curatolo, A., Inzerilli, N., Nuzzo, C.M.A., Vaccaro, V., Vari, S., Cognetti, F., Ciuffreda, L., 2015. PTEN: Multiple Functions in Human Malignant Tumors. Front. Oncol. 5, 24. https://doi.org/10.3389/fonc.2015.00024
Miller, B.W., Przepiorka, D., de Claro, R.A., Lee, K., Nie, L., Simpson, N., Gudi, R., Saber, H., Shord, S., Bullock, J., Marathe, D., Mehrotra, N., Hsieh, L.S., Ghosh, D., Brown, J., Kane, R.C., Justice, R., Kaminskas, E., Farrell, A.T., Pazdur, R., 2015. FDA approval: idelalisib monotherapy for the treatment of patients with follicular lymphoma and small lymphocytic lymphoma. Clin. Cancer Res. Off. J. Am. Assoc. Cancer Res. 21, 1525–1529. https://doi.org/10.1158/1078-0432.CCR-14-2522
Min, Y.H., Eom, J.I., Cheong, J.W., Maeng, H.O., Kim, J.Y., Jeung, H.K., Lee, S.T., Lee, M.H., Hahn, J.S., Ko, Y.W., 2003. Constitutive phosphorylation of Akt/PKB protein in acute myeloid leukemia: its significance as a prognostic variable. Leukemia 17, 995–997. https://doi.org/10.1038/sj.leu.2402874
Mitchell, K., Steidl, U., 2020. Targeting Immunophenotypic Markers on Leukemic Stem Cells: How Lessons from Current Approaches and Advances in the Leukemia Stem Cell (LSC) Model Can Inform Better Strategies for Treating Acute Myeloid Leukemia (AML). Cold Spring Harb. Perspect. Med. 10, a036251. https://doi.org/10.1101/cshperspect.a036251

Mitchell, R., Hopcroft, L.E.M., Baquero, P., Allan, E.K., Hewit, K., James, D., Hamilton, G., Mukhopadhyay, A., O'Prey, J., Hair, A., Melo, J.V., Chan, E., Ryan, K.M., Maguer-Satta, V., Druker, B.J., Clark, R.E., Mitra, S., Herzyk, P., Nicolini, F.E., Salomoni, P., Shanks, E., Calabretta, B., Holyoake, T.L., Helgason, G.V., 2018. Targeting BCR-ABL-Independent TKI Resistance in Chronic Myeloid Leukemia by mTOR and Autophagy Inhibition. J. Natl. Cancer Inst. 110, 467–478. https://doi.org/10.1093/jnci/djx236

Miyamoto, K., Araki, K.Y., Naka, K., Arai, F., Takubo, K., Yamazaki, S., Matsuoka, S., Miyamoto, T., Ito, K., Ohmura, M., Chen, C., Hosokawa, K., Nakauchi, H., Nakayama, K., Nakayama, K.I., Harada, M., Motoyama, N., Suda, T., Hirao, A., 2007. Foxo3a is essential for maintenance of the hematopoietic stem cell pool. Cell Stem Cell 1, 101–112. https://doi.org/10.1016/j.stem.2007.02.001

Mohi, M.G., Boulton, C., Gu, T.-L., Sternberg, D.W., Neuberg, D., Griffin, J.D., Gilliland, D.G., Neel, B.G., 2004. Combination of rapamycin and protein tyrosine kinase (PTK) inhibitors for the treatment of leukemias caused by oncogenic PTKs. Proc. Natl. Acad. Sci. U. S. A. 101, 3130–3135. https://doi.org/10.1073/pnas.0400063101

Moloney, J.N., Jayavelu, A.K., Stanicka, J., Roche, S.L., O'Brien, R.L., Scholl, S., Böhmer, F.-D., Cotter, T.G., 2017. Nuclear membrane-localised NOX4D generates pro-survival ROS in FLT3-ITD-expressing AML. Oncotarget 8, 105440–105457. https://doi.org/10.18632/oncotarget.22241

Muñoz-Maldonado, C., Zimmer, Y., Medová, M., 2019. A Comparative Analysis of Individual RAS Mutations in Cancer Biology. Front. Oncol. 9, 1088. https://doi.org/10.3389/fonc.2019.01088

Nagel, G., Weber, D., Fromm, E., Erhardt, S., Lübbert, M., Fiedler, W., Kindler, T., Krauter, J., Brossart, P., Kündgen, A., Salih, H.R., Westermann, J., Wulf, G., Hertenstein, B., Wattad, M., Götze, K., Kraemer, D., Heinicke, T., Girschikofsky, M., Derigs, H.G., Horst, H.A., Rudolph, C., Heuser, M., Göhring, G., Teleanu, V., Bullinger, L., Thol, F., Gaidzik, V.I., Paschka, P., Döhner, K., Ganser, A., Döhner, H., Schlenk, R.F., German-Austrian AML Study Group (AMLSG), 2017. Epidemiological, genetic, and clinical characterization by age of newly diagnosed acute myeloid leukemia based on an academic population-based registry study (AMLSG BiO). Ann. Hematol. 96, 1993–2003. https://doi.org/10.1007/s00277-017-3150-3

Nair-Gupta, P., Rudnick, S.I., Luistro, L., Smith, M., McDaid, R., Li, Y., Pillarisetti, K., Joseph, J., Heidrich, B., Packman, K., Attar, R., Gaudet, F., 2020. Blockade of VLA4 sensitizes leukemic and myeloma tumor cells to CD3 redirection in the bone marrow microenvironment. Blood Cancer J. 10, 65. https://doi.org/10.1038/s41408-020-0331-4

Nakanishi, A., Wada, Y., Kitagishi, Y., Matsuda, S., 2014. Link between PI3K/AKT/PTEN Pathway and NOX Proteinin Diseases. Aging Dis. 5, 203–211. https://doi.org/10.14336/AD.2014.0500203

Nakaso, K., Yano, H., Fukuhara, Y., Takeshima, T., Wada-Isoe, K., Nakashima, K., 2003. PI3K is a key molecule in the Nrf2-mediated regulation of antioxidative proteins by hemin in human neuroblastoma cells. FEBS Lett. 546, 181–184. https://doi.org/10.1016/s0014-5793(03)00517-9

Naseem, S., Binota, J., Varma, N., Virk, H., Varma, S., Malhotra, P., 2021. NPM1 and FLT3-ITD/TKD Gene Mutations in Acute Myeloid Leukemia. Int. J. Hematol.-Oncol. Stem Cell Res. 15, 15–26. https://doi.org/10.18502/ijhoscr.v15i1.5246

Natarajan, K., Xie, Y., Burcu, M., Linn, D.E., Qiu, Y., Baer, M.R., 2013. Pim-1 kinase phosphorylates and stabilizes 130 kDa FLT3 and promotes aberrant STAT5 signaling in acute myeloid leukemia with FLT3 internal tandem duplication. PloS One 8, e74653. https://doi.org/10.1371/journal.pone.0074653

Naymagon, L., Abdul-Hay, M., 2016. Novel agents in the treatment of multiple myeloma: a review about the future. J. Hematol. Oncol.J Hematol Oncol 9. https://doi.org/10.1186/s13045-016-0282-1

Nepstad, I., Hatfield, K.J., Aasebø, E., Hernandez-Valladares, M., Brenner, A.K., Bartaula-Brevik, S., Berven, F., Selheim, F., Skavland, J., Gjertsen, B.T., Reikvam, H., Bruserud, Ø., 2018. Two acute myeloid leukemia patient subsets are identified based on the constitutive PI3K-Akt-mTOR signaling of their leukemic cells; a functional, proteomic, and transcriptomic

comparison. Expert Opin. Ther. Targets 22, 639–653. https://doi.org/10.1080/14728222.2018.1487401
Nepstad, I., Hatfield, K.J., Gronningsaeter, I.S., Reikvam, H., 2020. The PI3K-Akt-mTOR Signaling Pathway in Human Acute Myeloid Leukemia (AML) Cells. Int. J. Mol. Sci. 21. https://doi.org/10.3390/ijms21082907
Netea, M.G., Nold-Petry, C.A., Nold, M.F., Joosten, L.A.B., Opitz, B., van der Meer, J.H.M., van de Veerdonk, F.L., Ferwerda, G., Heinhuis, B., Devesa, I., Funk, C.J., Mason, R.J., Kullberg, B.J., Rubartelli, A., van der Meer, J.W.M., Dinarello, C.A., 2009. Differential requirement for the activation of the inflammasome for processing and release of IL-1beta in monocytes and macrophages. Blood 113, 2324–2335. https://doi.org/10.1182/blood-2008-03-146720
Ng, K.L.N., Lynn, C., Leung, T.W.Y., So, E.C.W., Leung, A.Y.H., 2019. Targeting DNA Damage and Repair in Acute Myeloid Leukemia Carrying Internal Tandem Duplication of Fms-like Tyrosine Kinase 3 (FLT3-ITD) - a Mechanistic Study. Blood 134, 1261–1261. https://doi.org/10.1182/blood-2019-129472
Ng, S.W.K., Mitchell, A., Kennedy, J.A., Chen, W.C., McLeod, J., Ibrahimova, N., Arruda, A., Popescu, A., Gupta, V., Schimmer, A.D., Schuh, A.C., Yee, K.W., Bullinger, L., Herold, T., Görlich, D., Büchner, T., Hiddemann, W., Berdel, W.E., Wörmann, B., Cheok, M., Preudhomme, C., Dombret, H., Metzeler, K., Buske, C., Löwenberg, B., Valk, P.J.M., Zandstra, P.W., Minden, M.D., Dick, J.E., Wang, J.C.Y., 2016. A 17-gene stemness score for rapid determination of risk in acute leukaemia. Nature 540, 433–437. https://doi.org/10.1038/nature20598
Nguyen, L.X.T., Sesay, A., Mitchell, B.S., 2014. Effect of CAL-101, a PI3Kδ inhibitor, on ribosomal rna synthesis and cell proliferation in acute myeloid leukemia cells. Blood Cancer J. 4, e228. https://doi.org/10.1038/bcj.2014.49
Nilsson, S.K., Johnston, H.M., Whitty, G.A., Williams, B., Webb, R.J., Denhardt, D.T., Bertoncello, I., Bendall, L.J., Simmons, P.J., Haylock, D.N., 2005. Osteopontin, a key component of the hematopoietic stem cell niche and regulator of primitive hematopoietic progenitor cells. Blood 106, 1232–1239. https://doi.org/10.1182/blood-2004-11-4422
Nishioka, C., Ikezoe, T., Yang, J., Koeffler, H.P., Yokoyama, A., 2008. Blockade of mTOR signaling potentiates the ability of histone deacetylase inhibitor to induce growth arrest and differentiation of acute myelogenous leukemia cells. Leukemia 22, 2159–2168. https://doi.org/10.1038/leu.2008.243
Nitulescu, G.M., Margina, D., Juzenas, P., Peng, Q., Olaru, O.T., Saloustros, E., Fenga, C., Spandidos, D.A., Libra, M., Tsatsakis, A.M., 2016. Akt inhibitors in cancer treatment: The long journey from drug discovery to clinical use (Review). Int. J. Oncol. 48, 869–885. https://doi.org/10.3892/ijo.2015.3306
Nogami, A., Okada, K., Ishida, S., Akiyama, H., Umezawa, Y., Miura, O., 2019. Inhibition of the STAT5/Pim Kinase Axis Enhances Cytotoxic Effects of Proteasome Inhibitors on FLT3-ITD-Positive AML Cells by Cooperatively Inhibiting the mTORC1/4EBP1/S6K/Mcl-1 Pathway. Transl. Oncol. 12, 336–349. https://doi.org/10.1016/j.tranon.2018.11.001
Nogami, A., Oshikawa, G., Okada, K., Fukutake, S., Umezawa, Y., Nagao, T., Kurosu, T., Miura, O., 2015. FLT3-ITD confers resistance to the PI3K/Akt pathway inhibitors by protecting the mTOR/4EBP1/Mcl-1 pathway through STAT5 activation in acute myeloid leukemia. Oncotarget 6, 9189–9205. https://doi.org/10.18632/oncotarget.3279
Okada, K., Nogami, A., Ishida, S., Akiyama, H., Chen, C., Umezawa, Y., Miura, O., 2018. FLT3-ITD induces expression of Pim kinases through STAT5 to confer resistance to the PI3K/Akt pathway inhibitors on leukemic cells by enhancing the mTORC1/Mcl-1 pathway. Oncotarget 9, 8870–8886. https://doi.org/10.18632/oncotarget.22926
Okkenhaug, K., Graupera, M., Vanhaesebroeck, B., 2016. Targeting PI3K in Cancer: Impact on Tumor Cells, Their Protective Stroma, Angiogenesis, and Immunotherapy. Cancer Discov. 6, 1090–1105. https://doi.org/10.1158/2159-8290.CD-16-0716
Oran, B., Weisdorf, D.J., 2012. Survival for older patients with acute myeloid leukemia: a population-based study. Haematologica 97, 1916–1924. https://doi.org/10.3324/haematol.2012.066100

O'Reilly, E., Zeinabad, H.A., Szegezdi, E., 2021. Hematopoietic versus leukemic stem cell quiescence: Challenges and therapeutic opportunities. Blood Rev. 50, 100850. https://doi.org/10.1016/j.blre.2021.100850

Ossenkoppele, G.J., Stussi, G., Maertens, J., van Montfort, K., Biemond, B.J., Breems, D., Ferrant, A., Graux, C., de Greef, G.E., Halkes, C.J.M., Hoogendoorn, M., Hollestein, R.M., Jongen-Lavrencic, M., Levin, M.D., van de Loosdrecht, A.A., van Marwijk Kooij, M., van Norden, Y., Pabst, T., Schouten, H.C., Vellenga, E., Verhoef, G.E.G., de Weerdt, O., Wijermans, P., Passweg, J.R., Löwenberg, B., 2012. Addition of bevacizumab to chemotherapy in acute myeloid leukemia at older age: a randomized phase 2 trial of the Dutch-Belgian Cooperative Trial Group for Hemato-Oncology (HOVON) and the Swiss Group for Clinical Cancer Research (SAKK). Blood 120, 4706–4711. https://doi.org/10.1182/blood-2012-04-420596

Pan, R., Hogdal, L.J., Benito, J.M., Bucci, D., Han, L., Borthakur, G., Cortes, J., DeAngelo, D.J., Debose, L., Mu, H., Döhner, H., Gaidzik, V.I., Galinsky, I., Golfman, L.S., Haferlach, T., Harutyunyan, K.G., Hu, J., Leverson, J.D., Marcucci, G., Müschen, M., Newman, R., Park, E., Ruvolo, P.P., Ruvolo, V., Ryan, J., Schindela, S., Zweidler-McKay, P., Stone, R.M., Kantarjian, H., Andreeff, M., Konopleva, M., Letai, A.G., 2014. Selective BCL-2 inhibition by ABT-199 causes on-target cell death in acute myeloid leukemia. Cancer Discov. 4, 362–375. https://doi.org/10.1158/2159-8290.CD-13-0609

Pan, R., Ruvolo, V., Mu, H., Leverson, J.D., Nichols, G., Reed, J.C., Konopleva, M., Andreeff, M., 2017. Synthetic Lethality of Combined Bcl-2 Inhibition and p53 Activation in AML: Mechanisms and Superior Antileukemic Efficacy. Cancer Cell 32, 748-760.e6. https://doi.org/10.1016/j.ccell.2017.11.003

Park, I.-K., Mundy-Bosse, B., Whitman, S.P., Zhang, X., Warner, S.L., Bearss, D.J., Blum, W., Marcucci, G., Caligiuri, M.A., 2015. Receptor tyrosine kinase Axl is required for resistance of leukemic cells to FLT3-targeted therapy in acute myeloid leukemia. Leukemia 29, 2382–2389. https://doi.org/10.1038/leu.2015.147

Park, S., Chapuis, N., Saint Marcoux, F., Recher, C., Prebet, T., Chevallier, P., Cahn, J.-Y., Leguay, T., Bories, P., Witz, F., Lamy, T., Mayeux, P., Lacombe, C., Demur, C., Tamburini, J., Merlat, A., Delepine, R., Vey, N., Dreyfus, F., Béné, M.C., Ifrah, N., Bouscary, D., GOELAMS (Groupe Ouest Est d'Etude des Leucémies aiguës et Autres Maladies du Sang), 2013. A phase Ib GOELAMS study of the mTOR inhibitor RAD001 in association with chemotherapy for AML patients in first relapse. Leukemia 27, 1479–1486. https://doi.org/10.1038/leu.2013.17

Park, S., Chapuis, N., Tamburini, J., Bardet, V., Cornillet-Lefebvre, P., Willems, L., Green, A., Mayeux, P., Lacombe, C., Bouscary, D., 2010. Role of the PI3K/AKT and mTOR signaling pathways in acute myeloid leukemia. Haematologica 95, 819–828. https://doi.org/10.3324/haematol.2009.013797

Park, S.R., Yoo, Y.J., Ban, Y.-H., Yoon, Y.J., 2010. Biosynthesis of rapamycin and its regulation: past achievements and recent progress. J. Antibiot. (Tokyo) 63, 434–441. https://doi.org/10.1038/ja.2010.71

Parmar, A., Marz, S., Rushton, S., Holzwarth, C., Lind, K., Kayser, S., Döhner, K., Peschel, C., Oostendorp, R.A.J., Götze, K.S., 2011. Stromal niche cells protect early leukemic FLT3-ITD+ progenitor cells against first-generation FLT3 tyrosine kinase inhibitors. Cancer Res. 71, 4696–4706. https://doi.org/10.1158/0008-5472.CAN-10-4136

Passaro, D., Di Tullio, A., Abarrategi, A., Rouault-Pierre, K., Foster, K., Ariza-McNaughton, L., Montaner, B., Chakravarty, P., Bhaw, L., Diana, G., Lassailly, F., Gribben, J., Bonnet, D., 2017. Increased Vascular Permeability in the Bone Marrow Microenvironment Contributes to Disease Progression and Drug Response in Acute Myeloid Leukemia. Cancer Cell 32, 324-341.e6. https://doi.org/10.1016/j.ccell.2017.08.001

Patel, A.B., Pomicter, A.D., Yan, D., Eiring, A.M., Antelope, O., Schumacher, J.A., Kelley, T.W., Tantravahi, S.K., Kovacsovics, T.J., Shami, P.J., O'Hare, T., Deininger, M.W., 2020. Dasatinib overcomes stroma-based resistance to the FLT3 inhibitor quizartinib using multiple mechanisms. Leukemia 34, 2981–2991. https://doi.org/10.1038/s41375-020-0858-1

Patnaik, M.M., 2018. The importance of FLT3 mutational analysis in acute myeloid leukemia. Leuk. Lymphoma 59, 2273–2286. https://doi.org/10.1080/10428194.2017.1399312

Pearce, L.R., Huang, X., Boudeau, J., Pawłowski, R., Wullschleger, S., Deak, M., Ibrahim, A.F.M., Gourlay, R., Magnuson, M.A., Alessi, D.R., 2007. Identification of Protor as a novel Rictor-binding component of mTOR complex-2. Biochem. J. 405, 513–522. https://doi.org/10.1042/BJ20070540

Pei, S., Minhajuddin, M., Callahan, K.P., Balys, M., Ashton, J.M., Neering, S.J., Lagadinou, E.D., Corbett, C., Ye, H., Liesveld, J.L., O'Dwyer, K.M., Li, Z., Shi, L., Greninger, P., Settleman, J., Benes, C., Hagen, F.K., Munger, J., Crooks, P.A., Becker, M.W., Jordan, C.T., 2013. Targeting Aberrant Glutathione Metabolism to Eradicate Human Acute Myelogenous Leukemia Cells. J. Biol. Chem. 288, 33542–33558. https://doi.org/10.1074/jbc.M113.511170

Peña-Blanco, A., García-Sáez, A.J., 2018. Bax, Bak and beyond - mitochondrial performance in apoptosis. FEBS J. 285, 416–431. https://doi.org/10.1111/febs.14186

Pende, M., Um, S.H., Mieulet, V., Sticker, M., Goss, V.L., Mestan, J., Mueller, M., Fumagalli, S., Kozma, S.C., Thomas, G., 2004. S6K1(-/-)/S6K2(-/-) mice exhibit perinatal lethality and rapamycin-sensitive 5'-terminal oligopyrimidine mRNA translation and reveal a mitogen-activated protein kinase-dependent S6 kinase pathway. Mol. Cell. Biol. 24, 3112–3124. https://doi.org/10.1128/mcb.24.8.3112-3124.2004

Pepe, F., Bill, M., Papaioannou, D., Karunasiri, M., Walker, A., Naumann, E., Snyder, K., Ranganathan, P., Dorrance, A., Garzon, R., 2022. Targeting Wnt signaling in acute myeloid leukemia stem cells. Haematologica 107, 307–311. https://doi.org/10.3324/haematol.2020.266155

Perl, A.E., Kasner, M.T., Shank, D., Luger, S.M., Carroll, M., 2012. Single-cell pharmacodynamic monitoring of S6 ribosomal protein phosphorylation in AML blasts during a clinical trial combining the mTOR inhibitor sirolimus and intensive chemotherapy. Clin. Cancer Res. Off. J. Am. Assoc. Cancer Res. 18, 1716–1725. https://doi.org/10.1158/1078-0432.CCR-11-2346

Perl, A.E., Kasner, M.T., Tsai, D.E., Vogl, D.T., Loren, A.W., Schuster, S.J., Porter, D.L., Stadtmauer, E.A., Goldstein, S.C., Frey, N.V., Nasta, S.D., Hexner, E.O., Dierov, J.K., Swider, C.R., Bagg, A., Gewirtz, A.M., Carroll, M., Luger, S.M., 2009. A phase I study of the mammalian target of rapamycin inhibitor sirolimus and MEC chemotherapy in relapsed and refractory acute myelogenous leukemia. Clin. Cancer Res. Off. J. Am. Assoc. Cancer Res. 15, 6732–6739. https://doi.org/10.1158/1078-0432.CCR-09-0842

Perl, A.E., Martinelli, G., Cortes, J.E., Neubauer, A., Berman, E., Paolini, S., Montesinos, P., Baer, M.R., Larson, R.A., Ustun, C., Fabbiano, F., Erba, H.P., Di Stasi, A., Stuart, R., Olin, R., Kasner, M., Ciceri, F., Chou, W.-C., Podoltsev, N., Recher, C., Yokoyama, H., Hosono, N., Yoon, S.-S., Lee, J.-H., Pardee, T., Fathi, A.T., Liu, C., Hasabou, N., Liu, X., Bahceci, E., Levis, M.J., 2019. Gilteritinib or Chemotherapy for Relapsed or Refractory FLT3-Mutated AML. N. Engl. J. Med. 381, 1728–1740. https://doi.org/10.1056/NEJMoa1902688

Perlin, J.R., Sporrij, A., Zon, L.I., 2017. Blood on the tracks: hematopoietic stem cell-endothelial cell interactions in homing and engraftment. J. Mol. Med. Berl. Ger. 95, 809–819. https://doi.org/10.1007/s00109-017-1559-8

Pietras, E.M., Warr, M.R., Passegué, E., 2011. Cell cycle regulation in hematopoietic stem cells. J. Cell Biol. 195, 709–720. https://doi.org/10.1083/jcb.201102131

Piloto, O., Wright, M., Brown, P., Kim, K.-T., Levis, M., Small, D., 2007. Prolonged exposure to FLT3 inhibitors leads to resistance via activation of parallel signaling pathways. Blood 109, 1643–1652. https://doi.org/10.1182/blood-2006-05-023804

Pongas, G., Fojo, T., 2016. BEZ235: When Promising Science Meets Clinical Reality. The Oncologist 21, 1033–1034. https://doi.org/10.1634/theoncologist.2016-0243

Ponomaryov, T., Peled, A., Petit, I., Taichman, R.S., Habler, L., Sandbank, J., Arenzana-Seisdedos, F., Magerus, A., Caruz, A., Fujii, N., Nagler, A., Lahav, M., Szyper-Kravitz, M., Zipori, D., Lapidot, T., 2000. Induction of the chemokine stromal-derived factor-1 following DNA damage improves human stem cell function. J. Clin. Invest. 106, 1331–1339. https://doi.org/10.1172/JCI10329

Ponta, H., Sherman, L., Herrlich, P.A., 2003. CD44: From adhesion molecules to signalling regulators. Nat. Rev. Mol. Cell Biol. 4, 33–45. https://doi.org/10.1038/nrm1004
Port, M., Böttcher, M., Thol, F., Ganser, A., Schlenk, R., Wasem, J., Neumann, A., Pouryamout, L., 2014. Prognostic significance of FLT3 internal tandem duplication, nucleophosmin 1, and CEBPA gene mutations for acute myeloid leukemia patients with normal karyotype and younger than 60 years: a systematic review and meta-analysis. Ann. Hematol. 93, 1279–1286. https://doi.org/10.1007/s00277-014-2072-6
Potter, C.J., Pedraza, L.G., Xu, T., 2002. Akt regulates growth by directly phosphorylating Tsc2. Nat. Cell Biol. 4, 658–665. https://doi.org/10.1038/ncb840
Poulos, M.G., Guo, P., Kofler, N.M., Pinho, S., Gutkin, M.C., Tikhonova, A., Aifantis, I., Frenette, P.S., Kitajewski, J., Rafii, S., Butler, J.M., 2013. Endothelial Jagged-1 is necessary for homeostatic and regenerative hematopoiesis. Cell Rep. 4, 1022–1034. https://doi.org/10.1016/j.celrep.2013.07.048
Pugazhenthi, S., Nesterova, A., Sable, C., Heidenreich, K.A., Boxer, L.M., Heasley, L.E., Reusch, J.E., 2000. Akt/protein kinase B up-regulates Bcl-2 expression through cAMP-response element-binding protein. J. Biol. Chem. 275, 10761–10766. https://doi.org/10.1074/jbc.275.15.10761
Qian, H., Buza-Vidas, N., Hyland, C.D., Jensen, C.T., Antonchuk, J., Månsson, R., Thoren, L.A., Ekblom, M., Alexander, W.S., Jacobsen, S.E.W., 2007. Critical role of thrombopoietin in maintaining adult quiescent hematopoietic stem cells. Cell Stem Cell 1, 671–684. https://doi.org/10.1016/j.stem.2007.10.008
Qian, X., Li, Y., Yu, Y., Yang, F., Deng, R., Ji, J., Jiao, L., Li, X., Wu, R.-Y., Chen, W.-D., Feng, G.-K., Zhu, X.-F., 2015. Inhibition of DNA methyltransferase as a novel therapeutic strategy to overcome acquired resistance to dual PI3K/mTOR inhibitors. Oncotarget 6, 5134–5146. https://doi.org/10.18632/oncotarget.3016
Qin, X., Jiang, B., Zhang, Y., 2016. 4E-BP1, a multifactor regulated multifunctional protein. Cell Cycle Georget. Tex 15, 781–786. https://doi.org/10.1080/15384101.2016.1151581
Quek, L., Otto, G.W., Garnett, C., Lhermitte, L., Karamitros, D., Stoilova, B., Lau, I.-J., Doondeea, J., Usukhbayar, B., Kennedy, A., Metzner, M., Goardon, N., Ivey, A., Allen, C., Gale, R., Davies, B., Sternberg, A., Killick, S., Hunter, H., Cahalin, P., Price, A., Carr, A., Griffiths, M., Virgo, P., Mackinnon, S., Grimwade, D., Freeman, S., Russell, N., Craddock, C., Mead, A., Peniket, A., Porcher, C., Vyas, P., 2016. Genetically distinct leukemic stem cells in human CD34- acute myeloid leukemia are arrested at a hemopoietic precursor-like stage. J. Exp. Med. 213, 1513–1535. https://doi.org/10.1084/jem.20151775
Quentmeier, H., Reinhardt, J., Zaborski, M., Drexler, H.G., 2003. FLT3 mutations in acute myeloid leukemia cell lines. Leukemia 17, 120–124. https://doi.org/10.1038/sj.leu.2402740
Rabanal-Ruiz, Y., Otten, E.G., Korolchuk, V.I., 2017. mTORC1 as the main gateway to autophagy. Essays Biochem. 61, 565–584. https://doi.org/10.1042/EBC20170027
Rafii, S., Shapiro, F., Pettengell, R., Ferris, B., Nachman, R.L., Moore, M.A., Asch, A.S., 1995. Human bone marrow microvascular endothelial cells support long-term proliferation and differentiation of myeloid and megakaryocytic progenitors. Blood 86, 3353–3363.
Ragon, B.K., Kantarjian, H., Jabbour, E., Ravandi, F., Cortes, J., Borthakur, G., DeBose, L., Zeng, Z., Schneider, H., Pemmaraju, N., Garcia-Manero, G., Kornblau, S., Wierda, W., Burger, J., DiNardo, C.D., Andreeff, M., Konopleva, M., Daver, N., 2017. Buparlisib, a PI3K inhibitor, demonstrates acceptable tolerability and preliminary activity in a phase I trial of patients with advanced leukemias. Am. J. Hematol. 92, 7–11. https://doi.org/10.1002/ajh.24568
Rahmani, M., Aust, M.M., Attkisson, E., Williams, D.C., Ferreira-Gonzalez, A., Grant, S., 2013. Dual inhibition of Bcl-2 and Bcl-xL strikingly enhances PI3K inhibition-induced apoptosis in human myeloid leukemia cells through a GSK3- and Bim-dependent mechanism. Cancer Res. 73, 1340–1351. https://doi.org/10.1158/0008-5472.CAN-12-1365
Rahmani, M., Aust, M.M., Benson, E.C., Wallace, L., Friedberg, J., Grant, S., 2014. PI3K/mTOR inhibition markedly potentiates HDAC inhibitor activity in NHL cells through BIM- and MCL-1-dependent mechanisms in vitro and in vivo. Clin. Cancer Res. Off. J. Am. Assoc. Cancer Res. 20, 4849–4860. https://doi.org/10.1158/1078-0432.CCR-14-0034
Rahmani, M., Nkwocha, J., Hawkins, E., Pei, X., Parker, R.E., Kmieciak, M., Leverson, J.D., Sampath, D., Ferreira-Gonzalez, A., Grant, S., 2018. Cotargeting BCL-2 and PI3K Induces

BAX-Dependent Mitochondrial Apoptosis in AML Cells. Cancer Res. 78, 3075–3086. https://doi.org/10.1158/0008-5472.CAN-17-3024
Raimondo, L., D'Amato, V., Servetto, A., Rosa, R., Marciano, R., Formisano, L., Mauro, C.D., Orsini, R.C., Cascetta, P., Ciciola, P., De Maio, A.P., Di Renzo, M.F., Cosconati, S., Bruno, A., Randazzo, A., Napolitano, F., Montuori, N., Veneziani, B.M., Placido, S.D., Bianco, R., 2016. Everolimus induces Met inactivation by disrupting the FKBP12/Met complex. Oncotarget 7, 40073–40084. https://doi.org/10.18632/oncotarget.9484
Rashidi, A., DiPersio, J.F., 2016. Targeting the leukemia–stroma interaction in acute myeloid leukemia: rationale and latest evidence. Ther. Adv. Hematol. 7, 40–51. https://doi.org/10.1177/2040620715619307
Rebechi, M.T., Pratz, K.W., 2017. Genomic instability is a principle pathologic feature of FLT3 ITD kinase activity in acute myeloid leukemia leading to clonal evolution and disease progression. Leuk. Lymphoma 58, 1–11. https://doi.org/10.1080/10428194.2017.1283031
Reikvam, H., 2020. Inhibition of NF-κB Signaling Alters Acute Myelogenous Leukemia Cell Transcriptomics. Cells 9, 1677. https://doi.org/10.3390/cells9071677
Reikvam, H., Aasebø, E., Brenner, A.K., Bartaula-Brevik, S., Grønningsæter, I.S., Forthun, R.B., Hovland, R., Bruserud, Ø., 2019. High Constitutive Cytokine Release by Primary Human Acute Myeloid Leukemia Cells Is Associated with a Specific Intercellular Communication Phenotype. J. Clin. Med. 8, 970. https://doi.org/10.3390/jcm8070970
Reikvam, H., Nepstad, I., Bruserud, Ø., Hatfield, K.J., 2013. Pharmacological targeting of the PI3K/mTOR pathway alters the release of angioregulatory mediators both from primary human acute myeloid leukemia cells and their neighboring stromal cells. Oncotarget 4, 830–843.
Rieger, M.A., Schroeder, T., 2012. Hematopoiesis. Cold Spring Harb. Perspect. Biol. 4, a008250. https://doi.org/10.1101/cshperspect.a008250
Roboz, G.J., Ritchie, E.K., Dault, Y., Lam, L., Marshall, D.C., Cruz, N.M., Hsu, H.-T.C., Hassane, D.C., Christos, P.J., Ippoliti, C., Scandura, J.M., Guzman, M.L., 2018. Phase I trial of plerixafor combined with decitabine in newly diagnosed older patients with acute myeloid leukemia. Haematologica 103, 1308–1316. https://doi.org/10.3324/haematol.2017.183418
Rodrigues, D.A., Sagrillo, F.S., Fraga, C.A.M., 2019. Duvelisib: A 2018 Novel FDA-Approved Small Molecule Inhibiting Phosphoinositide. Pharm. Basel Switz. 12. https://doi.org/10.3390/ph12020069
Rollins-Raval, M., Pillai, R., Warita, K., Mitsuhashi-Warita, T., Mehta, R., Boyiadzis, M., Djokic, M., Kant, J.A., Roth, C.G., 2013. CD123 immunohistochemical expression in acute myeloid leukemia is associated with underlying FLT3-ITD and NPM1 mutations. Appl. Immunohistochem. Mol. Morphol. AIMM 21, 212–217. https://doi.org/10.1097/PAI.0b013e318261a342
Roskoski, R., 2019. Properties of FDA-approved small molecule protein kinase inhibitors. Pharmacol. Res. 144, 19–50. https://doi.org/10.1016/j.phrs.2019.03.006
Roskoski, R., 2012. ERK1/2 MAP kinases: structure, function, and regulation. Pharmacol. Res. 66, 105–143. https://doi.org/10.1016/j.phrs.2012.04.005
Rossi, H.A., O'Donnell, J., Sarcinelli, F., Stewart, F.M., Quesenberry, P.J., Becker, P.S., 2002. Granulocyte–macrophage colony-stimulating factor (GM-CSF) priming with successive concomitant low-dose Ara-C for elderly patients with secondary/refractory acute myeloid leukemia or advanced myelodysplastic syndrome. Leukemia 16, 310–315. https://doi.org/10.1038/sj.leu.2402368
Roux, P.P., Ballif, B.A., Anjum, R., Gygi, S.P., Blenis, J., 2004. Tumor-promoting phorbol esters and activated Ras inactivate the tuberous sclerosis tumor suppressor complex via p90 ribosomal S6 kinase. Proc. Natl. Acad. Sci. U. S. A. 101, 13489–13494. https://doi.org/10.1073/pnas.0405659101
Rücker, F.G., Du, L., Luck, T.J., Benner, A., Krzykalla, J., Gathmann, I., Voso, M.T., Amadori, S., Prior, T.W., Brandwein, J.M., Appelbaum, F.R., Medeiros, B.C., Tallman, M.S., Savoie, L., Sierra, J., Pallaud, C., Sanz, M.A., Jansen, J.H., Niederwieser, D., Fischer, T., Ehninger, G., Heuser, M., Ganser, A., Bullinger, L., Larson, R.A., Bloomfield, C.D., Stone, R.M., Döhner, H., Thiede, C., Döhner, K., 2021. Molecular landscape and prognostic impact of

FLT3-ITD insertion site in acute myeloid leukemia: RATIFY study results. Leukemia 1–10. https://doi.org/10.1038/s41375-021-01323-0
Ruvinsky, I., Meyuhas, O., 2006. Ribosomal protein S6 phosphorylation: from protein synthesis to cell size. Trends Biochem. Sci. 31, 342–348. https://doi.org/10.1016/j.tibs.2006.04.003
Sabers, C.J., Martin, M.M., Brunn, G.J., Williams, J.M., Dumont, F.J., Wiederrecht, G., Abraham, R.T., 1995. Isolation of a protein target of the FKBP12-rapamycin complex in mammalian cells. J. Biol. Chem. 270, 815–822. https://doi.org/10.1074/jbc.270.2.815
Sabio, G., Davis, R.J., 2014. TNF and MAP kinase signaling pathways. Semin. Immunol. 26, 237–245. https://doi.org/10.1016/j.smim.2014.02.009
Sadeghi, S., Esmaeili, S., Pourbagheri-Sigaroodi, A., Safaroghli-Azar, A., Bashash, D., 2020. PI3K abrogation using pan PI3K inhibitor BKM120 give rise to a weighty anti-cancer effect on AML-derived KG-1 cells by inducing apoptosis and G2/M arrest. Turk. J. Haematol. Off. J. Turk. Soc. Haematol. https://doi.org/10.4274/tjh.galenos.2020.2019.0440
Salazar, R., Garcia-Carbonero, R., Libutti, S.K., Hendifar, A.E., Custodio, A., Guimbaud, R., Lombard-Bohas, C., Ricci, S., Klümpen, H.-J., Capdevila, J., Reed, N., Walenkamp, A., Grande, E., Safina, S., Meyer, T., Kong, O., Salomon, H., Tavorath, R., Yao, J.C., 2018. Phase II Study of BEZ235 versus Everolimus in Patients with Mammalian Target of Rapamycin Inhibitor-Naïve Advanced Pancreatic Neuroendocrine Tumors. The Oncologist 23, 766-e90. https://doi.org/10.1634/theoncologist.2017-0144
Sallmyr, A., Fan, J., Datta, K., Kim, K.-T., Grosu, D., Shapiro, P., Small, D., Rassool, F., 2008a. Internal tandem duplication of FLT3 (FLT3/ITD) induces increased ROS production, DNA damage, and misrepair: implications for poor prognosis in AML. Blood 111, 3173–3182. https://doi.org/10.1182/blood-2007-05-092510
Sallmyr, A., Fan, J., Rassool, F.V., 2008b. Genomic instability in myeloid malignancies: increased reactive oxygen species (ROS), DNA double strand breaks (DSBs) and error-prone repair. Cancer Lett. 270, 1–9. https://doi.org/10.1016/j.canlet.2008.03.036
San José-Enériz, E., Gimenez-Camino, N., Agirre, X., Prosper, F., 2019. HDAC Inhibitors in Acute Myeloid Leukemia. Cancers 11. https://doi.org/10.3390/cancers11111794
Sanchez-Correa, B., Bergua, J.M., Campos, C., Gayoso, I., Arcos, M.J., Bañas, H., Morgado, S., Casado, J.G., Solana, R., Tarazona, R., 2013. Cytokine profiles in acute myeloid leukemia patients at diagnosis: survival is inversely correlated with IL-6 and directly correlated with IL-10 levels. Cytokine 61, 885–891. https://doi.org/10.1016/j.cyto.2012.12.023
Sandhöfer, N., Metzeler, K.H., Rothenberg, M., Herold, T., Tiedt, S., Groiß, V., Carlet, M., Walter, G., Hinrichsen, T., Wachter, O., Grunert, M., Schneider, S., Subklewe, M., Dufour, A., Fröhling, S., Klein, H.-G., Hiddemann, W., Jeremias, I., Spiekermann, K., 2015. Dual PI3K/mTOR inhibition shows antileukemic activity in MLL-rearranged acute myeloid leukemia. Leukemia 29, 828–838. https://doi.org/10.1038/leu.2014.305
Sands, W.A., Copland, M., Wheadon, H., 2013. Targeting self-renewal pathways in myeloid malignancies. Cell Commun. Signal. 11, 33. https://doi.org/10.1186/1478-811X-11-33
Santo, E.E., Stroeken, P., Sluis, P.V., Koster, J., Versteeg, R., Westerhout, E.M., 2013. FOXO3a is a major target of inactivation by PI3K/AKT signaling in aggressive neuroblastoma. Cancer Res. 73, 2189–2198. https://doi.org/10.1158/0008-5472.CAN-12-3767
Sarry, J.-E., Murphy, K., Perry, R., Sanchez, P.V., Secreto, A., Keefer, C., Swider, C.R., Strzelecki, A.-C., Cavelier, C., Récher, C., Mansat-De Mas, V., Delabesse, E., Danet-Desnoyers, G., Carroll, M., 2011. Human acute myelogenous leukemia stem cells are rare and heterogeneous when assayed in NOD/SCID/IL2Rγc-deficient mice. J. Clin. Invest. 121, 384–395. https://doi.org/10.1172/JCI41495
Sato, T., Yang, X., Knapper, S., White, P., Smith, B.D., Galkin, S., Small, D., Burnett, A., Levis, M., 2011. FLT3 ligand impedes the efficacy of FLT3 inhibitors in vitro and in vivo. Blood 117, 3286–3293. https://doi.org/10.1182/blood-2010-01-266742
Saultz, J.N., Garzon, R., 2016. Acute Myeloid Leukemia: A Concise Review. J. Clin. Med. 5. https://doi.org/10.3390/jcm5030033
Saxton, R.A., Sabatini, D.M., 2017. mTOR Signaling in Growth, Metabolism, and Disease. Cell 168, 960–976. https://doi.org/10.1016/j.cell.2017.02.004

Scheijen, B., Ngo, H.T., Kang, H., Griffin, J.D., 2004. FLT3 receptors with internal tandem duplications promote cell viability and proliferation by signaling through Foxo proteins. Oncogene 23, 3338–3349. https://doi.org/10.1038/sj.onc.1207456

Schlenk, R.F., Weber, D., Fiedler, W., Salih, H.R., Wulf, G., Salwender, H., Schroeder, T., Kindler, T., Lübbert, M., Wolf, D., Westermann, J., Kraemer, D., Götze, K.S., Horst, H.-A., Krauter, J., Girschikofsky, M., Ringhoffer, M., Südhoff, T., Held, G., Derigs, H.-G., Schroers, R., Greil, R., Grießhammer, M., Lange, E., Burchardt, A., Martens, U., Hertenstein, B., Marretta, L., Heuser, M., Thol, F., Gaidzik, V.I., Herr, W., Krzykalla, J., Benner, A., Döhner, K., Ganser, A., Paschka, P., Döhner, H., 2019. Midostaurin added to chemotherapy and continued single-agent maintenance therapy in acute myeloid leukemia with FLT3-ITD. Blood 133, 840–851. https://doi.org/10.1182/blood-2018-08-869453

Schofield, R., 1978. The relationship between the spleen colony-forming cell and the haemopoietic stem cell. Blood Cells 4, 7–25.

Scholl, S., Fleischmann, M., Schnetzke, U., Heidel, F.H., 2020. Molecular Mechanisms of Resistance to FLT3 Inhibitors in Acute Myeloid Leukemia: Ongoing Challenges and Future Treatments. Cells 9, E2493. https://doi.org/10.3390/cells9112493

Schreuder, H., Tardif, C., Trump-Kallmeyer, S., Soffientini, A., Sarubbi, E., Akeson, A., Bowlin, T., Yanofsky, S., Barrett, R.W., 1997. A new cytokine-receptor binding mode revealed by the crystal structure of the IL-1 receptor with an antagonist. Nature 386, 194–200. https://doi.org/10.1038/386194a0

Scott, M.T., Korfi, K., Saffrey, P., Hopcroft, L.E.M., Kinstrie, R., Pellicano, F., Guenther, C., Gallipoli, P., Cruz, M., Dunn, K., Jorgensen, H.G., Cassels, J.E., Hamilton, A., Crossan, A., Sinclair, A., Holyoake, T.L., Vetrie, D., 2016. Epigenetic Reprogramming Sensitizes CML Stem Cells to Combined EZH2 and Tyrosine Kinase Inhibition. Cancer Discov. 6, 1248–1257. https://doi.org/10.1158/2159-8290.CD-16-0263

Scully, R., Panday, A., Elango, R., Willis, N.A., 2019. DNA double strand break repair pathway choice in somatic mammalian cells. Nat. Rev. Mol. Cell Biol. 20, 698–714. https://doi.org/10.1038/s41580-019-0152-0

Seedhouse, C.H., Hunter, H.M., Lloyd-Lewis, B., Massip, A.-M., Pallis, M., Carter, G.I., Grundy, M., Shang, S., Russell, N.H., 2006. DNA repair contributes to the drug-resistant phenotype of primary acute myeloid leukaemia cells with FLT3 internal tandem duplications and is reversed by the FLT3 inhibitor PKC412. Leukemia 20, 2130–2136. https://doi.org/10.1038/sj.leu.2404439

Seita, J., Weissman, I.L., 2010. Hematopoietic stem cell: self-renewal versus differentiation. Wiley Interdiscip. Rev. Syst. Biol. Med. 2, 640–653. https://doi.org/10.1002/wsbm.86

Sekulić, A., Hudson, C.C., Homme, J.L., Yin, P., Otterness, D.M., Karnitz, L.M., Abraham, R.T., 2000. A direct linkage between the phosphoinositide 3-kinase-AKT signaling pathway and the mammalian target of rapamycin in mitogen-stimulated and transformed cells. Cancer Res. 60, 3504–3513.

Sepehrizadeh, Z., Mohammadi, M., Emami, A., Yazdi, M.T., Bozchlou, S.H., Khorramizadeh, M.R., Shapourabadi, M.B., Jaberi, E., Rajaei, N., Setayesh, N., 2014. Assessment of Cytokine Expression Profile in Acute Myeloid Leukemia Patients Before and After Chemotherapy. Turk. J. Hematol. 31, 149–154. https://doi.org/10.4274/tjh.2012.0164

Sexauer, A., Perl, A., Yang, X., Borowitz, M., Gocke, C., Rajkhowa, T., Thiede, C., Frattini, M., Nybakken, G.E., Pratz, K., Karp, J., Smith, B.D., Levis, M., 2012. Terminal myeloid differentiation in vivo is induced by FLT3 inhibition in FLT3/ITD AML. Blood 120, 4205–4214. https://doi.org/10.1182/blood-2012-01-402545

Shafat, M.S., Gnaneswaran, B., Bowles, K.M., Rushworth, S.A., 2017. The bone marrow microenvironment - Home of the leukemic blasts. Blood Rev. 31, 277–286. https://doi.org/10.1016/j.blre.2017.03.004

Shah, K., Moharram, S.A., Kazi, J.U., 2018. Acute leukemia cells resistant to PI3K/mTOR inhibition display upregulation of P2RY14 expression. Clin. Epigenetics 10, 83. https://doi.org/10.1186/s13148-018-0516-x

She, Q.-B., Solit, D.B., Ye, Q., O'Reilly, K.E., Lobo, J., Rosen, N., 2005. The BAD protein integrates survival signaling by EGFR/MAPK and PI3K/Akt kinase pathways in PTEN-deficient tumor cells. Cancer Cell 8, 287–297. https://doi.org/10.1016/j.ccr.2005.09.006

Shen, W.H., Balajee, A.S., Wang, J., Wu, H., Eng, C., Pandolfi, P.P., Yin, Y., 2007. Essential role for nuclear PTEN in maintaining chromosomal integrity. Cell 128, 157–170. https://doi.org/10.1016/j.cell.2006.11.042

Shi, Y., Liu, C.H., Roberts, A.I., Das, J., Xu, G., Ren, G., Zhang, Y., Zhang, L., Yuan, Z.R., Tan, H.S.W., Das, G., Devadas, S., 2006. Granulocyte-macrophage colony-stimulating factor (GM-CSF) and T-cell responses: what we do and don't know. Cell Res. 16, 126–133. https://doi.org/10.1038/sj.cr.7310017

Sillar, J.R., Germon, Z.P., DeIuliis, G.N., Dun, M.D., 2019. The Role of Reactive Oxygen Species in Acute Myeloid Leukaemia. Int. J. Mol. Sci. 20. https://doi.org/10.3390/ijms20236003

Siveen, K.S., Uddin, S., Mohammad, R.M., 2017. Targeting acute myeloid leukemia stem cell signaling by natural products. Mol. Cancer 16, 13. https://doi.org/10.1186/s12943-016-0571-x

Smith, C.C., 2020. FLT3 Inhibition in Acute Myeloid Leukemia. Clin. Lymphoma Myeloma Leuk. 20 Suppl 1, S5–S6. https://doi.org/10.1016/S2152-2650(20)30441-9

Smith, C.C., Lin, K., Stecula, A., Sali, A., Shah, N.P., 2015. FLT3 D835 Mutations Confer Differential Resistance to Type II FLT3 Inhibitors. Leukemia 29, 2390–2392. https://doi.org/10.1038/leu.2015.165

Smith, C.C., Wang, Q., Chin, C.-S., Salerno, S., Damon, L.E., Levis, M.J., Perl, A.E., Travers, K.J., Wang, S., Hunt, J.P., Zarrinkar, P.P., Schadt, E.E., Kasarskis, A., Kuriyan, J., Shah, N.P., 2012. Validation of ITD mutations in FLT3 as a therapeutic target in human acute myeloid leukaemia. Nature 485, 260–263. https://doi.org/10.1038/nature11016

Soares, H.P., Ming, M., Mellon, M., Young, S.H., Han, L., Sinnet-Smith, J., Rozengurt, E., 2015. Dual PI3K/mTOR inhibitors induce rapid over-activation of the MEK/ERK pathway in human pancreatic cancer cells through suppression of mTORC2. Mol. Cancer Ther. 14, 1014–1023. https://doi.org/10.1158/1535-7163.MCT-14-0669

Song, J.H., Padi, S.K.R., Luevano, L.A., Minden, M.D., DeAngelo, D.J., Hardiman, G., Ball, L.E., Warfel, N.A., Kraft, A.S., 2016. Insulin receptor substrate 1 is a substrate of the Pim protein kinases. Oncotarget 7, 20152–20165. https://doi.org/10.18632/oncotarget.7918

Song, J.H., Singh, N., Luevano, L.A., Padi, S.K.R., Okumura, K., Olive, V., Black, S.M., Warfel, N.A., Goodrich, D.W., Kraft, A.S., 2018. Mechanisms Behind Resistance to PI3K Inhibitor Treatment Induced by the PIM Kinase. Mol. Cancer Ther. 17, 2710–2721. https://doi.org/10.1158/1535-7163.MCT-18-0374

Souers, A.J., Leverson, J.D., Boghaert, E.R., Ackler, S.L., Catron, N.D., Chen, J., Dayton, B.D., Ding, H., Enschede, S.H., Fairbrother, W.J., Huang, D.C.S., Hymowitz, S.G., Jin, S., Khaw, S.L., Kovar, P.J., Lam, L.T., Lee, J., Maecker, H.L., Marsh, K.C., Mason, K.D., Mitten, M.J., Nimmer, P.M., Oleksijew, A., Park, C.H., Park, C.-M., Phillips, D.C., Roberts, A.W., Sampath, D., Seymour, J.F., Smith, M.L., Sullivan, G.M., Tahir, S.K., Tse, C., Wendt, M.D., Xiao, Y., Xue, J.C., Zhang, H., Humerickhouse, R.A., Rosenberg, S.H., Elmore, S.W., 2013. ABT-199, a potent and selective BCL-2 inhibitor, achieves antitumor activity while sparing platelets. Nat. Med. 19, 202–208. https://doi.org/10.1038/nm.3048

Spangle, J.M., Roberts, T.M., Zhao, J.J., 2017. The emerging role of PI3K/AKT-mediated epigenetic regulation in cancer. Biochim. Biophys. Acta Rev. Cancer 1868, 123–131. https://doi.org/10.1016/j.bbcan.2017.03.002

Spencer, A., Yoon, S.-S., Harrison, S.J., Morris, S.R., Smith, D.A., Brigandi, R.A., Gauvin, J., Kumar, R., Opalinska, J.B., Chen, C., 2014. The novel AKT inhibitor afuresertib shows favorable safety, pharmacokinetics, and clinical activity in multiple myeloma. Blood 124, 2190–2195. https://doi.org/10.1182/blood-2014-03-559963

Spencer, J.A., Ferraro, F., Roussakis, E., Klein, A., Wu, J., Runnels, J.M., Zaher, W., Mortensen, L.J., Alt, C., Turcotte, R., Yusuf, R., Côté, D., Vinogradov, S.A., Scadden, D.T., Lin, C.P., 2014. Direct measurement of local oxygen concentration in the bone marrow of live animals. Nature 508, 269–273. https://doi.org/10.1038/nature13034

Spiekermann, K., Bagrintseva, K., Schwab, R., Schmieja, K., Hiddemann, W., 2003. Overexpression and constitutive activation of FLT3 induces STAT5 activation in primary acute myeloid leukemia blast cells. Clin. Cancer Res. Off. J. Am. Assoc. Cancer Res. 9, 2140–2150.

Standal, T., Borset, M., Sundan, A., 2004. Role of osteopontin in adhesion, migration, cell survival and bone remodeling. Exp. Oncol. 26, 179–184.
Stanicka, J., Russell, E.G., Woolley, J.F., Cotter, T.G., 2015. NADPH oxidase-generated hydrogen peroxide induces DNA damage in mutant FLT3-expressing leukemia cells. J. Biol. Chem. 290, 9348–9361. https://doi.org/10.1074/jbc.M113.510495
Stemke-Hale, K., Gonzalez-Angulo, A.M., Lluch, A., Neve, R.M., Kuo, W.-L., Davies, M., Carey, M., Hu, Z., Guan, Y., Sahin, A., Symmans, W.F., Pusztai, L., Nolden, L.K., Horlings, H., Berns, K., Hung, M.-C., van de Vijver, M.J., Valero, V., Gray, J.W., Bernards, R., Mills, G.B., Hennessy, B.T., 2008. An integrative genomic and proteomic analysis of PIK3CA, PTEN, and AKT mutations in breast cancer. Cancer Res. 68, 6084–6091. https://doi.org/10.1158/0008-5472.CAN-07-6854
Stevens, A.M., Miller, J.M., Munoz, J.O., Gaikwad, A.S., Redell, M.S., 2017. Interleukin-6 levels predict event-free survival in pediatric AML and suggest a mechanism of chemotherapy resistance. Blood Adv. 1, 1387–1397. https://doi.org/10.1182/bloodadvances.2017007856
Stier, S., Ko, Y., Forkert, R., Lutz, C., Neuhaus, T., Grünewald, E., Cheng, T., Dombkowski, D., Calvi, L.M., Rittling, S.R., Scadden, D.T., 2005. Osteopontin is a hematopoietic stem cell niche component that negatively regulates stem cell pool size. J. Exp. Med. 201, 1781–1791. https://doi.org/10.1084/jem.20041992
Stirewalt, D.L., Kopecky, K.J., Meshinchi, S., Engel, J.H., Pogosova-Agadjanyan, E.L., Linsley, J., Slovak, M.L., Willman, C.L., Radich, J.P., 2006. Size of FLT3 internal tandem duplication has prognostic significance in patients with acute myeloid leukemia. Blood 107, 3724–3726. https://doi.org/10.1182/blood-2005-08-3453
Stirewalt, D.L., Radich, J.P., 2003. The role of FLT3 in haematopoietic malignancies. Nat. Rev. Cancer 3, 650–665. https://doi.org/10.1038/nrc1169
Stone, R.M., Mandrekar, S.J., Sanford, B.L., Laumann, K., Geyer, S., Bloomfield, C.D., Thiede, C., Prior, T.W., Döhner, K., Marcucci, G., Lo-Coco, F., Klisovic, R.B., Wei, A., Sierra, J., Sanz, M.A., Brandwein, J.M., de Witte, T., Niederwieser, D., Appelbaum, F.R., Medeiros, B.C., Tallman, M.S., Krauter, J., Schlenk, R.F., Ganser, A., Serve, H., Ehninger, G., Amadori, S., Larson, R.A., Döhner, H., 2017. Midostaurin plus Chemotherapy for Acute Myeloid Leukemia with a FLT3 Mutation. N. Engl. J. Med. 377, 454–464. https://doi.org/10.1056/NEJMoa1614359
Stucki, A., Rivier, A.-S., Gikic, M., Monai, N., Schapira, M., Spertini, O., 2001. Endothelial cell activation by myeloblasts: molecular mechanisms of leukostasis and leukemic cell dissemination. Blood 97, 2121–2129. https://doi.org/10.1182/blood.V97.7.2121
Su, Y., Li, X., Ma, J., Zhao, J., Liu, S., Wang, G., Edwards, H., Taub, J.W., Lin, H., Ge, Y., 2018. Targeting PI3K, mTOR, ERK, and Bcl-2 signaling network shows superior antileukemic activity against AML ex vivo. Biochem. Pharmacol. 148, 13–26. https://doi.org/10.1016/j.bcp.2017.11.022
Sugiyama, H., Inoue, K., Ogawa, H., Yamagami, T., Soma, T., Miyake, S., Hirata, M., Kishimoto, T., 1996. The expression of IL-6 and its related genes in acute leukemia. Leuk. Lymphoma 21, 49–52. https://doi.org/10.3109/10428199609067579
Suire, S., Coadwell, J., Ferguson, G.J., Davidson, K., Hawkins, P., Stephens, L., 2005. p84, a new Gbetagamma-activated regulatory subunit of the type IB phosphoinositide 3-kinase p110gamma. Curr. Biol. CB 15, 566–570. https://doi.org/10.1016/j.cub.2005.02.020
Sujobert, P., Bardet, V., Cornillet-Lefebvre, P., Hayflick, J.S., Prie, N., Verdier, F., Vanhaesebroeck, B., Muller, O., Pesce, F., Ifrah, N., Hunault-Berger, M., Berthou, C., Villemagne, B., Jourdan, E., Audhuy, B., Solary, E., Witz, B., Harousseau, J.L., Himberlin, C., Lamy, T., Lioure, B., Cahn, J.Y., Dreyfus, F., Mayeux, P., Lacombe, C., Bouscary, D., 2005. Essential role for the p110delta isoform in phosphoinositide 3-kinase activation and cell proliferation in acute myeloid leukemia. Blood 106, 1063–1066. https://doi.org/10.1182/blood-2004-08-3225
Sung, P.J., Sugita, M., Koblish, H., Perl, A.E., Carroll, M., 2019. Hematopoietic cytokines mediate resistance to targeted therapy in FLT3-ITD acute myeloid leukemia. Blood Adv. 3, 1061–1072. https://doi.org/10.1182/bloodadvances.2018029850
Swaminathan, M., Kantarjian, H.M., Levis, M., Guerra, V., Borthakur, G., Alvarado, Y., DiNardo, C.D., Kadia, T., Garcia-Manero, G., Ohanian, M., Daver, N., Konopleva, M., Pemmaraju,

N., Ferrajoli, A., Andreeff, M., Jain, N., Estrov, Z., Jabbour, E.J., Wierda, W.G., Pierce, S., Pinsoy, M.R., Xiao, L., Ravandi, F., Cortes, J.E., 2021. A phase I/II study of the combination of quizartinib with azacitidine or low-dose cytarabine for the treatment of patients with acute myeloid leukemia and myelodysplastic syndrome. Haematologica 106, 2121–2130. https://doi.org/10.3324/haematol.2020.263392

Szade, K., Gulati, G.S., Chan, C.K.F., Kao, K.S., Miyanishi, M., Marjon, K.D., Sinha, R., George, B.M., Chen, J.Y., Weissman, I.L., 2018. Where Hematopoietic Stem Cells Live: The Bone Marrow Niche. Antioxid. Redox Signal. 29, 191–204. https://doi.org/10.1089/ars.2017.7419

Taichman, R.S., Emerson, S.G., 1994. Human osteoblasts support hematopoiesis through the production of granulocyte colony-stimulating factor. J. Exp. Med. 179, 1677–1682. https://doi.org/10.1084/jem.179.5.1677

Takahashi, S., 2011. Downstream molecular pathways of FLT3 in the pathogenesis of acute myeloid leukemia: biology and therapeutic implications. J. Hematol. Oncol.J Hematol Oncol 4, 13. https://doi.org/10.1186/1756-8722-4-13

Tamburini, J., Chapuis, N., Bardet, V., Park, S., Sujobert, P., Willems, L., Ifrah, N., Dreyfus, F., Mayeux, P., Lacombe, C., Bouscary, D., 2008. Mammalian target of rapamycin (mTOR) inhibition activates phosphatidylinositol 3-kinase/Akt by up-regulating insulin-like growth factor-1 receptor signaling in acute myeloid leukemia: rationale for therapeutic inhibition of both pathways. Blood 111, 379–382. https://doi.org/10.1182/blood-2007-03-080796

Tamburini, J., Green, A.S., Bardet, V., Chapuis, N., Park, S., Willems, L., Uzunov, M., Ifrah, N., Dreyfus, F., Lacombe, C., Mayeux, P., Bouscary, D., 2009. Protein synthesis is resistant to rapamycin and constitutes a promising therapeutic target in acute myeloid leukemia. Blood 114, 1618–1627. https://doi.org/10.1182/blood-2008-10-184515

Tan, P., Tiong, I.S., Fleming, S., Pomilio, G., Cummings, N., Droogleever, M., McManus, J., Schwarer, A., Catalano, J., Patil, S., Avery, S., Spencer, A., Wei, A., 2017. The mTOR inhibitor everolimus in combination with azacitidine in patients with relapsed/refractory acute myeloid leukemia: a phase Ib/II study. Oncotarget 8, 52269–52280. https://doi.org/10.18632/oncotarget.13699

Taussig, D.C., Vargaftig, J., Miraki-Moud, F., Griessinger, E., Sharrock, K., Luke, T., Lillington, D., Oakervee, H., Cavenagh, J., Agrawal, S.G., Lister, T.A., Gribben, J.G., Bonnet, D., 2010. Leukemia-initiating cells from some acute myeloid leukemia patients with mutated nucleophosmin reside in the CD34(-) fraction. Blood 115, 1976–1984. https://doi.org/10.1182/blood-2009-02-206565

Taylor, J., Xiao, W., Abdel-Wahab, O., 2017. Diagnosis and classification of hematologic malignancies on the basis of genetics. Blood 130, 410–423. https://doi.org/10.1182/blood-2017-02-734541

Teh, T.-C., Nguyen, N.-Y., Moujalled, D.M., Segal, D., Pomilio, G., Rijal, S., Jabbour, A., Cummins, K., Lackovic, K., Blombery, P., Thompson, E., Ekert, P.G., Lessene, G., Glaser, S.P., Huang, D.C.S., Roberts, A.W., Guthridge, M.A., Wei, A.H., 2018. Enhancing venetoclax activity in acute myeloid leukemia by co-targeting MCL1. Leukemia 32, 303–312. https://doi.org/10.1038/leu.2017.243

Testa, U., Pelosi, E., Castelli, G., 2019. CD123 as a Therapeutic Target in the Treatment of Hematological Malignancies. Cancers 11, 1358. https://doi.org/10.3390/cancers11091358

Thépot, S., Lainey, E., Cluzeau, T., Sébert, M., Leroy, C., Adès, L., Tailler, M., Galluzzi, L., Baran-Marszak, F., Roudot, H., Eclache, V., Gardin, C., de Botton, S., Auberger, P., Fenaux, P., Kroemer, G., Boehrer, S., 2011. Hypomethylating agents reactivate FOXO3A in acute myeloid leukemia. Cell Cycle Georget. Tex 10, 2323–2330. https://doi.org/10.4161/cc.10.14.16399

Thomas, D., Majeti, R., 2017. Biology and relevance of human acute myeloid leukemia stem cells. Blood 129, 1577–1585. https://doi.org/10.1182/blood-2016-10-696054

Thomas, X., Hirschauer, C., Troncy, J., Assouline, D., Joly, M.O., Fiere, D., Archimbaud, E., 1997. Serum interleukin-6 levels in adult acute myelogenous leukemia: relationship with disease characteristics and outcome. Leuk. Lymphoma 24, 291–300. https://doi.org/10.3109/10428199709039016

Tiong, I.S., Tan, P., McManus, J., Cummings, N., Sadawarte, S., Catalano, J., Hills, R., Wei, A., 2018. Phase Ib study of the mTOR inhibitor everolimus with low dose cytarabine in elderly

acute myeloid leukemia. Leuk. Lymphoma 59, 493–496. https://doi.org/10.1080/10428194.2017.1334122
Toker, A., Marmiroli, S., 2014. Signaling Specificity in the Akt Pathway in Biology and Disease. Adv. Biol. Regul. 0, 28–38. https://doi.org/10.1016/j.jbior.2014.04.001
Tolcher, A.W., Patnaik, A., Papadopoulos, K.P., Rasco, D.W., Becerra, C.R., Allred, A.J., Orford, K., Aktan, G., Ferron-Brady, G., Ibrahim, N., Gauvin, J., Motwani, M., Cornfeld, M., 2015. Phase I study of the MEK inhibitor trametinib in combination with the AKT inhibitor afuresertib in patients with solid tumors and multiple myeloma. Cancer Chemother. Pharmacol. 75, 183–189. https://doi.org/10.1007/s00280-014-2615-5
Tong, L., Chuang, C.-C., Wu, S., Zuo, L., 2015. Reactive oxygen species in redox cancer therapy. Cancer Lett. 367, 18–25. https://doi.org/10.1016/j.canlet.2015.07.008
Tothova, Z., Gilliland, D.G., 2007. FoxO transcription factors and stem cell homeostasis: insights from the hematopoietic system. Cell Stem Cell 1, 140–152. https://doi.org/10.1016/j.stem.2007.07.017
Tothova, Z., Kollipara, R., Huntly, B.J., Lee, B.H., Castrillon, D.H., Cullen, D.E., McDowell, E.P., Lazo-Kallanian, S., Williams, I.R., Sears, C., Armstrong, S.A., Passegué, E., DePinho, R.A., Gilliland, D.G., 2007. FoxOs are critical mediators of hematopoietic stem cell resistance to physiologic oxidative stress. Cell 128, 325–339. https://doi.org/10.1016/j.cell.2007.01.003
Tsao, T., Shi, Y., Kornblau, S., Lu, H., Konoplev, S., Antony, A., Ruvolo, V., Qiu, Y.H., Zhang, N., Coombes, K.R., Andreeff, M., Kojima, K., Konopleva, M., 2012. Concomitant inhibition of DNA methyltransferase and BCL-2 protein function synergistically induce mitochondrial apoptosis in acute myelogenous leukemia cells. Ann. Hematol. 91, 1861–1870. https://doi.org/10.1007/s00277-012-1537-8
Turzanski, J., Grundy, M., Russell, N.H., Pallis, M., 2004. Interleukin-1beta maintains an apoptosis-resistant phenotype in the blast cells of acute myeloid leukaemia via multiple pathways. Leukemia 18, 1662–1670. https://doi.org/10.1038/sj.leu.2403457
Tutt, A., Robson, M., Garber, J.E., Domchek, S.M., Audeh, M.W., Weitzel, J.N., Friedlander, M., Arun, B., Loman, N., Schmutzler, R.K., Wardley, A., Mitchell, G., Earl, H., Wickens, M., Carmichael, J., 2010. Oral poly(ADP-ribose) polymerase inhibitor olaparib in patients with BRCA1 or BRCA2 mutations and advanced breast cancer: a proof-of-concept trial. Lancet Lond. Engl. 376, 235–244. https://doi.org/10.1016/S0140-6736(10)60892-6
Uy, G.L., Rettig, M.P., Motabi, I.H., McFarland, K., Trinkaus, K.M., Hladnik, L.M., Kulkarni, S., Abboud, C.N., Cashen, A.F., Stockerl-Goldstein, K.E., Vij, R., Westervelt, P., DiPersio, J.F., 2012. A phase 1/2 study of chemosensitization with the CXCR4 antagonist plerixafor in relapsed or refractory acute myeloid leukemia. Blood 119, 3917–3924. https://doi.org/10.1182/blood-2011-10-383406
Vachhani, P., Bose, P., Rahmani, M., Grant, S., 2014. Rational combination of dual PI3K/mTOR blockade and Bcl-2/-xL inhibition in AML. Physiol. Genomics 46, 448–456. https://doi.org/10.1152/physiolgenomics.00173.2013
Vadas, O., Burke, J.E., Zhang, X., Berndt, A., Williams, R.L., 2011. Structural basis for activation and inhibition of class I phosphoinositide 3-kinases. Sci. Signal. 4, re2. https://doi.org/10.1126/scisignal.2002165
Vainchenker, W., Constantinescu, S.N., 2013. JAK/STAT signaling in hematological malignancies. Oncogene 32, 2601–2613. https://doi.org/10.1038/onc.2012.347
van Alphen, C., Cloos, J., Beekhof, R., Cucchi, D.G.J., Piersma, S.R., Knol, J.C., Henneman, A.A., Pham, T.V., van Meerloo, J., Ossenkoppele, G.J., Verheul, H.M.W., Janssen, J.J.W.M., Jimenez, C.R., 2020. Phosphotyrosine-based Phosphoproteomics for Target Identification and Drug Response Prediction in AML Cell Lines*. Mol. Cell. Proteomics 19, 884–899. https://doi.org/10.1074/mcp.RA119.001504
van Gils, N., Denkers, F., Smit, L., 2021. Escape From Treatment; the Different Faces of Leukemic Stem Cells and Therapy Resistance in Acute Myeloid Leukemia. Front. Oncol. 11, 1454. https://doi.org/10.3389/fonc.2021.659253
van Rhenen, A., van Dongen, G.A.M.S., Kelder, A., Rombouts, E.J., Feller, N., Moshaver, B., Stigter-van Walsum, M., Zweegman, S., Ossenkoppele, G.J., Jan Schuurhuis, G., 2007. The novel AML stem cell associated antigen CLL-1 aids in discrimination between normal

and leukemic stem cells. Blood 110, 2659–2666. https://doi.org/10.1182/blood-2007-03-083048
Vanhaesebroeck, B., Guillermet-Guibert, J., Graupera, M., Bilanges, B., 2010. The emerging mechanisms of isoform-specific PI3K signalling. Nat. Rev. Mol. Cell Biol. 11, 329–341. https://doi.org/10.1038/nrm2882
Vargaftig, J., Farhat, H., Ades, L., Briaux, A., Benoist, C., Turbiez, I., Vey, N., Glaisner, S., Callens, C., 2018. Phase 2 Trial of Single Agent Gedatolisib (PF-05212384), a Dual PI3K/mTOR Inhibitor, for Adverse Prognosis and Relapse/Refractory AML: Clinical and Transcriptomic Results. Blood 132, 5233–5233. https://doi.org/10.1182/blood-2018-99-117485
Vazquez, F., Grossman, S.R., Takahashi, Y., Rokas, M.V., Nakamura, N., Sellers, W.R., 2001. Phosphorylation of the PTEN tail acts as an inhibitory switch by preventing its recruitment into a protein complex. J. Biol. Chem. 276, 48627–48630. https://doi.org/10.1074/jbc.C100556200
Velten, L., Story, B.A., Hernández-Malmierca, P., Raffel, S., Leonce, D.R., Milbank, J., Paulsen, M., Demir, A., Szu-Tu, C., Frömel, R., Lutz, C., Nowak, D., Jann, J.-C., Pabst, C., Boch, T., Hofmann, W.-K., Müller-Tidow, C., Trumpp, A., Haas, S., Steinmetz, L.M., 2021. Identification of leukemic and pre-leukemic stem cells by clonal tracking from single-cell transcriptomics. Nat. Commun. 12, 1366. https://doi.org/10.1038/s41467-021-21650-1
Venkatesan, A.M., Dehnhardt, C.M., Delos Santos, E., Chen, Z., Dos Santos, O., Ayral-Kaloustian, S., Khafizova, G., Brooijmans, N., Mallon, R., Hollander, I., Feldberg, L., Lucas, J., Yu, K., Gibbons, J., Abraham, R.T., Chaudhary, I., Mansour, T.S., 2010. Bis(morpholino-1,3,5-triazine) derivatives: potent adenosine 5'-triphosphate competitive phosphatidylinositol-3-kinase/mammalian target of rapamycin inhibitors: discovery of compound 26 (PKI-587), a highly efficacious dual inhibitor. J. Med. Chem. 53, 2636–2645. https://doi.org/10.1021/jm901830p
Vetrie, D., Helgason, G.V., Copland, M., 2020. The leukaemia stem cell: similarities, differences and clinical prospects in CML and AML. Nat. Rev. Cancer 20, 158–173. https://doi.org/10.1038/s41568-019-0230-9
Villatoro, A., Konieczny, J., Cuminetti, V., Arranz, L., 2020. Leukemia Stem Cell Release From the Stem Cell Niche to Treat Acute Myeloid Leukemia. Front. Cell Dev. Biol. 8, 607. https://doi.org/10.3389/fcell.2020.00607
Visser, O., Trama, A., Maynadié, M., Stiller, C., Marcos-Gragera, R., De Angelis, R., Mallone, S., Tereanu, C., Allemani, C., Ricardi, U., Schouten, H.C., RARECARE Working Group, 2012. Incidence, survival and prevalence of myeloid malignancies in Europe. Eur. J. Cancer Oxf. Engl. 1990 48, 3257–3266. https://doi.org/10.1016/j.ejca.2012.05.024
Vukovic, M., Guitart, A.V., Sepulveda, C., Villacreces, A., O'Duibhir, E., Panagopoulou, T.I., Ivens, A., Menendez-Gonzalez, J., Iglesias, J.M., Allen, L., Glykofrydis, F., Subramani, C., Armesilla-Diaz, A., Post, A.E.M., Schaak, K., Gezer, D., So, C.W.E., Holyoake, T.L., Wood, A., O'Carroll, D., Ratcliffe, P.J., Kranc, K.R., 2015. Hif-1α and Hif-2α synergize to suppress AML development but are dispensable for disease maintenance. J. Exp. Med. 212, 2223–2234. https://doi.org/10.1084/jem.20150452
Wagner, F., Henningsen, B., Lederer, C., Eichenmüller, M., Gödeke, J., Müller-Höcker, J., von Schweinitz, D., Kappler, R., 2012. Rapamycin blocks hepatoblastoma growth in vitro and in vivo implicating new treatment options in high-risk patients. Eur. J. Cancer Oxf. Engl. 1990 48, 2442–2450. https://doi.org/10.1016/j.ejca.2011.12.032
Wainberg, Z.A., Alsina, M., Soares, H.P., Braña, I., Britten, C.D., Del Conte, G., Ezeh, P., Houk, B., Kern, K.A., Leong, S., Pathan, N., Pierce, K.J., Siu, L.L., Vermette, J., Tabernero, J., 2017. A Multi-Arm Phase I Study of the PI3K/mTOR Inhibitors PF-04691502 and Gedatolisib (PF-05212384) plus Irinotecan or the MEK Inhibitor PD-0325901 in Advanced Cancer. Target. Oncol. 12, 775–785. https://doi.org/10.1007/s11523-017-0530-5
Wan, X., Harkavy, B., Shen, N., Grohar, P., Helman, L.J., 2007. Rapamycin induces feedback activation of Akt signaling through an IGF-1R-dependent mechanism. Oncogene 26, 1932–1940. https://doi.org/10.1038/sj.onc.1209990
Wander, S.A., Levis, M.J., Fathi, A.T., 2014. The evolving role of FLT3 inhibitors in acute myeloid leukemia: quizartinib and beyond. Ther. Adv. Hematol. 5, 65–77. https://doi.org/10.1177/2040620714532123

Wang, D., Li, C., Zhang, Y., Wang, M., Jiang, N., Xiang, L., Li, T., Roberts, T.M., Zhao, J.J., Cheng, H., Liu, P., 2016. Combined inhibition of PI3K and PARP is effective in the treatment of ovarian cancer cells with wild-type PIK3CA genes. Gynecol. Oncol. 142, 548–556. https://doi.org/10.1016/j.ygyno.2016.07.092

Wang, F., Liu, Z., Zeng, J., Zhu, H., Li, J., Cheng, X., Jiang, T., Zhang, L., Zhang, C., Chen, T., Liu, T., Jia, Y., 2015. Metformin synergistically sensitizes FLT3-ITD-positive acute myeloid leukemia to sorafenib by promoting mTOR-mediated apoptosis and autophagy. Leuk. Res. 39, 1421–1427. https://doi.org/10.1016/j.leukres.2015.09.016

Wang, J.M., Chao, J.R., Chen, W., Kuo, M.L., Yen, J.J., Yang-Yen, H.F., 1999. The antiapoptotic gene mcl-1 is up-regulated by the phosphatidylinositol 3-kinase/Akt signaling pathway through a transcription factor complex containing CREB. Mol. Cell. Biol. 19, 6195–6206. https://doi.org/10.1128/mcb.19.9.6195

Wang, L., Chen, Y., Sternberg, P., Cai, J., 2008. Essential Roles of the PI3 Kinase/Akt Pathway in Regulating Nrf2-Dependent Antioxidant Functions in the RPE. Invest. Ophthalmol. Vis. Sci. 49, 1671–1678. https://doi.org/10.1167/iovs.07-1099

Wang, X., Huang, S., Chen, J.-L., 2017. Understanding of leukemic stem cells and their clinical implications. Mol. Cancer 16, 2. https://doi.org/10.1186/s12943-016-0574-7

Wang, Y., Krivtsov, A.V., Sinha, A.U., North, T.E., Goessling, W., Feng, Z., Zon, L.I., Armstrong, S.A., 2010. The Wnt/β-catenin Pathway Is Required for the Development of Leukemia Stem Cells in AML. Science 327, 1650–1653. https://doi.org/10.1126/science.1186624

Wang, Y., Sun, X., Yuan, S., Hou, S., Guo, T., Chu, Y., Pang, T., Luo, H.R., Yuan, W., Wang, X., 2020. Interleukin-1β inhibits normal hematopoietic expansion and promotes acute myeloid leukemia progression via the bone marrow niche. Cytotherapy 22, 127–134. https://doi.org/10.1016/j.jcyt.2020.01.001

Watanabe, D., Nogami, A., Okada, K., Akiyama, H., Umezawa, Y., Miura, O., 2019. FLT3-ITD Activates RSK1 to Enhance Proliferation and Survival of AML Cells by Activating mTORC1 and eIF4B Cooperatively with PIM or PI3K and by Inhibiting Bad and BIM. Cancers 11. https://doi.org/10.3390/cancers11121827

Wei, A.H., Strickland, S.A., Hou, J.-Z., Fiedler, W., Lin, T.L., Walter, R.B., Enjeti, A., Tiong, I.S., Savona, M., Lee, S., Chyla, B., Popovic, R., Salem, A.H., Agarwal, S., Xu, T., Fakouhi, K.M., Humerickhouse, R., Hong, W.-J., Hayslip, J., Roboz, G.J., 2019. Venetoclax Combined With Low-Dose Cytarabine for Previously Untreated Patients With Acute Myeloid Leukemia: Results From a Phase Ib/II Study. J. Clin. Oncol. Off. J. Am. Soc. Clin. Oncol. 37, 1277–1284. https://doi.org/10.1200/JCO.18.01600

Weisberg, E., Liu, Q., Nelson, E., Kung, A.L., Christie, A.L., Bronson, R., Sattler, M., Sanda, T., Zhao, Z., Hur, W., Mitsiades, C., Smith, R., Daley, J.F., Stone, R., Galinsky, I., Griffin, J.D., Gray, N., 2012. Using combination therapy to override stromal-mediated chemoresistance in mutant FLT3-positive AML: synergism between FLT3 inhibitors, dasatinib/multi-targeted inhibitors and JAK inhibitors. Leukemia 26, 2233–2244. https://doi.org/10.1038/leu.2012.96

Weisberg, E., Liu, Q., Zhang, X., Nelson, E., Sattler, M., Liu, F., Nicolais, M., Zhang, J., Mitsiades, C., Smith, R.W., Stone, R., Galinsky, I., Nonami, A., Griffin, J.D., Gray, N., 2013. Selective Akt inhibitors synergize with tyrosine kinase inhibitors and effectively override stroma-associated cytoprotection of mutant FLT3-positive AML cells. PloS One 8, e56473. https://doi.org/10.1371/journal.pone.0056473

Welch, J.S., Ley, T.J., Link, D.C., Miller, C.A., Larson, D.E., Koboldt, D.C., Wartman, L.D., Lamprecht, T.L., Liu, F., Xia, J., Kandoth, C., Fulton, R.S., McLellan, M.D., Dooling, D.J., Wallis, J.W., Chen, K., Harris, C.C., Schmidt, H.K., Kalicki-Veizer, J.M., Lu, C., Zhang, Q., Lin, L., O'Laughlin, M.D., McMichael, J.F., Delehaunty, K.D., Fulton, L.A., Magrini, V.J., McGrath, S.D., Demeter, R.T., Vickery, T.L., Hundal, J., Cook, L.L., Swift, G.W., Reed, J.P., Alldredge, P.A., Wylie, T.N., Walker, J.R., Watson, M.A., Heath, S.E., Shannon, W.D., Varghese, N., Nagarajan, R., Payton, J.E., Baty, J.D., Kulkarni, S., Klco, J.M., Tomasson, M.H., Westervelt, P., Walter, M.J., Graubert, T.A., DiPersio, J.F., Ding, L., Mardis, E.R., Wilson, R.K., 2012. The origin and evolution of mutations in acute myeloid leukemia. Cell 150, 264–278. https://doi.org/10.1016/j.cell.2012.06.023

Weldetsadik, A.T., 2013. Clinical characteristics of patients with hematological malignancies at gondar university hospital, North West Ethiopia. Ethiop. Med. J. 51, 25–31.

Willis, S.N., Chen, L., Dewson, G., Wei, A., Naik, E., Fletcher, J.I., Adams, J.M., Huang, D.C.S., 2005. Proapoptotic Bak is sequestered by Mcl-1 and Bcl-xL, but not Bcl-2, until displaced by BH3-only proteins. Genes Dev. 19, 1294–1305. https://doi.org/10.1101/gad.1304105

Wingelhofer, B., Maurer, B., Heyes, E.C., Cumaraswamy, A.A., Berger-Becvar, A., de Araujo, E.D., Orlova, A., Freund, P., Ruge, F., Park, J., Tin, G., Ahmar, S., Lardeau, C.-H., Sadovnik, I., Bajusz, D., Keserű, G.M., Grebien, F., Kubicek, S., Valent, P., Gunning, P.T., Moriggl, R., 2018. Pharmacologic inhibition of STAT5 in acute myeloid leukemia. Leukemia 32, 1135–1146. https://doi.org/10.1038/s41375-017-0005-9

Wittwer, N.L., Brumatti, G., Marchant, C., Sandow, J.J., Pudney, M.K., Dottore, M., D'Andrea, R.J., Lopez, A.F., Ekert, P.G., Ramshaw, H.S., 2017. High CD123 levels enhance proliferation in response to IL-3, but reduce chemotaxis by downregulating CXCR4 expression. Blood Adv. 1, 1067–1079. https://doi.org/10.1182/bloodadvances.2016002931

Wright, S.C.E., Vasilevski, N., Serra, V., Rodon, J., Eichhorn, P.J.A., 2021. Mechanisms of Resistance to PI3K Inhibitors in Cancer: Adaptive Responses, Drug Tolerance and Cellular Plasticity. Cancers 13, 1538. https://doi.org/10.3390/cancers13071538

Wunderle, L., Badura, S., Lang, F., Wolf, A., Schleyer, E., Serve, H., Goekbuget, N., Pfeifer, H., Bug, G., Ottmann, O.G., 2013. Safety and Efficacy Of BEZ235, a Dual PI3-Kinase /mTOR Inhibitor, In Adult Patients With Relapsed Or Refractory Acute Leukemia: Results Of a Phase I Study. Blood 122, 2675–2675. https://doi.org/10.1182/blood.V122.21.2675.2675

Xia, B., Tian, C., Guo, S., Zhang, L., Zhao, D., Qu, F., Zhao, W., Wang, Y., Wu, X., Da, W., Wei, S., Zhang, Y., 2015. c-Myc plays part in drug resistance mediated by bone marrow stromal cells in acute myeloid leukemia. Leuk. Res. 39, 92–99. https://doi.org/10.1016/j.leukres.2014.11.004

Xiang, Z., Luo, H., Payton, J.E., Cain, J., Ley, T.J., Opferman, J.T., Tomasson, M.H., 2010. Mcl1 haploinsufficiency protects mice from Myc-induced acute myeloid leukemia. J. Clin. Invest. 120, 2109–2118. https://doi.org/10.1172/JCI39964

Xing, Y., Lin, N.U., Maurer, M.A., Chen, H., Mahvash, A., Sahin, A., Akcakanat, A., Li, Y., Abramson, V., Litton, J., Chavez-MacGregor, M., Valero, V., Piha-Paul, S.A., Hong, D., Do, K.-A., Tarco, E., Riall, D., Eterovic, A.K., Wulf, G.M., Cantley, L.C., Mills, G.B., Doyle, L.A., Winer, E., Hortobagyi, G.N., Gonzalez-Angulo, A.M., Meric-Bernstam, F., 2019. Phase II trial of AKT inhibitor MK-2206 in patients with advanced breast cancer who have tumors with PIK3CA or AKT mutations, and/or PTEN loss/PTEN mutation. Breast Cancer Res. BCR 21, 78. https://doi.org/10.1186/s13058-019-1154-8

Xu, M., Skaug, B., Zeng, W., Chen, Z.J., 2009. A ubiquitin replacement strategy in human cells reveals distinct mechanisms of IKK activation by TNFalpha and IL-1beta. Mol. Cell 36, 302–314. https://doi.org/10.1016/j.molcel.2009.10.002

Xu, Q., Simpson, S.-E., Scialla, T.J., Bagg, A., Carroll, M., 2003. Survival of acute myeloid leukemia cells requires PI3 kinase activation. Blood 102, 972–980. https://doi.org/10.1182/blood-2002-11-3429

Xu, Q., Thompson, J.E., Carroll, M., 2005. mTOR regulates cell survival after etoposide treatment in primary AML cells. Blood 106, 4261–4268. https://doi.org/10.1182/blood-2004-11-4468

Yalniz, F., Abou Dalle, I., Kantarjian, H., Borthakur, G., Kadia, T., Patel, K., Loghavi, S., Garcia-Manero, G., Sasaki, K., Daver, N., DiNardo, C., Pemmaraju, N., Short, N.J., Yilmaz, M., Bose, P., Naqvi, K., Pierce, S., Nogueras González, G.M., Konopleva, M., Andreeff, M., Cortes, J., Ravandi, F., 2019. Prognostic significance of baseline FLT3-ITD mutant allele level in acute myeloid leukemia treated with intensive chemotherapy with/without sorafenib. Am. J. Hematol. 94, 984–991. https://doi.org/10.1002/ajh.25553

Yang, G., Murashige, D.S., Humphrey, S.J., James, D.E., 2015. A Positive Feedback Loop between Akt and mTORC2 via SIN1 Phosphorylation. Cell Rep. 12, 937–943. https://doi.org/10.1016/j.celrep.2015.07.016

Yang, H., Rudge, D.G., Koos, J.D., Vaidialingam, B., Yang, H.J., Pavletich, N.P., 2013. mTOR kinase structure, mechanism and regulation. Nature 497, 217–223. https://doi.org/10.1038/nature12122

Yang, J., Nie, J., Ma, X., Wei, Y., Peng, Y., Wei, X., 2019. Targeting PI3K in cancer: mechanisms and advances in clinical trials. Mol. Cancer 18, 26. https://doi.org/10.1186/s12943-019-0954-x

Yang, J.-Y., Zong, C.S., Xia, W., Yamaguchi, H., Ding, Q., Xie, X., Lang, J.-Y., Lai, C.-C., Chang, C.-J., Huang, W.-C., Huang, H., Kuo, H.-P., Lee, D.-F., Li, L.-Y., Lien, H.-C., Cheng, X., Chang, K.-J., Hsiao, C.-D., Tsai, F.-J., Tsai, C.-H., Sahin, A.A., Muller, W.J., Mills, G.B., Yu, D., Hortobagyi, G.N., Hung, M.-C., 2008. ERK promotes tumorigenesis by inhibiting FOXO3a via MDM2-mediated degradation. Nat. Cell Biol. 10, 138–148. https://doi.org/10.1038/ncb1676

Yang, L., Yang, G., Ding, Y., Huang, Y., Liu, S., Zhou, L., Wei, W., Wang, J., Hu, G., 2018. Combined treatment with PI3K inhibitor BKM120 and PARP inhibitor olaparib is effective in inhibiting the gastric cancer cells with ARID1A deficiency. Oncol. Rep. 40, 479–487. https://doi.org/10.3892/or.2018.6445

Yang, Q., Jiang, W., Hou, P., 2019. Emerging role of PI3K/AKT in tumor-related epigenetic regulation. Semin. Cancer Biol. 59, 112–124. https://doi.org/10.1016/j.semcancer.2019.04.001

Yang, S., Li, X., Guan, W., Qian, M., Yao, Z., Yin, X., Zhao, H., 2017. NVP-BKM120 inhibits colon cancer growth via FoxO3a-dependent PUMA induction. Oncotarget 8, 83052–83062. https://doi.org/10.18632/oncotarget.20943

Yang, X., Sexauer, A., Levis, M., 2014. Bone marrow stroma-mediated resistance to FLT3 inhibitors in FLT3-ITD AML is mediated by persistent activation of extracellular regulated kinase. Br. J. Haematol. 164, 61–72. https://doi.org/10.1111/bjh.12599

Yao, C., Liu, J., Shao, L., 2011. Rapamycin inhibits the proliferation and apoptosis of gastric cancer cells by down regulating the expression of survivin. Hepatogastroenterology. 58, 1075–1080.

Yao, Y., Li, F., Huang, J., Jin, J., Wang, H., 2021. Leukemia stem cell-bone marrow microenvironment interplay in acute myeloid leukemia development. Exp. Hematol. Oncol. 10, 39. https://doi.org/10.1186/s40164-021-00233-2

Yilmaz, M., Kantarjian, H.M., Muftuoglu, M., Kadia, T.M., Konopleva, M., Borthakur, G., DiNardo, C.D., Pemmaraju, N., Short, N.J., Alvarado, Y., Montalban Bravo, G., Jurisprudencia, C., Pike, A.M., Ohanian, M., Jabbour, E., Garcia-Manero, G., Ruvolo, V., Ravandi, F., Andreeff, M., Daver, N., 2020. Quizartinib with Decitabine +/- Venetoclax Is Highly Active in Patients (Pts) with FLT3-ITD Mutated (mut) Acute Myeloid Leukemia (AML): Clinical Report and Signaling Cytof Profiling from a Phase IB/II Trial. Blood 136, 19–20. https://doi.org/10.1182/blood-2020-142687

Yilmaz, M., Kantarjian, H.M., Muftuoglu, M., Kadia, T.M., Konopleva, M., Borthakur, G., Dinardo, C.D., Pemmaraju, N., Short, N.J., Alvarado, Y., Montalban-Bravo, G., Jurisprudenica, C., Pike, A., Ohanian, M., Jabbour, E., Garcia-Manero, G., Ruvolo, V., Ravandi, F., Andreeff, M., Daver, N.G., 2021. Quizartinib with decitabine and venetoclax (triplet) is highly active in patients with FLT3-ITD mutated acute myeloid leukemia (AML). J. Clin. Oncol. 39, e19019–e19019. https://doi.org/10.1200/JCO.2021.39.15_suppl.e19019

Yilmaz, O.H., Valdez, R., Theisen, B.K., Guo, W., Ferguson, D.O., Wu, H., Morrison, S.J., 2006. Pten dependence distinguishes haematopoietic stem cells from leukaemia-initiating cells. Nature 441, 475–482. https://doi.org/10.1038/nature04703

Yoshihara, H., Arai, F., Hosokawa, K., Hagiwara, T., Takubo, K., Nakamura, Y., Gomei, Y., Iwasaki, H., Matsuoka, S., Miyamoto, K., Miyazaki, H., Takahashi, T., Suda, T., 2007. Thrombopoietin/MPL signaling regulates hematopoietic stem cell quiescence and interaction with the osteoblastic niche. Cell Stem Cell 1, 685–697. https://doi.org/10.1016/j.stem.2007.10.020

Yoshimoto, G., Miyamoto, T., Jabbarzadeh-Tabrizi, S., Iino, T., Rocnik, J.L., Kikushige, Y., Mori, Y., Shima, T., Iwasaki, H., Takenaka, K., Nagafuji, K., Mizuno, S., Niiro, H., Gilliland, G.D., Akashi, K., 2009a. FLT3-ITD up-regulates MCL-1 to promote survival of stem cells in acute myeloid leukemia via FLT3-ITD-specific STAT5 activation. Blood 114, 5034–5043. https://doi.org/10.1182/blood-2008-12-196055

Yoshimoto, G., Miyamoto, T., Jabbarzadeh-Tabrizi, S., Iino, T., Rocnik, J.L., Kikushige, Y., Mori, Y., Shima, T., Iwasaki, H., Takenaka, K., Nagafuji, K., Mizuno, S., Niiro, H., Gilliland, G.D., Akashi, K., 2009b. FLT3-ITD up-regulates MCL-1 to promote survival of stem cells in acute myeloid leukemia via FLT3-ITD–specific STAT5 activation. Blood 114, 5034–5043. https://doi.org/10.1182/blood-2008-12-196055

Zabkiewicz, J., Pearn, L., Hills, R.K., Morgan, R.G., Tonks, A., Burnett, A.K., Darley, R.L., 2014. The PDK1 master kinase is over-expressed in acute myeloid leukemia and promotes PKC-mediated survival of leukemic blasts. Haematologica 99, 858–864. https://doi.org/10.3324/haematol.2013.096487

Zada, A.A.P., Singh, S.M., Reddy, V.A., Elsässer, A., Meisel, A., Haferlach, T., Tenen, D.G., Hiddemann, W., Behre, G., 2003. Downregulation of c-Jun expression and cell cycle regulatory molecules in acute myeloid leukemia cells upon CD44 ligation. Oncogene 22, 2296–2308. https://doi.org/10.1038/sj.onc.1206393

Zeng, Z., Shi, Y.X., Samudio, I.J., Wang, R.-Y., Ling, X., Frolova, O., Levis, M., Rubin, J.B., Negrin, R.R., Estey, E.H., Konoplev, S., Andreeff, M., Konopleva, M., 2009. Targeting the leukemia microenvironment by CXCR4 inhibition overcomes resistance to kinase inhibitors and chemotherapy in AML. Blood 113, 6215–6224. https://doi.org/10.1182/blood-2008-05-158311

Zeng, Z., Shi, Y.X., Tsao, T., Qiu, Y., Kornblau, S.M., Baggerly, K.A., Liu, W., Jessen, K., Liu, Y., Kantarjian, H., Rommel, C., Fruman, D.A., Andreeff, M., Konopleva, M., 2012. Targeting of mTORC1/2 by the mTOR kinase inhibitor PP242 induces apoptosis in AML cells under conditions mimicking the bone marrow microenvironment. Blood 120, 2679–2689. https://doi.org/10.1182/blood-2011-11-393934

Zhang, F., Beharry, Z.M., Harris, T.E., Lilly, M.B., Smith, C.D., Mahajan, S., Kraft, A.S., 2009. PIM1 protein kinase regulates PRAS40 phosphorylation and mTOR activity in FDCP1 cells. Cancer Biol. Ther. 8, 846–853. https://doi.org/10.4161/cbt.8.9.8210

Zhang, J., Gao, Z., Yin, J., Quon, M.J., Ye, J., 2008. S6K directly phosphorylates IRS-1 on Ser-270 to promote insulin resistance in response to TNF-(alpha) signaling through IKK2. J. Biol. Chem. 283, 35375–35382. https://doi.org/10.1074/jbc.M806480200

Zhang, J., Gu, Y., Chen, B., 2019. Mechanisms of drug resistance in acute myeloid leukemia. OncoTargets Ther. 12, 1937–1945. https://doi.org/10.2147/OTT.S191621

Zhang, S., Broxmeyer, H.E., 1999. p85 subunit of PI3 kinase does not bind to human Flt3 receptor, but associates with SHP2, SHIP, and a tyrosine-phosphorylated 100-kDa protein in Flt3 ligand-stimulated hematopoietic cells. Biochem. Biophys. Res. Commun. 254, 440–445. https://doi.org/10.1006/bbrc.1998.9959

Zhang, X., Tang, N., Hadden, T.J., Rishi, A.K., 2011. Akt, FoxO and regulation of apoptosis. Biochim. Biophys. Acta 1813, 1978–1986. https://doi.org/10.1016/j.bbamcr.2011.03.010

Zhao, L., So, C.W.E., 2016. PARP-inhibitor-induced synthetic lethality for acute myeloid leukemia treatment. Exp. Hematol. 44, 902–907. https://doi.org/10.1016/j.exphem.2016.07.007

Zhao, W., Sachsenmeier, K., Zhang, L., Sult, E., Hollingsworth, R.E., Yang, H., 2014. A New Bliss Independence Model to Analyze Drug Combination Data. J. Biomol. Screen. 19, 817–821. https://doi.org/10.1177/1087057114521867

Zhou, F., Ge, Z., Chen, B., 2019. Quizartinib (AC220): a promising option for acute myeloid leukemia. Drug Des. Devel. Ther. 13, 1117–1125. https://doi.org/10.2147/DDDT.S198950

Zhou, H.-S., Carter, B.Z., Andreeff, M., 2016. Bone marrow niche-mediated survival of leukemia stem cells in acute myeloid leukemia: Yin and Yang. Cancer Biol. Med. 13, 248–259. https://doi.org/10.20892/j.issn.2095-3941.2016.0023

Zhou, J., Ching, Y.Q., Chng, W.-J., 2015. Aberrant nuclear factor-kappa B activity in acute myeloid leukemia: from molecular pathogenesis to therapeutic target. Oncotarget 6, 5490–5500. https://doi.org/10.18632/oncotarget.3545

Zhou, J., Chng, W.-J., 2014. Identification and targeting leukemia stem cells: The path to the cure for acute myeloid leukemia. World J. Stem Cells 6, 473–484. https://doi.org/10.4252/wjsc.v6.i4.473

Zhou, J., Chooi, J.-Y., Ching, Y.Q., Quah, J.Y., Toh, S.H.-M., Ng, Y., Tan, T.Z., Chng, W.-J., 2018. NF-κB promotes the stem-like properties of leukemia cells by activation of LIN28B. World J. Stem Cells 10, 34–42. https://doi.org/10.4252/wjsc.v10.i4.34

Zhou, J.-D., Zhang, T.-J., Xu, Z.-J., Gu, Y., Ma, J.-C., Li, X.-X., Guo, H., Wen, X.-M., Zhang, W., Yang, L., Liu, X.-H., Lin, J., Qian, J., 2019. BCL2 overexpression: clinical implication and biological insights in acute myeloid leukemia. Diagn. Pathol. 14, 68. https://doi.org/10.1186/s13000-019-0841-1

Zhou, Y., Zhao, R., Tseng, K., Li, K., Lu, Z., Liu, Y., Han, K., Gan, Z., Lin, S., Hu, H., Min, D., 2016. Sirolimus induces apoptosis and reverses multidrug resistance in human osteosarcoma cells in vitro via increasing microRNA-34b expression. Acta Pharmacol. Sin. 37, 519–529. https://doi.org/10.1038/aps.2015.153

Zhu, A.X., Abrams, T.A., Miksad, R., Blaszkowsky, L.S., Meyerhardt, J.A., Zheng, H., Muzikansky, A., Clark, J.W., Kwak, E.L., Schrag, D., Jors, K.R., Fuchs, C.S., Iafrate, A.J., Borger, D.R., Ryan, D.P., 2011. Phase 1/2 study of everolimus in advanced hepatocellular carcinoma. Cancer 117, 5094–5102. https://doi.org/10.1002/cncr.26165

Zhu, C., Anderson, A.C., Kuchroo, V.K., 2011. TIM-3 and its regulatory role in immune responses. Curr. Top. Microbiol. Immunol. 350, 1–15. https://doi.org/10.1007/82_2010_84

Zhu, J., Blenis, J., Yuan, J., 2008. Activation of PI3K/Akt and MAPK pathways regulates Myc-mediated transcription by phosphorylating and promoting the degradation of Mad1. Proc. Natl. Acad. Sci. U. S. A. 105, 6584–6589. https://doi.org/10.1073/pnas.0802785105

Zhu, R., Li, L., Nguyen, B., Seo, J., Wu, M., Seale, T., Levis, M., Duffield, A., Hu, Y., Small, D., 2021. FLT3 tyrosine kinase inhibitors synergize with BCL-2 inhibition to eliminate FLT3/ITD acute leukemia cells through BIM activation. Signal Transduct. Target. Ther. 6, 1–11. https://doi.org/10.1038/s41392-021-00578-4

Zimta, A.-A., Cenariu, D., Irimie, A., Magdo, L., Nabavi, S.M., Atanasov, A.G., Berindan-Neagoe, I., 2019. The Role of Nrf2 Activity in Cancer Development and Progression. Cancers 11. https://doi.org/10.3390/cancers11111755

Zöller, M., 2015. CD44, Hyaluronan, the Hematopoietic Stem Cell, and Leukemia-Initiating Cells. Front. Immunol. 6, 235. https://doi.org/10.3389/fimmu.2015.00235

Zong, H., Gozman, A., Caldas-Lopes, E., Taldone, T., Sturgill, E., Brennan, S., Ochiana, S.O., Gomes-DaGama, E.M., Sen, S., Rodina, A., Koren, J., Becker, M.W., Rudin, C.M., Melnick, A., Levine, R.L., Roboz, G.J., Nimer, S.D., Chiosis, G., Guzman, M.L., 2015. A Hyperactive Signalosome in Acute Myeloid Leukemia Drives Addiction to a Tumor-Specific Hsp90 Species. Cell Rep. 13, 2159–2173. https://doi.org/10.1016/j.celrep.2015.10.073